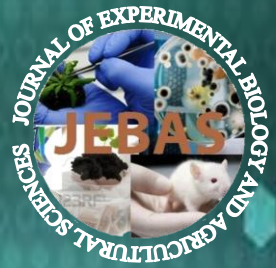


ISSN: 2320-8694

Journal of Experimental Biology And Agricultural Sciences



VOLUME 12

|| ISSUE I

|| FEBRUARY, 2024

Production and Hosting by Horizon Publisher India[HPI]
(<http://www.horizonpublisherindia.in>)
All rights reserved.

ISSN No. 2320 - 8694

Peer Reviewed - open access journal

Common Creative License - NC 4.0

Volume No - 12

Issue No - I

February, 2024

Journal of Experimental Biology and Agricultural Sciences (JEBAS) is an online platform for the advancement and rapid dissemination of scientific knowledge generated by the highly motivated researchers in the field of biological agricultural, veterinary and animal sciences. JEBAS publishes high-quality original research and critical up-to-date review articles covering all the aspects of biological sciences. Every year, it publishes six issues.

JEBAS has been accepted by SCOPUS UGC CARE, INDEX COPERNICUS INTERNATIONAL (Poland), AGRICOLA (USA), CAS (ACS, USA), CABI - Full Text (UK), International Committee of Medical Journal Editors (ICMJE), SHERPA - ROMEO; J gate and Indian Science Abstracts (ISA, NISCAIR) like well reputed indexing agencies.

[HORIZON PUBLISHER INDIA [HPI]

<http://www.horizonpublisherindia.in/>]

Editorial Board

Editor-in-Chief

Prof Y. Norma-Rashid
(University of Malaya, Kuala Lumpur)
editor.in.chief.jebas@gmail.com

Co-Editor-in-Chief

Dr. Kuldeep Dhama, M.V.Sc., Ph.D.
NAAS Associate, Principal Scientist, IVRI, Izatnagar India - 243 122
co_eic@jebas.org

Managing - Editor

Kamal K Chaudhary, Ph.D. (India)
jebasonline@gmail.com

Technical Editors

Hafiz M. N. Iqbal (Ph.D.)

Research Professor,
Tecnologico de Monterrey, School of Engineering and Sciences,
Campus Monterrey, Ave. Eugenio Garza Sada 2501,
Monterrey, N. L., CP 64849, Mexico
Tel.: +52 (81) 8358-2000Ext.5561-115
E-mail: hafiz.iqbal@my.westminster.ac.uk; hafiz.iqbal@itesm.mx

Prof. Dr. Mirza Barjees Baigis

Professor of Extension (Natural Resource Management),
Department of Agricultural Extension and Rural Society,
College of Food and Agriculture Sciences,
King Saud University, P.O. Box 2460, Riyadh 11451, Kingdom of Saudi Arabia
Email: mbaig@ksu.edu.sa

Dr. Mukesh Kumar Meghvansi

Scientist, Bioprocess Technology Division, Defence R & D Establishment, Gwalior-474002
Email: mk_meghvansi@yahoo.co.in

Dr. B L Yadav

Head – Botany, MLV Govt. College, Bhilwara, India
E mail: drblyadav@yahoo.com

Dr. K L Meena

Associate Professor – Botany, MLV Govt.
College, Bhilwara, India
E mail: kanhaiyameena211@yahoo.com

Dr. Yashpal S. Malik

ICAR – National Fellow Indian Veterinary Research Institute (IVRI)
Izatnagar 243 122, Bareilly, Uttar Pradesh, India

Associate Editors

Dr. Sunil K. Joshi

Laboratory Head, Cellular Immunology
Investigator, Frank Reidy Research Center of Bioelectrics, College of Health Sciences, Old Dominion University,
4211 Monarch Way, IRP-2, Suite # 300, Norfolk, VA 23508 USA
Email: skjoshi@odu.edu

Dr. Vincenzo Tufarelli

Department of Emergency and Organ Transplantation (DETO),
Section of Veterinary Science and Animal Production,
University of Bari 'Aldo Moro', s.p. Casamassima km 3, 70010 Valenzano, Italy
Email: vincenzo.tufarelli@uniba.it

Prof. Sanjay-Swami, Ph.D. (Soil Science & Agril. Chemistry),

School of Natural Resource Management,
College of Post Graduate Studies in Agricultural Sciences,
(Central Agricultural University),
UMIAM (Barapani)-793 103, Meghalaya, INDIA
Email: sanjay.nrm.cpgsas@cau.ac.in

Chiranjib Chakraborty, Ph.D.

Professor, School of Life Science and Biotechnology,
Adamas University, Kolkata, India
Email: drchiranjib@yahoo.com

Jose M. Lorenzo

Centro Tecnológico de la Carne de Galicia
Ourense, Spain
Email: jmlorenzo@ceteca.net

Assistant Editors

Dr Ayman EL Sabagh

Assistant professor, agronomy department, faculty of agriculture
kafresheikh university, Egypt
E-mail: ayman.elsabagh@agr.kfs.edu.eg

Safar Hussein Abdullah Al-Kahtani (Ph.D.)

King Saud University-College of Food and Agriculture Sciences,
Department of the Agricultural Economics
P.O.Box: 2460 Riyadh 11451, KSA
email: safark@ksu.edu.sa

Dr Ruchi Tiwari

Assistant Professor (Sr Scale)
Department of Veterinary Microbiology and Immunology,
College of Veterinary Sciences,
UP Pandit Deen Dayal Upadhayay Pashu Chikitsa Vigyan Vishwavidyalay Evum Go-Anusandhan Sansthan (DUVASU),
Mathura, Uttar Pradesh, 281 001, India
Email: ruchi.vet@gmail.com

Dr. ANIL KUMAR (Ph.D.)

Asstt. Professor (Soil Science)
Farm Science Centre (KVK)
Booh, Tarn Taran, Punjab (India) – 143 412
Email: anilkumarhpkv@gmail.com

Akansha Mishra

Postdoctoral Associate, Ob/Gyn lab
Baylor College of Medicine,
1102 Bates Ave, Houston Tx 77030
Email: akansha.mishra@bcm.edu; aksmisra@gmail.com

Dr. Muhammad Bilal

Associate Professor
School of Life Science and Food Engineering,
Huaiyin Institute of Technology, Huaian 223003, China
Email: bilaluaf@hotmail.com

Dr. Senthilkumar Natesan

Associate Professor

Department of Infectious Diseases, Indian Institute of Public Health

Gandhinagar, Opp to Airforce station HQ, Lekawada, Gandhinagar, Gujarat - 382042, India

Email: snatesan@iiphg.org

Mr. Ram Bahadur Khadka (Microbiologist)

Assistant Professor (Pokhara University)

Crimson College of Technology (CCT)

Butwal-13, Rupandehi, Lumbini Province, Nepal

Email: rambahadurkhadka00@gmail.com

Prof. A. VIJAYA ANAND

Professor

Department of Human Genetics and Molecular Biology

Bharathiar University

Coimbatore – 641 046

Dr. Phetole Mangena

Department of Biodiversity, School of Molecular and Life Sciences,

Faculty of Science and Agriculture, University of Limpopo, Republic of South Africa

Private Bag X1106, Sovenga, 0727

Email: Phetole.Mangena@ul.ac.za ; mangena.phetole@gmail.com

Table of contents

Production, characterization, and applications of a novel thermo-acidophilic L-asparaginase of <i>Pseudomonas aeruginosa</i> CSPA4 <i>10.18006/2024.12(1).1.15</i>	1 – 15
FIRST REPORT ON TRUFFLE-INHABITING FUNGI AND METAGENOMIC COMMUNITIES OF <i>TUBER AESTIVUM</i> COLLECTED IN RUSSIA <i>10.18006/2024.12(1).16.35</i>	16 – 35
Role of Probiotic Strain <i>Lactobacillus acidophilus</i> in the Reversal of Gut Dysbiosis Induced Brain Cognitive Decline <i>10.18006/2024.12(1).36.48</i>	36 – 48
Highlighting the Importance of Matrix Metalloproteinase 1, 8, and 9 Expression during the Progression of <i>Mycobacterium tuberculosis</i> Infection <i>10.18006/2024.12(1).49.59</i>	49 – 59
Exploration and Profiling of Potential Thermo-alkaliphilic <i>Bacillus licheniformis</i> and <i>Burkholderia</i> sp. from varied Soil of Delhi region, India and their Plant Growth-Promoting Traits <i>10.18006/2024.12(1).60.75</i>	60 – 75
Phytotoxicity and genotoxicity assessment of organic and inorganic contaminants detected in pharmaceutical industrial wastewaters using <i>Vigna radiata</i> and <i>Allium cepa</i> <i>10.18006/2024.12(1).76.92</i>	76 – 92
Ethnopharmacological study of medicinal plants used in the treatment of skin diseases in the Western Middle Atlas region (Morocco) <i>10.18006/2024.12(1).93.105</i>	93 – 105
Effects of Elicitation on <i>Invitro</i> Regeneration of two Tomato (<i>Solanum lycopersicum</i> L.) Cultivars in Tissue Culture <i>10.18006/2024.12(1).106.123</i>	106 – 123
ARTIFICIAL INTELLIGENCE IN TACKLING CORONAVIRUS AND FUTURE PANDEMICS <i>10.18006/2024.12(1).124.137</i>	124 – 137
Residue-specific orientation of arrestin in 5-HTR_{1B} (Serotonin Receptor)-βArrestin-1 interaction <i>10.18006/2024.12(1).138.144</i>	138 – 144
Analyzing the antimicrobial efficacy of the economically important tree <i>Knema linifolia</i> (Roxb.) Warb <i>10.18006/2024.12(1).145.152</i>	145 – 152
Molecular regulation of <i>Mycobacterium tuberculosis</i> Sigma factor H with Anti-sigma factor RshA under stress condition <i>10.18006/2024.12(1).153.162</i>	153 – 162



Journal of Experimental Biology and Agricultural Sciences

<http://www.jebas.org>

ISSN No. 2320 – 8694

Production, characterization, and applications of a novel thermo-acidophilic L-asparaginase of *Pseudomonas aeruginosa* CSPS4

Vinay Kumar¹ , Swati Joshi² , Bhupendra Kumar³ , Digvijay Verma^{1*} 

¹Department of Environmental Microbiology, Babasaheb Bhimrao Ambedkar University, Lucknow- 226025, Uttar Pradesh, India

²ICMR-National Institute of Occupational Health (NIOH) Meghani Nagar, Ahmedabad-380016, Gujarat, India

³CSIR-National Botanical Research Institute, Lucknow, Academy of Scientific and Innovative Research (AcSIR), Ghaziabad, Uttar Pradesh, India

Received – October 13, 2023; Revision – January 11, 2024; Accepted – February 12, 2024

Available Online – March 15, 2024

DOI: [http://dx.doi.org/10.18006/2024.12\(1\).1.15](http://dx.doi.org/10.18006/2024.12(1).1.15)

KEYWORDS

L-asparaginase

Pseudomonas aeruginosa

Thermo-acidophilic enzyme

Acrylamide reduction

Food industry

ABSTRACT

In present investigation, a potential L-asparaginase-producing bacterial isolate, *Pseudomonas aeruginosa* CSPS4, has been explored to enhance the production and purification of the asparaginase enzyme. Production of L-asparaginase is enhanced using the 'one variable at a time approach (OVAT)'. In Plackett Burman (PB) analysis, pH, sucrose, and temperature significantly influence L-asparaginase production. Thereafter, L-asparaginase enzyme was recovered from culture broth using fractional precipitation with chilled acetone. The partially purified L-asparaginase showed a molecular weight of ~35 KDa on SDS-PAGE. L-asparaginase was characterized as a thermo-acidophilic enzyme exhibiting optimum pH and temperature of 6.0 and 60 °C, respectively. These characteristics render this enzyme novel from other available asparaginases of *Pseudomonas* spp. L-asparaginase activity remained unaffected by different modulators. L-asparaginase of this investigation was successfully employed for acrylamide degradation in commercial fried potato chips, establishing its applicability in food industries.

* Corresponding author

E-mail: digvijay.udsc@gmail.com (Digvijay Verma)

Peer review under responsibility of Journal of Experimental Biology and Agricultural Sciences.

Production and Hosting by Horizon Publisher India [HPI]
(<http://www.horizonpublisherindia.in/>).
All rights reserved.

All the articles published by [Journal of Experimental Biology and Agricultural Sciences](#) are licensed under a [Creative Commons Attribution-NonCommercial 4.0 International License](#) Based on a work at www.jebas.org.



1 Introduction

L-asparaginase (EC 3.5.1.1) hydrolyzes the amide group of L-asparagine and liberates aspartic acid and ammonia (Qeshmi et al. 2022; Zhou et al. 2022). The enzyme finds several biotechnological applications related to human health in the food and pharmaceutical industries (Batool et al. 2016; Brumano et al. 2019). L-asparaginases grabbed special attention due to their major role as an antitumor agent (Shrivastava et al. 2016; Luo et al. 2018; Osama et al. 2023). Tumor cells cannot synthesize asparagine due to the lack of an asparagine synthase enzyme, which leads to inhibition of translation followed by complete cell cycle arrest (Povlova et al. 2018). By taking advantage of this fact, asparaginase was employed as an antitumor agent for diminishing the essential L-asparagine for the growth of leukemic cells (Mahajan et al. 2014; Ali et al. 2016; Osama et al. 2023). Several commercial L-asparaginases (Bionase®, Spectrila®, Erwinase®, and Oncaspar®) are available in the market that are chiefly sourced from either *Escherichia coli* or *Erwinia chrysanthemi* (Kataria et al. 2015; Vimal and Kumar 2022). Besides, using L-asparaginase has also proven acrylamide degradation (Xu et al. 2016). Therefore, this enzyme exhibits a significant role in the starch-based food industry, where it reduces the concentration of acrylamide, which is generated due to the Maillard reaction between sugars and L-asparagine at high temperatures (Stadler et al. 2002; Kukurova et al. 2009; Jia et al. 2021). Despite many available L-asparaginases from various sources, industries compromise with the enzyme characteristics. For example, weak thermostability at higher temperatures makes this enzyme unsuitable for food and baking industries (Li et al. 2019; Qeshmi et al. 2022; Muzuni et al. 2023). Similarly, glutaminase-free L-asparaginases are the pre-requisite of pharmaceutical industries to minimize the immunogenic response while treating acute lymphoblastic leukaemia (ALL). Therefore, further research is required to achieve the L-asparaginase with desired properties. In the present investigation, wild-type L-asparaginase of *Pseudomonas aeruginosa* CSPS4 is studied for the production, characterization, and application. The enzyme finds applicability and could be a candidate in the starch-based food industry due to the degradation of acrylamide.

2 Materials and Methods

2.1 Qualitative L-asparaginase assay for screening of L-asparaginase

Soil samples from a slaughter shop market in Lucknow, Uttar Pradesh, India, were collected in sterile polybags. Samples were stored at 4 °C in a refrigerator till their use. The serial dilution was performed to isolate bacteria from the samples (Yan et al. 2015). An appropriate dilution of 10^{-5} was spread on the C-Dox agar medium from 1.0 gm of soil suspension made in 10 ml of dH₂O.

The composition of 1L modified C-DOX agar medium was [Na₂HPO₄·2H₂O (6 gm), KH₂PO₄ (3 gm), NaCl (0.5 gm), L-asparagine (5 gm), 1M MgSO₄·7H₂O (2 ml), 0.1M CaCl₂·2H₂O (1 ml), 20% Glucose stock solution (10 ml), Agar (20 gm), 2.5% phenol red indicator (0.04-0.36 ml), and pH 7.0] as described by Mahajan et al. (2012) along with 0.5 (w/v) % of L-asparagine as substrate (Mahajan et al. 2012; Doriya and Kumar 2016). The colonies that were able to turn the orange-yellow colour of the media into pink-red color due to hydrolysis of L-asparagine into L-aspartate and ammonia (NH⁴⁺) were picked as L-asparaginase-producers (Doriya and Kumar 2016).

2.2 Thermal screening of the L-asparaginase enzyme

Bacterial isolates were further screened at 50 °C to obtain a thermostable L-asparaginase. For this, 50 ml C-Dox medium was inoculated with 1% (v/v) overnight grown inoculum of bacterial isolates. The culture broth was collected at 24 and 48 hrs to assess the L-asparaginase activity at 50°C. A bacterium exhibiting the highest L-asparaginase activity was selected for further investigation.

2.3 L-asparaginase and L-glutaminase assay

L-asparaginase and L-glutaminase activity was measured by assaying the cell-free supernatant of overnight grown culture (Shirfrin et al. 1974). The supernatant (L-asparaginase) was mixed with an equal volume of 1 % of respective substrates, either L-asparagine or L-glutamine solutions (dissolved in 0.1 M tris-HCl; pH 6.0) for hydrolysis of these substrates followed by measurement of ammonia using Nessler's reagent (Simas et al. 2021).

One international unit (IU) of L-asparaginase or L-glutaminase is defined as the amount of enzyme required for liberating 1 nanomole of ammonia at pH 6.0 and temperature 60 °C from these substrates. For the standard curve, varying concentrations (10-100 µM) of ammonium sulfate were prepared, where ammonia was assayed using Nessler's reagent.

2.4 Morphological, biochemical, and molecular characterization of isolated strain CSPS4

The isolated bacterial isolate was characterized for its morphology and biochemical properties according to Bergey's Manual of Determinative Bacteriology (Williams et al. 1989). Colour, shape, margins, texture, opacity, and odour were observed for morphological characterization. Besides, Gram staining was also performed to determine the characteristics of the bacteria (Dipali and Ajit 2012; Tripathi and Sapra 2023). For molecular-level identification of the bacterium, 3.0 ml of overnight-grown bacterial broth was sedimented at 10,000 rpm to collect the bacterial pellet. The pellet was homogenized in 1 ml of 1% extraction buffer (*N,N*-

,*N,N*-cetyltrimethylammonium bromide (CTAB), 2% polyvinylpyrrolidone (PVPP), 1.5 M NaCl, 100 mM EDTA, 0.1 M TE buffer (pH 8.0), 0.1 M sodium phosphate buffer (pH 8.0), and 100 µL RNaseA and treated with 5 µL of lysozyme (10 mg/ml) and proteinase-K (10 mg/ml) (Verma and Satyanarayana 2011). The suspension was kept at 37 °C for 1 hr, followed by adding 100 µL of 10% (w/v) SDS solution. The bacteria were further lysed at 60 °C for 1 hr. The cell debris was separated by centrifuging the suspension at 10,000 rpm for 5 min. The supernatant was collected and treated with an equal volume of phenol: chloroform: iso-amyl alcohol (25:24:1) solution to remove the proteins (Simpson and Beynon 2010; Verma and Satyanarayana 2011). The aqueous phase was collected by centrifugation at 10,000 rpm and treated with 0.7 V of isopropanol to precipitate the DNA. The precipitated DNA pellet was obtained after high-speed centrifugation of 10,000 rpm for 10 min. The pellet was washed with 70% (v/v) ethanol and dried at room temperature for 2 hrs. The pellet was suspended in 50 µL sterile TE buffer (0.1 M; pH 8.0). Thus, obtained genomic DNA was used for the amplification of bacterial-specific 16S rRNA gene using bacterial-specific primers (Forward: 5'AGAGTTTGATCMTGGCTCAG 3'; Reverse: 5'AAGGAGGTGATCCANCCRA3') to identify the bacterial species. A PCR reaction was set up at initial denaturation of 95 °C followed by 29 cycles of denaturation (95 °C for 1 min), annealing (56 °C for 1 min), and extension (72 °C for 1 min) was carried out in a thermal cycler (Bio-Rad, China) with a final extension of 10 min at 72 °C. The amplified DNA was sequenced, followed by BLASTn analysis to determine the % identity for bacterial identification.

2.5 Production of the L-asparaginase from *P. aeruginosa* CSPS4

Asparaginase production from *P. aeruginosa* CSPS4 was optimized using the C-Dox medium as a base medium by the 'one variable at a time' (OVAT) approach. Various physical (pH, temperature, inoculum age, inoculum size, agitation rate, and flask volume) and nutritional (carbon and nitrogen) parameters, along with detergent levels, were optimized to enhance the asparaginase production by the bacterial isolate.

2.6 Statistical optimization for L-asparaginase production using Plackett-Burman Design

The selected parameters obtained by OVAT analysis were further used to generate the Plackett-Burman (PB) factorial design for identifying the significant factors/culture variables for the L-asparaginase enzyme production. Nine variables (pH, temperature, incubation time, inoculum age, inoculum size, agitation rate, flask volume, sucrose, and peptone) were selected for PB design by considering higher (+) and lower (-) levels (Table 1). Statistical tool Design Expert Software 6.1.10 (<https://www.statease.com/software/design-expert/>) was used to design the PB model for analyzing the predicted enzyme production under the given conditions of the model. The experiment was performed in triplicates to calculate the standard deviations in each set of experiments. The experimental design was the estimated mean of L-asparaginase production that followed the first-order model with the following equation (El-Naggar et al. 2019).

Table 1 Statistical optimization for L-asparaginase production from *P. aeruginosa* CSPS4 using Plackett-Burman design

Run	Block 1	Incubation time (hrs.)	pH	Temp (°C)	Inoculum size (%)	Inoculum age (hrs)	RPM	Flask volume (ml)	Sucrose (%)	Peptone (%)	Enzyme Activity (nM/min)
1.	Block 1	72	8	25	6	12	100	10	4	4	249.77±2.03
2.	Block 1	24	8	45	1	24	100	10	0.5	4	70.22±3.35
3.	Block 1	72	8	45	1	24	250	10	4	0.5	498.66 ±3.35
4.	Block 1	24	4	25	6	24	250	10	4	4	19.55±2.77
5.	Block 1	24	4	45	6	24	100	200	4	0.5	56.88±0.76
6.	Block 1	24	8	25	1	12	250	200	4	0.5	453.33±4.07
7.	Block 1	72	4	25	1	24	250	200	0.5	4	101.77±2.03
8.	Block 1	24	4	25	1	12	100	10	0.5	0.5	131.55±3.35
9.	Block 1	24	8	45	6	12	250	200	0.5	4	204.88±4.33
10.	Block 1	72	8	25	6	24	100	200	0.5	0.5	521.33±4.07
11.	Block 1	72	4	45	1	12	100	200	4	4	159.11±3.33
12.	Block 1	72	4	45	6	12	250	10	0.5	0.5	161.77±2.03

Here ± indicates standard deviation (SD); Experiments were carried out in triplicates to calculate SD

$$Y = \beta_0 + \sum \beta_i x_i \quad \text{Eq. 1}$$

Where Y depicts L-asparaginase activity response, β_i is a linear variable coefficient, β_0 is the model intercept, x_i is the level independent variable, and i is the variable number. Design Expert 6.1.10 software was used to scan the variables. Nessler's reagent was used to measure the L-asparaginase activity (Table 1).

2.7 Purification of L-asparaginase

Extracellular L-asparaginase was purified by the acetone precipitation method (Simpson and Beynon 2010). Briefly, 1 L C-Dox medium was inoculated with 1% (v/v) overnight grown culture of *P. aeruginosa* CS4. L-asparaginase production was achieved by incubating the bacteria at 150 rpm at 37 °C for 48 hrs. The culture was centrifugated at 10000 rpm, and the culture supernatant was harvested to recover extracellular L-asparaginase. The total protein was precipitated from one liter of supernatant by gradually adding 6V of prechilled acetone (-20 °C) into one liter of cell-free supernatant on a continuous stirrer at 4 °C and the precipitated protein was collected using centrifugation followed by complete evaporation of acetone. The crude protein was suspended in 5.0 ml of Tris-Cl buffer (0.1M; pH 6.0). This suspension was further used for collecting various fractions of precipitated proteins to achieve the purified L-asparaginase. Acetone was added to 5.0 ml of suspended protein under varying concentrations. The first protein fraction was precipitated by adding 10% (v/v) prechilled acetone into 5.0 ml of suspended protein through the tube wall and incubated for 1 hr at low temperature. Thereafter, the precipitated crude protein was collected using centrifugation followed by complete evaporation of acetone. The crude protein was dissolved in 5.0 ml of Tris-HCl buffer (0.1M; pH 6.0). The supernatant was further used to precipitate the remaining protein in another cycle. It was carried out by sequentially adding chilled acetone by using 20%, 40%, 60%, 80%, and 100% (v/v) into the supernatant obtained from each cycle. The precipitated protein obtained from each cycle was dried at 4 °C by uncapping the respective tubes at 4 °C for 6 hrs and solubilized into 0.5 ml of 0.1 M Tris-HCl buffer of pH 6.0. Each precipitated protein fraction was subjected to protein estimation (Kruger 1994). The fractions of precipitated proteins were checked for L-asparaginase activity and also on SDS-PAGE. The purified L-asparaginase was further analyzed using high-pressure liquid chromatography (HPLC).

2.8 Biophysical and biochemical characterization of L-asparaginase

Various buffers (pH 3-12) were used for determining the optimum pH of L-asparaginase. Similarly, the optimum temperature of L-asparaginase was obtained by assaying the enzyme at different temperatures (40-80 °C). The stability of the enzyme was characterized by incubating the purified enzymes at varying pH

and temperatures. The samples were collected at different time intervals and assayed for residual enzyme activity. Biochemical characterization was done by incubating the purified enzyme with different modulators (Tweens, SDS, and EDTA) followed by an L-asparaginase assay. The substrate specificity was also assessed in the presence of L-glutamine to determine the glutaminase activity in the L-asparaginase enzyme. Activity on other protein-based substrates like casein and keratin was also evaluated.

2.9 Applications of L-asparaginase

2.9.1 inhibition of acrylamide gel polymerization

Inhibition of acrylamide polymerization was checked by using 20% and 30% acrylamide solutions. The reaction was set by mixing different concentrations of L-asparaginase into 5.0 ml of 20% and 30% acrylamide solution along with 2.5 ml dH₂O and kept at 60 °C for 30 min for enzymatic catalysis of acrylamide. To check the polymerization, polymerization of the acrylamide gel was initiated by adding 200 µL of 10% APS (ammonium persulfate) along with 20 µL of TEMED (tetra-methyl-ethylene-diamine) solution into the reaction tubes. The inhibition of polymerization was observed by recording the solidification time in respective tubes. The gel flow was also observed in similar reactions to determine the inhibition of polyacrylamide gel formation.

2.9.2 Acrylamide degradation in potato chips

10 gm commercial potato chips were soaked into 10 ml of MilliQ water and vortexed to solubilize the acrylamide present in the chips. The supernatant was collected using high-speed centrifugation, and 2.0 ml of supernatant was treated with ~30 IU of L-asparaginase and incubated at 60 °C for 30 min. 200 µL of the sample was collected at varying time intervals and assessed for the presence of ammonia using Nessler's reagent (Simas et al. 2021). The control samples were also collected similarly from another set of 2.0 ml supernatant without adding L-asparaginase.

2.10 Statistical tool

For PB analysis, Design-Expert version 9.0 (Stat-Ease Inc., Minneapolis, USA) was used. All other experiments were carried out in triplicates to determine the mean values and their standard deviation wherever required.

3 Results

3.1 Thermal screening and selection of L-asparaginase-producing bacteria

Of the seven potential isolates (CGRS, CS4, RNF, GSS, GSPS, NBB1, and NBB2) selected through qualitative screening, one isolate (CS4) showed the maximum production at 50 °C after 24

hrs of incubation as compared to other L-asparaginase-producing bacteria (Figure 1A). Study of colony characteristics showed that isolated bacterium formed greenish colour circular colonies with rough margins and umbonate surface after 24 hrs of incubation on nutrient agar at 37 °C (Figure 1B). The bacterium CSPS4 was identified as a Gram-negative stain (Figure 1C). BLASTn analysis of 16S rRNA sequence showed the identity with various strains of *P. aeruginosa*. The maximum identity was observed with *P. aeruginosa* strain OLB-1 (99.87%; LR130528.1), strain JADE-X (99.80%; CP114374.1), and strain M6A146 (99.80%; accession no. CP113974.1) (Figure 1D).

3.2 Production of L-asparaginase from *Pseudomonas aeruginosa* CSPS4

The OVAT approach for media optimization resulted in maximum L-asparaginase production of 512 ± 16.87 nM/min at pH 6.0, temperature 37 °C and incubation time of 48 hrs (Table 2; Figure 2A and 2B). Other optimized physical conditions were inoculum size (3%), inoculum age (18 hrs.), aeration (150 rpm), and flask volume (250 ml) (Figure 2C, 2D, 2E, and 2F). Whereas optimized nutrient parameters were carbon (1% sucrose) and nitrogen sources (1% peptone) (Figure 3A, 3B, 3C, and 3D).

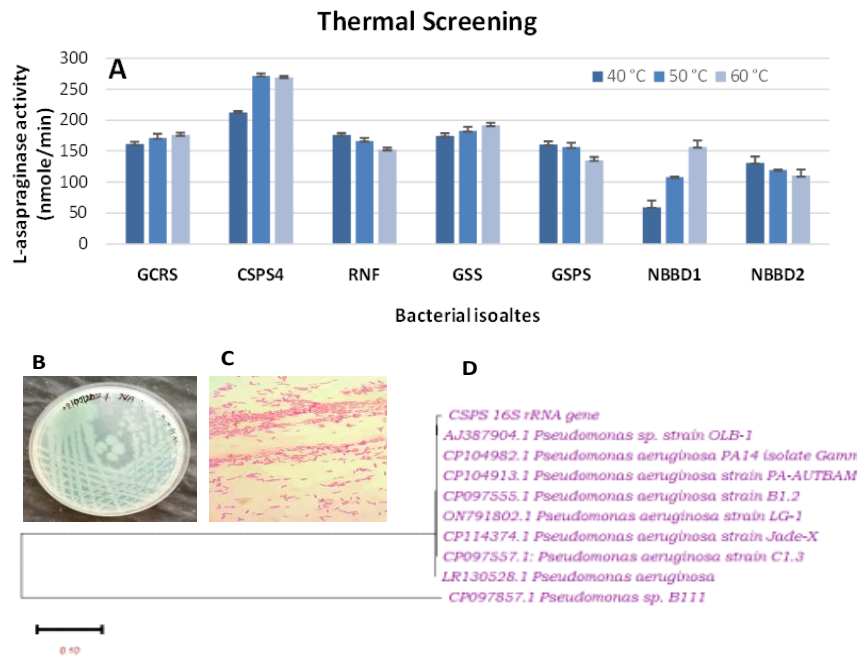


Figure 1 Thermal screening of the (A) bacterial isolates, (B) Colony morphology, (C) Gram-staining, and (D) Phylogenetic tree of the strain CSPS4. The phylogenetic tree was constructed using MEGA11 software by picking Neighbor-joining (NJ) method.

Table 2 Various parameters for L-asparaginase production using OVAT approach

S. No.	Parameters	Optimized condition	Optimum activity (nM/min)
1.	Incubation time	48	268±10.65
2.	pH	6.0	318±8.76
3.	Incubation temperature	37	332±11.32
4.	Inoculum size-3%	3	438±10.14
5.	Inoculum age-18 hrs	18	447±15.90
6.	RPM-150	150	468±14.32
7.	Flask volume-50ml	250	469±13.23
8.	Carbon source	1% (Sucrose)	480±12.22
9.	Sucrose	3%	504±13.32
10.	Nitrogen source	1% (Peptone)	474±13.22
11.	Optimized parameters		512±16.87

Here ± indicates standard deviation (SD); Experiments were carried out in triplicates to calculate SD

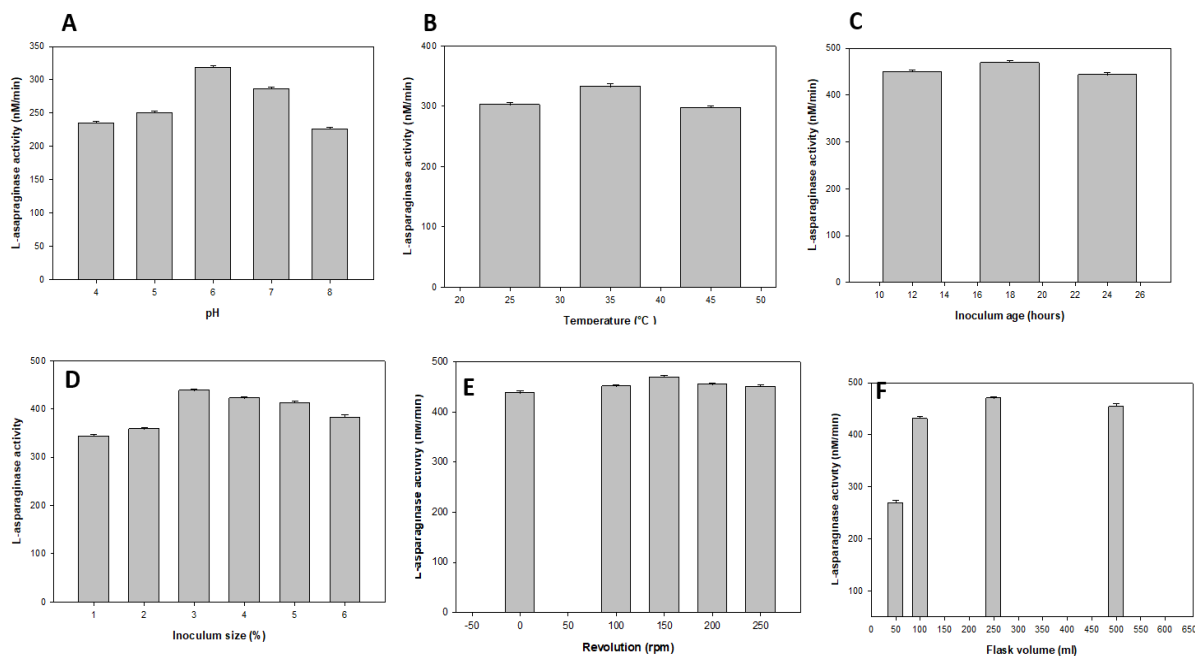


Figure 2 Optimization of physical parameters such as (A) pH, (B) temperature, (C) inoculum age, (D) inoculum size, (E) agitation rate, and (F) aeration conditions to produce L-asparaginase from *P. aeruginosa* CSPS4.

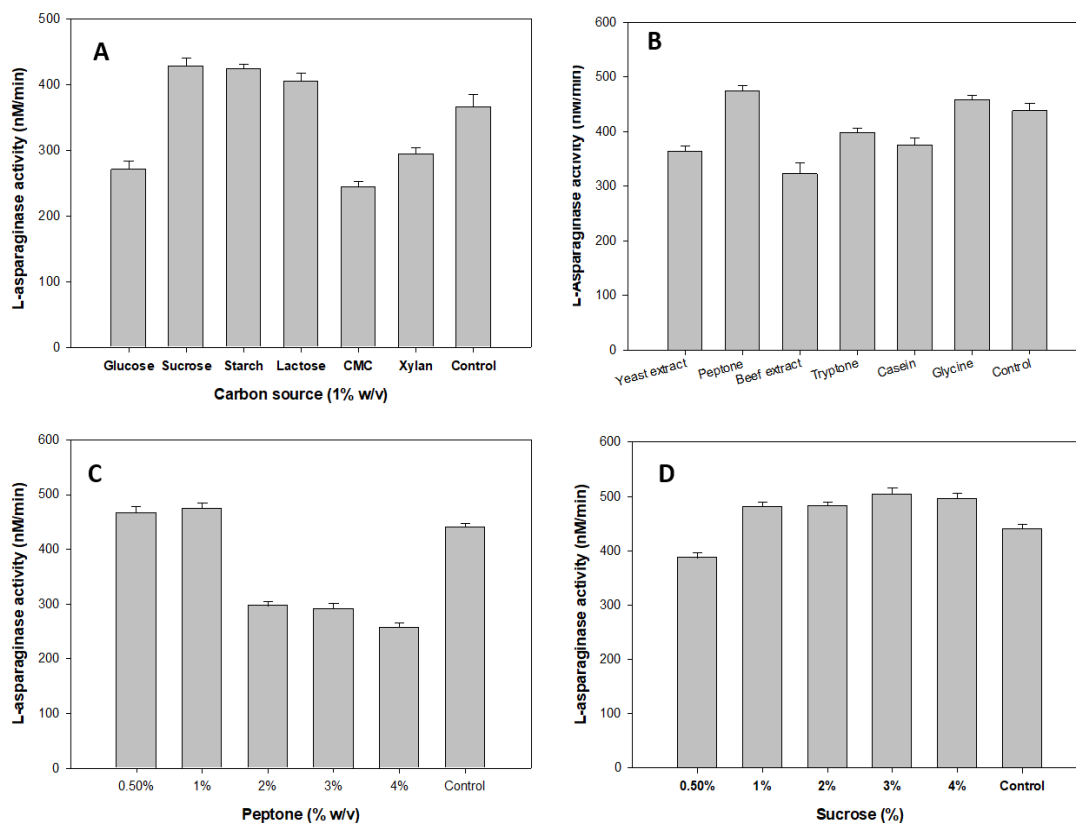


Figure 3 Optimization of nutrient components such as (A) carbon source, (B) nitrogen source, (C) peptone, and (D) sucrose to produce L-asparaginase from *P. aeruginosa* CSPS4.

Table 3 ANOVA analysis

	Source	Sum of Squares	Df	Mean Square	<i>f</i> -value	<i>p</i> -value Prob>F	Significant/Non-significant
	Model	2.28	9	0.25	83.99	0.0118	Significant
A	Incubation time	0.024	1	0.024	8.13	0.1041	Non-Significant
B	pH	1.43	1	1.43	475.38	0.0021	Significant
E	Inoculum age	2.407E-003	1	2.407E-003	0.80	0.4656	Non-Significant
F	Agitation (rpm)	0.023	1	0.023	7.53	0.1111	Non-Significant
G	Flask volume	0.027	1	0.027	8.91	0.0963	Non-Significant
H	Sucrose	0.12	1	0.12	38.44	0.0250	Significant
J	Peptone	0.58	1	0.58	193.32	0.0051	Significant
K	Dummy1	0.021	1	0.021	6.98	0.1183	Non-Significant
L	Dummy2	0.049	1	0.049	16.40	0.0559	Significant
	Residual	6.024E-003	2	3.012E-003			
	Cor Total	2.28	11				

3.3 Statistical optimization for L-asparaginase production using Plackett-Burman Design

Nine factors were assessed to identify the significant variables for achieving maximum L-asparaginase production. The model provided 12 runs, where columns and rows correspond to the variables and experimental conditions. During the trials, L-asparaginase production ranged from 19.55±2.77 nM/min (4th run) to 521.33±4.07 nM/min units (10th run). Multiple linear regression analysis was performed to determine the *F*- and *p*-value of respective components based on the PB design. First order linear model showed the effect of independent variables on L-asparaginase production [Eqn. 2 (coded factors) and Eqn. 3 (actual factors)].

3.3.1 Final equation in terms of coded factors

$$Y (\text{L-asparaginase}) = \text{Log}_{10}(\text{Response } 1) = +1.81 + 0.045 * A + 0.35 * B + 0.014 * E - 0.043 * F + 0.047 * G + 0.098 * H - 0.22 * J - 0.042 * K + 0.064 * L \quad (\text{Eq. } 2)$$

3.3.2 Final equation in terms of actual factors

$$Y (\text{L-asparaginase}) = \text{Log}_{10}(\text{Response } 1) = +0.84449 + 1.88230E-003 * \text{Incubation time} + 0.17271 * \text{pH} + 2.36062E-003 * \text{Inoculum age} - 5.79674E-004 * \text{RPM} + 4.97897E-004 * \text{Flask volume} + 0.056129 * \text{Sucrose} - 0.12587 * \text{Peptone} - 0.041861 * \text{Dummy } 1 + 0.064154 * \text{Dummy } 2 \quad (\text{Eq. } 3)$$

$$Y = \beta_0 + \sum \beta_i x_i$$

Where Y is the response of L-asparaginase enzyme activity, β_0 is the model intercept, β_i is a linear variable coefficient, *i* is the

variable number, and *x_i* is the level independent variable. Analysis of variance (ANOVA) (root mean squares) identified the significant model terms affecting the production of L-asparaginase (Table 3). B, H, and J were identified as significant model terms in this case.

In this case, pH (model term B) and peptone (model term J) were the only significant model terms. Values >0.1000 indicate that the model terms are non-significant. Overall, the model was significant, having a *p*-value of 0.011. Moreover, the model *F*-value of 83.99 implies that the model is significant. There is only a 1.18% chance that a "Model *F*-value" this large could occur due to noise. Moreover, the R-squared value and Adj R-squared values were 0.9974 and 0.9855, with a predicted R-squared value of 0.9050. Thus, the model can explain more than 99% of the variation. Here, the 'adeq-precision' ratio was 28.551, which indicates an adequate signal and can be used to navigate the design space.

3.4 Purification of L-asparaginase

During fractional precipitation, fraction number four (F4) showed the maximum L-asparaginase activity (Table 4). The purified enzyme exhibited a molecular weight of ~35 KDa on SDS-PAGE gel (Figure 4A). The purified L-asparaginase was also identified as a single peak during HPLC analysis (Figure 4B) that showed the pink/red zone on plate assay of L-asparaginase (Figure 4C).

3.5 Biophysical and Biochemical Characterization of L-asparaginase

Purified L-asparaginase exhibited an optimum temperature of 60 °C (Figure 5A) under an acidic condition of pH 6.0 (Opt. pH) (Figure

Table 4 Fractional precipitation and purification of L-asparaginase.

Fractions (F)	Acetone fractions (%)	L-asparaginase activity (nM/min)	Protein concentration (mg)	Specific L-asparaginase activity (nM/min/mg)
Total soluble protein (TSP)	Nil	842.22 ±1.31	3.8	221.63 ±1.23
F1.	0-20%	102.22 ±2.13	0.2	511.11 ±2.01
F2.	20-40%	468.00±1.85	1.1	425.45 ±1.87
F3.	40-60%	351.11±1.63	0.48	731.48 ±1.66
F4.	60-80%	796.89±1.87	0.68	1171.89±1.98
F5.	80-100%	66.67 ±1.54	0.43	155.04 ±1.55

Here ± indicates standard deviation (SD); Experiments were carried out in triplicates to calculate SD

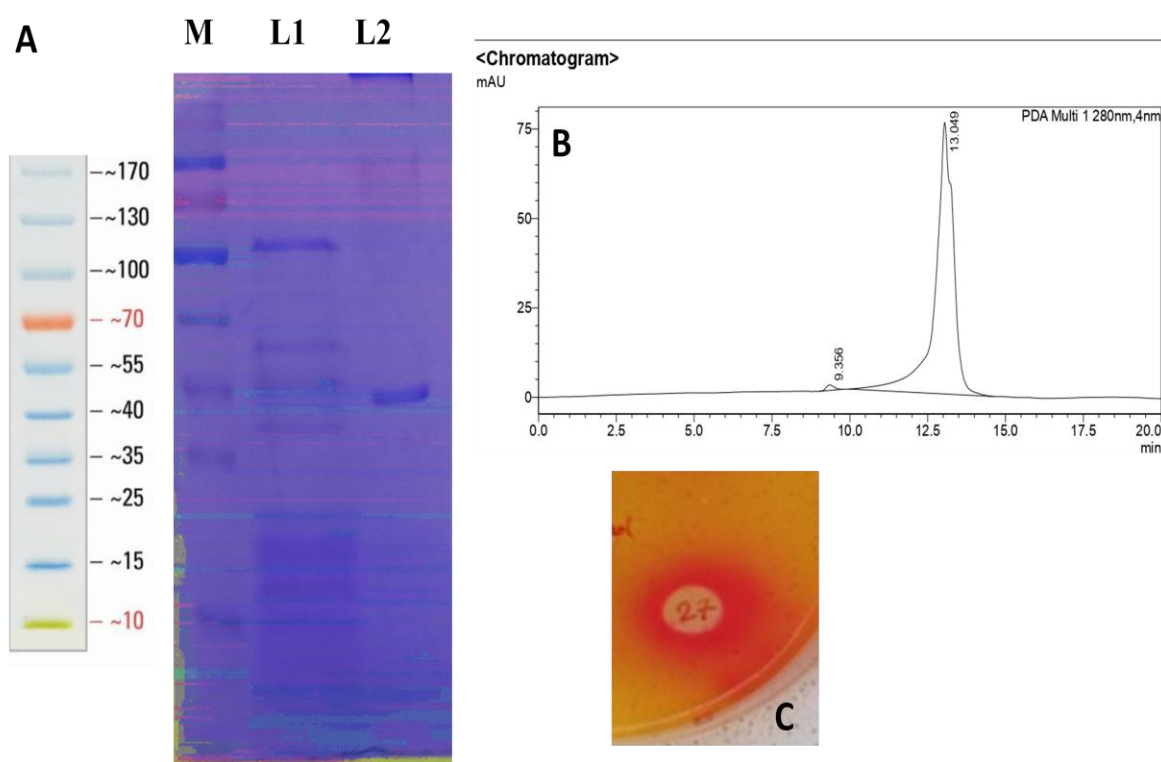


Figure 4 (A) SDS-PAGE analysis of extracellular L-asparaginase of *P. aeruginosa* CS4, where M, L1, and L2 can be defined as protein ladder (Thermo Scientific™ PageRuler™), total precipitated protein, and purified L-asparaginase enzyme, (B) HPLC analysis of the purified L-asparaginase enzyme, (C) Confirmation of purified L-asparaginase enzyme activity on L-asparagine containing agar plate

5B). The enzyme exhibited adequate stability at 50°, 60°, and 70 °C for 180 min (Figure 5C). The enzyme retained almost 50% activity at 80 °C after 3 hrs. Similarly, the purified L-asparaginase was stable at a broader pH scale from 4 to 8. The enzyme could hold greater than 60% activity even after 40 hours under pH 4.0 and 5.0 acidic conditions. However, at neutral pH, the L-asparaginase enzyme lost 50% activity at 40 hrs. In alkaline pH, the enzyme was comparatively less stable over the neutral and acidic conditions (Figure 5D). The enzymes retained > 90% activity in the presence of detergents and were slightly stimulated by adding 10% SDS.

Negligible inhibition was observed in L-asparaginase activity in the presence of EDTA (Table 5).

3.6 Glutaminase activity

The enzyme also exhibited significant glutaminase (419.5±1.55 nM/min; 81.20%) under assay conditions of pH 6.0 and temperature of 60 °C. Other protein-based substrates, such as casein and keratin, showed no activity towards L-asparaginase (Table 6).

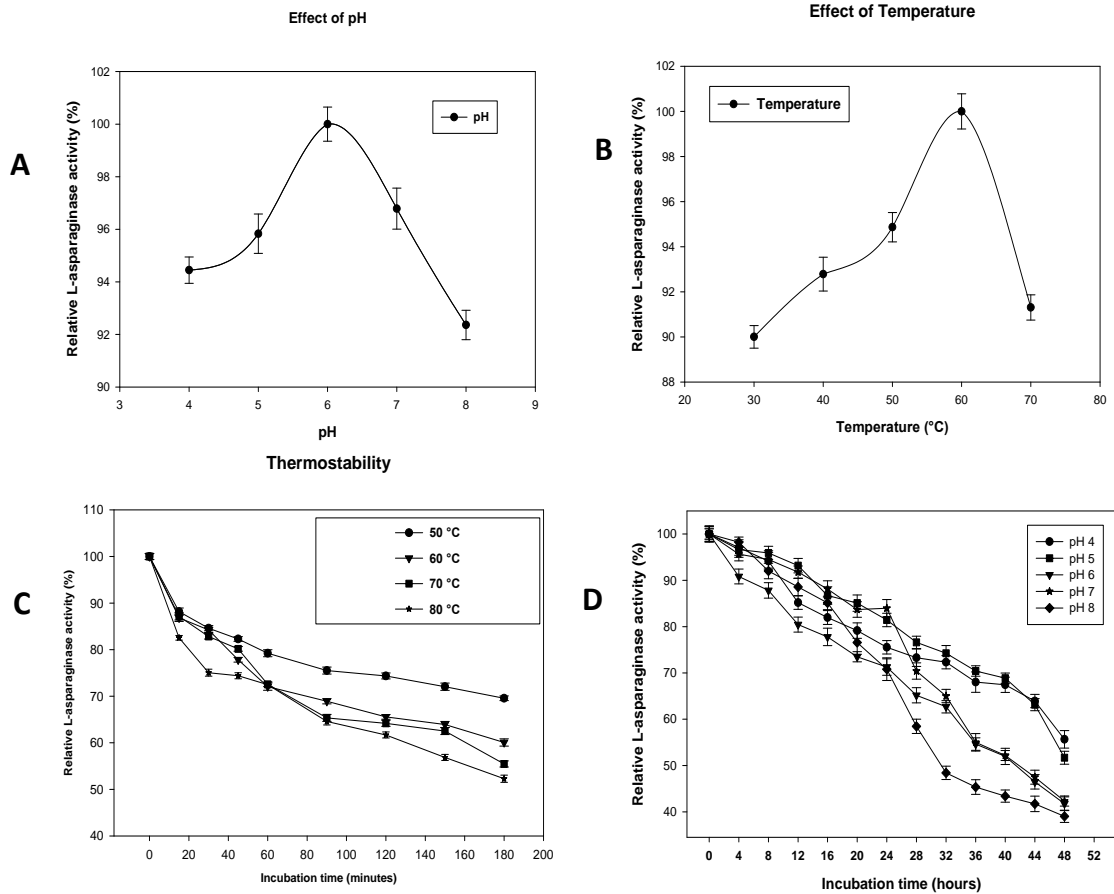


Figure 5 Biophysical characterization of L-asparaginase enzyme for determining optimum (A) pH, (B) optimum temperature, (C) thermostability, and (D) pH stability

Table 5 Effect of modulators on L-asparaginase activity.

S. No.	Modulators	Residual Enzyme activity (%)
1.	Control	100
2.	1% Tween 20	93.13 ± 1.73
3.	1% Tween 80	91.55 ± 1.89
4.	5% SDS	99.07 ± 2.32
5.	10% SDS	104.57 ± 1.45
6.	1mM EDTA	95.15 ± 1.03

Here ± indicates standard deviation (SD); Experiments were carried out in triplicates to calculate SD

Table 6 Effect of substrates on L-asparaginase activity.

S. No.	Modulators	Residual Enzyme activity (%)
1.	L-asparagine	100 ± 2.02
2.	Glutamine	81.20 ± 1.55
3.	Casein	0
4.	Keratin	0

Here ± indicates standard deviation (SD); Experiments were carried out in triplicates to calculate SD

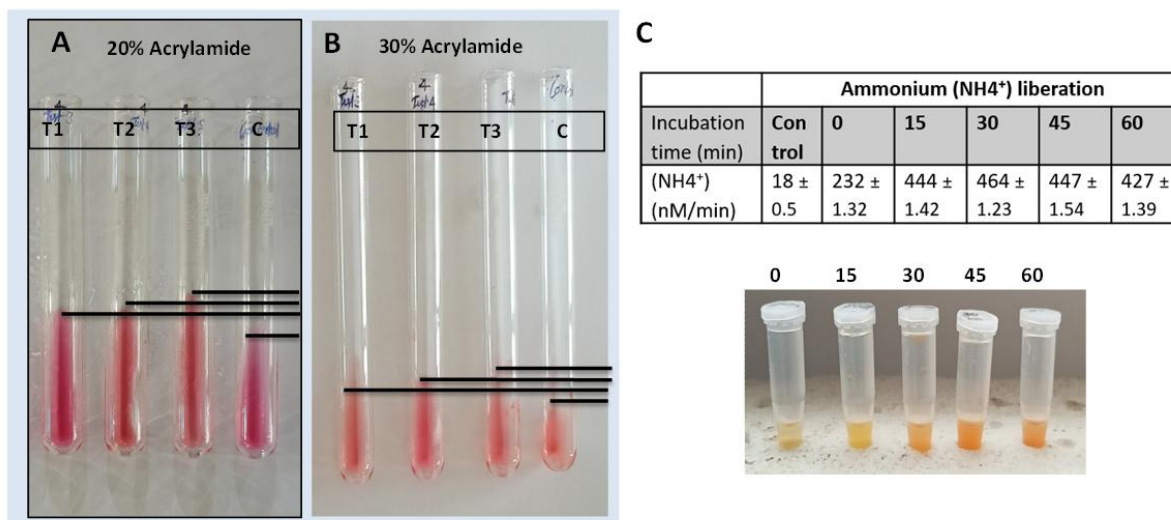


Figure 6 A and B Applications of L-asparaginase of *P. aeruginosa* CSPS4 in inhibition of acrylamide gel polymerization and (C) acrylamide degradation in fried-potato chips

3.7 Applications of L-asparaginases

3.7.1 inhibition of acrylamide polymerization

The purified L-asparaginase showed inhibition in gel polymerization at both the concentrations of acrylamide (20% and 30%) tested. It was observed by visualizing the enhanced flow of gel at varying concentrations of L-asparaginase (Figure 6A and 6B).

3.7.2 Acrylamide degradation in potato chips

The liberation of ammonia was detected in the potato chips in the presence of L-asparaginase over the control groups (Figure 6C). L-asparaginase showed a maximum liberation of 464 ± 1.23 nM/min after 30 min in potato chips.

4 Discussion

L-asparaginase belongs to one of the important biotechnological groups of therapeutic and industrial enzymes that share 40% of global sales of enzymes (Qeshmi et al. 2022). Due to the potential to hydrolyze L-asparagine (an essential amino acid), the enzyme has been successfully employed for destroying leukemia cells (Osama et al. 2023). Recent investigations have also reported the role of the enzyme in treating human neoplastic cells (Alrumman et al. 2019). However, most of the available L-asparaginase also exhibits glutaminase activity along with L-asparaginase activity (EI-Bessoumy et al. 2004; EI-Sharkawy et al. 2016). Glutaminase has several side effects, such as enhanced hypersensitivity, immunogenic response, and coagulation abnormalities (Duval et al. 2002; Mahajan et al. 2014). Therefore, pharmaceutical industries demand glutaminase-free L-asparaginase enzymes.

Streptomyces olivaceus NEAE-119 (EI-Naggar et al. 2015), *Erwinia carotovora* subsp. *Atroseptica* SCRI 1043 (Goswami et al. 2015), *Pectobacterium carotovorum* MTCC 1428 (Kumar et al. 2017) and *Bacillus paralicheniformis* (Mahajan et al. 2014) are the names of a few bacterial sources that show glutaminase free L-asparaginase activity. Recently, *Pseudomonas* spp. has gained attention for harnessing L-asparaginase activity (Badoei-Dalfard 2015; Fatima et al. 2019; Kumar et al. 2022). In the present investigation, a strain of *P. aeruginosa* was isolated from soil samples of poultry slaughter regions exhibiting L-asparaginase activity. Amany et al. (2021) reported several L-asparaginase producers from fish, meat, and egg sources (Amany et al. 2021). Similarly, a potential anticancer activity was reported from L-asparaginase of the *P. aeruginosa* strain. Several Gram-negative bacteria have been shown to produce L-asparaginase activity (Kamble et al. 2012; Managamuri et al. 2017; Brumano et al. 2019). However, most of the *Pseudomonas*-derived L-asparaginase also exhibit L-glutaminase activity (Brumano et al. 2019; Kumar et al. 2022). This was consistent with our findings too, where reduced L-glutaminase activity was observed in the asparaginase of *P. aeruginosa* CSPS4 strain. Moreover, these strains were reported to produce extracellular L-asparaginase, followed by their OVAT approach production. The present study enhanced the extracellular enzyme using the OVAT approach, where a ~2-fold increase was observed. Nutrient source Sucrose (3%) and peptone (1%) showed maximum L-asparaginase production at 37 °C under acidic pH 6.0 after 48 hrs of incubation (Table 1). Very similar parameters were reported to produce L-asparaginase from another *P. aeruginosa* strain, where 1% (w/v) asparagine and glucose were reported for the maximum productivity after 48 hrs incubation at 35 °C (Amany et al. 2021). Statistical optimization using PB and Response Surface Methodology (RSM) is always beneficial to

understand the interaction among the physical and chemical parameters for enhancing the production of enzymes (Sharma and Satyanarayana 2011; Joshi and Satyanarayana 2015; Talluri et al. 2019). Here, the results of this study observed maximum L-asparaginase production from 19.55 ± 2.77 nM/min (4th run) to 521.33 ± 4.07 nM/min units (10th run) during the PB analysis. Further, the study's results revealed that pH, sucrose, and peptone significantly interacted significantly in enhanced L-asparaginase production. It was also found that the OVAT approach was comparable in L-asparaginase activity to the PB design in this case. It may be due to the temperature (25 °C) and pH (8.0) that do not support the maximal production of the enzyme as optimized through the OVAT approach. However, a significant difference in the range of L-asparaginase production under varying conditions (runs) suggests the influence of physicochemical parameters on enzyme production. Sharma and Satyanarayana (2011) successfully used statistical optimization to enhance the production of acidic amylase from *Bacillus acidicola* PB analysis showed the influence of media components and physical parameters on L-asparaginase production from *Acinetobacter baumannii* ZAS1 (Abhini et al. 2022).

Purified L-asparaginase from *P. aeruginosa* CSPS4 strain showed a molecular weight of ~35 kDa. Qeshmi et al. (2022) reported a similar molecular weight of ~35 kDa of a recombinant L-asparaginase from *P. aeruginosa* HR03 (Qeshmi et al. 2022). It was consistent with the recombinant L-asparaginase of *P. aeruginosa* CSPS4 (Kumar et al. 2024). However, L-asparaginase of *P. aeruginosa* WCHPA075019 (Amany et al. 2021) and *P. aeruginosa* 50071 (EI-Bessoumy et al. 2004) showed a higher molecular weight L-asparaginases of 123 kDa and 160 kDa, respectively. Kumar et al. (2022) also reported a high molecular mass L-asparaginase of 148.0 kDa from *Pseudomonas* sp. PCH44 (Kumar et al. 2022), however, it was unveiled as a homo-tetrameric protein of molecular weight of 37 kDa. In another report, a homo-hexamer of L-asparaginase of ~205 kDa was observed on native PAGE that was identified as a monomeric protein of ~34 kDa on SDS-PAGE (Husain et al. 2016). It suggests that *Pseudomonas* spp. harbor a wide variety of L-asparaginases that may exhibit homomeric forms. On the physiological characterization of purified L-asparaginase from *P. aeruginosa* CSPS4, the optimum pH and temperature of the enzyme were 6.0 and 60 °C. These properties render this enzyme unique from the other available L-asparaginases from *Pseudomonas* spp. and categorize it as a thermo-acidophilic L-asparaginase. It was further confirmed at the molecular level by cloning and expressing the L-asparaginase encoding gene (*rAsn_PA*) of *P. aeruginosa* CSPS4 (Kumar et al. 2024). To the best of our information, only one thermo-acidophilic L-asparaginase has been reported from *P. aeruginosa* that exhibits optimum pH and temperature at an acidic pH of 5.0 and temperature of 50 °C (Badoei-Dalfard 2015).

Comparable properties in another L-asparaginase (T_{opt} : 60 °C and pH_{opt} : 5.6) were also observed; however, it was from a fungal strain *Aspergillus tubingensis* SY1 (Yahya et al. 2016). Most of the *Pseudomonas*-derived L-asparaginases exhibit optimum activity at neutral pH (Fatima et al. 2019; Amany et al. 2021; Kambe et al. 2012). Alkaline L-asparaginases have also been reported from various species of *Pseudomonas* (Qeshmi et al. 2022; EI-Bessoumy et al. 2004; Kumar et al. 2022). Most of the L-asparaginase cluster was recorded at the optimum temperature of 37 °C (EI-Bessoumy et al. 2004; Fatima et al. 2019; Brumano et al. 2022). The enzyme reported in the present investigation showed the optimum temperature at 60 °C. L-asparaginase from *Pseudomonas* sp. PCH44 and *P. aeruginosa* HR03; however, they showed optimum activity at 45 °C and 40 °C, respectively. L-asparaginase from *P. aeruginosa* CSPS4 was stable at higher temperature ranges of 50 °C to 80 °C even after 3 hrs of incubation. These properties find the applicability of this enzyme in pharmaceutical and starch-based food industries. L-asparaginase of *P. aeruginosa* HR03 was also thermostable at 40-90 °C (Qeshmi et al. 2022). This enzyme could hold 50% of its activity at 90 °C after 10-min of incubation. Similarly, 76.53% of L-asparaginase activity was retained at 45 °C after 120 min of incubation from *Pseudomonas* sp. PCH44 (Kumar et al. 2022). In addition to thermostability, L-asparaginase from *P. aeruginosa* CSPS4 also showed stability at a broad pH range (4 to 8). The enzyme retained better stability under acidic pH compared to the alkaline conditions which makes this enzyme suitable for different biotechnological applications. Only a handful of reports are available that discuss the pH stability of L-asparaginase from *Pseudomonas* spp. (Qeshmi et al. 2022). For example, L-asparaginase of *Pseudomonas aeruginosa* HR03 retained 52% and 60% residual activity at pH 4.0 and 11.0, respectively (Qeshmi et al. 2022). Modulators showed a marginal effect on L-asparaginase activity in this investigation. The enzyme was able to retain 90% activity in the presence of detergents (SDS and Tween) which confirm the suitability of this enzyme in pharmaceutical industries. Besides, a non-significant inhibition was recorded in L-asparaginase activity in the presence of EDTA. *P. aeruginosa* WCHPA075019-derived L-asparaginase was also not inhibited by EDTA (Amany et al. 2021). It indicates that this L-asparaginase lacks metals in its structure and does not belong to the group of metalloenzymes. However, Ps44-ASNase II of *Pseudomonas* spp. PCH44 was strongly inhibited by EDTA (Kumar et al. 2022), suggesting diversity among L-asparaginase of *Pseudomonas* spp.

Due to the hydrolysis ability of amide groups, L-asparaginase of the present investigation was successfully employed to hydrolyze acrylamide. Here, we first report for assessing the L-asparaginase activity in acrylamide hydrolysis from a *P. aeruginosa* strain. A significant delay was observed in acrylamide gel polymerization as compared to the control, where immediate solidification was

observed. Mahajan et al. (2014) also reported a delayed polymerization of acrylamide gel by using L-asparaginase of *B. licheniformis* (Mahajan et al. 2014). The associated application of acrylamide reduction was also performed in fried potato chips. Here, acrylamide degradation was observed indirectly by estimating the liberation of ammonia in the enzyme-treated fried potato chips. L-asparaginase of *P. oryzae* has also been reported to reduce the acrylamide levels in fried potato slices (Bhagat et al. 2016). The permissible limit of acrylamide in food ranges from 13.76-71.13 g for fried snack foods and 12.97- 93.88 gm for baked food items for a person of average weight of 57 Kg (WHO). However, acrylamide concentration in snack foods ranges from 371.56 µg/kg to 6391.73 µg per kg, which is quite high and keeps humans at high health risks. Therefore, pretreatment of starch-based fried food products with L-asparaginase must be strictly implemented.

Conclusion

The study resulted in identification of a novel thermo-acidophilic L-asparaginase from *P. aeruginosa* strains CS4. The optimum temperature and pH at 60 °C and 6.0, respectively, renders this enzyme novel from other L-asparaginases of *Pseudomonas* spp. Besides, L-asparaginase also exhibits stability under a broad pH range of 4 to 8, indicating its potential applicability in the pharmaceutical and food industries. The enzyme successfully inhibited acrylamide polymerization and degraded acrylamide in commercial fried potato chips. Because of its potential in acrylamide reduction in food products and to meet industrial demands, further studies are required to develop its recombinant version.

Acknowledgement

DV and VK are thankful to Babasaheb Bhimrao Ambedkar University, Lucknow for providing infrastructure and useful resources.

Data Availability Statement

The manuscript has no associated data.

Funding

No funding was received to perform this investigation.

Conflict of Interest

The authors have no financial competing interests to declare

Compliance with Ethical Standards

There is no participation of human and animals or their biological materials; therefore, no ethical approval is required.

Author's Contribution

DV conceived the idea and designed the experiments. VK performed the experimental work and analyzed the data. SJ assisted in media optimization experiments. BK assisted in protein purification and analysis. VK and DV wrote the manuscript. VK, SJ, and DV edited the manuscript. All the authors read and approved the final version of the manuscript.

References

- Abhini, K.N., Rajan, A.B., Fathimathu, Z.K., & Sebastian, D. (2022). Response surface methodological optimization of L-asparaginase production from the medicinal plant endophyte *Acinetobacter baumannii* ZAS1. *Journal of Genetic Engineering and Biotechnology*, 20 (1), 1-13. doi: 10.1186/s43141-022-00309-4.
- Ali, U., Naveed, M., Ullah, A., Ali, K., Shah, S.A., Fahad, S., & Mumtaz, A.S. (2016). L-asparaginase, as a critical component to combat acute lymphoblastic leukemia (ALL): A novel approach to target ALL. *European Journal of Pharmacology*, 77 (1), 199-210. doi.org/10.1016/j.ejphar.2015.12.023.
- Alrumman, S.A., Mostafa, Y.S., Al-Izran, K.A., Alfaifi, M.Y., Taha, T.H., Elbehairi, S.E. (2019). Production and anticancer activity of aL-Asparaginase from *Bacillus licheniformis* isolated from the red sea, Saudi Arabia. *Scientific Reports*, 6, 3756. doi.org/10.1038/s41598-019-40512-x.
- Amany, B., Abd El-Aziz, Wesam, A., Hassanein Zakaria, A., Mattar, Rabab, A., & El-Didamony (2021). Production of chemotherapeutic agent L-asparaginase from gamma-Irradiated *Pseudomonas aeruginosa* WCHPA075019. *Jordan journal of Biological Sciences*, 14, 403-412. doi.org/10.54319/jjbs/140304.
- Badoei-Dalfard, A. (2015). Purification and characterization of L-asparaginase from *Pseudomonas aeruginosa* strain SN004: production optimization by statistical methods. *Biocatalysis and Agricultural Biotechnology*, 4, 388-397. doi.org/10.1016/j.bcab.2015.06.007.
- Batool, T., Makky E.A., Jalal, M., & Yusoff, M.M. (2016). A comprehensive review on L-asparaginase and its applications. *Applied biochemistry and biotechnology*, 178, 900-923. doi:10.1007/s12010-015-1917-3.
- Bhagat, J., Kaur, A., & Chadha, B.S. (2016). Single step purification of asparaginase from endophytic bacteria *Pseudomonas oryzae* exhibiting high potential to reduce acrylamide in processed potato chips. *Food and Bioprocess Technology*, 99, 222-230. doi.org/10.1016/j.fbp.2016.05.010.
- Brumano, L.P., da Silva, F.V.S., Costa-Silva, T.A., Apolinário, A.C., Santos J.H.P.M., et al. (2019). Development of L-

- Asparaginase Biobetters: current research status and review of the desirable quality profiles. *Frontiers in Bioengineering and Biotechnology*, 6, 212. doi.org/10.3389/fbioe.2018.00212.
- Brumano, L.P., Moguel, I.S., Yamakawa, C.K., Pessoa, A.Jr., & Mussatto, S.I. (2022). Selection and optimization of medium components for the efficient production of L-asparaginase by *Leucosporidium scottii* L115—A Psychrotolerant Yeast. *Fermentation*, 8, 398. doi.org/10.3390/fermentation8080398.
- Dipali, P., & Ajit, P. (2012). Characterization of amylase producing bacterial isolates. *Pharmaceutical Life Science*, 1, 42–47. doi.org/10.1155/2021/5592885.
- Doriya, K., & Kumar, D.S. (2016) Isolation and screening of L-asparaginase free of glutaminase and urease from fungal sp. 3 *Biotech*, 6, 239.
- Duval, M., Suci, S., Ferster, A., Riolland, X., Nelken, B., et al. (2002). Comparison of *Escherichia coli*-asparaginase with *Erwinia*-asparaginase in the treatment of childhood lymphoid malignancies: results of a randomized European Organization for Research and Treatment of Cancer-Children's Leukemia Group phase 3 trial. *Blood*, 99, 2734–2739. doi.org/10.1182/blood.V99.8.2734.
- El-Bessoumy, A.A., Sarhan, M., & Mansour, J. (2004). Production, isolation, and purification of L-asparaginase from *Pseudomonas aeruginosa* 50071 using solid-state fermentation. *Korean Society for Biochemistry and Molecular Biology. BMB Reports*, 37, 387-393. doi.org/10.5483/BMBRep
- El-Naggar, N.E.A., Moawad, H., El-Shweihy, N.M. et al (2019). Process development for scale-up production of a therapeutic L-asparaginase by *Streptomyces brolllosae* NEAE-115 from shake flasks to bioreactor. *Scientific Reports*, 9, 13571.
- El-Naggar, Nel-A., Moawad, H., El-Shweihy, N.M., & El-Ewasy, S.M. (2015). Optimization of culture conditions for production of the anti-leukemic glutaminase free L-asparaginase by newly isolated *Streptomyces olivaceus* NEAE-119 using response surface methodology. *BioMed Research International*, 2015 (17). doi.org/10.1155/2015/627031.
- El-Sharkawy, A.S., Farag, A.M., Embaby, A.M., Saeed H., & El-Shenawy, M. (2016) Cloning, expression and characterization of *Pseudomonas aeruginosa* EGYII *L-Asparaginase* from *Pseudomonas aeruginosa* strain EGYII DSM 101801 in *E. coli* BL21(DE3) pLysS. *Journal of Molecular Catalysis B: Enzymatic*, 132, 16-23. doi.org/10.1016/j.molcatb.2016.06.011.
- Fatima, N., Khan, M.M., & Khan, I.A. (2019). L-asparaginase produced from soil isolates of *Pseudomonas aeruginosa* shows potent anticancer activity on HeLa cells. *Saudi Journal of Biological Sciences*, 26, 1146-1153. doi.org/10.1016/j.sjbs.2019.05.001.
- Goswami, R., Hegde, K., & Veeranki, V.D. (2015). Production and characterization of novel glutaminase free recombinant L-asparaginase II of *Erwinia carotovora* subsp. *atroseptica* SCRI 1043 in *E. coli* BL21 (DE3) *British Microbiology Research Journal*, 6, 95-112. DOI: 10.9734/BMRJ/2015/13867
- Husain, I., Sharma, A., Kumar, S., & Malik, F. (2016). Purification and characterization of glutaminase free asparaginase from *Enterobacter cloacae*: in-vitro evaluation of cytotoxic potential against human Myeloid Leukemia HL-60 cells. *PLoS One*, 1811, e0148877. doi.org/10.1371/journal.pone.0148877.
- Jia, R., Wan, X., Geng, X., Xue, D., Xie, Z., & Chen, C. (2021). Microbial L-asparaginase for application in acrylamide mitigation from food: Current research status and future perspectives. *Microorganisms*, 9, 1659.
- Joshi, S., & Satyanarayana, T. (2015). Bioprocess for efficient production of recombinant *Pichia anomala* phytase and its applicability in dephytinizing chick feed and whole wheat flat Indian breads. *Journal of Industrial Microbiology and Biotechnology*, 42, 1389-1400 doi.org/10.1007/s10295-015-1670-1.
- Kamble, K.D., Bidwe, P.R., Muley, V.Y., Kamble, L.H., Bhadange, D.G., & Musaddiq, M. (2012). Characterization of l-asparaginase producing bacteria from water, farm, and saline soil. *Bioscience discovery*, 3, 116-119.
- Kataria, M., Kaur, N., Narula, R., Kumar, K., Kataria, S., & Verma, N. (2015). L-Asparaginase from novel source: *Solanum nigrum* and development of asparagine biosensor. *The Pharma Innovation Journal*, 4, 81.
- Kruger, N.J. (1994). Detection of polypeptides on immunoblots using secondary antibodies or protein A. *Methods in Molecular Biology*, 32, 17–24.
- Kukurova, K., Morales, F.J., Bednářiková, A., & Ciesarová, Z. (2009). Effect of l-asparaginase on acrylamide mitigation in a fried-dough pastry model. *Molecular Nutrition & Food Research*, 53, 1532-1539. doi: 10.1002/mnfr.200800600.
- Kumar, S., Ashish, P.A., Venkata, D.V., & Pakshirajan, K. (2017). Kinetics of growth on dual substrates, production of novel glutaminase-free L-asparaginase and substrates utilization by *Pectobacterium carotovorum* MTCC 1428 in a batch bioreactor. *Korean Journal of Chemical Engineering*, 34, 118-126. doi: 10.1007/s11814-016-0216-1.
- Kumar, S., Darnal, S., Patial, V., Kumar, V., Kumar, S., & Singh, D. (2022). Molecular cloning, characterization, and in-silico

- analysis of L-asparaginase from Himalayan *Pseudomonas* sp. PCH44. *3 Biotech*, *12*, 162. doi.org/10.1007/s13205-022-03224-0
- Kumar, V., Kumar, R., Sharma, S., Shah, A., Chaturvedi, C.P., & Verma, D. (2024) Cloning, expression, and, characterization of a novel thermo-acidophilic l-asparaginase of *Pseudomonas aeruginosa* CS4. *3 Biotech* *14*, 54. doi.org/10.1007/s13205-024-03916-9.
- Li, X., Zhang, X., Xu, S., Xu, M., Yang, T., et al. (2019). Insight into the thermostability of thermophilic L-asparaginase and non-thermophilic L-asparaginase II through bioinformatics and structural analysis. *Applied microbiology and biotechnology*, *103*, 7055-7070. doi.org/10.1007/s00253-019-09967-w.
- Luo, M., Brooks, M., & Wicha, M.S. (2018). Asparagine and Glutamine: Co-conspirators Fueling Metastasis. *Cell Metabolism*, *27*, 947-949. doi: 10.1016/j.cmet.2018.04.012.
- Mahajan, R.V., Kumar, V., Rajendran, V., Saran, S., Ghosh, P.C., & Saxena, R.K. (2014). Purification and characterization of a novel and robust L-asparaginase having low-glutaminase activity from *Bacillus licheniformis*: in vitro evaluation of anti-cancerous properties. *PLoS One*, *6*, 99037.
- Mahajan, R.V., Saran, S., Kameswaran, K., Kumar, V., & Saxena, R.K. (2012). Efficient production of L-asparaginase from *Bacillus licheniformis* with low-glutaminase activity: optimization, scale up and acrylamide degradation studies. *Bioresource Technology*, *125*, 11-6. doi.org/10.1016/j.biortech.2012.08.086.
- Managamuri, U., Vijayalakshmi, M., Ganduri, VSRK., Babu, S., & Poda, S. (2017). Optimization of culture conditions by response surface methodology and unstructured kinetic modeling for L-asparaginase production by *Pseudonocardia endophytica* VUK-10. *Journal of Applied Pharmaceutical Science*, *7*, 42–50. doi: 10.7324/JAPS.2017. 70106.
- Muzuni, Aprilyani, R., Ardiansyah, S., Farij, M., & Gultom, M.T. (2023). Characterization of the type 2 l-asparaginase gene in thermo-halophilic bacterial from *Wawolesea* hot springs, Southeast Sulawesi, Indonesia. *Pakistan Journal of Biological Sciences* *26*, 392-402. doi: 10.3923/pjbs.2023.392.402.
- Osama, S., El-Sherei, M.M., Al-Mahdy, D.A., Bishr, M., Salama, O., & Raafat, M.M (2023). Optimization and characterization of antileukemic L-asparaginase produced by *Fusarium solani* endophyte. *AMB Express*, *13*, 96. doi: 10.1186/s13568-023-01602-2
- Pavlova, N.N., Hui, S., Ghergurovich, J.M., Fan, J., Intlekofer, A.M., et al. (2018). As extracellular glutamine levels decline, asparagine becomes an essential amino acid. *Cell Metabolism*, *6*, 428-438.e5. doi.org/10.1016/j.cmet.2017.12.006.
- Qeshmi, I.F., Homaei, A., Khajeh, K., Kamrani, E., & Fernandes, P. (2022). Production of a Novel Marine *Pseudomonas aeruginosa* recombinant L-asparaginase: Insight on the structure and biochemical characterization. *Marine Biotechnology*, *24*, 599-613. doi.org/10.1007/s10126-022-10129-9.
- Sharma, A., & Satyanarayana, T. (2011). Optimization of medium components and cultural variables for enhanced production of acidic high maltose-forming and Ca²⁺-independent α -amylase by *Bacillus acidicola*. *Journal of Biosciences Bioengineering*, *111* (5), 550-3.
- Shirfrin, S., Parrott, C.L., & Luborsky, S.W. (1974). Substrate binding and inter-subunit interactions in L-asparaginase. *Journal of Biological Chemistry*, *249*, 1335–1340.
- Shrivastava, A., Khan, A.A., Khurshid, M., Kalam, M.A., Jain, S.K., & Singhal, P.K. (2016). Recent developments in L-asparaginase discovery and its potential as anticancer agent. *Critical reviews in oncology/hematology*, *100*, 1-10. doi: 10.1016/j.critrevonc.2015.01.002.
- Simas, R.G., Krebs Kleingesinds, E., Pessoa Junior, A., & Long, P.F. (2021). An improved method for simple and accurate colorimetric determination of l-asparaginase Enzyme Activity Using Nessler's Reagent. *Journal of Chemical Technology & Biotechnology*, *96*, 1326–1332.
- Simpson, D.M., & Beynon, R.J. (2010). Acetone precipitation of proteins and the modification of peptides. *Journal of Proteome Research*, *9*, 444-450. doi: 10.1021/pr900806x.
- Stadler, R.H., Blank, I., Varga, N., Robert F, Hau J, et al. (2002). Acrylamide from Maillard reaction products. *Nature*, *3,449-50*. doi: 10.1038/419449a.
- Talluri, P.V., Lanka, S.S., Rajagopal Saladi, V., & Avicenna, J. (2019). Statistical Optimization of Process Parameters by Central Composite Design (CCD) for an Enhanced Production of L-asparaginase by *Myroides gitamensis* BSH-3, a Novel Species. *Avicenna Journal of Medical Biotechnology*, *11*, 59-66.
- Tripathi, N., & Sapra, A. (2023) Gram Staining. In: Stat-Pearls [Internet]. Treasure Island (FL): StatPearls Publishing.
- Verma, D., & Satyanarayana, T. (2011). An improved protocol for DNA extraction from alkaline soil and sediment samples for constructing metagenomic libraries. *Applied Biochemistry and Biotechnology*, *165*, 454-64. doi: 10.1007/s12010-011-9264-5.
- Vimal, A., & Kumar, A., (2022) L-asparaginase: need for an expedition from an enzymatic molecule to antimicrobial drug.

- International Journal of Peptide Research and Therapeutics*, 28, 9. <https://doi.org/10.1007/s10989-021-10312-x>.
- Williams, S.T., Sharpe, M.E., & Holt, J.G. (1989). *Bergey's Manual of Systematic Bacteriology*. 2nd. Baltimore, MD, USA: Springer Science+Business Media, LLC.
- Xu, F., Oruna-Concha, M.J., & Elmore, J.S. (2016). The use of asparaginase to reduce acrylamide levels in cooked food. *Food chemistry*, 105, 163–171. doi: 10.1016/j.foodchem.2016.04.105.
- Yahya, S., Jahagir, S., Shaukat, S., Sohail, M., & Khan, S. (2016). Production optimization by using Plackett-Burman design and partial characterization of amylase from *Aspergillus tubingensis* SY1. *Pakistan Journal of Botany*, 48., 2557-2561.
- Yan, Y., Kuramae, E.E., Klinkhamer, P.G., & van Veen, J.A. (2015). Revisiting the dilution procedure used to manipulate microbial biodiversity in terrestrial systems. *Applied Environmental Microbiology*, 81, 4246-52.
- Zhou, Y., Jiao, L., Shen, J., Chi, H., Lu, Z., et al. (2022). Enhancing the Catalytic Activity of Type II L-Asparaginase from *Bacillus licheniformis* through Semi-Rational Design. *International Journal of Molecular Sciences*, 23, 9663. doi.org/10.3390/ijms23179663.













Journal of Experimental Biology and Agricultural Sciences

<http://www.jebas.org>

ISSN No. 2320 – 8694

FIRST REPORT ON TRUFFLE-INHABITING FUNGI AND METAGENOMIC COMMUNITIES OF *TUBER AESTIVUM* COLLECTED IN RUSSIA

Ekaterina V. Malygina¹ , Natalia A. Imidoeva¹ , Maria M. Morgunova^{1,2} ,
Maria E. Dmitrieva¹ , Alexander Y. Belyshenko¹ , Anfisa A. Vlasova¹ ,
Victoria N. Shelkovnikova¹ , Tamara Y. Telnova¹ , Alexander S. Konovalov¹ ,
Denis V. Axenov-Gribanov^{1,3,4*} 

¹Irkutsk State University, 664003 Irkutsk, Russia

²Irkutsk National Research Technical University, 664074 Irkutsk, Russia

³GreenTechBaikal, LLC, 664007 Irkutsk, Russia

⁴Mycotech, LLC, 664007 Irkutsk, Russia

Received – January 31, 2024; Revision – February 13, 2024; Accepted – February 27, 2024

Available Online – March 15, 2024

DOI: [http://dx.doi.org/10.18006/2024.12\(1\).16.35](http://dx.doi.org/10.18006/2024.12(1).16.35)

KEYWORDS

Truffle

Tuber aestivum

Microbial community

Symbionts

Fusarium sp.

Clonostachys sp.

Plectosphaerella sp.

Trichothecium sp.

ABSTRACT

Truffles are one of the least studied groups of fungi in terms of their biological and biotechnological aspects. This study aimed to isolate truffle-inhabiting fungi and assess the metagenomic communities of the most common Russian summer truffle, *Tuber aestivum*. This study is the first to characterize the biodiversity of prokaryotic and eukaryotic organisms living in the truffle *T. aestivum* using molecular analysis and sequencing. Plant pathogens involved in a symbiotic relationship with truffles were identified by sequencing the hypervariable fragments of the 16S rRNA and 18S rRNA genes. In addition, some strains of fungal symbionts and likely pathogens were isolated and recognized for the first time from the truffles. This study also compared and characterized the general diversity and distribution of microbial taxa of *T. aestivum* collected in Russia and Europe. The results revealed that the Russian and European truffle study materials demonstrated high similarity. In addition to the truffles, representatives of bacteria, fungi, and protists were found in the fruiting bodies. Many of these prokaryotic and eukaryotic species inhabiting truffles might influence them, help them form mycorrhizae with trees, and regulate biological processes. Thus, truffles are interesting and promising sources for modern biotechnological and agricultural studies.

* Corresponding author

E-mail: denis.axengri@gmail.com (Denis V. Axenov-Gribanov)

Peer review under responsibility of Journal of Experimental Biology and Agricultural Sciences.

Production and Hosting by Horizon Publisher India [HPI]
(<http://www.horizonpublisherindia.in/>).
All rights reserved.

All the articles published by [Journal of Experimental Biology and Agricultural Sciences](#) are licensed under a [Creative Commons Attribution-NonCommercial 4.0 International License](#) Based on a work at www.jebas.org.



1 Introduction

Truffles belong to the group of hypogean (underground) ascomycetes. This order includes approximately 80–220 species characterized by underground fruiting bodies, usually truffles (Leonardi et al. 2021a). The fruiting bodies of truffles have a round or tuber-like shape, and their texture can be fleshy or cartilaginous. Depending on the species, truffles can vary in size from that of a hazelnut to that of a large potato. The outer part of the truffle forms a skin layer called the peridium, which can be smooth, cracked, or covered with large polyhedral tubercles. When cut, the fleshy tissue inside the truffle has a distinct marbled pattern with alternating light and dark (Taschen et al. 2022). The asci, which contain spores, are located inside the fruiting body on internal veins, forming a layer similar to the hymenium. The asci can also be distributed in a nest-like pattern within the truffle, a characteristic trait. The shape of the asci can be spherical, broadly oval, club-shaped, sac-shaped, or sometimes cylindrical. They can contain one, two, four, or eight spores (Ljubojević et al. 2022). The ascospores are always unicellular, colourless or brown, and globular or elliptical. One ascus can reach 0.08 mm in size, while the spores can reach 0.02 mm under normal conditions. The surfaces of truffles are typically rough or spiky. Spores are released passively when the ascocarp is destroyed or when the truffle is consumed by an animal (Thomas and Thomas 2022).

Truffles obligatorily form mycorrhizae, and they grow near taller plants. Typically, black truffles such as *Tuber melanosporum* and *T. aestivum* grow in forests with deciduous trees such as oak, beech, hornbeam, and hazel. These trees and special soil types provide favourable conditions for truffle growth (Vlahova 2021). White truffles, such as *T. magnatum*, grow in forests with birch, poplar, elm, lime, willow, mountain ash, and hawthorn trees (Leonardi et al. 2021b). Truffles also form mycorrhizae with juniper, fir, and pine trees (Allen and Bennett 2021).

Among the truffles with practical value, the most valuable and important is the black French truffle, which is related to *T. melanosporum* (Perigord truffle) (Oliach et al. 2022). The aroma, taste, and biomedical value of true black truffles drive a constant high demand for these mushrooms (Dogan 2021). Moreover, many pharmaceutical and cosmetic companies produce products with black truffle extracts.

Currently, in the agricultural field, there is an increasing demand to understand the connections between the bacterial communities associated with the ascomata of *Tuber* spp. and those found in the surrounding soils. Additionally, there is a need to investigate the unique microbial diversity present in areas where truffles are cultivated and harvested (Sillo et al. 2022). Due to the symbiotic nature of truffles, artificial growth and planting are complicated compared with these processes for other gastronomic fungi.

Microbial communities associated with truffles have been characterized using different microbiological and molecular ecological methods (Perlińska-Lenart et al. 2020a; Bragato et al. 2021). Such studies have focused mainly on bacteria and rarely on the yeasts and fungi inhabiting *T. magnatum*, *T. melanosporum*, *T. borchii*, and *T. aestivum*; therefore, the fungi and bacteria inhabiting truffles are less characterized. Researchers worldwide do not agree that each truffle species has its unique microbiome. Some studies have shown that the symbiotic composition of truffle mushrooms correlates with the microbiological composition of the soil in which they grow (Liu et al. 2021a). This study aimed to isolate truffle-inhabiting fungi and assess the metagenomic communities of the most common summer truffle (*Tuber aestivum*) collected in Russia.

2 Materials and Methods

2.1 Sampling and description of true truffles

The summer truffle (*Tuber aestivum*) has a large fruiting body, up to the size of a chicken's egg. The shape is irregularly rounded. The peridium is covered with large, hard, slightly striped polyhedral tubercles with black–brown colouring. The gleba of *T. aestivum* is yellowish-white, light brown, or chocolate-coloured when heated. The growth of the fruiting bodies is shallow (near the ground surface), sometimes even in the foliage or under oak, beech, birch, pine, and hazel trees, and especially under hornbeams in clay-lime soil. Because *T. aestivum* is on the Red List of Threatened Species of the Russian Federation, so, permission from the Federal Service for Supervision of Natural Recourses was obtained for this study (Permission No. 183, 70A-10-04-GU/10015 on 23/09/2022).

For this study, truffles ranging in size from 3 to 5 cm were collected in a hornbeam forest in the Matsesta area (Sochi, Krasnodar region, Russia). The humus-calcareous and podzolic yellow earth soil types are predominant in this area. During sampling, the pH ranged from 6.0 to 7.0, and the air temperature ranged from 20 to 27 °C. The fruiting bodies of the truffles were found in August with the help of trained truffle-hunting dogs and were collected using a rake to keep them intact. Then, the truffles were transferred to Irkutsk by air post under temperature-controlled conditions at 6–10 °C, along with some soil and rice to avoid putrefaction.

Truffle dissection and spore microscopy were carried out in the laboratory. The fruiting bodies of the truffles were cleaned with a soft toothbrush and then sterilized with 70% ethyl alcohol. Then, the truffles were fractured, and pieces of the gleba were collected for microbiological and metagenomic analysis. For microscopic analysis, a piece of gleba was homogenized and crushed between glass layers. Observations were made using an immersion system at a magnification of 1000× on a bright-field microscope (Mikromed-3–20, Russia, Saint Petersburg) equipped with a digital camera.

2.2 Isolation of nucleic acids, sequencing, and phylogenetic analysis

Two to five pieces of the gleba were dissected from each truffle. Each piece was approximately 0.5 × 0.5 × 0.5 cm in size. The biomaterials were homogenized in TE buffer (10 mM Tris-HCl, 1 M EDTA) and transferred to BioSpark LLC (Russia, Moscow) for DNA isolation, sequencing, and basic bioinformatic analysis.

Total DNA was extracted using a DNeasy Plant Mini Kit (Art. 6910, Qiagen, Germany, Hilden). Fragments of the 16S rRNA gene containing the hypervariable regions V3–V4 were amplified using a mixture of eubacterial primers. The fungal internal transcribed spacer was amplified using primers for the hypervariable ITS2 region of the 18S rRNA gene. The amplification was performed in 25 µL of a mixture containing 5x KTN-mix (Evrogen, Russia, Moscow) (5 µL), primer mix (2 µL), and 50x SYBR (0.5 µL) in a real-time amplifier CFX96 Touch (Bio-Rad, USA, CA). The nucleotide sequences of the primers and the amplification program are presented in Table 1.

Then, the libraries were synthesized for sequencing. Amplification of the PCR products obtained at the first stage for the purpose of barcoding (indexing) the libraries was carried out in 25 µL of a mixture containing 5x KTN mix (5 µL), the primer mixture (2 µL), and 50x SYBR (0.5 µL) in a real-time amplifier under the following conditions: primary denaturation for 3 min at 95 °C; 7 cycles of denaturation for 30 s at 95°C, annealing for 30 s at 55°C,

and elongation for 30 s at 72°C; and a final elongation for 5 min at 72 °C. The Nextera Index Kit was used for amplification with the indices recommended by the manufacturer (Illumina, USA, San Diego).

Sequencing was performed on the Illumina platform. After the second stage, the amplicons were purified using AMPure XP magnetic particles (Kapa Biosystems, United Kingdom, London) at the ratios of 1:0.6 for purification of the PCR products of the 16S rRNA genes and 1:0.7 for purification of the PCR products using primers for amplification of the hypervariable ITS2 region of the 18S rRNA gene. These purified amplicons are ready-made libraries for multiplex sequencing on the Illumina platform. The libraries were mixed and brought to a total concentration of 2 nM. Next, 5 µL of 0.2 M NaOH was added to 5 µL of the mixture and incubated for 5 min. Then, 990 µL of HTI and 1 µL of 12.5 mM pre-denatured PhyX (Kapa Biosystems, United Kingdom, London) were added to the denatured DNA. Library sequencing was performed on the Illumina MiSeq next-generation sequencer using the paired-end read method, generating at least 10,000 paired reads per sample and using reagents from the MiSeq Reagent Nano Kit v2 and the MiSeq v2 Reagent Kit (Illumina, USA, San Diego) (500 cycles PE).

The obtained sequencing data were processed using QIIME 1.9.1. The program included alignment of the forward and reverse reads and deletion of the technical sequences. Sequences with low quality (less than Q30) and chimeric sequences were removed. The

Table 1 Mixture of primers used for sequencing metagenomic communities

Type of primer	Name	Sequence 5'–3'	Concentration µM	Amplification program
Amplification of the hypervariable region V3-V4 of the 16S rRNA gene				
F	GPro341F	CCTACGGGNBGCASCAG	0.625	95 °C for 3 min (initial denaturation); 95 °C for 30 s, 57 °C for 30 s, 72 °C for 30 s (35 cycles); 72 °C for 5 min (final extension step)
R	GPro806R	GGACTACNVGGGTWTCTAATCC	0.625	
F	NR_16_341F1	TCGTCGGCAGCGTCAGATGTGTATAAGAGA CAGTGCCTACGGGNBGCASCAG	2.5	
F	NR_16_341F2	TCGTCGGCAGCGTCAGATGTGTATAAGAGA CAGCTGCCTACGGGNBGCASCAG	2.5	
F	NR_16_341F3	TCGTCGGCAGCGTCAGATGTGTATAAGAGA CAGTCTGCCTACGGGNBGCASCAG	2.5	
R	NR_16_806R1	GTCTCGTGGGCTCGGAGATGTGTATAAGAG ACAGCCGGACTACNVGGGTWTCTAATCC	2.5	
R	NR_16_806R2	GTCTCGTGGGCTCGGAGATGTGTATAAGAG ACAGACCGACTACNVGGGTWTCTAATCC	2.5	
R	NR_16_806R3	GTCTCGTGGGCTCGGAGATGTGTATAAGAG ACAGAACCGACTACNVGGGTWTCTAATCC	2.5	
Amplification of the hypervariable region ITS2 of the 18S rRNA gene				
F	NR_5.8SR	TCGTCGGCAGCGTCAGATGTGTATAAGAG ACAGATCTCGATGAAGAACGCAGCG,	5	95 °C for 3 min (initial denaturation); 95 °C for 30 s, 55 °C for 30 s, 72 °C for 30 s (7 cycles); 72 °C for 5 min (final extension step).
R	NR ITS4R	GTCTCGTGGGCTCGGAGATGTGTATAAGA GACAGGCATCCTCCGCTTATTGATATGC	5	

Table 2 The list of bacterial phyla associated with *T. aestivum* collected in different countries.

Fungus	Country	Bacterial diversity (%)					Ref.
		Proteobacteria	Bacteroidetes	Firmicutes	Actinobacteria	Others	
<i>Tuber aestivum</i>	Italy	76.5	4.7	5.15	13.65	-	Monaco et al. 2020
	France	88	-	5	-	7	Vahdatzadeh et al. 2019
	Russia	99.8	0.04	0.09	0.01	0.1	

distribution of sequences by taxonomic units was determined using the SILVA database (version 132) and UNITE v8. A classification algorithm for operational taxonomic units (OTUs) with an open reference and a threshold of 97% was used.

The sequences were compared with the known 16S rRNA and ITS gene sequences and analyzed using BLAST. The data obtained from metagenomic analysis of prokaryotic and eukaryotic communities were registered in the NCBI database as Bioproject PRJNA1026823.

The evolutionary relationships among the taxa were inferred using the maximum likelihood method (Tamura and Nei 1993), with *Morchella* sp. (NCBI ID KY462590.1) serving as an outgroup. This analysis involved 41 nucleotide sequences. The final dataset contained a total of 600 positions. Evolutionary analysis was conducted in MEGA X (Kumar et al. 2018). The nucleotide sequences were deposited in the NCBI database under the accession numbers ON398998 and ON391736–ON391740.

2.3 Isolation and molecular identification of *T. aestivum* fungal symbionts

The gleba pieces that were aseptically dissected from the central part of *T. aestivum* were homogenized and plated on solid nutrient media. Nutrient media such as malt and potato–dextrose agar were used to isolate the fungal symbionts from the truffles. The composition of the nutrient media was as follows: the malt agar included malt extract (20 g/L), glucose (20 g/L), peptone (1 g/L), and agar (20 g/L), while the composition of the potato–dextrose agar was potato extract (20 g/L), glucose (50 g/L), peptone (30 g/L), MgSO₄ (5 g/L), K₂HPO₄ (10 g/L), and agar (20 g/L).

Truffle-associated fungal mycelial strains were isolated under thermostatic conditions at 24 °C. Only strains characterized by a white aerial mycelium were collected. Each fungal mycelial colony was transferred into Petri dishes with fresh nutrient media. Then, the isolated fungi were cultivated in liquid nutrient media for DNA isolation. Inoculation of pure cultures was performed in sterile 250–300 mL conical flasks with deflectors with the addition of glass beads. Cultivation was performed under thermostatic conditions at 22–24 °C with constant stirring at 180 rpm on an orbital shaker for 5 days.

The samples were ground using steel balls in a laboratory ball mill to isolate fungal DNA. Next, the potassium acetate method was used for DNA isolation and PCR analysis (Rodríguez et al. 2014). The following primers were used to perform PCR on the obtained fungal DNA samples: ITS5: 5'-GGA AGT AAA AGT CGT AAC AAG-3' (F); ITS7: 5'-ACT CGC CGT TAC TGA GGC AAT-3' (R) (Table 2).

PCR was performed in an automatic amplifier (Biometra, Germany) under the following conditions: denaturation for 5 min at 94 °C (first cycle), annealing for 15 s at 60 °C, and elongation for 40 s and 72 °C (subsequent cycles). The final elongation was performed at 72 °C for 7 min. The total number of cycles was 33. The PCR products were purified using a cleanup kit for purifying DNA from the agarose gel and reaction. The purified PCR products, together with the primers, were sent to Evrogen LLC for sequencing. Nucleotide sequences were sequenced using the Sanger method (Valencia et al. 2013). The contigs were assembled using BioEdit software and then uploaded to the NCBI database for comparison and identification. The nucleotide sequences were aligned with the sequences from the NCBI database that showed the highest similarity using the ClustalW multiple alignment algorithm in the MEGA-11 software package. The evolutionary relationships among the taxa were inferred using the maximum likelihood method (Tamura and Nei 1993), with *Penicillium* sp. (NCBI ID OL838180.1) serving as an outgroup. The phylogenetic tree was constructed with 1000 bootstrap replicates. Bootstrap support values above 70% are indicated in the figures. The nucleotide sequences of truffle-inhabiting fungi were deposited in the NCBI database under accession numbers ON386018.1 - ON386020.1, OR335550, and OR335570.

2.4 Statistical analysis

Metagenomic analysis was performed for 6 fruiting bodies of *T. aestivum*. Mean data ± standard deviations are presented in the study. The Shannon diversity index was calculated using QIIME.

3 Results

3.1 Phylogenetic characterization of the truffles collected in Russia

Tuber aestivum, sampled for this study near Sochi, was grown in a hornbeam forest in the Matsesta area (Figure 1). The fruiting bodies and spores of *T. aestivum* are shown in Figure 2.



Figure 1 Photographs of the sampling location; left – *Tuber aestivum* found in leaf litter; right – Hornbeam forest in the Matsesta region, Sochi, Russia 43.57187 N, 39.80306 E

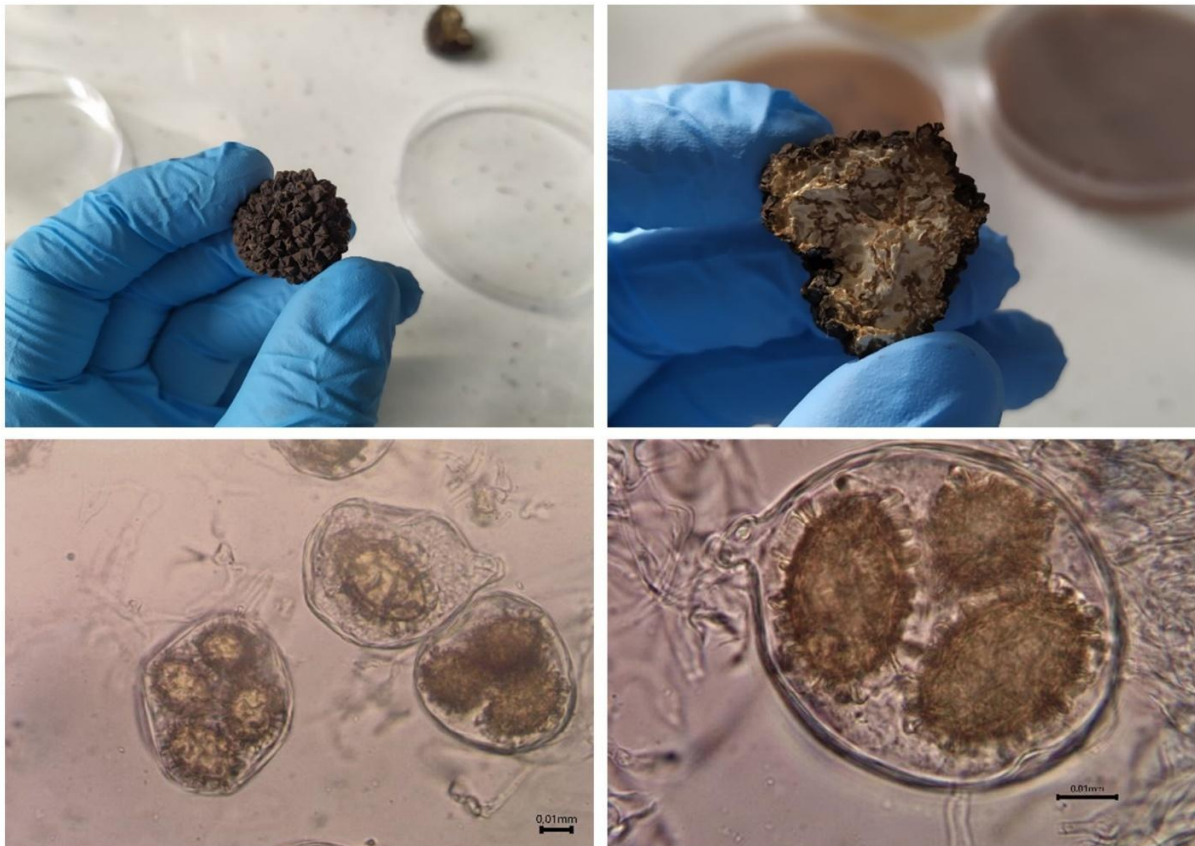


Figure 2 Images of the fruiting body (top) and spores in asci (bottom) of *T. aestivum* used in this study (Scale bars = 0.01 mm).

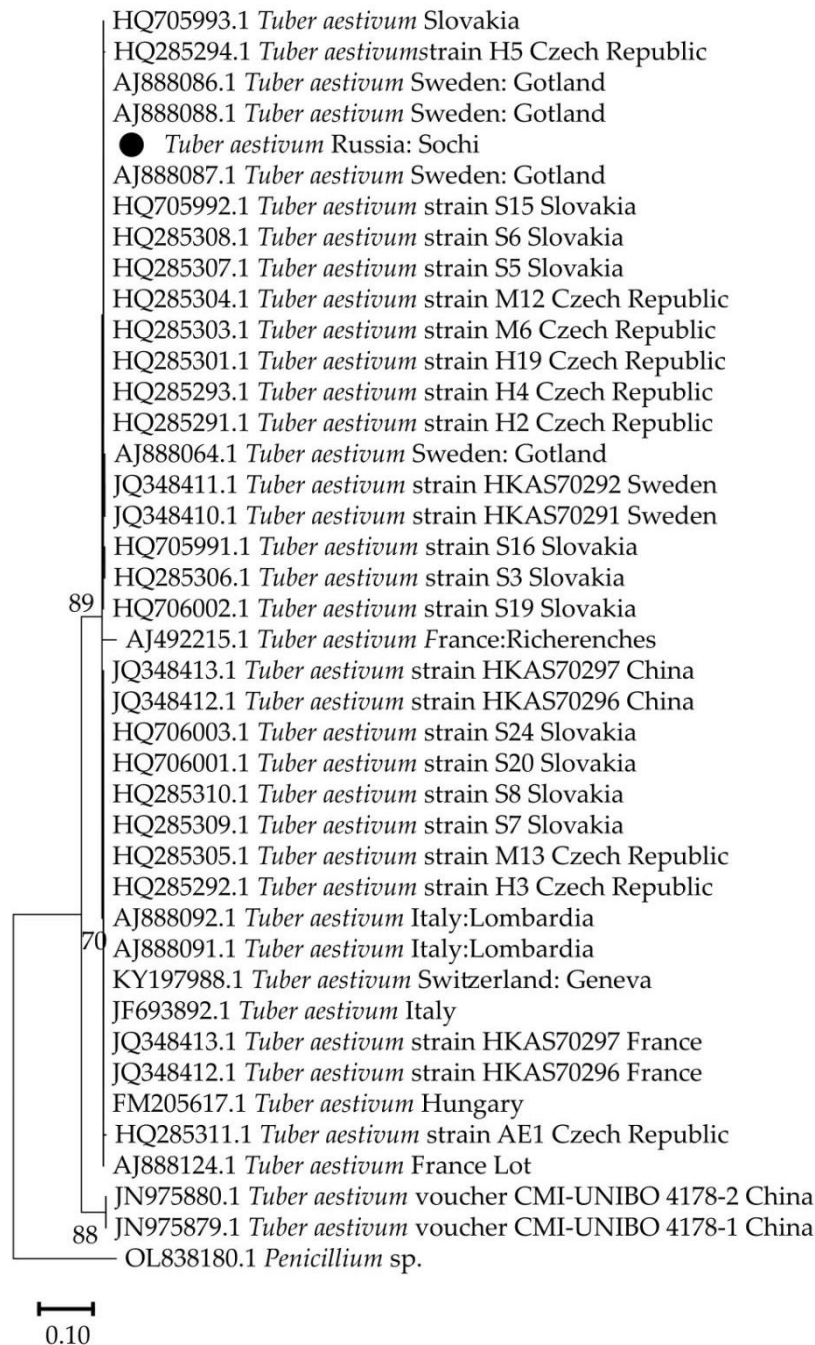


Figure 3 Evolutionary analysis via the maximum likelihood method (the black marker is the strain of *T. aestivum* found in this study).

Based on the results of this study and an analysis of the nucleotide sequences aligned with the nucleotide sequence of this study, the Russian truffle was identified as *Tuber aestivum* (summer truffle). Nucleotide sequences were aligned and compared with those of the studied summer truffle and were used in the analysis (Zambonelli et al. 2012; Zhang et al. 2012; Truong et al. 2017). The phylogenetic analysis was performed

based on the fragment of the 18S rRNA gene, the nucleotide sequence of the internal transcribed spacer, and the 5.8S rRNA gene and revealed high similarity between the truffles collected in Russia and the truffles collected in Europe (Czech Republic, Slovakia, etc.). The Russian truffles (*T. aestivum*) were characterized by their high divergence from truffles collected in China (Figure 3).

The evolutionary history was inferred using the maximum likelihood method and the Tamura–Nei model (Tamura and Nei 1993). The percentage of trees in which the associated taxa clustered is shown next to the branches. The initial tree(s) for the heuristic search were obtained automatically by applying the neighbour joining and BioNJ algorithms to a matrix of the pairwise distances estimated using the Tamura–Nei model and then selecting the topology with the superior log likelihood value. The tree is drawn to scale, with the branch lengths measured as the number of substitutions per site. This analysis involved 41 nucleotide sequences, and there were 608 positions in total in the final dataset.

3.2 Characterization of the prokaryotic and eukaryotic communities of truffles collected in Russia

According to the materials used for the metagenomic analysis, the prokaryotic community of *T. aestivum* collected in Russia (Sochi) was represented by the phylum *Proteobacteria* (OTU 99.88 ± 0.11%) and several minor phyla, including *Actinobacteria*, *Bacteroides*, *Cyanobacteria*, and *Firmicutes*. The classes of microorganisms and their distribution are shown in Figure 4. The dominant class was *Gammaproteobacteria*, and representatives of *Pseudomonas* were the dominant group of bacteria inhabiting the

ascomata of *T. aestivum*. The major groups of bacteria were represented by bacterial genera such as *Rahnella*, *Enterobacter*, and *Stenotrophomonas*. In addition, several minor groups of bacteria were found in the fruiting bodies of the truffles (OTU <1%). These genera included *Acinetobacter*, *Citrobacter*, *Comamonas*, *Enterobacter*, *Klebsiella*, *Lactobacillus*, *Massilia*, *Nitrobacter*, *Nocardioidea*, *Pedobacter*, *Ralstonia*, *Raoultella*, *Rahnella*, *Rhizobium*, *Sphingobacterium*, and *Staphylococcus*. Among the diverse bacteria, several were identified as *Bacillus anthracis*, *Bacillus cereus*, and *Enterobacter aerogenes*.

The eukaryotic community of the *T. aestivum* collected in Russia (Sochi) contained fungi (OTU 74.3 ± 3.17%), protists (OTU 10.6 ± 4.7), and undescribed taxa (15.06 ± 1.32%) (Figure 5). The fungal community of *T. aestivum* was represented by 13 genera and unclassified taxa: *Alternaria*, *Ascobolus*, *Cladophialophora*, *Holtermanniella*, *Hyaloscypha*, *Malassezia*, *Mycosphaerella*, *Mortierella*, *Penicillium*, *Papulaspora*, *Psathyrella*, *Rhodotorula*, and *Tylospora*. Among the diverse fungi, several were identified as the following species: *Alternaria metachromatica*, *Cladophialophora chaetospora*, *Holtermanniella festucosa*, *Mortierella polygonia*, *Papulaspora equi*, *Penicillium aethiopicum*, *Penicillium bialowiezense*, *Penicillium thomii*, *Psathyrellapygmaea*, and *Rhodotorula dairenensis*.

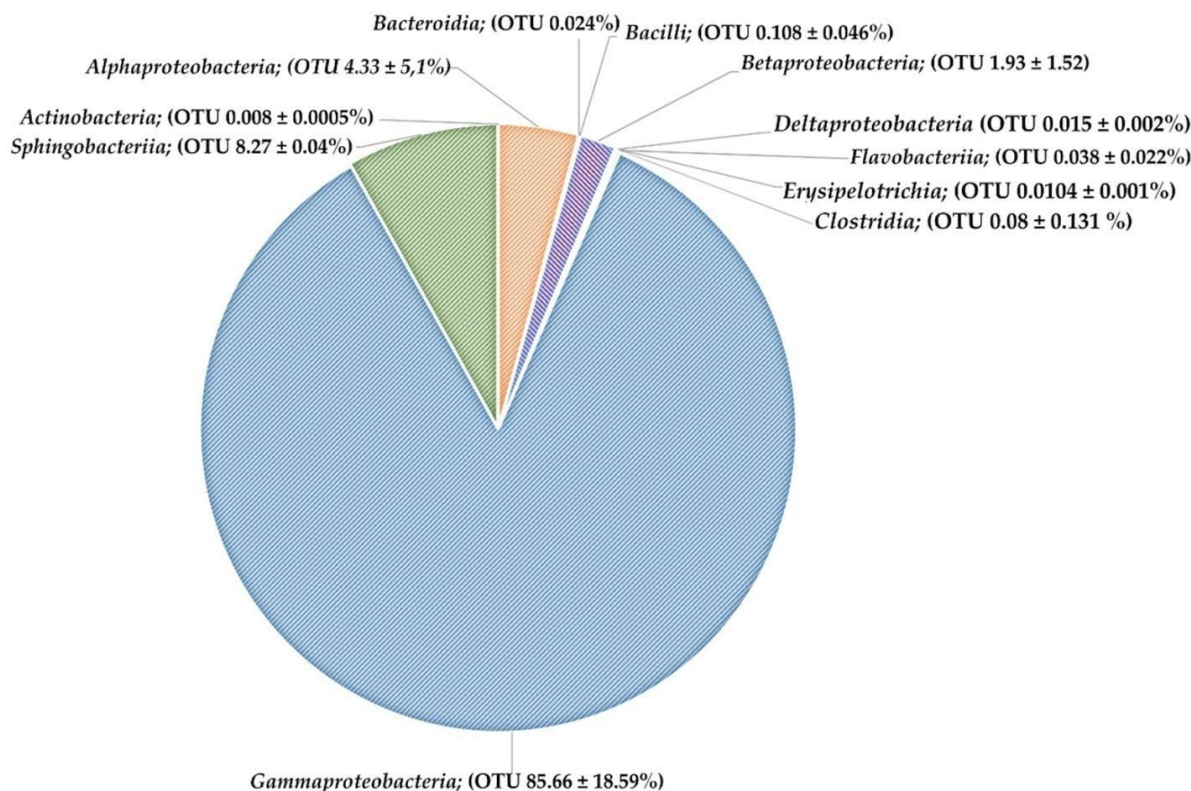


Figure 4 Total distribution of the classes of prokaryotic organisms (OTUs, %) inhabiting *T. aestivum* collected in Russia.

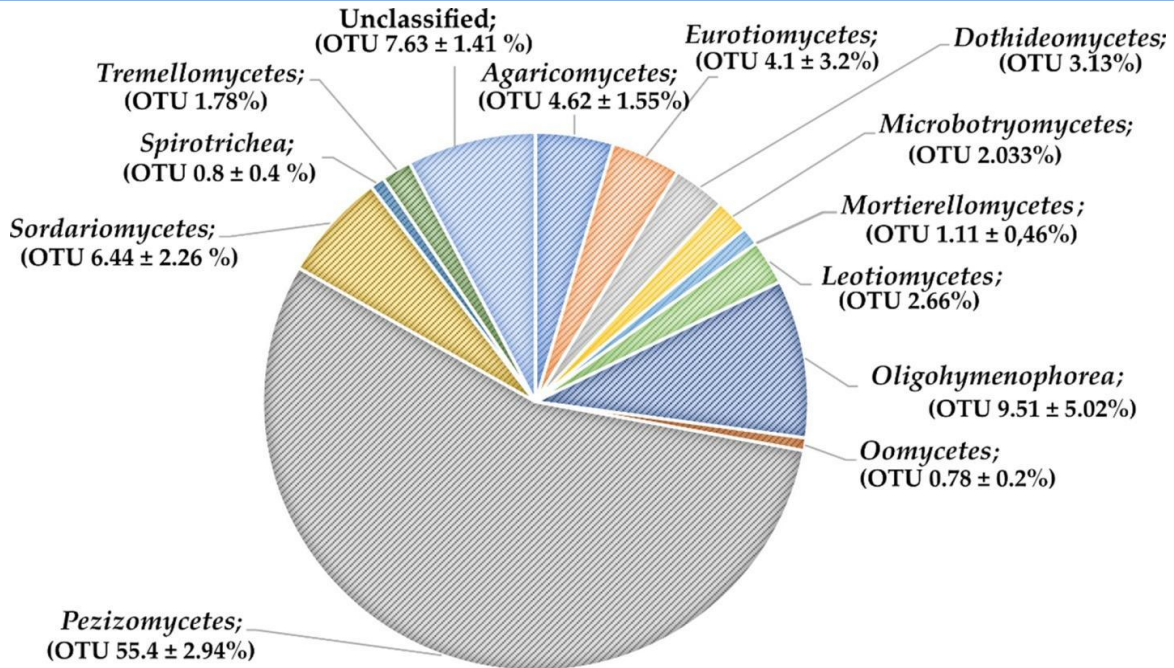


Figure 5 Total distribution of eukaryotic organisms (OTUs, %) found in the ascospores of *T. aestivum* collected in Russia.

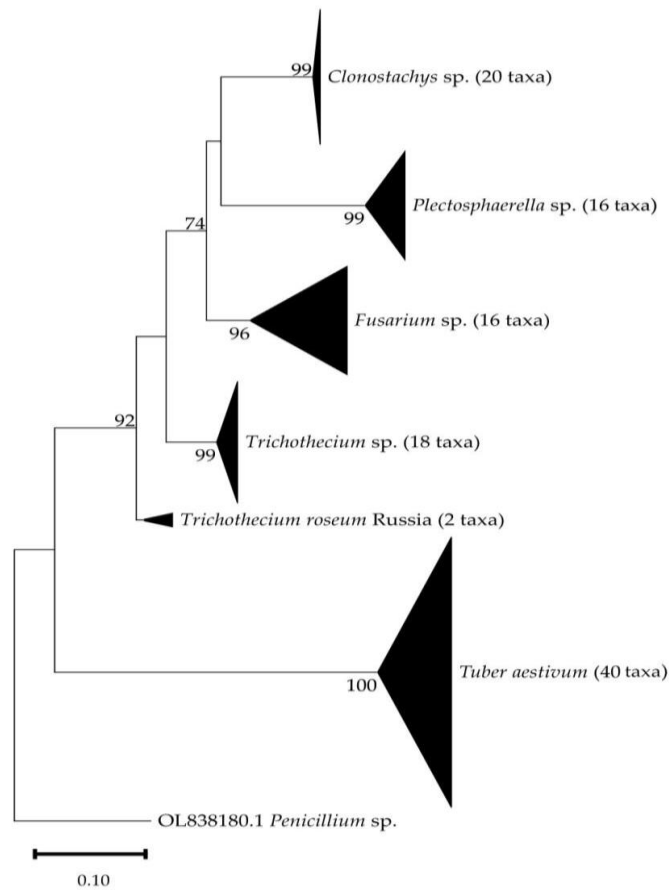


Figure 6 General topology of the phylogenetic tree of the truffle-associated fungi

This study also analyzed the diversity of bacteria, fungi, and other eukaryotes inhabiting the fruiting bodies of truffles. The microorganisms found in Russian, Italian, and French truffles were estimated. The general diversity of the microbial phyla is presented in Table 2. The results suggested a general similarity among the diverse microbial phyla of Russian, Italian, and French truffles.

3.3 Phylogenetic characterization of fungal symbionts isolated from Russian truffles

This study isolated and identified several truffle-inhabiting fungi from black truffles. These strains belong to four genera of mycelial fungi: *Clonostachys* sp., *Fusarium* sp., *Plectosphaerella* sp., and *Trichothecium* sp. The results of the phylogenetic analysis of the

sequences are presented in Figures 6–10. The *Clonostachys* sp. LPB202216 strain isolated from *T. aestivum* formed a clade with other *Clonostachys* sp. representatives from the USA, China, Russia, Italy, Mongolia, etc. *Clonostachys* sp. strains from Russia did not constitute a separate clade with each other or with isolated strains (Figure 7).

Another strain, identified as *Fusarium* sp. LPB148, formed a mixed clade with the strains deposited in the NCBI database. The highest similarity was shown for strains from the Netherlands and Switzerland (Figure 8). *Plectosphaerella* sp. LPB202213, which is associated with *T. aestivum* and was isolated during this study, formed a weakly supported clade with a strain found in China (Figure 9).

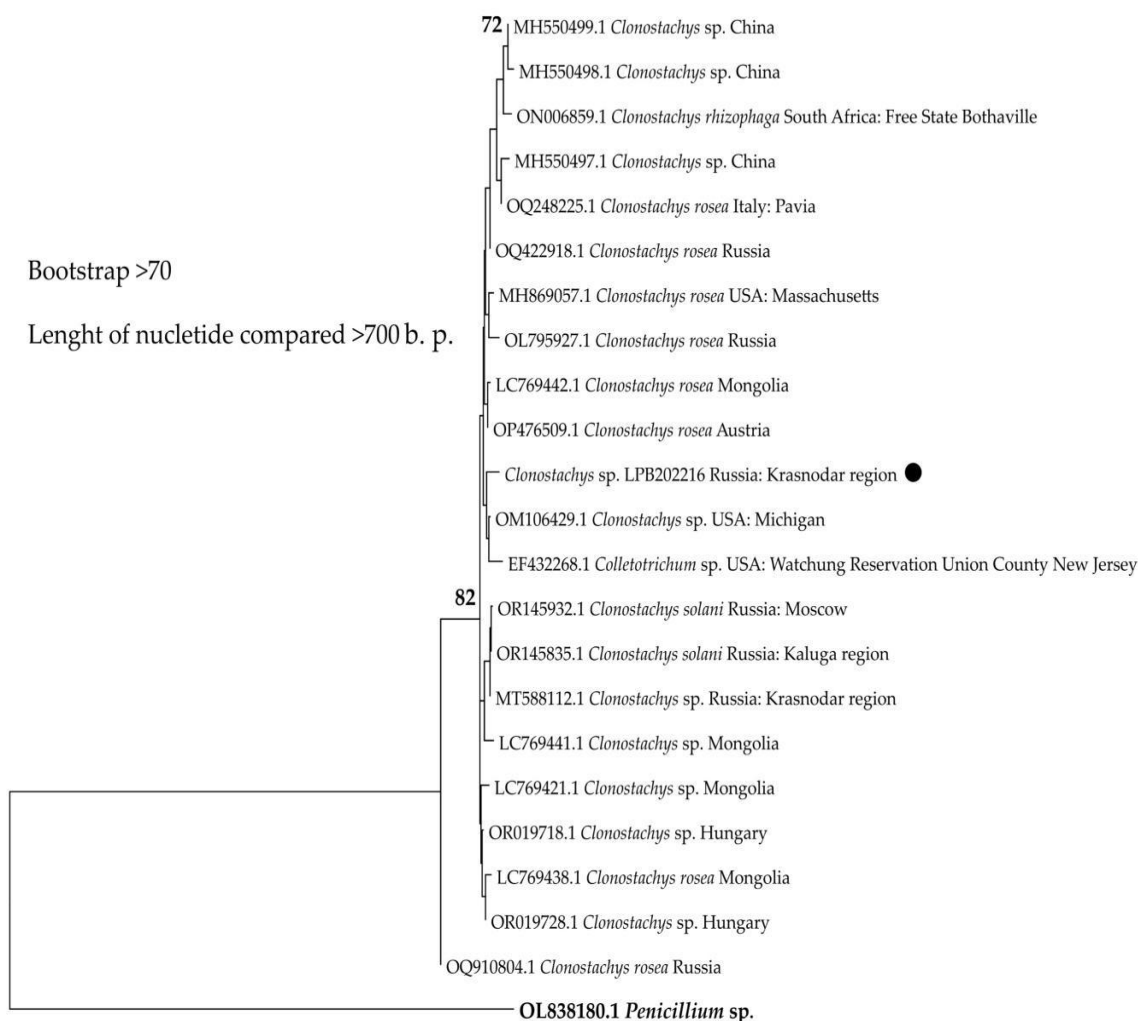


Figure 7 Evolutionary analysis via the maximum likelihood method for *Clonostachys* sp. LPB202216

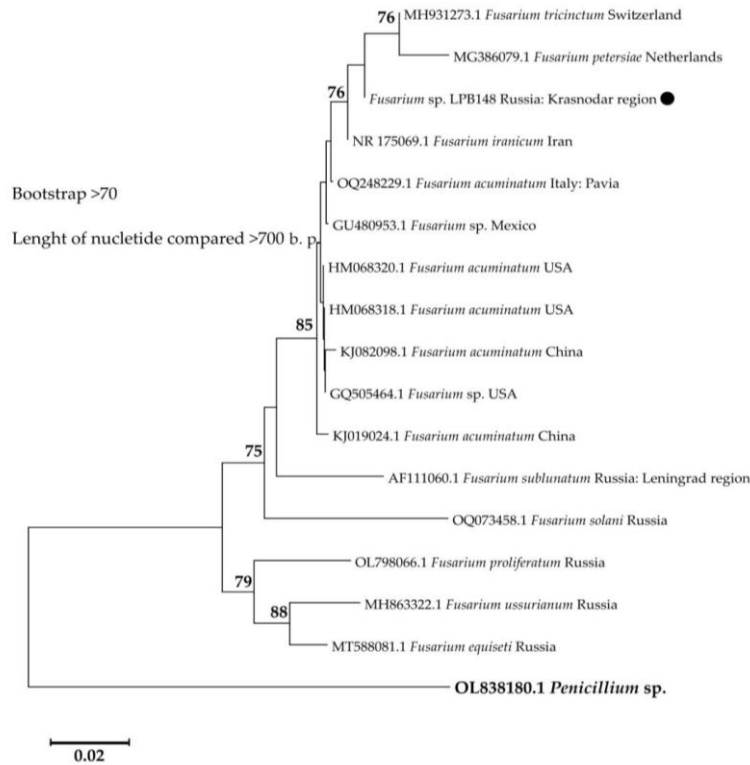


Figure 8 Evolutionary analysis via the maximum likelihood method for *Fusarium* sp. LPB148.

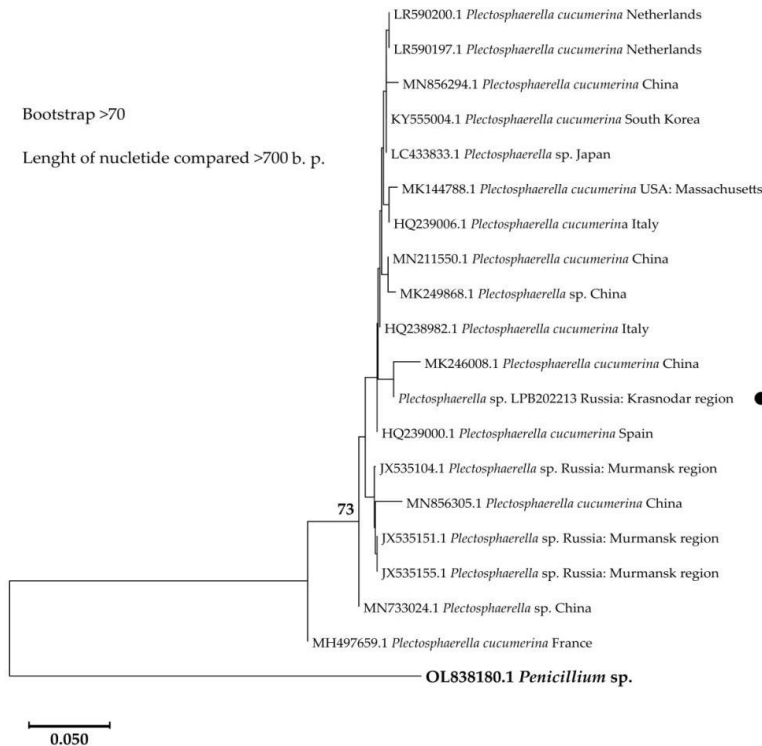


Figure 9 Evolutionary analysis via the maximum likelihood method for *Plectosphaerella* sp. LPB202213.

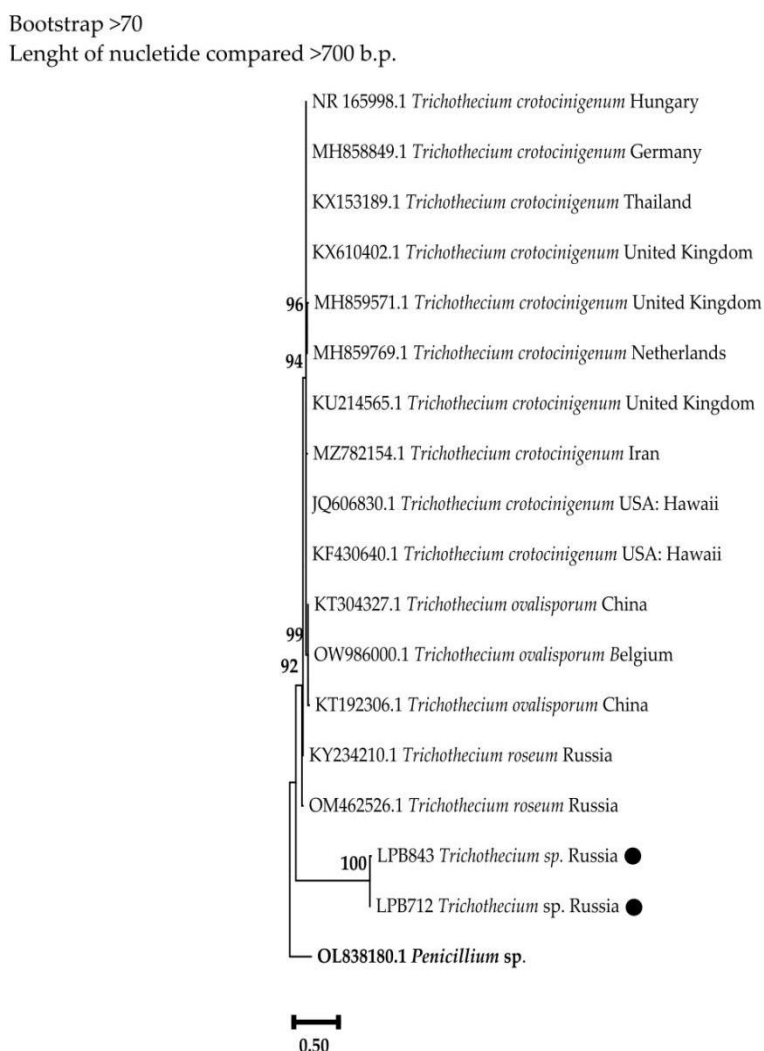


Figure 10 Evolutionary analysis via the maximum likelihood method for *Trichothecium* sp. LPB712 and *Trichothecium* sp. LPB843.

Trichothecium sp. LPB712 and *Trichothecium* sp. LPB843 strains formed a separate clade from the other strains. This indicated a large difference between the isolated truffle-associated strains and those isolated in Russia and other countries' territories (Figure 10). Moreover, the large differences between the isolated strains and the different strains deposited in the NCBI can be explained by new species of *Trichothecium* spp. inhabiting *T. aestivum* in Russia.

4 Discussion

Many published studies focused on the biomedical properties of truffle fruiting bodies in a pure culture of *Tuber* sp. However, the fruiting bodies of truffles contain a consortium of organisms (Das et al. 2022). This can lead to an unstable composition and different therapeutic effects of the extracts obtained from the ascomata (Khalifa et al. 2019; Tejedor-Calvo et al. 2021). Furthermore, the

diversity of prokaryotic and eukaryotic organisms in the fruiting bodies of truffles makes obtaining pure cultures problematic (Siebyła and Szyp-Borowska 2021).

Microorganisms that are symbiotic with truffles are understudied, and their biological and biomedical potential has not been described. Several studies on the composition of truffle-associated microbial communities have assessed truffles collected in European countries (Vahdatzadeh et al. 2019; Monaco et al. 2020; Siebyła and Szyp-Borowska 2022; Herero de Aza et al. 2022). However, in Russia, studies on this topic are now being reported for the first time. Thus, for the first time, this study demonstrated that Russian truffles belonging to the genus *T. aestivum* do not form an independent phylogenetic clade. The question of truffle identification was discussed in the study performed by Molinier et al. (2013) demonstrated that European *T. uncinatum* and *T. aestivum* belong to the same species. In addition, it was hypothesized that *T. aestivum* is

most likely self-reproductive. This might explain the high similarity of truffles collected in Russia to other representatives of *T. aestivum*.

The analysis of the symbiotic bacteria genera described in Table 3 revealed that the representatives of *Enterobacter* are typical symbionts of truffles. This bacterium was found in fruiting bodies

collected in Russia, Italy, and France. In addition, the results of this study revealed the presence of several bacterial genera only in Russian truffles. These bacteria include the following: *Achromobacter*, *Acinetobacter*, *Comamonas*, *Delftia*, *Enterohabdus*, *Klebsiella*, *Lactobacillus*, *Massilia*, *Rahnella*, *Ralstonia*, *Raoultella*, and *Stenotrophomonas*.

Table 3 Comparative list of bacteria associated with the fruiting bodies of *T. aestivum* collected in different countries.

Genus of bacteria	Known prokaryotic communities of the black truffle <i>T. aestivum</i>		
	<i>T. aestivum</i> (region of Sochi, Russia) (current study)	<i>T. aestivum</i> (region of Molise, Italy) (Monaco et al. 2020)	<i>T. aestivum</i> (region of Var, France) (Vahdatzadeh et al. 2019)
<i>Achromobacter</i> sp.	+	-	-
<i>Acidovorax</i> sp.	-	+	-
<i>Acinetobacter</i> sp.	+	-	-
<i>Bacillus</i> sp.	+	+	-
<i>Bacteroides</i> sp.	+	+	-
<i>Bifidobacterium</i> sp.	-	+	-
<i>Buttiauxella</i> sp.	-	+	-
<i>Bradyrhizobium</i> sp.	-	+	+
<i>Carnobacterium</i> sp.	-	-	+
<i>Chryseolinea</i> sp.	-	+	-
<i>Citrobacter</i> sp.	+	-	+
<i>Comamonas</i> sp.	+	-	-
<i>Delftia</i> sp.	+	-	-
<i>Devosia</i> sp.	-	+	-
<i>Dongia</i> sp.	-	+	-
<i>Ensifer</i> sp.	-	+	-
<i>Enterobacter</i> sp.	+	+	+
<i>Enterohabdus</i> sp.	+	-	-
<i>Frankia</i> sp.	-	+	-
<i>Hydrogenophaga</i> sp.	-	+	-
<i>Klebsiella</i> sp.	+	-	-
<i>Lactobacillus</i> sp.	+	-	-
<i>Lactococcus</i> sp.	-	-	+
<i>Massilia</i> sp.	+	-	-
<i>Mesorhizobium</i> sp.	-	+	-
<i>Nocardioides</i> sp.	+	+	-
<i>Paenibacillus</i> sp.	-	+	-
<i>Pantoea</i> sp.	-	+	-
<i>Pedobacter</i> sp.	+	-	+
<i>Pedomicrobium</i> sp.	-	+	-

Genus of bacteria	Known prokaryotic communities of the black truffle <i>T. aestivum</i>		
	<i>T. aestivum</i> (region of Sochi, Russia) (current study)	<i>T. aestivum</i> (region of Molise, Italy) (Monaco et al. 2020)	<i>T. aestivum</i> (region of Var, France) (Vahdatzadeh et al. 2019)
<i>Polaromonas</i> sp.	-	+	+
<i>Pseudomonas</i> sp.	+	+	-
<i>Pseudonocaria</i> sp.	-	+	-
<i>Rahnella</i> sp.	+	-	-
<i>Ralstonia</i> sp.	+	-	-
<i>Raoultella</i> sp.	+	-	-
<i>Reyranella</i> sp.	-	+	-
<i>Rhizobium</i> sp.	+	+	-
<i>Rubrobacter</i> sp.	-	+	-
<i>Serratia</i> sp.	+	-	+
<i>Sphingobacterium</i> sp.	+	+	-
<i>Spingomonas</i> sp.	-	+	-
<i>Staphylococcus</i> sp.	+	+	-
<i>Stenotrophomonas</i> sp.	+	-	-
<i>Varivorax</i> sp.	-	-	+

The "+" symbol indicates the presence of this bacterial genus in the truffle microbiome; the "-" symbol indicates the absence of this bacterial genus in the truffle microbiome

Several bacteria were found in European *T. aestivum* but not in Russian truffles, including the following: *Acidovorax*, *Buttiauxella*, *Chryseolinea*, *Devosia*, *Ensifer*, *Frankia*, *Hydrogenophaga*, *Lactococcus*, *Mesorhizobium*, and *Pantoea*. Representatives of *Bradyrhizobium* and *Polaromonas* were found only in the fruiting bodies of *T. aestivum* sampled in Italy and France (Vahdatzadeh et al. 2019).

During the evaluation of the prokaryotic composition of three samples of the fruiting bodies of the truffle *T. aestivum*, classes belonging to *Gammaproteobacteria* and *Bacilli* were detected in all the samples. A study by Vahdatzadeh et al. (2019) demonstrated that the bacteria associated with *T. aestivum* classes depended on the product's freshness and storage conditions. A comparison of recently published data and the data obtained in this study allowed us to establish that the classes of bacteria found in the truffle samples are markers of staleness (Ramos-Pereira et al. 2019) despite their fresh appearance and appropriate transport conditions. The diverse fungi found in the fruiting bodies of *T. aestivum* collected in different countries included four common genera: *Malassezia*, *Papulaspora*, *Psathyrella*, and *Penicillium* (Table 4).

In the microbiome of the truffles, we also found fungi of the genus *Penicillium*. The presence of these fungi in the metagenome of

food products is a marker of food spoilage (Ramos-Pereira et al. 2019). In addition, the following fungal genera were found in Russian truffles: *Ascobolus*, *Mortierella*, *Holtermanniella*, *Papulaspora*, *Psathyrella*, and *Rhodotorula*. These are soil microorganisms previously isolated from rotting plant residues or ruminant manure. This peculiarity indicates that these microorganisms that enter symbiosis allow the truffles to colonize plant roots more efficiently, utilizing a specific set of cellulases and hydrolases (Siebyła 2022).

Thus, despite the external quality of truffles, molecular analysis revealed a high diversity of pathogenic and nonpathogenic organisms associated with their fruiting bodies. The potential importance of these genera of prokaryotic and eukaryotic organisms is presented in Table 5. The diversity of prokaryotic (Dahal et al. 2021; Rosenberg et al. 2014; Zafar and Saier 2021; Araújo et al. 2021; Ke et al. 2021; Muszyński et al. 2021; Evangelista et al. 2022; Riahi et al. 2022) and eukaryotic (Litvinov 2013; Mesanza et al. 2021; Vohník et al. 2022; Ianiri et al. 2022; Lin et al. 2022) organisms and the high number of pathogenic species in the fruiting bodies of truffles indicate the complexity of the symbiotic interactions that can be observed and studied in the truffle model. Many prokaryotic and eukaryotic organisms mentioned here might influence truffles and help them form effective mycorrhizae with trees.

Table 4 Comparative list of fungi associated with the fruiting bodies of *T. aestivum* collected in different countries.

Genus	Known eukaryotic communities of the black truffle <i>T. aestivum</i>	
	<i>T. aestivum</i> (region of Sochi, Russia) (current study)	<i>T. aestivum</i> (region of the Nida river, Poland) (Perlińska-Lenart et al. 2020b)
<i>Sphaerodes</i> sp.	-	+
<i>Alternaria</i> sp.	+	-
<i>Ascobolus</i> sp.	+	-
<i>Cladophialophora</i> sp.	+	-
<i>Coprinellus</i> sp.	-	+
<i>Holtermanniella</i> sp.	+	-
<i>Hyaloscypha</i> sp.	+	-
<i>Leptolegnia</i> sp.	-	+
<i>Malassezia</i> sp.	+	+
<i>Mortierella</i> sp.	+	-
<i>Mucor</i> sp.	-	+
<i>Mycosphaerella</i> sp.	+	-
<i>Papulaspora</i> sp.	+	+
<i>Penicillium</i> sp.	+	+
<i>Phlebia</i> sp.	-	+
<i>Piptoporus</i> sp.	-	+
<i>Psathyrella</i> sp.	+	+
<i>Rhodotorula</i> sp.	-	+
<i>Trichoderma</i> sp.	-	+
<i>Tylospora</i> sp.	+	-
<i>Umbelopsis</i> sp.	-	+
<i>Veluticeps</i> sp.	-	+

The "+" symbol indicates the presence of this fungal genus in the truffle microbiome; the "-" symbol indicates the absence of this fungal genus in the truffle microbiome

The truffle-inhabiting fungi isolated in this study were identified as *Fusarium* sp., *Clonostachys* sp., *Plectosphaerella* sp., and *Trichothecium* sp. *Trichothecium crotoconigenum* (also widely known as *Acremonium crotoconigenum*) is responsible for a widespread rot epidemic affecting the cultivation of *T. melanosporum* in Australia. This epidemic has lasted for several years and has resulted in the loss of more than 50% of the truffle harvest in some cases. The pathogenicity of *T. crotoconigenum* has been directly confirmed in the field by inoculating the conidia or gleba of rotten truffles. However, it is worth noting that *T. crotoconigenum* was previously found in healthy ascocarps of *Tuber maculatum* Vittad in the Netherlands (Pacioni and Leonardi 2016). Another similar species, *Trichothecium roseum*, has been isolated from rotten pink Chinese truffles and observed on stored

desert truffles, *Terfeziapinoi* Maire and *Terfeziacaveryi* Chatin. This mushroom is a truffle symbiont and, presumably, can be useful for combating soil parasites (Satish et al. 2022).

The fungal strain identification results identified a small, studied oligotrophic fungal species belonging to *Plectosphaerella*. Most of the known fungi of the genus *Plectosphaerella* were isolated from soils (Soledad et al. 2023). They are pathogens of several plant species and are described as a component of the core fungal genera associated with forests producing white truffles (Giorgio et al. 2023). However, previously, representatives of *Plectosphaerella* were never reported as organisms living inside the ascomata of truffles, and we found no mention of these fungi as pathogens of truffles, especially black truffles.

Table 5 The potential biological importance of organisms found in association with *T. aestivum*

Organism	Importance
Prokaryotic organisms	
<i>Achromobacter</i> sp.	Soil bacteria, arsenic oxidizers
<i>Acidovorax</i> sp.	Phytopathogens, heavy metal oxidizers
<i>Acinetobacter</i> sp.	Saprophytes, chemoorganotrophs
<i>Bacillus</i> sp.	Saprophytes, plant and animal pathogens
<i>Bacteroides</i> sp.	Saprophytes, human pathogens
<i>Bifidobacterium</i> sp.	Saprophytes, the member of normal human microflora
<i>Buttiauxella</i> sp.	Soil bacteria, endophytes
<i>Bradyrhizobium</i> sp.	Soil nitrogen-fixing bacteria
<i>Carnobacterium</i> sp.	Acidophilic bacteria, producers of bacteriocins
<i>Chryseobacterium</i> sp.	Soil bacteria, phytopathogenic
<i>Citrobacter</i> sp.	Human and vertebrate pathogens
<i>Comamonas</i> sp.	Denitrifying bacteria
<i>Delftia</i> sp.	Detoxification of heavy metals, ability to decompose herbicides, etc.
<i>Devosia</i> sp.	Nitrogen-fixing nodule bacteria
<i>Desulfovibrio</i> sp.	Oil destructors, metal oxidizers
<i>Dongia</i> sp.	Soil bacteria
<i>Ensifer</i> sp.	Nitrogen-fixing nodule bacteria
<i>Enterobacter</i> sp.	Vertebrate pathogens
<i>Frankia</i> sp.	Nitrogen-fixing bacteria, plant symbionts
<i>Granulibacter</i> sp.	Human and vertebrate pathogens
<i>Klebsiella</i> sp.	Animal pathogens
<i>Lachnospiraceae</i> sp.	Human intestinal symbionts, destroyer of cellulose
<i>Lactobacillus</i> sp.	Animal pathogens
<i>Lactococcus</i> sp.	Animal pathogens
<i>Massilia</i> sp.	Nitrogen-fixing bacteria, plant symbionts, decomposers of chlorine-based herbicides
<i>Mesorhizobium</i> sp.	Nitrogen-fixing nodule bacteria
<i>Nitrobacter</i> sp.	Soil-nitrifying bacteria
<i>Nocardioides</i> sp.	Detoxifiers, symbionts of algae and vertebrates
<i>Paenibacillus</i> sp.	Destroyers of biopolymers, including cellulose and agar-agar
<i>Pantoea</i> sp.	Pathogen of plants, saprophytes
<i>Pedobacter</i> sp.	Soil bacteria
<i>Pedomicrobium</i> sp.	Oxidizers of manganese
<i>Polaromonas</i> sp.	Psychrophilic bacteria
<i>Pseudomonas</i> sp.	Wide effects and products of biosynthesis
<i>Pseudonocardia</i> sp.	Wide effects and products of biosynthesis

Organism	Importance
<i>Rahnella</i> sp.	Human pathogens in the environment
<i>Ralstonia</i> sp.	Phytopathogens
<i>Raoultella</i> sp.	Human and vertebrate pathogens
<i>Reyranella</i> sp.	Soil bacteria, symbionts of plants
<i>Rhizobium</i> sp.	Nitrogen-fixing nodule bacteria
<i>Ruminococcus</i> sp.	Human pathogens
<i>Serratia</i> sp.	Destroyers of biopolymers, symbionts of plants
<i>Sphingobacterium</i> sp.	Human pathogens
<i>Spingomonas</i> sp.	Plant symbionts, involved in bioremediation processes
<i>Staphylococcus</i> sp.	Human and vertebrate pathogens
<i>Stenotrophomonas</i> sp.	Wide effects and products of biosynthesis
<i>Varivorax</i> sp.	Phytopathogens, nitrogen-fixing bacteria
Eukaryotic organisms	
<i>Alternaria</i> sp.	Soil fungi, phytopathogens
<i>Ascobolussp.</i>	Coprophilous. Found in manure of herbivorous mammals and on plant residues
<i>Cladophialophora</i> sp.	Human pathogens
<i>Coprinellus</i> sp.	Coprophilous. Found in manure of herbivorous mammals and on plant residues
<i>Holtermanniella</i> sp.	Biological destroyers
<i>Hyaloscypha</i> sp.	Symbionts of plant roots
<i>Leptolegnia</i> sp.	Pathogens of insects
<i>Malassezia</i> sp.	Pathogens of humans and mammals
<i>Mortierella</i> sp.	Biological destroyer, pathogens
<i>Mucor</i> sp.	Biological destroyer, pathogens
<i>Mycosphaerella</i> sp.	Phytopathogens
<i>Papulaspora</i> sp.	Producers of amylase
<i>Penicillium</i> sp.	Soil fungi, plant parasites
<i>Phlebia</i> sp.	Phytopathogens
<i>Piptoporus</i> sp.	Biological destroyers
<i>Psathyrella</i> sp.	Found in the manure of herbivores
<i>Rhodotorula</i> sp.	Denitrifiers
<i>Trichoderma</i> sp.	Phytopathogens
<i>Tylospora</i> sp.	Biological destroyers
<i>Umbelopsis</i> sp.	Producers of oils
<i>Veluticeps</i> sp.	Phytopathogens

From an analysis of literary sources, it is known that the fungus *Clonostachys rosea* is of great interest. It is a saprotroph used as an agent for the biological control of phytopathogenic fungi (Funk Jensen et al. 2022). *C. rosea* is short and was mentioned in

(Rennick et al. 2022). However, the role of *Clonostachys* sp. and other truffle-inhabiting fungi in the life of truffles is unclear.

Truffles are special kinds of fungi with unique adaptations and complexes of unknown and rarely studied interactions with other organisms, including fungal symbionts. One of the reasons for having so many fungal symbionts is that they help truffles resist competition from other fungi and microorganisms living in the soil. The variety of fungal symbionts provides the truffle with maximum efficiency in obtaining nutrients for forming fruiting bodies (García-Barreda et al. 2023). Truffles are also known to grow in different ecological conditions, including various types of soils, climatic zones, and plant communities (Mrak et al. 2024). The variety of fungal and bacterial symbionts allows truffles to adapt to these different environmental conditions (Barou et al. 2023). Each fungal symbiont has its own characteristics that help truffles survive under certain climatic conditions and form mycorrhizae with host plants (García-Montero et al. 2024). Thus, the diversity of bacterial and fungal symbionts in truffles plays an important role in their growth and reproduction (Liu et al. 2021b).

Conclusion

In this study, we first demonstrated the diversity of prokaryotic and eukaryotic organisms associated with the Russian truffle *T. aestivum*. The microbiome of the black truffle *T. aestivum* mainly consisted of soil bacteria and fungi. This study also estimated the diversity of microorganisms inhabiting Russian truffles compared with *T. aestivum* collected in Italy and France and found that the general distribution of the microbial taxa was similar. We found a high similarity between Russian and European truffles. Sequencing the hypervariable fragments of the 16S rRNA and 18S rRNA genes allowed us to identify the plant pathogens involved in symbiotic relationships with the truffles. In addition, some strains of fungal symbionts and likely pathogens were isolated and identified in truffles for the first time. Because they are associated with truffles, many species of these prokaryotic and eukaryotic organisms might influence truffles and help them form mycorrhizae with trees. Thus, truffles are interesting and promising sources for modern biotechnological and agricultural studies.

Author Contributions

E.V.M., M.E.D., M.M.M., N.A.I., A.A.V., T.Y.T., V.N.S., A.S.K. and A.Y.B. performed the experiments and analysed the data. E.V.M. and M.M.M. isolated the strains. MED, MMM, and NAI identified the strains. EVM wrote the first draft of the manuscript. DVAG and EVM planned the experiments, analysed the data, and edited the manuscript. All authors have read and agreed to the published version of the manuscript.

Funding

The study was performed at the Laboratory of Pharmaceutical Biotechnology (ISU) and supported by GreenTechBaikal LLC. The Russian Science Foundation funded the study project ID 22-76-10036.

Data Availability Statement

The sequence data used to support the findings of this study have been deposited in the NCBI Genbank repository (<https://www.ncbi.nlm.nih.gov/genbank/>).

Acknowledgments

We thank all the researchers and students of the biological and soils faculty at ISU, the director of the botanical garden at ISU, and the administration of ISU for their support, and Innovation Centre Skolkovo for technical help and translation of the potential of innovation of this project.

Conflicts Of Interest

The authors declare no conflicts of interest.

References

- Allen, K., & Bennett, J.W. (2021). Tour of truffles: aromas, aphrodisiacs, adaptogens, and more. *Mycobiology*, 49 (3).<https://doi.org/10.1080/12298093.2021.1936766>
- Araújo, R.C., Rodrigues, F.A., Nadal, M.C., Ribeiro, M.S., Antônio, C.A., et al. (2021). Acclimatization of *Musa* spp. seedlings using endophytic *Bacillus* spp. and *Buttiauxellaagrestis* strains. *Microbiological Research*, 248, 126750. <https://doi.org/10.1016/j.micres.2021.126750>
- Barou, V., Rincón, A., Calvet, C., Camprubí, A., & Parladé, J. (2023). Aromatic plants and their associated arbuscular mycorrhizal fungi outcompete *Tuber melanosporum* in compatibility assays with truffle-oaks. *Biology*, 12 (4), 628. <https://doi.org/10.3390/biology12040628>
- Bragato, G., Fornasier, F., Bagi, I., Egli, S., & Marjanović, Ž. (2021). Soil parameters explain short-distance variation in production of *Tuber aestivum* Vittad. in an oak plantation in the Central-Northern part of the great Hungarian plain (Jászság Region, Hungary). *Forest Ecology of Management*, 479, 118578. <https://doi.org/10.1016/j.foreco.2020.118578>
- Dahal, R.H., Chaudhary, D.K., Kim, D.U., Pandey, R.P., & Kim, J. (2021). *Chryseobacterium antibioticum* sp. nov. with antimicrobial activity against Gram-negative bacteria, isolated from arctic soil.

- The Journal of Antibiotics*, 74 (2), 115–123. <https://doi.org/10.1038/s41429-020-00367-1>
- Das, M., Pal, A., Banerjee, S., Dey, S., & Banerjee, R. (2022). Phylogenomics, microbiome and morphological insights of truffles: the tale of a sensory stimulating ectomycorrhizal filamentous fungus. S. Sahay (Eds) *Extremophilic Fungi* (pp. 709-730). Springer, Singapore. https://doi.org/10.1007/978-981-16-4907-3_29
- Dogan, H. (2021). A New truffle species addition, *Tuber macrosporum*, to Turkish mycota. *Trakya University Journal of Natural Sciences*, 22 (2), 139-146. <https://doi.org/10.23902/trkjnat.873651>
- Evangelista, A.G., Danielski, G.M., Corrêa, J.A.F., Cavalari, C.M. deA., et al. (2022). *Carnobacterium* as a bioprotective and potential probiotic culture to improve food quality, food safety, and human health – a scoping review. *Critical Reviews in Food Science and Nutrition*, 63 (24), 1–14. <https://doi.org/10.1080/10408398.2022.2038079>
- Funck Jensen, D., Dubey, M., Jensen, B., & Karlsson, M. (2022). *Clonostachys rosea* to control plant diseases. In J. and Ravensberg, W. (Eds.), *Microbial bioprotectants for plant disease management* (pp. 30-35). Burleigh Dodds Science Publishing. DOI: 10.19103/AS.2021.0093.14
- García-Barreda, S., Marco, P., Bonito, G., Parladé, J., Sánchez, S., et al. (2023). Interannual dynamics of *Tuber melanosporum* and fungal communities in productive black truffle orchards amended with truffle nests. *FEMS Microbiology Ecology*, 99 (8), fiad084. <https://doi.org/10.1093/femsec/fiad084>
- García-Montero, L.G., Monleón, V.J., Valverde-Asenjo, I., Menta, C., & Kuyper, T.W. (2024). Niche construction by two ectomycorrhizal truffle species (*Tuber aestivum* and *T. melanosporum*). *Soil Biology and Biochemistry*, 189, 109276. <https://doi.org/10.1016/j.soilbio.2023.109276>
- Giorgio, M., Niccolò, B.G.M., Benedetta, T., Luisa, M., Leonardo, B.F., et al. (2023). Fungal and bacterial diversity in the *Tuber magnatum* ecosystem and microbiome. *Microbial Ecology*, 85, 508-521. <https://doi.org/10.1007/s00248-021-01950-1>
- Herero de Aza, C., Armenteros, S., McDermott, J., Mauceri, S., Olaizola, J., et al. (2022). Fungal and Bacterial communities in *tuber melanosporum* plantations from northern Spain. *Forests*, 13 (3), 385. <https://doi.org/10.3390/f13030385>
- Ianiri, G., LeibundGut-Landmann, S., & Dawson Jr., L. T. (2022). *Malassezia*: A commensal, pathogen, and mutualist of human and animal skin. annual review of *Microbiology*, 76, 757-782. <https://doi.org/10.1146/annurev-micro-040820-010114>
- Ke, Z., Lan, M., Yang, T., Jia, W., Gou, Z., Chen, K., & Jiang, J. (2021). A Two-Component Monooxygenase for Continuous denitration and dechlorination of chlorinated 4-nitrophenol in *Ensifer* sp. strain 22-1. *Environmental Research*, 198, 111216. <https://doi.org/10.1016/j.envres.2021.111216>
- Khalifa, S.A.M., Farag, M.A., Yosri, N., Sabir, J.S.M., Saeed, A., et al. (2019). Truffles: from islamic culture to chemistry, pharmacology, and food trends in recent times. *Trends in Food Science & Technology*, 91, 193–218. <https://doi.org/10.1016/j.tifs.2019.07.008>
- Kumar, S., Stecher, G., Li, M., Knyaz, C., & Tamura, K. (2018). MEGA X: molecular evolutionary genetics analysis across computing platforms. *Molecular Biology and Evolution*, 35 (6), 1547–1549. <https://doi.org/10.1093/molbev/msy096>
- Leonardi, M., Iotti, M., Pacioni, G., Hall, I.R., & Zambonelli, A. (2021a). Truffles: Biodiversity, ecological significances, and biotechnological applications. In A.M. Abdel-Azeem, A.N. Yadav, N. Yadav, Z. Usmani (Eds.), *Industrially Important Fungi for Sustainable Development. Fungal Biology* (pp. 107-146). Springer, Cham. <https://doi.org/10.1007/978-3-030-67561-5>
- Leonardi, P., Baroni, R., Puliga, F., Iotti, M., Salerni, E., Perini, C., & Zambonelli, A. (2021b). Co-occurrence of true truffle mycelia in *Tuber magnatum* fruiting sites. *Mycorrhiza*, 31, 389-394. <https://doi.org/10.1007/s00572-021-01030-9>
- Lin, X., Zhou, H., Zeng, F., Jiang, L., OkokonAtakpa, E., et al. (2022). A biosurfactant-producing yeast *Rhodotorula* sp.CC01 utilizing landfill leachate as nitrogen source and its broad degradation spectra of petroleum hydrocarbons. *World Journal of Microbiology and Biotechnology*, 38, 68. <https://doi.org/10.1007/s11274-022-03254-z>
- Litvinov, M.A. (2013). *A determinant of microscopic soil fungi*. Ripol Classic. Pp. 311 (Russian).
- Liu, D., Chater, C.C.C., Yu, F., & Perez-Moreno, J. (2021a). *Tuber pseudohimalayense* ascomata-compartments strongly select their associated bacterial microbiome from nearby pine forest soils independently of their maturation stage. *Pedobiologia*, 87-88. <https://doi.org/10.1016/j.pedobi.2021.150743>
- Liu, D., He, X., Chater, C.C.C., Perez-Moreno, J., & Yu, F. (2021b). Microbiome community structure and functional gene partitioning in different micro-niches within a sporocarp-forming fungus. *Frontiers in Microbiology*, 12, 629352. <https://doi.org/10.3389/fmicb.2021.629352>
- Ljubojević, S., Vasilišin, L., Vučić, G., & Velemir, A. (2022). Morphological Characteristics of summer truffle (*Tuber*

- aestivum*Vittad.) from Bosnia and Herzegovina. *Agricultural and Biological Sciences*, 2, 9-20. <https://doi.org/10.21303/2504-5695.2022.002382>
- Mesanza, N., Hernández, M., Raposo, R., & Iturrutxa, E. (2021). First report of *Mycosphaerella dearnessii*, teleomorph of *Lecanostictaacicola*, in Europe. *Plant Health Progress*, 22 (4), 565-566. <https://doi.org/10.1094/PHP-03-21-0060-BR>
- Molinier, V., Tuinen, D., Chevalier, G., & Golotte, A. (2013). A multigene phylogeny demonstrates that *Tuber aestivum* and *Tuber uncinatum* are conspecific. *Organisms Diversity & Evolution*, 13 (4). <https://doi.org/10.1007/s13127-013-0146-2>
- Monaco, P., Toumi, M., Sferra, G., Tóth, E., Naclerio, G., & Bucci, A. (2020). The bacterial communities of *Tuber aestivum*: preliminary investigations in Molise region, southern Italy. *Annual Microbiology*, 70 (1), 37. <https://doi.org/10.1186/s13213-020-01586-5>
- Mrak, T., Grebenc, T., Friedrich, S., & Münzenberger, B. (2024). Description, identification, and growth of *Tuber borchii* Vittad. mycorrhizal *Pinus sylvestris* L. seedlings on different lime contents. *Mycorrhiza*. <https://doi.org/10.1007/s00572-023-01135-3>
- Muszyński, A., Zarembek, K.A., Heiss, C., Shiloach, J., Berg, L.J., et al. (2021). *Granulibacterbethesdensis*, a pathogen from patients with chronic granulomatous disease, produces a penta-acylated hypostimulatory glycerol-d-talo-oct-2-ulosonic acid-lipid a glycolipid (ko-lipid a). *International Journal of Molecular Sciences*, 22 (7), 3303. <https://doi.org/10.3390/ijms22073303>
- Oliach, D., Castaño, C., Fischer, C.R., Barry-Etienne, D., Bonet, J.A., Colinas, C., & Oliva, J. (2022). Soil fungal community and mating type development of *Tuber melanosporum* in a 20-year chronosequence of black truffle plantations. *Soil Biology and Biochemistry*, 165, 108510. <https://doi.org/10.1016/j.soilbio.2021.108510>
- Pacioni, G., & Leonardi, M. (2016). Truffle-inhabiting fungi. In A. Zambonelli, M. Iotti, & C. Murat, (Eds.), *True Truffle (Tuber spp.) in the World* (pp. 1-436). Springer, Cham. https://doi.org/10.1007/978-3-319-31436-5_17
- Perlińska-Lenart, U., Piłyk, S., Gryz, E., Turlo, J., Hilszczańska, D., & Kruszewska, J.S. (2020a). Identification of bacteria and fungi inhabiting fruiting bodies of burgundy truffle (*Tuber aestivum*Vittad.). *Archives of Microbiology*, 202 (10), 2727-2738. <https://doi.org/10.1007/s00203-020-02002-x>
- Perlińska-Lenart, U., Piłyk, S., Gryz, E., Turlo, J., Hilszczańska, D., & Kruszewska, J.S. (2020b). Identification of Bacteria and fungi inhabiting fruiting bodies of burgundy truffle (*Tuber aestivum*Vittad.). *Archives of Microbiology*, 202 (10), 2727-2738. <https://doi.org/10.1007/s00203-020-02002-x>
- Ramos-Pereira, J., Mareze, J., Patrino, E., Santos, J.A., & López-Díaz, T.M. (2019). Polyphasic identification of *Penicillium* spp. isolated from Spanish semi-hard ripened cheeses. *Food Microbiology*, 84, 103253. <https://doi.org/10.1016/j.fm.2019.103253>
- Rennick, B., Benucci, G.M.N., Zhi-Yan, D. Healy, R., & Bonito, G. (2022). *Tuber rugosum*, a new species from northeastern North America: Slug mycophagy aides in electron microscopy of ascospores. *Mycologia*, 115 (3), 340-356. <https://doi.org/10.1080/00275514.2023.2184983>
- Riahi, H.S., Heidarieh, P., & Fatahi-Bafghi, M. (2022). Genus *Pseudonocardia*: What we know about its biological properties, abilities and current application in biotechnology. *Journal of Applied Microbiology*, 132 (2), 890-906. <https://doi.org/10.1111/jam.15271>
- Rodríguez, I., Fraga, J., Noda, A. A., Mayet, M., Duarte, Y., Echevarria, E., & Fernández, C. (2014). An alternative and rapid method for the extraction of nucleic acids from ixodid ticks by potassium acetate procedure. *Brazilian Archives of Biology and Technology*, 57, 542-547. <https://doi.org/10.1590/S1516-8913201402005>
- Rosenberg, E., DeLong, EF, & Lory, S. (2014). *The Prokaryotes* (4th ed.). Springer. Pp. 1013.
- Satish, L., Barak, H., Keren, G., Yehezkel, G., Kushmaro, A., et al. (2022). The Microbiome structure of the symbiosis between the desert truffle *Terfeziaboudieri* and its host plant *Helianthemum sessiliflorum*. *Journal of Fungi*, 8 (10), 1062. <https://doi.org/10.3390/jof8101062>
- Siebyła, M. (2022). Metabolic activity of soil bacteria associated with summer truffle *Tuber aestivum*. *Sylwan*, 166 (1), 54-70. <https://doi.org/10.26202/sylwan.2022003>
- Siebyła, M., & Szyp-Borowska, I. (2021). Comparison of bacterial communities in roots of selected trees with and without summer truffle (*Tuber aestivum*) ectomycorrhiza. *Folia Forestalia Polonica*, 63 (2), 97 – 111. <https://doi.org/10.2478/ffp-2021-0011>
- Siebyła, M., & Szyp-Borowska, I. (2022). Bacterial communities inhabiting the ascomata of the ectomycorrhizal summer truffle (*Tuber aestivum*). *Research Square*. <https://doi.org/10.21203/rs.3.rs-2297836/v1>
- Sillo, F., Vergine, M., Luvisi, A., Calvo, A., Petruzzelli, G., et al. (2022). Bacterial communities in the fruiting bodies and background soils of the white truffle *Tuber magnatum*. *Frontiers in Microbiology*, 13. <https://doi.org/10.3389/fmicb.2022.864434>

- Soledad, N.G., Sosa, A.L., Loyola, J.G., & Passone, M.A. (2023). Ecophysiological characteristics of the nematophagous fungus, *Plectosphaerella plurivora*, with biocontrol potential on *Nacobbus aberrans*. L. in tomato. *European Journal of Plant Pathology*. <https://doi.org/10.21203/rs.3.rs-2762633/v1>
- Tamura, K., & Nei, M. (1993). Estimation of the number of nucleotide substitutions in the control region of mitochondrial DNA in humans and chimpanzees. *Molecular Biology and Evolution*, 10 (3), 512–26. <https://doi.org/10.1093/oxfordjournals.molbev.a040023>
- Taschen, E., Callot, G., Sauve, M., Penuelas-samaniego, Y., Rousset, F., et al. (2022). Efficiency of the traditional practice of traps to stimulate black truffle production, and its ecological mechanisms. *Scientific Reports*, 12, 16201. <https://doi.org/10.1038/s41598-022-19962-3>
- Tejedor-Calvo, E., Amara, K., Reis, F.S., Barros, L., Martins, A., et al. (2021). Chemical composition and evaluation of antioxidant, antimicrobial and antiproliferative activities of *Tuber* and *Terfeziatruffles*. *Food Research International*, 140, 110071. <https://doi.org/10.1016/j.foodres.2020.110071>
- Thomas, P.W., & Thomas, H.W. (2022). Mycorrhizal fungi and invertebrates: Impacts on *Tuber melanosporum* ascospore dispersal and lifecycle by isopod mycophagy. *Food Webs*, 33, e00260. <https://doi.org/10.1016/j.fooweb.2022.e00260>
- Truong, C., Mujic, A., Healy, R., Kuhar, F., Furci, G., et al. (2017). How to know the fungi: combining field inventories and DNA-barcoding to document fungal diversity. *New Phytologist*, 214, 913–919. <https://doi.org/10.1111/nph.14509>
- Vahdatzadeh, M., Deveau, A., & Splivallo, R. (2019). Are bacteria responsible for aroma deterioration upon storage of the black truffle *Tuber aestivum*: amicrobiome and volatilome study. *Food Microbiology*, 84, 103251. <https://doi.org/10.1016/j.fm.2019.103251>
- Valencia, C.A., Pervaiz, M.A., Husami, A., Qian, Y., & Zhang, K. (2013). Sanger sequencing principles, history, and landmarks. In *Next Generation Sequencing Technologies in Medical Genetics* (pp. 3-11). Springer Briefs in Genetics. Springer, New York. https://doi.org/10.1007/978-1-4614-9032-6_1
- Vlahova, V. (2021). Study of the successful approach to truffle growing in Europe - review. *Scientific Papers. Series E. Land Reclamation, Earth Observation & Surveying, Environmental Engineering*, 10.
- Vohník, M., Figura, T., & Réblová, M. (2022). *Hyaloscyphagabretae* and *Hyaloscyphagryndleri* spp. nov. (Hyaloscyphaceae, Helotiales), two new mycobionts colonizing conifer, ericaceous and orchid roots. *Mycorrhiza*, 32, 105-122. <https://doi.org/10.1007/s00572-021-01064-z>
- Zafar, H., & Saier, M.H. (2021). Gut bacteroides species in health and disease. *Gut Microbes*, 13 (1), 1848158. <https://doi.org/10.1080/19490976.2020.1848158>
- Zambonelli, A., Iotti, M., & Piattoni, F. (2012). Chinese *Tuber aestivum* Sensu Lato in Europe. *Open Mycology Journal*, 6, 22–26. <https://doi.org/10.2174/1874437001206010022>
- Zhang, J.P., Liu, P.G., & Chen, J. (2012). *Tuber sinoaestivum* sp. nov., an edible truffle from southwestern China. *Mycotaxon*, 122, 73–82. <https://doi.org/10.5248/122.73>



Journal of Experimental Biology and Agricultural Sciences

<http://www.jebas.org>

ISSN No. 2320 – 8694

Role of Probiotic Strain *Lactobacillus acidophilus* in the Reversal of Gut Dysbiosis Induced Brain Cognitive Decline

Murugan Mukilan^{1,2*} , Mepully Thomas Antony Mathew² ,
Siva Yaswanth² , Vivekanandan Mallikarjun² 

¹Advanced Technology Development Centre, Indian Institute of Technology, Kharagpur 721 302, West Bengal, India

²Department of Biotechnology, Sri Ramakrishna College of Arts & Science, Coimbatore 641 006, Tamil Nadu, India

Received – October 12, 2023; Revision – October 21, 2023; Accepted – February 11, 2024

Available Online – March 15, 2024

DOI: [http://dx.doi.org/10.18006/2024.12\(1\).36.48](http://dx.doi.org/10.18006/2024.12(1).36.48)

KEYWORDS

Learning

Memory

Pseudomonas aeruginosa

Bacillus subtilis

Escherichia coli

Lactobacillus acidophilus

Enterotoxin

Cognitive impairment

ABSTRACT

In the central nervous system, bidirectional communication between the brain and gut results in memory formation due to synaptic plasticity changes. During a healthy state, oral balanced microflora plays a pivotal role in memory formation by inhibiting the enterotoxin level produced by infectious pathogens. In disease conditions, beneficial microbial dysbiosis may result in excess enterotoxin production. Further, excess enterotoxin secretion prevents beneficial bacteria's proliferation and impairs neurotransmitter precursor compounds' transport to the brain. Blockade of neurotransmitter precursor compounds may result in the development of memory loss. The present study stated the role of *Lactobacillus acidophilus* in recovering memory loss. Reversal of cognitive impairment is shown with the help of a three-step behavioural analysis, which consists of one pre-infusive behavioural analysis and two post-infusive behavioural analyses (phase 1 and 2). The pre-infusive analysis showed no cognitive impairment in an assimilated environment without any infusions. After oral microbial infusions, phase 1 of post-infusive behavioural analysis showed the presence of cognitive impairment in the experimental groups who received oral infusions. Formed cognitive impairment is reverted with the help of *L. acidophilus* oral infusion in phase 2 of post-infusive analysis. Comparative three-step behavioural analysis proved that *Pseudomonas aeuroginosa* induced cognitive impairment may revert to normal conditions with the help of *L. acidophilus*. The outcome of the present study proves that cognitive impairment developed due to poor oral hygiene can be treated with the help of probiotic microorganisms.

* Corresponding author

E-mail: mukilan@srcas.ac.in (Murugan Mukilan)

Peer review under responsibility of Journal of Experimental Biology and Agricultural Sciences.

Production and Hosting by Horizon Publisher India [HPI]
(<http://www.horizonpublisherindia.in/>).
All rights reserved.

All the articles published by [Journal of Experimental Biology and Agricultural Sciences](#) are licensed under a [Creative Commons Attribution-NonCommercial 4.0 International License](#) Based on a work at www.jebas.org.



1 Introduction

Learning and memory formation (LMF) plays a major role in developing cognitive functions during repeated exposure to a non-harmful/harmful stimulus (Bisaz et al. 2014; Abraham et al. 2019; Mukilan 2023). Repeated exposure to this stimulus results in brain neuronal circuit changes. Changes in brain neuronal circuits happen during short-term memory (STM) formation and long-term memory (LTM) formation due to LMF. In LMF, STM formation uses existing proteins for memory formation, which lasts 24 hours. Compared to STM, LTM formation employs a unique neuronal signaling pathway for the acquaintance of information and its storage in different brain regions for a long period (throughout the life span) (Abraham et al. 2019; Evans et al. 2021; Lin et al. 2021; Mukilan 2023). Formation of LTM uses RNA-dependent protein synthesis machinery along with pre and post-synaptic neurons. This LTM formation begins with repeated exposure to a particular defined stimulus for a limited time in subsequent days. As a result of exposure, pre-synaptic neurons (PrSN) release specific neurotransmitters into the synaptic cleft (SC). Released neurotransmitters bind to specific receptors of post-synaptic neurons (PoSN) and trigger the activation of cyclic adenosine monophosphate (cAMP) (Bai and Suzuki 2020; Lin et al. 2021). Further upregulated cAMP activates protein kinase A (PKA) and enzyme-regulated kinase 1/2 (ERK-1/2). Activated ERK-1/2 molecules may add phosphate molecules to the cAMP response element binding protein-1 (CREB-1) for its activation. Further phosphorylated and activated CREB-1 initiates the induction of immediate-early genes (especially *Egr-1*, *C-fos*, and *C-jun*) responsible for forming post-synaptic density proteins. Cumulative expression of these neuronal signaling proteins results in the LTM formation (Ganesh et al. 2010; Rajan et al. 2011; Ganesh et al. 2012; Mendez et al. 2015; Mukilan et al. 2015; Mukilan et al. 2018a; Thangaleela et al. 2018; Mukilan 2023). This formed LTM is majorly impaired due to stress, gut-microbiota dysbiosis, and poor oral hygiene (Evans et al. 2021; Lin et al. 2021; Dai et al. 2022; Mukilan 2023).

In healthy individuals, oral and intestinal microbiotas play a major role in regulating the homeostasis mechanism of an endocrine and neural system through the central nervous system (CNS) (Luca et al. 2018; Ma et al. 2019; Myers Jr et al. 2021). The homeostasis state of the host is majorly disturbed by chronic stress (CS)/pathogenic infection (PI). This CS increases corticotrophin-releasing hormones (CRH) in the bloodstream through the hypothalamic-pituitary-adrenal axis (HPA). Produced CRH released from the axon terminals may stimulate the production of endotoxins (ET) in the gut (Herman et al. 2016; Fung et al. 2017; Misiak et al. 2020; Sheng et al. 2021; Hinds and Sanchez 2022). These ETs regulate the secretion of neurotransmitter precursor compounds responsible for gut

microbiota interaction with CNS (Strandwitz 2018; García-Cabrerizo et al. 2021; Salami 2021; Miri et al. 2023). Later on, secreted neurotransmitter precursor compounds are transported to the brain (CNS) from the gut via the vagus nerve. The PrSN uses transported precursor compounds to produce brain neurotransmitters like 5-hydroxytryptamine (5-HT). Synthesized 5-HT released into the SC results in the binding with PoSN and activates the CREB-mediated neuronal signaling pathway (CMNSP). Activated CMNSP may further result in the formation of LTM (Mukilan et al. 2015; Mukilan et al. 2018b; Thangaleela et al. 2018; Mukilan 2022; Mukilan 2023).

An imbalance in this CMNSP results in the development of cognitive memory impairment/neurodegeneration. Recent studies have proved that stress formation may result in the induction of impaired cognitive dysfunction along with gut/oral dysbiosis. Thus, the formed cognitive decline may be reversed with the intake of live probiotic microorganisms along with diet may block the release of endotoxins (Wong et al. 2018; Angelucci et al. 2019; Asl et al. 2019; Bermúdez-Humarán et al. 2019; Morshedi et al. 2020; Naomi et al. 2022). Earlier reports from our group showed that poor oral hygiene plays an important role in forming declined cognitive functions via the oral administration of microorganisms (Mukilan 2023). In the present study, we predicted that probiotic microorganisms may participate in reversing the microorganism-induced cognitive impairment by suppressing ET. Goldfish were subject to the three-step behavioural analysis with the infusions of isolates and probiotic microorganisms through the oral passage to test the hypothesis.

2 Materials and Methods

2.1 Study Animals and Home Tank Design

Commercially available naïve adult goldfish *Carassius auratus* (Mean length: 6.5 – 8 cm, and weight 6 – 15 g) were purchased from a local aquarium of P.N. Palayam, Coimbatore, Tamil Nadu, India. After purchase, animals were carefully examined for non-microbial colonization in the skin and housed in home tanks as groups (n = 6/group). The aquarium (glass rectangular tank with a length, breadth, and height of 42 X 30 X 21 inches) was provided with continuous air circulation, temperature (26 ± 2° C), and light: dark cycle (12: 12 hours). Commercial dry round food pellets (Taiyo Pet Products Pvt. Ltd., India) were provided twice a day (9.00 and 18.00 h) at their aquarium on alternative days, and the aquarium was routinely cleaned and replaced with pure water to maintain dissolved oxygen level and dust free environment. Fishes were identified according to their phenotypic/morphological differences. The study design and experimental protocol follow the institutional animal care guidelines of Sri Ramakrishna Institutions, Coimbatore, Tamil Nadu, India.

2.2 Study Design and Experimental Setup (ES)

The experimental chamber was separated into three different parts as per the need of the study. These three chambers include two feeding chambers (FC) and one central chamber (CC). Each FC had a LBH of 6 X 30 X 21 inches with a central opening, and CC had a LBH of 30 X 30 X 21 inches. In the two FCs, one FC is designated for positive (with food reward), and the other is for negative chambers (without food reward). The FC's central opening facilitates the fish's movement into the positive and negative reward chambers. Developed ES was used for pre-infusive and post-infusive behavioural analysis (Figure 1).

2.3 Behavioural study

2.3.1 Experimental Groups (EGs)

Fishes were randomly separated into four different groups. These are control (C), Group 1 (G - 1) received oral infusions of *Pseudomonas aeruginosa*, Group - 2 (G - 2) received oral infusions of *Bacillus subtilis*, and Group - 3 (G - 3) received oral infusions of *Escherichia coli* during post-infusive behavioural analysis (phase - 1). Infused groups (G - 1, 2, and 3) received oral infusions of *Lactobacillus acidophilus* after completion of phase - 1 post-infusive analysis.

2.3.2 Reward-Based Learning (RBL)

Reward-based learning used in this study was followed to understand the development of cognitive memory formation with

the help of color cues. During the training phase, individuals were trained to use blue and red color cues at the opposite sides of the experimental chamber. FC with a blue color cue acts as a positive chamber with a food reward, and FC with a red color cue acts as a negative chamber without a food reward.

2.4 Microbial Cultures Used

Three isolates used in the present study (*P. aeruginosa*, *B. subtilis*, and *E. coli*) were availed on request from the PSG Institute of Medical Sciences & Research (PSG IMSR). Probiotic strain *L. acidophilus* (MTCC No. 10307) was received from MTCC, IMTECH, Chandigarh, Punjab, India.

2.5 Purity Confirmation and Oral Infusion Mixture Preparation

Pure culture was isolated on a nutrient agar medium with the help of simple streak and quadrant streak methods for the isolates and probiotic strains. Once the purity was confirmed, an individual probiotic colony (IPC) was selected from quadrant-streaked nutrient agar plates. Selected IPC again streaked on *Lactobacillus* MRS Agar plates for further confirmation. Later on, from the quadrant plates individual colonies were picked up and used for the arousal of overnight cultures of isolates and probiotic strains. Nutrient broth and MRS broth were used to grow the overnight culture. Grown overnight cultures were used to prepare the oral infusion mixture and phosphate buffer saline (PBS) in a ratio of 50:50 (Mukilan 2023).

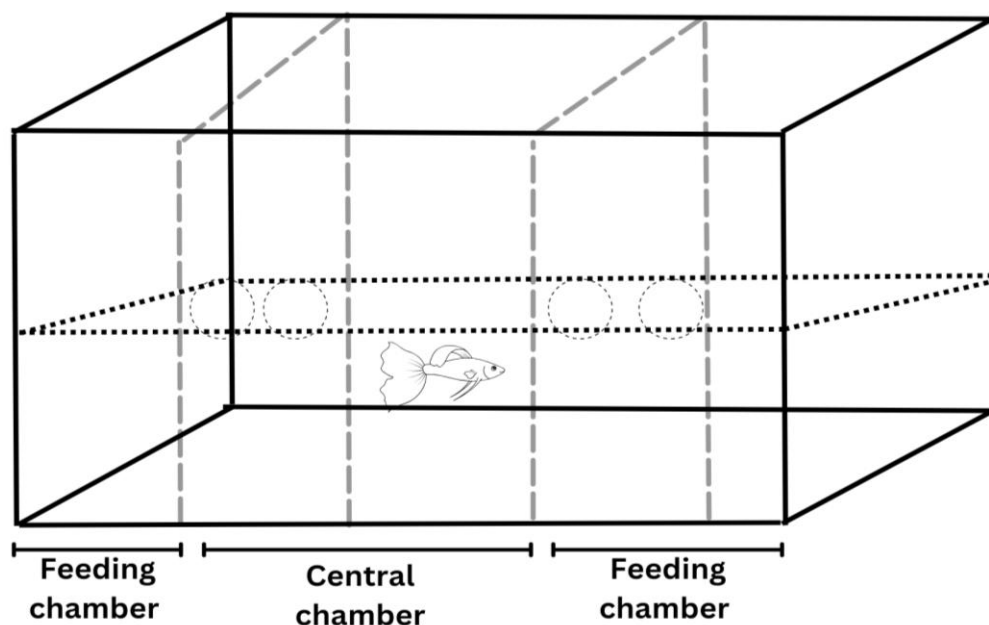


Figure 1 Diagrammatic representation of the experimental setup (ES) used to test cognitive functions development in the three-step behavioural analysis. Represented ES consists of one central chamber (CC) and two feeding chambers [right chamber (RC) and left chamber (LC)].

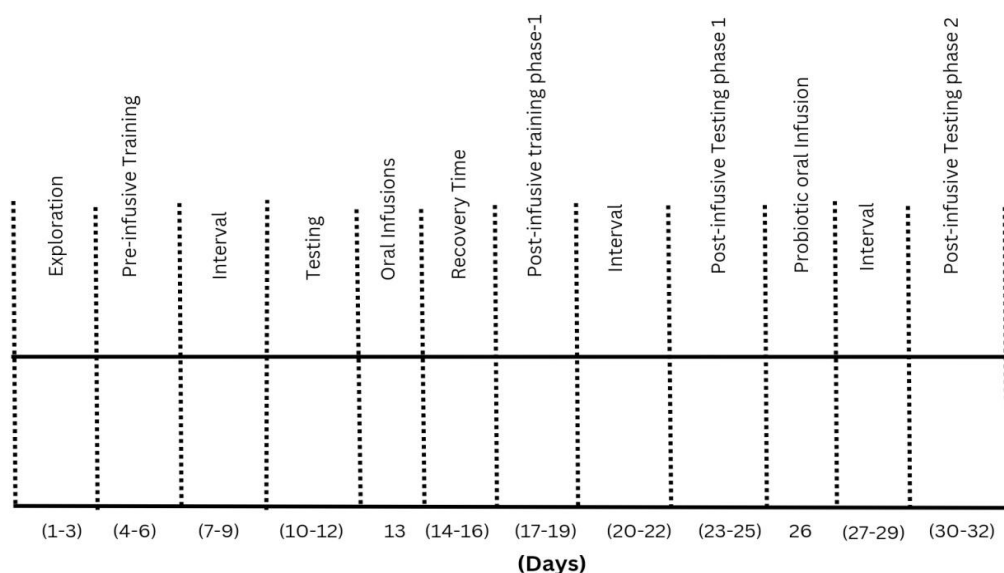


Figure 2 Line diagram showing the experimental time period of the three-step behavioural analysis used in this present study

2.6 Behavioural Analysis

Three-step behavioural analysis was designed for the study, consisting of one pre-infusive and two post-infusive analyses (Phases 1 and 2). The timeline followed for the behavioural study is shown in Figure 2.

2.6.1 Pre-infusive Behavioural Analysis (PrBA)

Experimental groups of EGs were allowed to stay in the aquarium to adapt to the laboratory conditions for 3 days during the habituation process. In the exploration phase, EGs were acquainted with the experimental setup for 3 days between days 1 – 3. Followed by exploration, training, and testing phase takes place in the ES in two different time intervals (4-6 days and 10-12 days). Further 72 hours of interval (3 days) was given between the training and testing phase for memory consolidation (Mukilan 2023).

2.6.2 Post-infusive Behavioural Analysis (PoBA)

Post-infusive behavioural analysis (PoBA) was carried out for the three EGs (Groups – 2, 3, and 4) after the completion of PrBA. On day 13th, oral infusion mixtures of isolates (*P. aeruginosa*, *E. coli*, and *B. subtilis*) were infused into respective EGs. Oral infusions were given into respective EGs with the help of an oral gauge. An interval period of 72 hours (Days 13 – 15) was given to infused EGs for their transportation to the gut (Mukilan 2023).

2.7 Statistical Analysis

Behavioural responses of four EGs (pre-infusive and post-infusive analysis) are plotted as a bar graphical representation with the help of KyPlot (Version 5.0).

3 Results

The present study employs a three-step behavioural analysis to prove a serene environment's role in forming cognitive memory. Three-step behavioural analysis showed the impact of a stress-free environment, oral infusions of isolates (*P. aeruginosa*, *B. subtilis*, and *E. coli*), and probiotic strain (*L. acidophilus*) on cognitive memory formation. Behavioural studies consist of one PrBA and two phases of PoBA (Phases 1 and 2).

3.1 Impact of stress-free habituated environment on cognition

Initially, the role of a stress-free environment was tested against cognitive learning and memory formation with the help of PrBA. PrBA consists of three different kinds of behavioural scores taken up from the exploration (Days 1-3), training (Days 4-6), and testing (Days 10-12) periods in the ES. In pre-infusive behavioural analysis, behavioural scores showed that animals spent more time in CC than the two FCs [LC and RC]. Exploration data revealed that animals were active in the ES. All experimental groups were allowed to explore the three chambers present in the ES with the help of brain navigation without color cues (Figure 3).

The training phase of the PrBA showed that all experimental groups (n = 6/group) tried to learn the presence of positive cues (blue color) based on reward-based learning. Behavioural scores of the training phase showed that animals learned about both positive and negative stimuli during the training period (Days 4 - 6). On day 4, the number of entries to the positive chamber was low compared to the negative chamber; later on, it got reversed due to learning of provided information/stimuli. Cumulative behavioural

scores showed a decrease in time spent in CC compared to the time spent in the FC. When comparing the time spent in each FC, RC has more attempts/time spent due to reward-based learning (Figure 4).

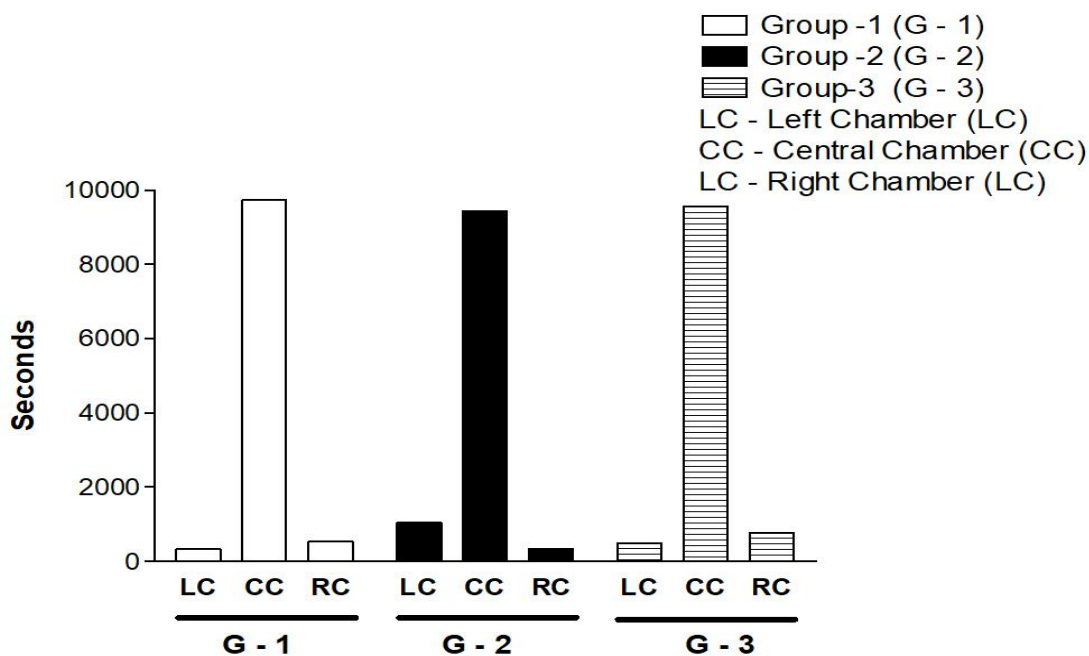


Figure 3 Behavioural scores of the exploration phase (Pre-injusive behavioural analysis) showed that animals spent more time in the central chamber (CC) compared to the left chamber (LC), and right chamber (RC). The outcome of the exploration phase stated that animals were active and tried to explore both LC and RC of the experimental setup (ES) in a serene habituated environment.

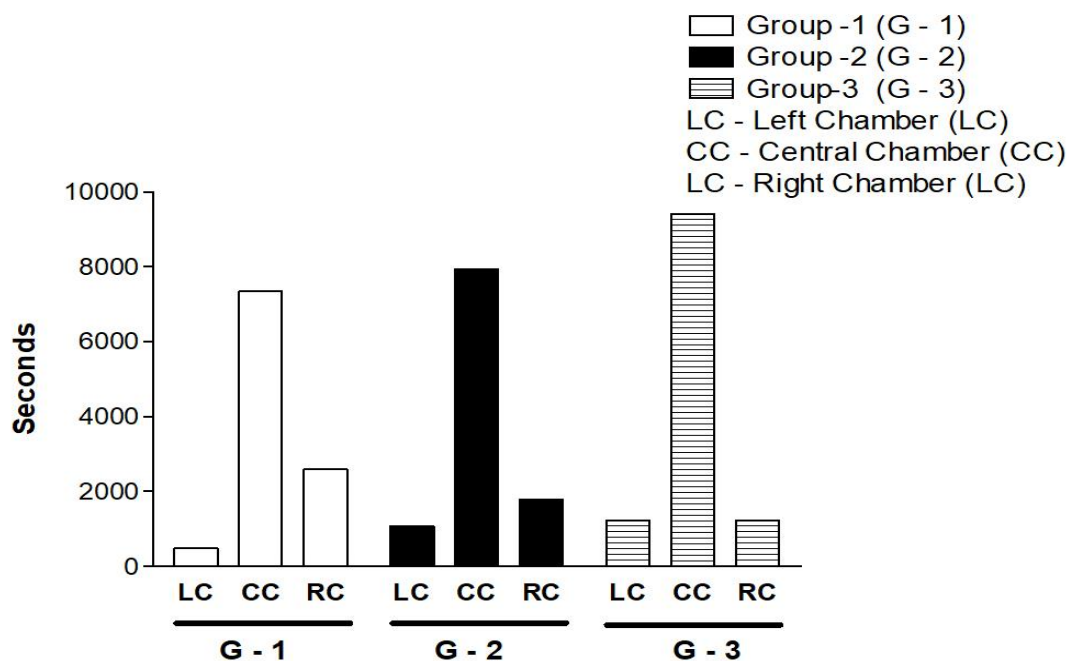


Figure 4 Training phase of the pre-injusive behavioural analysis showed that the experimental animals tried to learn the presence of positive cues based on reward-based learning. Behavioural scores of the training phase (pre-injusive analysis) showed that during the training period (Days 4 -6) animals learned about the positive and negative stimuli. During the training phase, time spent in the CC gradually decreased compared to the amount of time spent in the FC (LC, and RC).

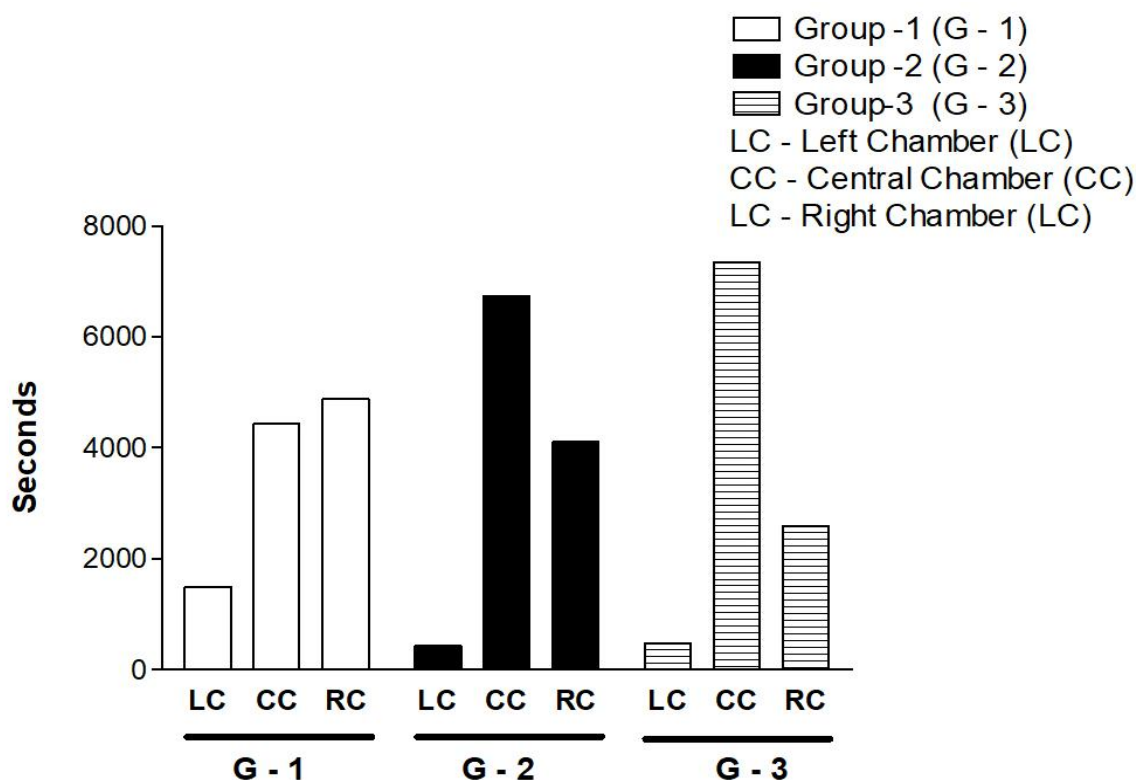


Figure 5 Pre-infusive testing phase showed that animals learned about the positive and negative stimuli; and were able to retrieve the learned information during the testing phase. Compared to the training phase, the identification of positive stimuli was high compared to the negative stimuli identification. Identification of negative stimuli was gradually decreased in the days – 2, and 3 of testing.

After the PrBA training phase, all experimental groups were given an interval period of three days. Three days of time interval is given to consolidate learned information in the brain. Testing was done between days 10 – 12 to test the retrieval of learned information. Behavioural responses of the testing phase showed that correct choices were high compared to the PrBA training period. Thus, it was proved that there was no hindrance in developing cognitive functions during pre-infusive behavioural studies (without any infusions) (Figure 5).

3.2 Role of *P. aeruginosa*, *B. subtilis*, and *E. coli* oral infusions on the development of cognitive impairment

Before PoBA, all desired microorganisms, including three isolates (*P. aeruginosa*, *B. subtilis*, and *E. coli*) and one probiotic strain (*L. acidophilus*), were streaked on the nutrient agar medium to confirm the purity of microorganisms used in the study by the use of simple and quadrant streaking method. For *Lactobacillus* strain confirmation, the individual colony was again streaked on the *Lactobacillus* MRS agar plates for double confirmation from the nutrient agar plate. After purity confirmation, three isolates were used to prepare an overnight culture with the specified volume of 5 ml (Figure 6). Later, overnight-grown cultures were mixed with PBS in the ratio of 50:50 as oral infusion mixtures. Prepared oral

infusion mixtures were given to the animal with the help of an oral gauge on day 13. After infusions, an interval of 72 hours was given to transport oral infusion toward the gut of animals (Days 14 – 16).

PoBA Phase 1 analysis was done after the completion of interval time from day 17. In the first phase of PoBA, training (Days 17 – 19) and testing (Days 23-25) were done for three infused groups that received oral microbial infusions of *P. aeruginosa*, *B. subtilis*, and *E. coli*. Behavioural scores of the training period showed that oral microbial infusions do not impact the brain homeostasis mechanism (Figure 7). Followed by training, testing was done between days 23 – 25 which showed the impairment in the memory retrieval from brain regions. Behavioural scores of PoBA testing phase 1 showed increased response in CC and decreased response in RC. Decreased response in RC showed memory retrieval imbalance in the experimental group treated with *P. aeruginosa* (Figure 8). Memory retrieval may be impaired due to microbial metabolite transport from the gut to the brain through BBB. Excess amounts of enterotoxin present in this microbial metabolite may inhibit the growth and proliferation of beneficial bacteria. Inhibition of beneficial bacterial proliferation may decrease the synthesis of neurotransmitter precursor compounds responsible for the brain neurotransmitter synthesis. The least amount of neurotransmitter synthesis results in impaired LTM formation.

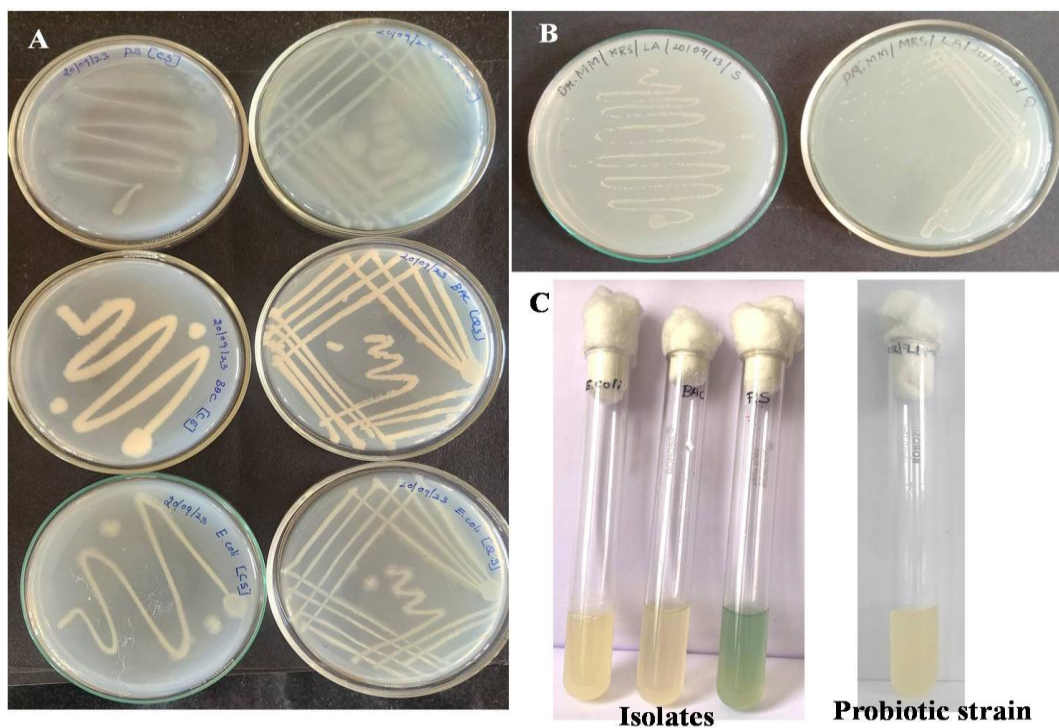


Figure 6 Representative plate photographs showing the purity of isolates and probiotic strain used in the present study. All four microorganisms [Three isolates (*P. aeruginosa*, *B. subtilis*, and *E.coli*) and one probiotic strain (*L. acidophilus*)] were streaked in nutrient agar medium by the way of simple and quadrant streaking method. For lactobacillus strain confirmation, an individual colony of lactobacillus was streaked on lactobacillus MRS medium for its double confirmation from the nutrient agar plate.

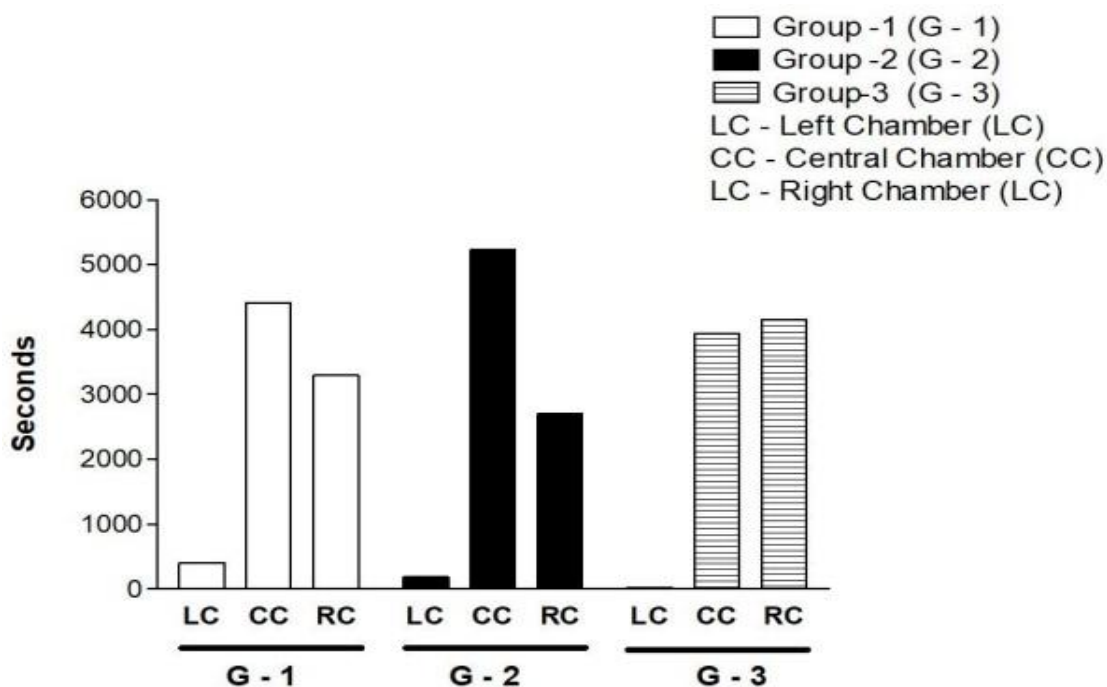


Figure 7 The training phase of post-infusive behavioural analysis (phase -1) showed that oral infusions of *P. aeruginosa*, *B. subtilis*, and *E.coli* do not have an impact on the animal learning abilities. Behavioural scores of the training period showed that there is no imbalance in homeostasis mechanisms due to oral infusions of isolates.

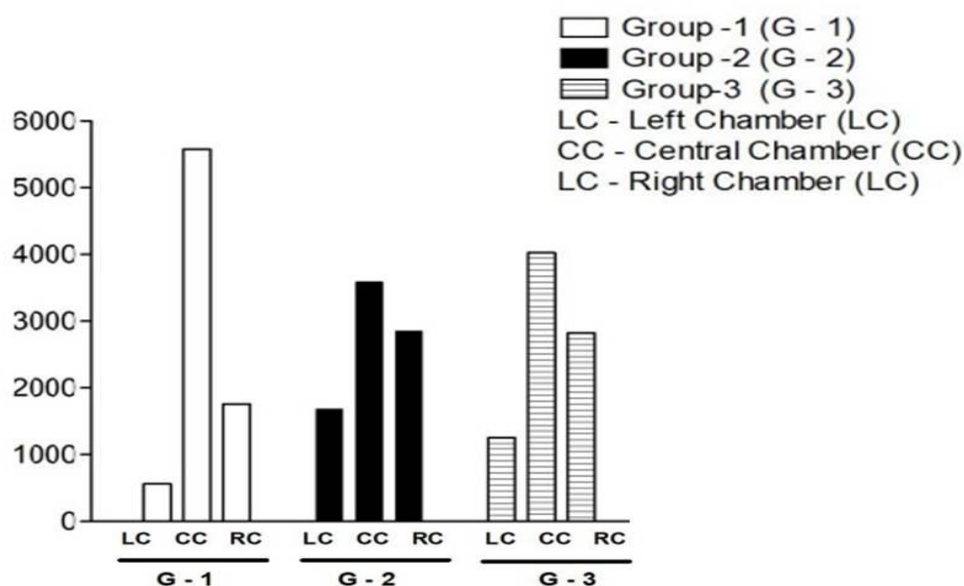


Figure 8 The testing phase of post-infusive behavioural analysis (phase -1) showed that oral infusions of *P. aeruginosa*, *B. subtilis*, and *E.coli* have an impact on information processing and memory retrieval in the experimental groups.

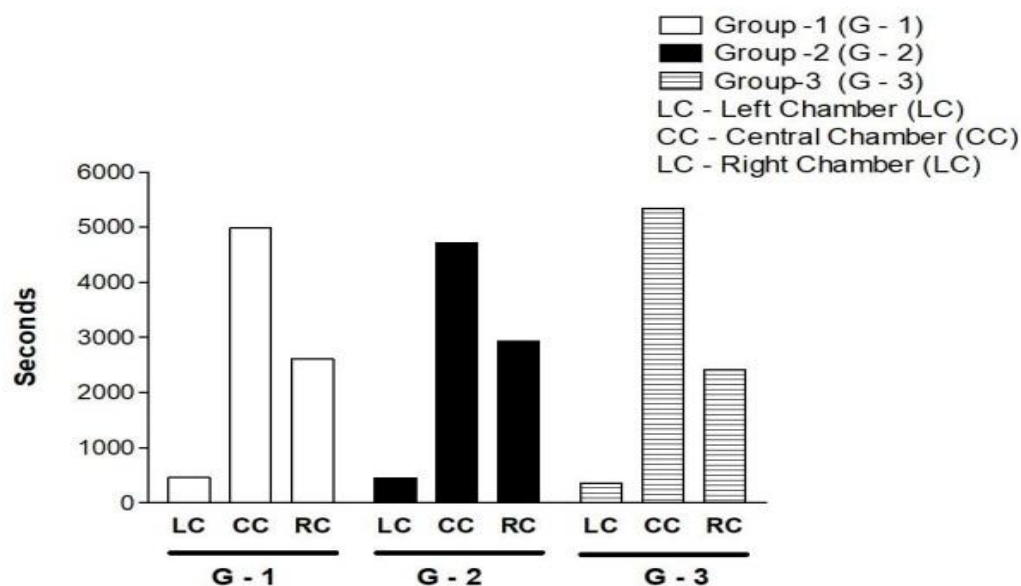


Figure 9 Post-infusive testing phase - 2 showed that probiotic infusion (*L. acidophilus*) reversed the oral infusions induced cognitive impairment. During testing, the number of correct responses was high compared to wrong responses, which shows the recovery of cognitive impairment.

3.3 Reversal of microbial metabolite-induced cognitive impairment using the probiotic strain (*L. acidophilus*)

To identify the role of *L. acidophilus* in the reversal of cognitive impairment, PoBA Phase -2 was carried out between days 30 – 32. Experimental behavioural scores proved that probiotics reversed microbial metabolite-induced cognitive impairment (LTM impairment). In the Phase -2 testing, the number of responses

towards the correct responses increased like the Phase -1 training. Other than that, the number of wrong choices also concerned PrBA testing. The resulting outcome showed that the number of correct and wrong choices resembled the same as the testing phase of a stress-free environment (PrBA). Thus, from the PoBA Phase 2 testing study, this study proved that the probiotic strain (*L. acidophilus*) reversed the *P. aeruginosa*-induced cognitive impairment (Figure 9).

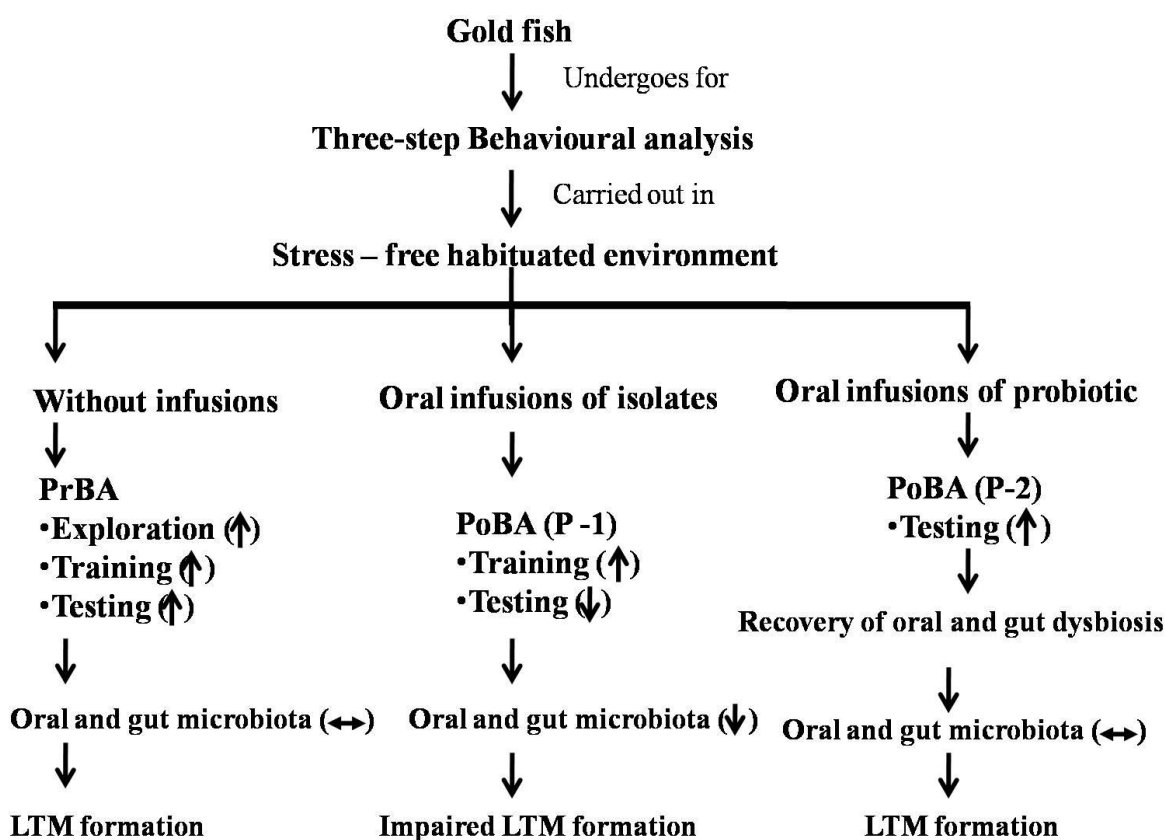


Figure 10 Flow-diagram showing the role of oral and gut microbiota in the development of LTM formation

4 Discussion

In the gut-brain axis, gut microbiota plays (GM) a major role in the regulation of neurotransmitter production (Ma et al. 2019; Misiak et al. 2020; Sheng et al. 2021; Hinds and Sanchez 2022; Mukilan 2023). This GM consists of microorganisms like bacteria, viruses, and fungi and these microbiotas may control intestinal hydrogen ion concentration (pH), and inhibit the growth of infectious pathogens (IP) in the gut (Jiang et al. 2017; Kaczmarek et al. 2017; Gentile and Weir 2018; Hillemaicher et al. 2018; Savin et al. 2018; Ng et al. 2023). Growth inhibition of IP results in the development of a healthy state (HS) via probiotic treatment. Further, HS will show the mutual exchange and regulation of neurotransmitter precursor compounds (NPC) and enterotoxin (ET) (Aponte et al. 2020; Piatek et al. 2020; Raheem et al. 2021; Shandilya et al. 2022; Mazziotta et al. 2023). In the brain, these transported NPC from the gut used for the synthesis of neurotransmitters like serotonin (5-HT), γ -aminobutyric acid (GABA), dopamine (DA), and noradrenaline (NA) (Chen et al. 2017; O'Donnell et al. 2020; Shandilya et al. 2022; Mazziotta et al. 2023). These synthesized neurotransmitters may positively regulate the calcium influx (CI), adenylyl cyclase (AC), PKA, and cAMP levels in a stress-free environment. Regulation of these abovementioned molecules

results in the phosphorylation of CREB followed by the activation of IEGs and PSD proteins (Mukilan et al. 2015; Mukilan et al. 2018a; Thangaleela et al. 2018; Mukilan 2023). However, an imbalance in the regulation and phosphorylation of these neuronal signaling molecules may result in cognitive memory decline. Formed cognitive memory decline was a result of reduced synaptic plasticity formation (Ganesh et al. 2012; Preethi et al. 2012; Mukilan et al. 2015; Ortega-Martínez 2015; Sen et al. 2017; Mukilan et al. 2018b; Thangaleela et al. 2018; Mukilan 2023).

This memory impairment may occur due to oral/gut dysbiosis. These oral and gut dysbiosis shows an increase in pathogenic microorganisms and a decrease in beneficial microorganisms (Orr et al. 2020; Sarkar et al. 2020; Lotz et al. 2021; Park and Wu 2022; Da et al. 2023; Jemimah et al. 2023). Recently, it was reported that oral infusions of *P. aeruginosa*, *B. subtilis*, *S. aureus*, and *E. coli* impact cognitive memory development. Recent reports showed that probiotic microorganisms may be a potential agent to increase synaptic plasticity development by regulating ET. During cognitive impairment, there is a reduced expression of neuronal signaling molecules due to the transport of an excess amount of ET from the enteric nervous system to the central nervous system (Aponte et al. 2020; Piatek et al. 2020; Raheem et al. 2021; Shandilya et al. 2022;

Mazziotta et al. 2023). This condition may be reversed with the help of short-chain fatty acids (SCFA). Production of SCFA may be regulated by the probiotic organisms present in the gut. These SCFAs will interact with the ET produced by the IP. As a result of interaction, there is a regulation of infectious pathogens and ET levels through the blood-brain barrier (Daliri et al. 2018; Asadpoor et al. 2021; Ma et al. 2022; Qian et al. 2022; Ney et al. 2023). Regulation of ET results in the reduction of memory impairment through the expression recovery of neuronal signaling molecules involved in CMNSP (Ganesh et al. 2012; Preethi et al. 2012; Mukilan et al. 2015; Ortega-Martínez 2015; Sen et al. 2017; Mukilan et al. 2018a; Thangaleela et al. 2018; Mukilan 2023). The present study tried to elucidate the effect of probiotic microorganisms against the reversal of cognitive impairment. Initially, cognitive impairment was induced by the oral infusion of periodontic microorganisms, like *P. aeruginosa*, *B. subtilis*, and *E.coli*. Later, reversals of cognitive impairments were proved by infusing probiotic microorganisms into the impaired experimental groups. Ongoing studies in our lab may identify the impact of ET on cognitive memory formation through its transportation via the blood-brain barrier (BBB).

Conclusion

The present study proved probiotic microorganisms' role in retrieving induced cognitive memory decline through oral administration. The study's outcome showed that improper oral hygiene caused by microbiota imbalance can be reverted back into normal conditions with the help of probiotic supplementations. Experimental results also showed that enterotoxin produced by infectious pathogens may inhibit the formation of neurotransmitter precursor compounds and block its transportation from the gut to the brain through the blood-brain barrier. Three-step behavioural analysis showed impaired memory development occurred in the infused groups compared to the control initially. Later on, impaired cognition was reversed with the oral infusions of probiotics. Retrieval of impaired cognition may happen due to the transmission of microbial precursor compounds from the gut to the brain through the blood-brain barrier (BBB). Thus, the present study proved the role of probiotic oral microbial infusions on the development of cognitive memory. The overall outcome of the study showed that improper oral hygiene played a crucial factor in the development of cognitive dysfunction through the gut-brain axis.

Acknowledgements

MM thanks the Indian Institute of Technology (IIT), Kharagpur (KGP), India (IN), for the Institutional Post-Doctoral Fellowship (IIT/ACD(PGS&R)/PDF/Offer/2018-2019/AT), Tamilnadu State Council for Science and Technology for the Student Project Scheme (TNSCST/SPS/2021-2022/MS-320), and DST-FIST (SR/FST/COLLEGE-/2022/1203) for the financial support.

Author Contributions

MM performed the conceptualization, research design, funding acquisition, original investigation, draft preparation, review and editing of the manuscript. MTAM, SY, and VM did the experiment performance and data collection.

References

- Abraham, W.C., Jones, O.D., & Glanzman, D.L. (2019). Is plasticity of synapses the mechanism of long-term memory storage? *Npj Science of learning*, 4, 9.
- Angelucci, F., Cechova, K., Amlerova, J., & Hort, J. (2019). Antibiotics, gut microbiota, and Alzheimer's disease. *Journal of Neuroinflammation*, 16, 108.
- Aponte, M., Murru, N., & Shoukat, M. (2020). Therapeutic, Prophylactic, and Functional Use of Probiotics: A Current Perspective. *Frontiers in Microbiology*, 11, 562048.
- Asadpoor, M., Ithakisiou, G., Henricks, P.A., Pieters, R., et al. (2021). Non-Digestible Oligosaccharides and Short Chain Fatty Acids as Therapeutic Targets against Enterotoxin-Producing Bacteria and Their Toxins. *Toxins*, 13, 175.
- Asl, Z.R., Sepehri, G., & Salami, M. (2019). Probiotic treatment improves the impaired spatial cognitive performance and restores synaptic plasticity in an animal model of alzheimer's disease. *Behavioural Brain Research*, 376, 112183.
- Bai, Y., & Suzuki, T. (2020). Activity-Dependent Synaptic Plasticity in *Drosophila melanogaster*. *Frontiers in physiology*, 11, 161.
- Bermúdez-Humarán, L.G., Salinas, E., Ortiz, G.G., Ramirez-Jirano, L.J., et al. (2019). From Probiotics to Psychobiotics: Live Beneficial Bacteria Which Act on the Brain-Gut Axis. *Nutrients*, 11, 890.
- Bisaz, R., Travaglia, A., & Alberini, C.M. (2014). The neurobiological bases of memory formation: from physiological conditions to psychopathology. *Psychopathology*, 47, 347-356.
- Chen, D., Yang, X., Yang, J., Lai, G., et al. (2017). Prebiotic effect of fructooligosaccharides from *Morinda officinalis* on alzheimer's disease in rodent models by targeting the microbiota-gut-brain axis. *Frontiers in Aging Neuroscience*, 9, 403.
- Da, D., Zhao, Q., Zhang, H., Wu, W., et al. (2023). Oral microbiome in older adults with mild cognitive impairment. *Journal of Oral Microbiology*, 15, 2173544.
- Dai, W., Liu, J., Qiu, Y., Teng, Z., et al. (2022). Gut Microbial Dysbiosis and Cognitive impairment in Bipolar Disorder: Current Evidence. *Frontiers in Pharmacology*, 13, 893567.

- Daliri, E.B., Tango, C.N., Lee, B.H., & Oh, D. (2018). Human microbiome restoration and safety. *International Journal of Medical Microbiology*, *30*, 487-497.
- Evans, H.T., Blackmore, D., Götz, J., & Bodea, L. (2021). *De novo* proteomic methods for examining the molecular mechanisms underpinning long-term memory. *Brain Research Bulletin*, *169*, 94-103.
- Fung, T.C., Olson, C.A., & Hsiao, E.Y. (2017). Interactions between the microbiota, immune and nervous systems in health and disease. *Nature Neuroscience*, *20*, 145-155.
- Ganesh, A., Bogdanowicz, W., Balamurugan, K., Marimuthu, G., & Rajan, K.E. (2012). Egr-1 antisense oligodeoxynucleotide administration into the olfactory bulb impairs olfactory learning in the greater short-nosed fruit bat *Cynopterus sphinx*. *Brain Research*, *1471*, 33-45.
- Ganesh, A., Bogdanowicz, W., Haupt, M., Marimuthu, G., & Rajan, K.E. (2010). Role of olfactory bulb serotonin in olfactory learning in the greater short-nosed fruit bat, *Cynopterus sphinx* (Chiroptera: Pteropodidae). *Brain Research*, *1352*, 108-117.
- García-Cabrerizo, R., Carbia, C., Óriordan, K.J., Schellekens, H., & Cryan, J.F. (2021). Microbiota-gut-brain axis as a regulator of reward processes. *Journal of Neurochemistry*, *157*, 1495-1524.
- Gentile, C.L., & Weir, T.L. (2018). The gut microbiota at the intersection of diet and human health. *Science*, *362*, 776-780.
- Herman, J., McKlveen, J.M., Ghosal, S., Kopp, B., et al. (2016). Regulation of the Hypothalamic-Pituitary-Adrenocortical Stress Response. *Comprehensive Physiology*, *6*, 603-621.
- Hillemacher, T., Bachmann, O., Kahl, K.G., & Frieling, H. (2018). Alcohol, microbiome, and their effect on psychiatric disorders. *Progress in Neuropsychopharmacology and Biological Psychiatry*, *85*, 105-115.
- Hinds, J.A., & Sanchez, E.R. (2022). The Role of the Hypothalamus-Pituitary-Adrenal (HPA) Axis in Test-Induced Anxiety: Assessments, Physiological Responses, and Molecular Details. *Stresses*, *2*, 146-155.
- Jemimah, S., Chabib, C.M.M., Hadjileontiadis, L., & Alshehhi, A. (2023). Gut microbiome dysbiosis in Alzheimer's disease and mild cognitive impairment: A systematic review and meta-analysis. *PLOS ONE*, *18*, e0285346.
- Jiang, C., Li, G., Huang, P., Liu, Z., & Zhao, B. (2017). The gut microbiota and alzheimer's disease. *Journal of Alzheimer's Disease*, *58*, 1-15.
- Kaczmarek, J.L., Thomps, S.V., & Holscher, H.D. (2017). Complex interactions of circadian rhythms, eating behaviours, and the gastrointestinal microbiota and their potential impact on health. *Nutrition Reviews*, *75*, 673-682.
- Lin, H., Chen, C., deBelle, J.S., Tully, T., & Chiang, A. (2021). CREB A and CREB B in two identified neurons gate long-term memory formation in *Drosophila*. *Proceedings of the National Academy of Sciences of the United States of America*, *118*, e2100624118.
- Lotz, S.K., Blackhurst, B.M., Reagin, K.L., & Funk, K.E. (2021). Microbial Infections Are a Risk Factor for Neurodegenerative Diseases. *Frontiers in Cellular Neuroscience*, *15*, 691136.
- Luca, C.D., Colangelo, A.M., Alberghina, L., & Papa, M. (2018). Neuro-Immune Hemostasis: Homeostasis and Diseases in the Central Nervous System. *Frontiers in Cellular Neuroscience*, *12*, 459.
- Ma, J., Piao, X., Mahfuz, S., Long, S., & Wang, J. (2022). The interaction among gut microbes, the intestinal barrier and short chain fatty acids. *Animal Nutrition*, *9*, 159-174.
- Ma, Q., Xing, C., Long, W., Wang, H.Y., Liu, Q., & Wang, R. (2019). Impact of microbiota on central nervous system and neurological diseases: the gut-brain axis. *Journal of Neuroinflammation*, *16*, 53.
- Mazziotta, C., Tognon, M., Martini, F., Torreggiani, E. & Rotondo, J.C. (2023). Probiotics Mechanism of Action on Immune Cells and Beneficial Effects on Human Health. *Cells*, *12*, 184.
- Mendez, M., Arias, N., Uceda, S., & Arias, J.L. (2015). c-Fos expression correlates with performance on novel object and novel place recognition tests. *Brain Research Bulletin*, *117*, 16-23.
- Miri, S., Yeo, J., Abubaker, S., Hammami, R. (2023). Neuromicrobiology, an emerging neurometabolic facet of the gut microbiome? *Frontiers in Microbiology*, *14*, 1098412.
- Misiak, B., Łoniewski, I., Marlicz, W., Freydeca, W., et al. (2020). The HPA axis dysregulation in severe mental illness: can we shift the blame to gut microbiota. *Progress in Neuro-Psychopharmacology and Biological Psychiatry*, *102*, 109951.
- Morshedi, M., Saghafi-Asl, M., & Hosseinfard, E.S. (2020). The potential therapeutic effects of the gut microbiome manipulation by symbiotic containing-Lactobacillus plantarum on neuropsychological performance of diabetic rats. *Journal of Translational Medicine*, *18*, 18.

- Mukilan, M. (2022). Effect of Probiotics, Prebiotics and Synbiotic Supplementation on Cognitive Impairment: A Review. *Journal of Experimental Biology and Agricultural Sciences*, 10, 1-11.
- Mukilan, M. (2023). Impact of *Pseudomonas aeruginosa*, *Bacillus subtilis*, *Staphylococcus aureus*, and *Escherichia coli* Oral Infusions on Cognitive Memory Decline in Mild Cognitive Impairment. *Journal of Experimental Biology and Agricultural Sciences*, 11, 581-592.
- Mukilan, M., Bogdanowicz, W., Marimuthu, G., & Rajan, K.E. (2018a). Odour discrimination learning in the Indian greater short-nosed fruit bat (*Cynopterus sphix*): differential expression of *Egr-1*, *C-fos* and PP-1 in the olfactory bulb, amygdala and hippocampus. *Journal of Experimental Biology*, 221, jeb175364.
- Mukilan, M., Rajathej, D.M., Jeyaraj, E., Kayalvizhi, N., & Rajan, K.E. (2018b). MiR-132 regulated olfactory bulb proteins linked to olfactory learning in greater short-nosed fruit bat *Cynopterus sphinx*. *Gene*, 671, 10-20.
- Mukilan, M., Varman, D.R., Sudhakar, S., & Rajan, K.E. (2015). Activity-dependent expression of miR-132 regulates immediate early gene induction during olfactory learning in the greater short-nosed fruit bat, *Cynopterus sphinx*. *Neurobiology of Learning and Memory*, 120, 41-51.
- Myers Jr, M.G., Affinati, A.H., Richardson, N., & Schwartz, M.W. (2021). Central nervous system regulation of organismal energy and glucose homeostasis. *Nature Metabolism*, 3, 737-750.
- Naomi, R., Embong, H., Othman, F., Ghazi, H.F., et al. (2022). Probiotics for Alzheimer's Disease: A Systematic Review. *Nutrients*, 14, 20.
- Ney, L., Wipplinger, M., Grossmann, M., Engert, N., et al. (2023). Short chain fatty acids: Key regulators of the local and systemic immune response in inflammatory diseases and infections. *Open Biology*, 13, 230014.
- Ng, K.M., Pannu, S., Liu, S., Burckhardt, J.C., et al. (2023). Single-strain behavior predicts responses to environmental pH and osmolality in the gut microbiota. *mBio*, 14, e0075323.
- O'Donnell, M.P., Fox, B.W., Chao, P., Schroeder, F.C., & Sengupta, P. (2020). A neurotransmitter produced by gut bacteria modulates host sensory behaviour. *Nature*, 583, 415-420.
- Orr, M.E., Reveles, K.R., Yeh, C., Young, E.H., et al. (2020). Can oral health and oral-derived biospecimens predict progression of dementia? *Oral Diseases*, 26, 249-258.
- Ortega-Martínez S. (2015). A new perspective on the role of the CREB family of transcription factors in memory consolidation via adult hippocampal neurogenesis. *Frontiers in Molecular Neuroscience*, 8, 46.
- Park, S., & Wu, X. (2022). Modulation of the Gut Microbiota in Memory Impairment and Alzheimer's Disease via the Inhibition of the Parasympathetic Nervous System. *International Journal of Molecular Sciences*, 23, 13574.
- Piatek, J., Krauss, H., Ciecchelska-Rybarczyk, A., Bernatek, M., et al. (2020). In-Vitro Growth Inhibition of Bacterial Pathogens by Probiotics and a Synbiotic: Product Composition Matters. *International Journal of Environmental Research and Public Health*, 17, 3332.
- Preethi, J., Singh, H.K., Charles, P.D., Charles, P.D., & Rajan, K.E. (2012). Participation of microRNA 124-CREB pathway: a parallel memory enhancing mechanism of standardized extract of *Bacopa monniera* (BESEB CDRI-08). *Neurochemical Research*, 37, 2167-2177.
- Qian, X., Xie, R., Liu, X., Chen, S., & Tang, H. (2022). Mechanisms of Short-Chain Fatty Acids Derived from Gut Microbiota in Alzheimer's Disease. *Aging and Disease*, 13, 1252-1266.
- Raheem, A., Liang, L., Zhang, G., & Cui, S. (2021). Modulatory Effects of Probiotics using Pathogenic Infections With Emphasis on Immune Regulation. *Frontiers in Immunology*, 12, 616713.
- Rajan, K.E., Ganesh, A., Dharaneedharan, S., & Radhakrishnan, K. (2011). Spatial learning-induced egr-1 expression in telencephalon of gold fish *Carassius auratus*. *Fish Physiology and Biochemistry*, 37, 153-159.
- Salami, M. (2021). Interplay of Good Bacteria and Central Nervous System: Cognitive Aspects and Mechanistic Considerations. *Frontiers in Neuroscience*, 15, 613120.
- Sarkar, S.P., Mazumder, P.M., & Banerjee, S. (2020). Probiotics protect against gut dysbiosis associated decline in learning and memory. *Journal of Neuroimmunology*, 348, 577390.
- Savin, Z., Kivity, S., Yonath, H., & Yehuda, S. (2018). Smoking and the intestinal microbiome. *Archives of Microbiology*, 200, 677-684.
- Sen, T., Gupta, R., Kaiser, H., & Sen, N. (2017). Activation of PERK Elicits Memory Impairment through Inactivation of CREB and Downregulation of PSD95 After Traumatic Brain Injury. *The Journal of Neuroscience*, 37, 5900-5911.
- Shandilya, S., Kumar, S., Jha, N.J., Kesari, K.K., & Ruokolainen, J. (2022). Interplay of gut microbiota and oxidative stress: Perspective on neurodegeneration and neuroprotection. *Journal of Advanced Research*, 38, 223-244.

- Sheng, J.A., Bales, N.J., Myers, S.A., Bautista, A.I., et al. (2021). The Hypothalamic-Pituitary-Adrenal Axis: Development, Programming Actions of Hormones, and Maternal-Fetal Interactions. *Frontiers in Behavioral Neuroscience, 14*, 601939.
- Strandwitz, P. (2018). Neurotransmitter modulation by the gut microbiota. *Brain Research, 1693*, 128-133.
- Thangaleela, S., Shanmugapriya, S., Mukilan, M., Radhakrishnan, K., & Rajan, K.E. (2018). Alterations in MicroRNA-132/212 Expression Impairs Fear Memory in Goldfish *Carassius auratus*. *Annals of Neurosciences, 25*, 90-97.
- Wong, C.B., Kobayashi, Y., & Xiao, J. (2018). Probiotics for preventing cognitive impairment in alzheimer's disease. In A. Evrensel, & B.O. Ünsalver, (eds), Gut Microbiota, IntechOpen.



Journal of Experimental Biology and Agricultural Sciences

<http://www.jebas.org>

ISSN No. 2320 – 8694

Highlighting the Importance of Matrix Metalloproteinase 1, 8, and 9 Expression during the Progression of *Mycobacterium tuberculosis* Infection

Sasikumar Pitchaikani¹ , Murugan Mukilan^{2,3} , Pothiaraj Govindan¹ ,
Ganesan Kathiravan¹ , Harshavardhan Shakila^{1*} 

¹Department of Molecular Microbiology, School of Biotechnology, Madurai Kamaraj University, Madurai 625 021, Tamil Nadu, India.

²Advanced Technology Development Centre, Indian Institute of Technology, Kharagpur 721 302, West Bengal, India.

³Department of Biotechnology, Sri Ramakrishna College of Arts & Science, Coimbatore 641006, Tamil Nadu, India.

Received – December 08, 2023; Revision – February 17, 2024; Accepted – February 28, 2024

Available Online – March 15, 2024

DOI: [http://dx.doi.org/10.18006/2024.12\(1\).49.59](http://dx.doi.org/10.18006/2024.12(1).49.59)

KEYWORDS

Tuberculosis

Drug resistance TB

Matrix metalloproteinase

Antimicrobial resistance

ABSTRACT

Tuberculosis (TB) is one of the major threats to public health; annually it kills more than 1.5 million people around the globe. Tuberculosis is caused by an intracellular pathogen named *Mycobacterium tuberculosis* (*Mtb*). This *Mtb* enters the lung through the respiratory passage by inhalation in healthy individuals. Infection of this disease starts from the settlement of *Mtb* to the lung alveoli of the host from the external bacilli air droplets. After settlement, the multiplication of *Mtb* results in the induction of innate immunity through the alveolar macrophages. Compared to other infectious diseases, tuberculosis infection was transmitted rapidly by the infected aerosols released from infected persons to healthy persons through the air. After infection, disease development results in the formation of drug-resistance TB (DR-TB) with four subcategories, i.e. Single-drug resistant TB (SDR-TB), multi-drug resistant TB (MDR-TB), extensive drug-resistant TB (XDR-TB), and total-drug resistant TB (TDR-TB). As a result, this DR-TB may act as a major source of TB death due to spontaneous antimicrobial resistance (AMR). This AMR makes the anti-TB drugs ineffective. In the current scenario, researchers are trying to find the drug target to decrease tuberculosis progression instead of drug resistance. The present review reports that the outcome of research studies showed that matrix metalloproteinase (MMP) may act as a suitable target for treating *Mtb* infection with the help of specific proteinase inhibitors. Recent reports have shown the specific role of matrix metalloproteinases 1, 8, and 9 in the disease progression and its role in normal homeostasis mechanism with the help of specific animal models/*In vitro* models.

* Corresponding author

E-mail: mohanshakila@yahoo.com (Harshavardhan Shakila)

Peer review under responsibility of Journal of Experimental Biology and Agricultural Sciences.

Production and Hosting by Horizon Publisher India [HPI]
(<http://www.horizonpublisherindia.in/>).
All rights reserved.

All the articles published by [Journal of Experimental Biology and Agricultural Sciences](#) are licensed under a [Creative Commons Attribution-NonCommercial 4.0 International License](#) Based on a work at www.jebas.org.



1 Introduction

Infectious diseases like tuberculosis (TB), smallpox (SP), and polio (P) have been present since the evolution of humans, and these infectious diseases are primarily caused by *Mycobacterium tuberculosis* (*Mtb*), variola virus, and poliovirus, which will affect the lungs, skin, and brain stem respectively. Recent developments in vaccination technologies resulted in the maximal eradication of smallpox and polio disease development in the human population (Chai et al. 2018; Pollard and Bijker 2020; Kayser and Ramzan 2021; Sakai and Morimoto 2022). As a result, nowadays more attention is given to identifying effective drug targets for treating TB. At present, TB is ranked among the top 10 leading causes of death on a global scale and stands as the primary cause of death resulting from an infectious disease (Tiberi et al. 2018; Dartois and Rubin 2022; Singh 2023). During diseased conditions, the causative pathogen (CP) of *Mtb* spreads through the air when it is released by coughing or sneezing by the infected person. After release into the air, CP travels as an aerosol through the natural ventilation pattern (NVP). As a result of NVP, it reaches the lungs of an uninfected person through inhalation of aerosols. Once *Mtb* reaches the lung alveoli, it will try for multiplication with the help of the host system and colonize the lungs. Majorly the progression of TB occurs in the host system due to the weakening of the host immune response (Jones-López et al. 2016; Patterson and Wood 2019; Dartois and Rubin 2022; Singh 2023). In normal conditions, the progression of initial TB infection cannot be controlled easily, and it may advance to active primary disease (APD), particularly in children. Treatment of APD may result in partial control of *Mtb* progression, and further, it enters a latent state which further weakens the immune system. This progression was typically

triggered by the breakdown of granulomas and uncontrolled replication of *Mycobacteria*, leading to disease in the host system's primary and secondary organs (Figure 1). This *Mtb* infection and its progression may also depend on contact with the infected person, social, behavioural, and environmental factors like poor hygiene, alcohol consumption, pollution, and smoking (Lönmroth et al. 2009; Narasimhan et al. 2013; Bhargava et al. 2013; Chandrasekaran et al. 2017; Stewart et al. 2020; Dartois and Rubin 2022; Singh 2023). In the present review, we have shown the unexplored role of matrix metalloproteinases (MMPs) and their sub-classes in the progression of TB.

2 Role of *M. tuberculosis* pathogenesis in the development of tuberculosis

Tuberculosis (TB) is one of the leading causes of mortality spread by the transmission of *M. tuberculosis* (Adami and Cervantes 2015; Bloom et al. 2017; Bussi and Gutierrez 2019; Furin et al. 2019; Sia and Rengarajan 2019; Chai et al. 2020; Boom et al. 2021; Zhou et al. 2021). According to the reports of the Centers for Disease Control and Prevention (CDC), nearly 1.6 million people die due to this infectious disease which affects the lungs. Infection of the disease caused by the settlement of *Mtb* to the lung alveoli of the host from the external bacilli air droplets (Smith 2003; Adami and Cervantes 2015; Cohen et al. 2018; Chai et al. 2020; Boom et al. 2021). After settlement, the multiplication of *Mtb* results in the activation of the innate immune response through the alveolar macrophages through sequential steps involved in disease development (Figure 2) (Smith 2003; Adami and Cervantes 2015; Cohen et al. 2018; Chai et al. 2020; Boom et al. 2021; Lovey et al. 2022; de Waal et al. 2022).

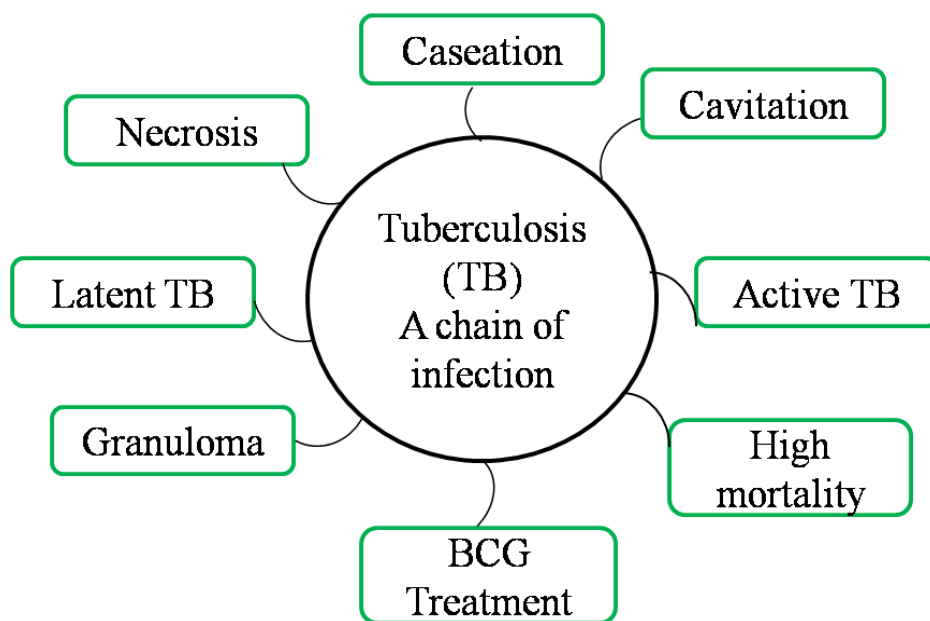


Figure 1 Cyclic diagram showing the chain of infection caused by *Mycobacterium tuberculosis*

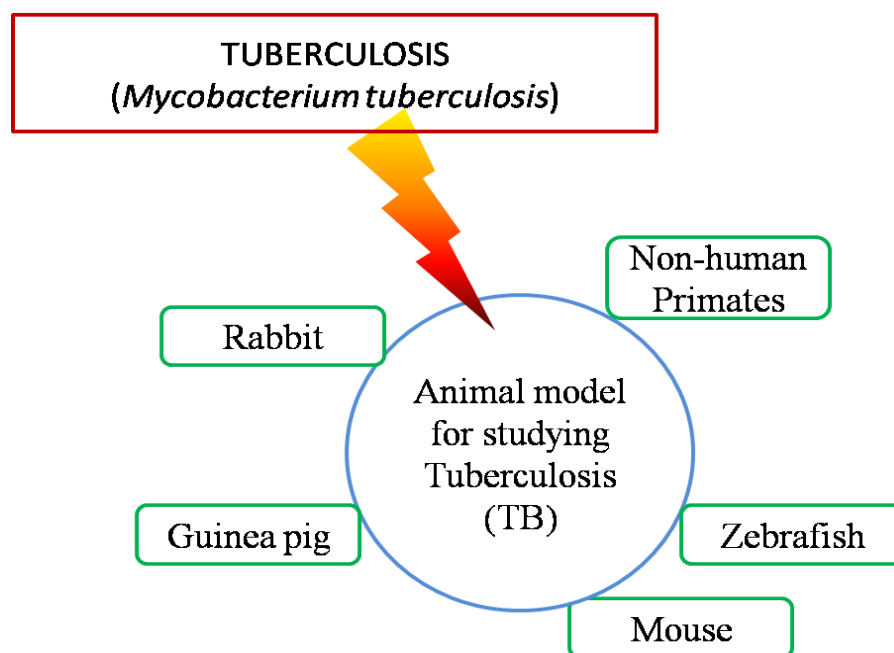


Figure 2 Animal model for studying *Mycobacterium tuberculosis* infection

In disease development, different *Mtb* strains are involved with genotypic resistance. The development of genotypic resistance results in the formation of drug-resistant TB (DR-TB). Later on, DR-TB is further classified into four subcategories i.e. single-drug resistant TB (SDR-TB), multi-drug resistant TB (MDR-TB), extensive-drug resistant TB (XDR-TB), and totally-drug resistant TB (TDR-TB) (Furin et al. 2019; Pontali et al. 2019; Singh et al. 2020; Khawbung et al. 2021; Singh and Chibale 2021).

Recent reports have shown that DR-TB acts as a major source of TB death due to spontaneous antimicrobial resistance (AMR) (Palomino and Martin 2014; Kurz et al. 2016; Murray et al. 2022). This AMR may also reduce the activity of certain drugs used in the treatment of TB including rifampicin, isoniazid, ethambutol, pyrazinamide, ethionamide, moxifloxacin, streptomycin, kanamycin, amikacin, capreomycin, cycloserine, Linezolid, Bedaquiline, Delamanid and Pretomanid (Kurz et al. 2016; Angula et al. 2021; dos Anjos et al. 2022; Ushtanit et al. 2022). Other than reducing the effect of the drug, TDR-TB will make the available first and second lines of anti-TB drugs made it to ineffective (Gothi and Joshi 2011; Vasava et al. 2017; Adeniji et al. 2020; Singh and Chibale 2021; Yusoof et al. 2022). Limitations in drug susceptibility testing lead to develop biomarkers to identify TDR-TB (Singh and Chibale 2021; Yusoof et al. 2022).

3 Impact of Matrix Metalloproteinase in the normal homeostasis mechanism

Matrix metalloproteinase (MMPs) belongs to a superfamily (metzincin) of enzymatic proteins, which depends on zinc and

calcium. This MMPs family is highly conserved across different species, and till today, 25 MMPs have been identified in vertebrates, and 24 of them are present in humans (LaFever et al. 2017; Sabir et al. 2019; Laronha and Caldeira 2020). Identified MMPs are responsible for functions that vary from the release of growth factors, acting as membrane-bound enzymes, growth & death receptors, and regulating extracellular matrix in different species. These identified MMPs are further differentiated into five different sub-families: collagenases, gelatinases, stromelysins, elastases, and membrane-type MMPs (Rosenberg 2002; Visse and Nagase 2003; Laronha and Caldeira 2020; Cabral-Pacheco et al. 2020; Zipfel et al. 2020). Representative MMPs of five different sub-families are tabulated in Table 1.

Among the representative MMPs, MMP-1, 3, 7, and 8 are located together in a single gene cluster, which will emphasize their critical role in initial physiological processes. These MMPs are responsible for the tissue remodelling of connective tissues including angiogenesis, morphogenesis, etc. MMP – 1, 8 plays a major role and includes the degradation of triple-helical fibrillar collagen in bone and ligaments. MMP-3 and MMP-7 are responsible for the degradation of extracellular matrix. Thus, the above-listed MMP plays a fundamental digestive process in the maintenance of physiological hemostasis mechanism (Loffek et al. 2011; Cui et al. 2017; Gonzalez-Avila et al. 2019; Cabral-Pacheco et al. 2020; Zipfel et al. 2020). The general functions of different MMPs are indicated in Table 2.

These MMPs are initially synthesized as inactive proenzymes (also known as zymogens), which consist of an N-terminal signal peptide,

Table 1 MMP subfamily and its examples

S. No	Matrix metalloproteinase (MMP) Subfamily	Examples	References
1	Collagenases	MMP-1,8 and 13	Gho et al. 2018; Falconer et al. 2019; Bocaneti et al. 2023
2	Gelatinases	MMP-2, and 9	Hannocks et al. 2019; Ligi et al. 2020; Nikolov and Popovski 2021
3	Stromelysins	MMP-3, and 10	Piskór et al. 2020; Raeeszadeh-Sarmazdeh et al. 2022
4	Elastases	MMP-7, and 12	Hao et al. 2019; Heinz 2020
5	Membrane-type MMPs	MMP-1 to 5	Kumar et al. 2018; Rohlwink et al. 2019; Cabral-Pacheco et al. 2020

Table 2 General functions of MMPs

S.No	Process	Functional activity	References
1.	Development	1. Embryonic development 2. Blastocyst implantation 3. Nerve growth	Loffek et al. 2011; Rohlwink et al. 2019
2.	Homoeostasis	1. Nerve regeneration 2. Bone remodelling 3. Angiogenesis 4. Wound-healing	Loffek et al. 2011; Rohlwink et al. 2019
3.	Reproduction	1. Cervical dilatation 2. Ovulation 3. Endometrial cycling	Loffek et al. 2011; Rohlwink et al. 2019

prodomain, and catalytic domain. Activation of inactive proenzymes results in the cleavage of N-terminal signal peptide by the secretory pathway followed by the prodomain and catalytic domain (Yong et al. 2001; Cerdá-Costa and Gomis-Rüth 2014; Rohlwink et al. 2019; Gomis-Ruth and Stöcker 2023). As a result of cleavage, minimal pro-MMPs are formed in the intermittent stage of MMP activation. Further, activation of pro-MMPs can occur in *in vitro* and *in vivo* conditions. During *in vitro* conditions, the pro-MMPs can be activated using chemical agents like sodium dodecyl sulphate (SDS), thiol-modifying agents and oxidized glutathione. However, *in-vivo* conditions use more complex processes in the activation of pro-MMPs, like recruitments of other MMPs or different classes of proteinases such as neutrophil elastases and plasmin (English et al. 2001; Rosenblum et al. 2007; Vandenbroucke and Libert 2014; Sabir et al. 2019; Zipfel et al. 2020; Almutairi et al. 2023).

To prevent excessive and destructive activity during normal haemostasis mechanism, MMPs activity is subjected to control at multiple levels, including gene expression regulation (both transcriptional and post-transcriptional), proenzyme activation, and the action of natural inhibitors (Wang and Khalil 2018; Gonzalez-Avila et al. 2019; Madzharova et al. 2019; Laronha and Caldeira 2020; He et al. 2023). These inhibitors include α 2-macroglobulin found in the bloodstream and tissue inhibitors of metalloproteinase (TIMPs) in the tissues. TIMPs are endogenous proteins that serve as regulators and exhibit tissue-specific, constitutive, or inducible expression. Four members in the TIMP family, known as TIMPs 1-4, inhibit MMP activity through non-covalent binding. TIMP-3 is noteworthy for its ability to act on both MMPs and tumor necrosis

factor (TNF)- α converting enzyme (TACE) (Murphy 2011; Gonzalez-Avila et al. 2019; Madzharova et al. 2019; Rohlwink et al. 2019; Laronha and Caldeira 2020; Zapata-Acevedo et al. 2022; He et al. 2023).

4 Role of matrix metalloproteinase (MMP) expression in disease management

The significance of MMPs and TIMPs in maintaining health and their involvement in disease processes has attracted increasing attention. Exploring how the control of these substances influences pathological conditions and their impact on the release of cytokines, reactive oxygen species (ROS), and growth factors could provide valuable insights for improving disease management. Dysregulated MMPs and their TIMPs are notably associated with various pathological conditions, such as matrix weakening, microglial activation, autoimmune diseases, inflammation, tissue damage, cancer development, fibrosis and improper blood vessel formation. However, these substances are involved in additional activity, including cell proliferation, apoptosis, and adhesion, by cleaving bioactive molecules that regulate these activities (Quintero-Fabián et al. 2019; Cabral-Pacheco et al. 2020; Ma et al. 2021; He et al. 2023).

4.1 Role of metalloproteinase 1 (MMP1) as a therapeutic target for the treatment of *M. tuberculosis* infection

Recent reports showed that whenever *Mtb* infected with human primary monocytes results in the regulated MMP1 more effectively

than other MMPs like MMP3, MMP7, MMP8, MMP10, MMP12, and MMP14 (Kumar et al. 2018; Rohlwink et al. 2019; Sabir et al. 2019). Initially, Elkington et al. (2011) reported that an increase in MMP-1 secretion/upregulation might link to TLR-2 signaling instead of live mycobacterial induction in its upregulation. Furthermore, *Mtb* infection enhanced monocyte migration through an extracellular matrix-coated transwell system. Consequently, the upregulation of MMPs led to a functional increase in matrix degradation by the infected cells (Elkington et al. 2011; Randall et al. 2015; Peddireddy et al. 2017; Rohlwink et al. 2019; Sabir et al. 2019; Tiwari and Martineau 2023).

Targeting MMP-1 activity makes it possible to reduce the pathological processes contributing to the morbidity and mortality associated with tuberculosis infection. P-amino-salicylic acid, which has been employed in TB treatment for six decades but with an unclear mechanism of action, inhibits MMP-1 secretion by *Mtb*-infected macrophages (Rand et al. 2009; Elkington et al. 2011; Stek et al. 2018; Sabir et al. 2019; Kirwan et al. 2021). This suggests that an established TB treatment might work by limiting tissue damage. Furthermore, they demonstrated that Ro32-3555, a compound that has been evaluated in phase III clinical trials for arthritis, can effectively suppress MMP-1 activity driven by *Mtb* (Rohlwink et al. 2019; Sabir et al. 2019; Tiwari and Martineau 2023). Since MMP-1 may be responsible for causing matrix destruction in TB, hence it is a promising therapeutic target for mitigating immunopathology in the disease (Elkington et al. 2011; Rohlwink et al. 2019; Sabir et al. 2019; Guler et al. 2021; Tiwari and Martineau 2023).

4.2 Impact of matrix metalloproteinase 9 (MMP 9) in the regulation of immune response

A robust link between the activity and immune response of matrix metalloproteinase 9 (MMP 9) has become increasingly evident. MMPs have been demonstrated to play a role in regulating the immune response to infectious pathogens and the broader inflammatory processes (Lee et al. 2005; Cabral-Pacheco et al. 2020; Quintero-Fabián et al. 2019; Sabir et al. 2019; de Almeida et al. 2022). Multiple investigations have revealed that MMPs, with a particular focus on MMP-9, are expressed during different stages of tuberculosis, such as active cavitary tuberculosis, pleuritis and cases of meningitis. Infection of THP-1 cells with *Mtb* results in an increased expression of MMP-9. Signaling pathways mediated by specific receptors control this upregulation of MMP-9. In tuberculosis (TB) patients, the levels of various MMPs in the blood may vary between genders, but this variation doesn't appear to be associated with the severity of the disease (Hoheisel et al. 2001; Ravimohan et al. 2018; Rohlwink et al. 2019; Sabir et al. 2019).

Azikin et al. (2017) evaluated MMP-9 levels in children who lived in the same household as those with active TB. Their study found

no significant differences in the expression levels of MMP-9 between the group of children exposed to TB and those infected with *Mtb*. Furthermore, the levels of MMP-9 were not affected by factors such as sex, age, nutritional status, or the status of BCG immunization (Rohlwink et al. 2019; Sabir et al. 2019). The reported study shows that the extracellular matrix (ECM) plays a vital role in shaping the structure and composition of the granuloma. It influences how different types of white blood cells move in and out of this dynamic environment and may also affect the positioning of various subpopulations of white blood cells within the granuloma (Gonzalez-Juarrero et al. 2001; Taylor et al. 2006; Diller and Tabor 2022). Mice exposed to *Mtb* through inhalation have been categorized into two groups: susceptible and resistant, determined by their survival rates. This division aligns with variations in aspects such as the recruitment of white blood cells, the structure of granulomas, the production of cytokines, and the expression of adhesion molecules. A recent discovery has indicated that when subjected to *Mtb* infection in a laboratory setting, macrophages from a mouse strain known for its resistance to the disease (C57BL/6) produced notably higher levels of MMP-9 mRNA compared to macrophages from a mouse strain known for susceptibility (CBA/J) (Taylor et al. 2006; Carow et al. 2019).

In one study, Taylor et al. (2006) investigated the activity of MMPs in promoting the initial spread of *Mtb* bacilli outside the lungs of the resistant strain. C57BL/6 mice were exposed to about 500 colony-forming units (CFUs) of *Mtb* H37Rv through inhalation. Following infection, they were promptly administered an MMP activity inhibitor called batimastat (BB-94). These findings indicated that the dissemination of viable bacilli into the bloodstream was more pronounced in mice receiving the control vehicle than in those receiving the MMP inhibitor. This suggests that MMPs may play a role in the hematogenous spread of *Mtb* (Taylor et al. 2006; Polena et al. 2016; Rohlwink et al. 2019). While there were statistically significant differences between the groups in terms of CFU counts in the spleen and blood during the early phase of infection at day 14, there was no observable impact on the growth of *Mtb* in the lungs of mice treated with BB-94 compared to those treated with the carrier later in the infection process (Taylor et al. 2006; Ammerman et al. 2018; Zhu et al. 2021).

4.3 Role of matrix metalloproteinase 8 (MMP 8) in the regulation of NF- κ B pathway

In tuberculosis (TB), neutrophils were found to produce matrix metalloproteinase-8 (MMP-8) through a process regulated by the NF- κ B pathway. This upregulation of MMP-8 secretion by neutrophils led to the degradation of the extracellular matrix, both in laboratory settings and in samples from respiratory specimens of TB patients. The destruction of collagen caused by TB infection was effectively prevented by doxycycline, an approved inhibitor of

MMPs. Neutrophils release MMP-8, a highly effective enzyme capable of breaking down collagen. Elevated levels of MMPs produced by neutrophils are linked to the progression of disease in Central Nervous System Tuberculosis (CNS-TB), suggesting that neutrophils play a role in the immune response and disease progression in human tuberculosis (Price et al. 2001; Green et al. 2009; Ong et al. 2015; Ravimohan et al. 2018; Rohlwick et al. 2019; Sabir et al. 2019; Poh et al. 2021; Lee and Kim 2022; Tiwari and Martineau 2023).

Furthermore, it was also observed that neutrophil extracellular traps (NETs) contained MMP-8 and were elevated in samples obtained from TB patients. Neutrophils were observed surrounding the edges of cavities in the lungs of individuals with pulmonary TB, and the concentration of MMP-8 in sputum samples correlated with the radiological and clinical severity of TB disease. The protein AMP-activated protein kinase (AMPK), a central regulator of catabolic processes, was identified as a driver of MMP-8 secretion by neutrophils. Neutrophils from individuals lacking AMPK secreted lower concentrations of MMP-8. Furthermore, AMPK-expressing neutrophils were detected in lung biopsies from individuals with TB, with evidence of AMPK activation observed in cell nuclei. These findings highlight the significant role of neutrophil-derived MMP-8 in the immunopathology of TB and suggest that it could serve as a potential target for host-directed therapy in the context of this infectious disease (Ong et al. 2015; Ravimohan et al. 2018; Rohlwick et al. 2019; Sabir et al. 2019; Poh et al. 2021; Lee and Kim 2022; Tiwari and Martineau 2023). Besides TB, these MMPs are also involved in developing normal brain and synaptic plasticity. However, aberrant expression of MMPs may lead to neuronal cell death, inflammation, and demyelination in the brain. Further, it develops cognitive impairment due to oral/gut dysbiosis within a host system (Beuron et al. 2019; Behl et al. 2021; Mukilan 2023).

Conclusion

Matrix metalloproteinases (MMPs) belong to a proteolytic family of enzymes and have numerous functions in regulating physiological functions. Some of their important functions include extracellular matrix remodelling, cell migration facilitating, cytokine cleaving, and activation of defensins. These MMPs can result in extracellular matrix breakdown during tuberculosis in the lungs, especially under neutral pH conditions. In normal conditions, MMPs are typically controlled in the body to maintain normal homeostasis mechanisms in the host. During tuberculosis, their uncontrolled activity results in the development of immunopathological processes like tuberculosis, chronic obstructive pulmonary disease, sarcoidosis, and acute respiratory distress syndrome. Dysregulation of MMPs is a significant characteristic of the immunopathology associated with tuberculosis. By downregulating the expression of MMP with the

help of some specific protease inhibitors, we can regulate the progress of tuberculosis. The present review laid a path to identify drug targets for tuberculosis as matrix metalloproteinases (MMP) in the near future. Thereby present review focused on the role of MMPs in the maintenance of homeostasis mechanisms and disease progression in a host system. Other than tuberculosis, these MMPs are also involved in brain inflammation and other systematic disorders in a host system. It also opens up the use of MMPs as a potential target for treating neurodegenerative disorders like Alzheimer's disease.

Acknowledgements

SP thank DBT (BT/IN/Indo-US/Foldscope/39/2015) and RUSA 2.0. (RUSA/MKU/Internship/2022) for the financial support in the form of fellowship. MM sincerely thank Indian Institute of Technology, Kharagpur, West Bengal, India, for the Post-Doctoral Fellowship (IIT/ACD(PGS&R)/PDF/Offer/2018-2019/AT), and DST-FIST (SR/FST/COLLEGE-/2022/1203) for the infrastructural project (PG college level – A program) sanctioned to the Department of Biotechnology, Sri Ramakrishna College of Arts & Science (Autonomous), Coimbatore – 641 006, Tamil Nadu, India.

Author Contributions

SP, and MM performed the conceptualization, study design, original draft preparation, review and editing of the manuscript. PG, GK did the data collection and its organization. HS approved the final manuscript.

Conflicts of Interest

The author declares no conflict of interest to express

References

- Adami, A.J., & Cervantes, J.L. (2015). The microbiome at the pulmonary alveolar niche and its role in *Mycobacterium tuberculosis* infection. *Tuberculosis*, 95, 651-658.
- Adeniji, A.A., Knoll, K.E., & Loots, D.T. (2020). Potential anti-TB investigational compounds and drugs with repositioning potential in TB therapy: a conspectus. *Applied Microbiology and Biotechnology*, 104, 5633-5662.
- Almutairi, S., Kalloush H.M., Manoon N.A., & Bardaweel S.K. (2023). Matrix Metalloproteinases Inhibitors in Cancer Treatment: An Updated Review (2013-2023). *Molecules*, 28, 5567.
- Ammerman, N.C., Swanson, R.V., Bautista, E.M., Almeida, D.V., et al. (2018). Impact of Clofazimine Dosing on Treatment Shortening of the First-Line Regimen in a Mouse Model of Tuberculosis. *Antimicrobial Agents and Chemotherapy*, 62, e00636-18.

- Angula, K.T., Legoabe, L.J., & Beteck, R.M. (2021). Chemical Classes Presenting Novel Antituberculosis Agents Currently in Different Phases of Drug Development: A 2010-2020 Review. *Pharmaceuticals*, *14*, 461.
- Azikin, W., Amiruddin, L., Husein, A., et al. (2017). Matrix Metalloproteinase-9 (MMP-9) Level in Tuberculosis Exposed and Infected Children. *American Journal of Health Research*, *1*, 7-10.
- Behl, T., Kaur, G., Sehgal, A., Bhardwaj, S., et al. (2021). Multifaceted Role of Matrix Metalloproteinases in Neurodegenerative Diseases: Pathophysiological and Therapeutic Perspectives. *International Journal of Molecular Sciences*, *22*, 1413.
- Beroun, A., Mitra, S., Michaluk, P., Pijet, B., et al. (2019). MMPs in learning and memory and neuropsychiatric disorders. *Cellular and Molecular Life Sciences*, *76*, 3207-3228.
- Bhargava, A., Chatterjee, M., Jain, Y., Chatterjee, B., et al. (2013). Nutritional status of adult patients with pulmonary tuberculosis in rural central India and its association with mortality. *PLoS One*, *8*, e77979.
- Bloom, B.R., Atun, R., Cohen, T., Dye, C., et al. (2017). Tuberculosis. editors. In: Major Infectious Diseases. 3rd Edition. Washington (DC): The international Bank for Reconstruction and Development/The World Bank. DOI: 10.1596/978-1-648-0524-0_ch11.
- Bocaneti, F.D., Altamura, G., Corteggio, A., Tanase, O.I., et al. (2023). Expression of collagenases (matrix metalloproteinase-1, -8, -13) and tissue inhibitor of metalloproteinase-3 (TIMP-3) in naturally occurring bovine cutaneous fibropapillomas. *Frontiers in Veterinary Science*, *9*, 1072672.
- Boom, W.H., Schaible, U.E., & Achkar, J.M. (2021). The knowns and unknowns of latent Mycobacterium tuberculosis infection. *The Journal of Clinical Investigation*, *131*, e136222.
- Bussi, C., & Gutierrez, M.G. (2019). Mycobacterium tuberculosis infection of host cells in space and time. *FEMS Microbiology Reviews*, *43*, 341 – 361.
- Cabral-Pacheco, G.A., Garza-Veloz, I., la Rosa, C.C., Ramirez-Acuña, J.M., et al. (2020). The Roles of Matrix Metalloproteinases and Their Inhibitors in Human Diseases. *International Journal of Molecular Sciences*, *21*, 9739.
- Carow, B., Hauling, T., Qian, X., Kramnik, I., et al. (2019). Spatial and temporal localization of immune transcripts defines hallmarks and diversity in the tuberculosis granuloma. *Nature Communications*, *10*, 1823.
- Cerdá-Costa, N., & Gomis-Rüth F.X. (2014). Architecture and function of metallopeptidase catalytic domains. *Protein Science*, *23*, 123-144.
- Chai, Q., Lu, Z., & Liu, C.H. (2020). Host defense mechanisms against *Mycobacterium tuberculosis*. *Cellular and Molecular Life Sciences* *77*, 1859-878.
- Chai, Q., Zhang, Y., & Liu, C.H. (2018). *Mycobacterium tuberculosis*: An Adaptable Pathogen Associated With Multiple Human Diseases. *Frontiers in Cellular and Infection Microbiology*, *8*, 158.
- Chandrasekaran, P., Saravanan, N., Bethunaickan, R., & Tripathy, S. (2017). Malnutrition: modulator of immune responses in tuberculosis. *Frontiers in immunology*, *8*, 1316.
- Cohen, S.B., Gern, BH, Delahaye, J.L., Adams, K.N., & Plumlee, C.R. (2018). Alveolar Macrophages Provide an Early *Mycobacterium tuberculosis* Niche and Initiate dissemination. *Cell Host & Microbe*, *24*, 439-446.
- Cui, N., Hu, M, & Khalil, R.A. (2017). Biochemical and Biological Attributes of Matrix Metalloproteinases. *Progress in Molecular Biology and Translational Science*, *147*, 1-13.
- Dartois, V.A., & Rubin, E.J. (2022). Anti-tuberculosis treatment strategies and drug development: challenges and priorities. *Nature Reviews Microbiology*, *20*, 685-701.
- de Almeida, L.G.N., Thode, H., Eslambolchi, Y., Chopra, S., et al. (2022). Matrix Metalloproteinases: From Molecular Mechanisms to Physiology, Pathophysiology, and Pharmacology. *Pharmacological Reviews*, *74*, 714-770.
- de Waal A.M., Hiemstra, P.S., Ottenhoff, T.H., Joosten, S.A., & van der Does AM. (2022). Lung epithelial cells interact with immune cells and bacteria to shape the microenvironment in tuberculosis. *Thorax*, *77*, 408-416.
- Diller, R.B., & Tabor, A.J. (2022). The Role of the Extracellular Matrix (ECM) in wound Healing: A Review. *Biomimetics*, *7*, 87.
- dos Anjos, T.R., Castro, V.S., Filho, E.S.M., Suffys, P.N., et al. (2022). Genomic analysis of *Mycobacterium tuberculosis* variant *bovis* strains isolated from bovine in the state of Mato Grosso, Brazil. *Frontiers in Veterinary Science*, *9*, 1006090.
- Elkington, P., Shiomi, T., Breen, R., Nuttall, R.K., et al. (2011). MMP-1 drives immunopathology in human tuberculosis and transgenic mice. *The Journal of clinical investigation*, *121*, 1827-1833.
- English, W.R., Holtz, B., Vogt, G., Knäuper, V., & Murphy, G. (2001). Characterization of the role of the “MT-loop”: an

- eight-amino acid insertion specific to progelatinase a (MMP2) activating membrane-type matrix metalloproteinases. *Journal of Biological Chemistry*, 276, 42018-42026.
- Falconer, A.M.D., Chan, C.M., Gray, J., Nagashima, I., et al. (2019). Collagenolytic matrix metalloproteinases antagonize proteinase-activated receptor-2 activation, providing insights into extracellular matrix turnover. *Journal of Biological Chemistry*, 294, 10266-10277.
- Furin, J., Cox, H., & Pai, M. (2019). Tuberculosis. *Lancet*, 393, 1642-1656.
- Gho, W.G., Choi, Y., Park, K., & Huh, J. (2018). Expression of collagenases (matrix metalloproteinase-1,8, 13) and tissue inhibitor of metalloproteinase-1 of retrodiscal tissue in temporomandibular joint disorder patients. *Journal of The Korean Association of Oral and Maxillofacial Surgeons*, 44, 120-127.
- Gomis-Ruth, F.X., & Stöcker W. (2023). Structural and evolutionary insights into astacin metallopeptidases. *Frontiers in Molecular Biosciences*, 9, 1080836.
- Gonzalez-Avila, G., Sommer, B., Mendoza-Posada, D.A., Ramos, C., et al. (2019). Matrix metalloproteinases participation in the metastatic process and their diagnostic and therapeutic applications in cancer. *Critical Reviews in Oncology/Hematology*, 137, 57-83.
- Gonzalez-Juarrero, M., Turner, O. C., Turner, J., Marietta, P., et al. (2001). Temporal and spatial arrangement of lymphocytes within lung granulomas induced by aerosol infection with *Mycobacterium tuberculosis*. *Infection and Immunity*, 69, 1722-1728.
- Gothi, D., & Joshi, J.M. (2011). Resistant TB: Newer Drugs and Community Approach. *Recent Patents on Anti-infective Drug Discovery*, 6, 27-37.
- Green, J.A., Tran, C.T., Farrar, J.J., Nguyen, M.T., et al. (2009). Dexamethasone, cerebrospinal fluid matrix metalloproteinase concentrations and clinical outcomes in tuberculous meningitis. *PLoS One*, 4, e7277.
- Guler, R., Ozturk, M., Sabeel, S., Motaung, B., et al. (2021). Targeting Molecular Inflammatory Pathways in Granuloma as Host-Directed Therapies for Tuberculosis. *Frontiers in Immunology*, 12, 733853.
- Hannocks, M.J., Zhang, X., Gerwien, H., Chashchina, A., et al. (2019). The gelatinases, MMP-2 and MMP-9, as fine tuners of neuroinflammatory processes. *Matrix Biology*, 75-76, 102-113.
- Hao, W., Li, M., Zhang, Y., Zhang, C., & Xue, Y. (2019). Expressions of MMP-12, TIMP-4, and Neutrophil Elastase in PBMCs and Exhaled Breath Condensate in Patients with COPD and Their Relationships with Disease Severity and Acute Exacerbations. *Journal of Immunology Research*, 2019, 7142438.
- He, L., Kang, Q., Chan, K.I., Zhang, Y., et al. (2023). The immunomodulatory role of matrix metalloproteinases in colitis-associated cancer. *Frontiers in Immunology*, 13, 1093990.
- Heinz, A. (2020). Elastases and elastokines: elastin degradation and its significance in health and disease. *Critical Reviews in Biochemistry and Molecular Biology*, 55, 252-273.
- Hoheisel, G., Sack, U., Hui D.S., Huse, K., et al. (2001). Occurrence of matrix metalloproteinases and tissue inhibitors of metalloproteinases in tuberculous pleuritis. *Tuberculosis*, 81, 203-209.
- Jones-López, E., Acuña-Villaorduña, C., Ssebidandi, M., Gaeddert, M., et al. (2016). Cough Aerosols of Mycobacterium tuberculosis in the Prediction of Incident Tuberculosis Disease in Household Contacts. *Clinical Infectious Diseases*, 63, 10-20.
- Kayser, V., & Ramzan, I. (2021). Vaccines and vaccination: history and emerging issues. *Human Vaccines & Immunotherapeutics*, 17, 525-5268.
- Khawbung, J.L., Nath, D., & Chakraborty, S. (2021). Drug resistant Tuberculosis: A review. *Comparative Immunology, Microbiology and Infectious Diseases*, 74, 101574.
- Kirwan D.E., Chong, D.L.W., & Friedland, J.S. (2021). Platelet Activation and the Immune Response to Tuberculosis. *Frontiers in Immunology*, 12, 631696.
- Kumar, N.P., Moideen, K., Viswanathan, V., Shruthi, B.S., et al. (2018). Elevated levels of matrix metalloproteinases reflect severity and extent of disease in tuberculosis-diabetes co-morbidity and are predominantly reversed following standard antituberculosis or metformin treatment. *BMC Infectious Diseases*, 18, 345.
- Kurz, S.G., Furin, J.J., & Bark, C.M. (2016). Drug Resistant Tuberculosis: Challenges and Progress. *Infectious Disease Clinics of North America*, 30, 509-522.
- LaFever, K.S., Wang, X., Page-McCaw, P., Bhawe, G., & Page-McCaw, A. (2017). Both Drosophila matrix metalloproteinases have releases and membrane-tethered forms but have different substrates. *Scientific Reports*, 7, 44560.
- Laronha, H., & Caldeira, J. (2020). Structure and Function of Human Matrix Metalloproteinases. *Cells*, 9, 1076.
- Lee, H.S., & Kim, W.J. (2022). The Role of Matrix Metalloproteinase in Inflammation with a Focus on Infectious Diseases. *International Journal of Molecular Sciences*, 23, 10546.

- Lee, M.M., Yoon, B.J., Osiewicz, K., Preston, M., et al (2005). Tissue inhibitor of metalloproteinase 1 regulates resistance to infection. *Infection and Immunity*, *73*, 661-665.
- Ligi, D., Maniscalco, R., & Mannello, F. (2020). MMP-2 and MMP-9 in Human Peripheral Blood: Optimizing Gelatinase Calibrator for Degradome Research and Discovering a Novel Gelatinolytic Enzyme. *Journal of Proteome Research*, *19*, 525-536.
- Loffek, S., Schilling, O., & Franzke, C.W. (2011). Series “matrix metalloproteinases in lung health and disease”: Biological role of matrix metalloproteinases: A critical balance. *The European Respiratory Journal*, *38*, 191–208.
- Lönnroth, K., Jaramillo, E., Williams, B.G., Dye, C., & Raviglione, M. (2009). Drivers of tuberculosis epidemics: the role of risk factors and social determinants. *Social Science & Medicine*, *68*, 2240–6.
- Lovey, A., Verma, S., Kaipilyawar, V., Ribeiro-Rodrigues, R., et al. (2022). Early alveolar macrophage response and IL-1R-dependent T cell priming determine transmissibility of *Mycobacterium tuberculosis* strains. *Nature Communications*, *13*, 884.
- Ma, B., Ran, R., Liao, H., & Zhang, H. (2021). The paradoxical role of matrix metalloproteinase-11 in cancer. *Biomedicine & Pharmacotherapy*, *141*, 111899.
- Madzharova, E., Kastl, P., Sabino, F., & dem Keller, U.A. (2019). Post-Translational Modification-Dependent Activity of Matrix Metalloproteinases. *International Journal of Molecular Sciences*, *20*, 3077.
- Mukilan, M. (2023). Impact of *Pseudomonas aeruginosa*, *Bacillus subtilis*, *Staphylococcus aureus*, and *Escherichia coli* Oral Infusions on Cognitive Memory Decline in Mild Cognitive Impairment. *Journal of Experimental Biology and Agricultural Sciences*, *11*, 581-592.
- Murphy, G. (2011). Tissue inhibitors of metalloproteinases. *Genome Biology*, *12*, 233.
- Murray, C.J.L., Ikuta, K.S., Sharara, F., Swetschinski, L., et al. (2022). Global burden of bacterial antimicrobial resistance in 2019: a systematic analysis. *The Lancet*, *399*, 629-655.
- Narasimhan, P., Wood, J., MacIntyre, C.R., & Mathai, D. (2013). Risk factors for tuberculosis. *Pulmonary Medicine*, *2013*, 828939.
- Nikolov, A., & Popovski, N. (2021). Role of Gelatinases MMP-2, and MMP-9 in Healthy and Complicated Pregnancy and Their Future Potential as Preeclampsia Biomarkers. *Diagnostics*, *11*, 480.
- Ong, C.W., Elkington, P.T., Brilha, S., Ugarte-Gil, C., et al. (2015). Neutrophil-Derived MMP-8 Drives AMPK-Dependent Matrix Destruction in Human Pulmonary Tuberculosis. *PLoS Pathogens*, *11*, e1004917.
- Palomino, J.C., & Martin, A. (2014). Drug Resistance Mechanisms in *Mycobacterium tuberculosis*. *Antibiotics*, *3*, 317-340.
- Patterson, B., & Wood, R. (2019). Is cough really necessary for TB transmission. *Tuberculosis*, *117*, 31-35.
- Peddireddy, V., Doddam, S.N., & Ahmed, N. (2017). Mycobacterial Dormancy Systems and Host Responses in Tuberculosis. *Frontiers in Immunology*, *8*, 84.
- Piskór, B.M., Przyłipiak, A., Dabrowska, E., Niczyporuk, M., & Lawicki, S. (2020). Matrilysins and Stromelysins in Pathogenesis and Diagnostics of Cancers. *Cancer Management and Research*, *12*, 10949-10694.
- Poh, X.Y., Loh, F.K., Friedland, J.S., & Ong, C.W.M. (2021). Neutrophil-Mediated Immunopathology and Matrix Metalloproteinases in Central Nervous System – Tuberculosis. *Frontiers in Immunology*, *12*, 788976.
- Polena, H., Boudou, F., Tilleul, S., Dubois-Colas, N., et al. (2016). *Mycobacterium tuberculosis* exploits the formation of new blood vessels for its dissemination. *Scientific Reports*, *6*, 33162.
- Pollard, A.J., & Bijker, E.M. (2020). A guide to vaccinology: from basic principles to new developments. *Nature Reviews Immunology*, *21*, 83-100.
- Pontali, E., Raviglione, M.C., Migliori, G.B., et al. (2019). Regimens to treat multidrug-resistant tuberculosis: past, present and future perspectives. *European Respiratory Review*, *28*, 190035.
- Price, N.M., Farrar, J., Tran, T.T., Nguyen, T.H., Tran TH, et al. (2001). Identification of a matrix-degrading phenotype in human tuberculosis in vitro and in vivo. *Journal of Immunology*, *166*, 4223–4230.
- Quintero-Fabián, S., Arreola, R., Becerril-Villanueva, E., Tores-Romero, J.C., et al. (2019). Role of Matrix Metalloproteinase in Angiogenesis and Cancer. *Frontiers in Oncology*, *9*, 1370.
- Rand, L., Green, J.A., Saraiva, L., Friedland, J.S., & Elkington, P.T. (2009). Matrix metalloproteinase-1 is regulated in tuberculosis by a p38 MAPK-dependent, p-aminosalicylic acid-sensitive signaling cascade. *Journal of Immunology*, *182*, 5865–5872.
- Raezadeh-Sarmazdeh, M., Coban, M., Mahajan, S., Hockla, A., et al. (2022). Engineering of tissue inhibitor of metalloproteinases TIMP-1 for fine discrimination between closely related

- stromelysins MMP-3 and MMP-10. *Journal of Biological Chemistry*, 298, 101654.
- Randall, P.J., Hsu, N., Quesniaux, V., Ryffel, B., & Jacobs, M. (2015). Mycobacterium tuberculosis infection of the 'non-classical immune cell'. *Immunology & Cell Biology*, 93, 789-795.
- Ravimohan, S., Kornfield, H., Weissman, D., & Bisson, G.P. (2018). Tuberculosis and lung damage: from epidemiology to pathophysiology. *European Respiratory Review*, 27, 170077.
- Rohlwink, U.K., Walker, N.F., Ordonez, A.A., Li, Y.J., et al. (2019). Matrix Metalloproteinases in Pulmonary and Central Nervous System Tuberculosis-A Review. *International Journal of Molecular Sciences*, 20, 1350.
- Rosenberg, G.A. (2002). Matrix metalloproteinases in neuroinflammation. *Glia*, 40, 130.
- Rosenblum, G., Meroueh, S., Toth, M., Fisher, J.F., et al. (2007). Molecular Structures and Dynamics of the Stepwise Activation Mechanism of a Matrix Metalloproteinase Zymogen: Challenging the Cysteine Switch Dogma. *Journal of the American Chemical Society*, 129, 13566-13574.
- Sabir, N., Hussian, T., Mangi, M.H., Zhao, D., & Zhou, X. (2019). Matrix metalloproteinases: Expression, regulation and role in the immunopathology of tuberculosis. *Cell Proliferation*, 52, e12649.
- Sakai, T., & Morimoto, Y. (2022). The History of Infectious Diseases and Medicine. *Pathogens*, 11, 1147.
- Sia, J.K., & Rengarajan, J. (2019). Immunology of *Mycobacterium tuberculosis* infections. *Microbiology Spectrum*, 7, 10.1128/microbiolspec.GPP3-0022-2018.
- Singh, B. (2023). Bedaquiline in Drug-Resistant Tuberculosis: A Mini-Review. *Current Molecular Pharmacology*, 16, 243-253.
- Singh, R., Dwivedi, S.P., Gaharwar, U.S., Meena, R., et al. (2020). Recent updates on drug resistance in *Mycobacterium tuberculosis*. *Journal of Applied Microbiology*, 128, 1547-1567.
- Singh, V., & Chibale, K. (2021). Strategies to Combat Multi-Drug Resistance in Tuberculosis. *Accounts of Chemical Research*, 54, 2361-2376.
- Smith, I. (2003). *Mycobacterium tuberculosis* Pathogenesis and Molecular Determinants of Virulence. *Clinical Microbiology Reviews*, 16, 463-496.
- Stek, C., Allwood, B., Walker, N.F., Wilkinson, R.J., et al. (2018). The Immune Mechanisms of Lung Parenchymal Damage in Tuberculosis and the Role of Host-Directed Therapy. *Frontiers in Microbiology*, 9, 2603.
- Stewart, R.J., Wortham, J., Parvez, F., Morris, S.B., et al. (2020). Tuberculosis Infection in Children. *The Journal of nurse practitioners*, 16, 673-678.
- Taylor, J.L., Hattle, J.M., Dreitz, S.A., Troudt, J.M., et al. (2006). Role for matrix metalloproteinase 9 in granuloma formation during pulmonary *Mycobacterium tuberculosis* infection. *Infection and Immunity*, 74, 6135-44.
- Tiberi, S., du Plessis, N., Walzl, G., Vjecha, M.J., et al. (2018). Tuberculosis: progress and advances in development of new drugs, treatment regimens, and host-directed therapies. *The Lancet. Infectious diseases*, 18, e183-e198.
- Tiwari, D., & Martineau, A.R. (2023). Inflammation-mediated tissue damage in pulmonary tuberculosis and host-directed therapeutic strategies. *Seminars in Immunology*, 65, 101672.
- Ushtanit, A., Kulagina, E., Mikhailova, Y., Makarova, M., et al. (2022). Molecular Determinants of Ethionamide Resistance in Clinical Isolates of *Mycobacterium tuberculosis*. *Antibiotics*, 11, 133.
- Vandenbroucke, R.E., & Libert, C. (2014). Is there new hope for therapeutic matrix metalloproteinase inhibition? *Nature Reviews Drug Discovery*, 13, 904-927.
- Vasava, M.S., Bhoi, M.J., Rathwa, S.K., Borad, M.A., et al. (2017). Drug development against tuberculosis: Past, present and future. *The Indian Journal of Tuberculosis*, 64, 252-275.
- Visse, R., & Nagase, H. (2003). Matrix metalloproteinases and tissue inhibitors of metalloproteinases: Structure, function, and biochemistry. *Circulation Research*, 92, 827-839.
- Wang, X., & Khalil, R.A. (2018). Matrix Metalloproteinases, Vascular Remodeling, and Vascular Disease. *Advances in Pharmacology*, 81, 241-330.
- Yong, V.W., Power, C., Forsyth, P., & Edwards, D.R. (2001). Metalloproteinases in biology and pathology of the nervous system. *Nature Reviews Neuroscience*, 2, 502-511.
- Yusoof, K.A., Garcia, J.I., Schami, A., Garcia-Vilanova, A., et al. (2022). Tuberculosis Phenotypic and Genotypic Drug Susceptibility Testing and Immunodiagnosics: A Review. *Frontiers in Immunology*, 13, 870768.
- Zapata-Acevedo, J.F., García-Pérez, V., Cabezas- Pérez, R., Losada-Barragán, M., et al. (2022). Laminin as a Biomarker of Blood-Brain Barrier Disruption under Neuroinflammation: A Systematic Review. *International Journal of Molecular Sciences*, 23, 6788.

- Zhou, J., Lv, J., Carlson, C., Liu, H., et al. (2021). Trained immunity contributes to the prevention of *Mycobacterium tuberculosis* infection, a novel role of autophagy. *Emerging Microbes & Infections*, *10*, 578-588.
- Zhu, H., Fu, L., Wang, B., Chen, X., et al. (2021). Activity of Clofazimine and TBI-166 against *Mycobacterium tuberculosis* in Different Administration Intervals in Mouse Tuberculosis Models. *Antimicrobial Agents and Chemotherapy*, *65*, e02164-20.
- Zipfel, P., Rochais, C., Baranger, K., Rivera, S., & Dallemagne, P. (2020). Matrix metalloproteinases as new targets in Alzheimer's disease: Opportunities and Challenges. *Journal of Medicinal Chemistry*, *63*, 10705-10725.












Journal of Experimental Biology and Agricultural Sciences

<http://www.jebas.org>

ISSN No. 2320 – 8694

Exploration and Profiling of Potential Thermo-alkaliphilic *Bacillus licheniformis* and *Burkholderia* sp. from varied Soil of Delhi region, India and their Plant Growth-Promoting Traits

Charu Singh¹ , Abhishek Chauhan^{2*} , Jayati Arora¹ , Anuj Ranjan³ ,
Hardeep Singh Tuli⁴ , Moyad Shahwan^{5,6} , Vishnu D. Rajput³ , Tatiana Minkina³ ,
Sambasivan Venkat Eswaran⁷ , Tanu Jindal^{2,*} 

¹Amity Institute of Environmental Sciences, Amity University, Noida, Uttar Pradesh, India

²Amity Institute of Environmental Toxicology, Safety, and Management, Amity University, Noida, Uttar Pradesh, India

³Academy of Biology and Biotechnology, Southern Federal University, Rostov-on-Don, Russia

⁴Department of Bio-Sciences and Technology, Maharishi Markandeshwar Engineering College, Maharishi Markandeshwar (Deemed to Be University), Mullana, Ambala, 133207, India

⁵Department of Clinical Sciences, College of Pharmacy and Health Sciences, Ajman University, Ajman 346, United Arab Emirates

⁶Centre of Medical and Bio-Allied Health Sciences Research, Ajman University, Ajman 346, United Arab Emirates

⁷Ex-Head (Chemistry Department) and Dean (Academics), St Stephen's College, Delhi, 110007; Amity University, Noida, Uttar Pradesh-201313, India

Received – January 15, 2024; Revision – February 21, 2024; Accepted – March 05, 2024

Available Online – March 15, 2024

DOI: [http://dx.doi.org/10.18006/2024.12\(1\).60.75](http://dx.doi.org/10.18006/2024.12(1).60.75)

KEYWORDS

PGPR

Sustainable Agriculture

Crop Health

Oryza sativa

ABSTRACT

Soilless cultivation has emerged as a fundamental alternative for large-scale vegetable production because it generates high-quality yields and uses resources efficiently. While plant growth-promoting bacteria (PGPB) are known to enhance growth and physiological aspects in crops grown in soil, their application in soilless cultivation has been relatively less explored. This study aimed to isolate potential PGPBs from soil samples collected from five locations in and around the Delhi-National Capital Region (NCR), India, which were further screened for significant PGPB attributes. Among these, 51 isolated were selected for assessing the impact on *Oryza sativa* (rice) growth and yield grown on a hydroponic set. The results indicated that isolates AFSI16 and ACSIO2 significantly improved the physiological parameters of the plants. For instance, treatment with AFSI16 showed a 23.27% increase in maximum fresh shoot mass, while ACSIO2 resulted in a 46.8% increase in root fresh mass. Additionally, ACSIO2 exhibited the highest shoot length (34.07%), whereas AFSI16 exhibited the longest root length (46.08%) in *O. sativa*. Treatment with AFSI16 also led to significant increases in total protein content (4.94%) and chlorophyll content (23.44%), while ACSIO2 treatment showed a 13.48% increase in maximum carotenoid

* Corresponding author

E-mail: akchauhan@amity.edu (Abhishek Chauhan); tjindal@amity.edu (Tanu Jindal)

Peer review under responsibility of Journal of Experimental Biology and Agricultural Sciences.

Production and Hosting by Horizon Publisher India [HPI]
(<http://www.horizonpublisherindia.in/>).
All rights reserved.

All the articles published by [Journal of Experimental Biology and Agricultural Sciences](http://www.jebas.org) are licensed under a [Creative Commons Attribution-NonCommercial 4.0 International License](https://creativecommons.org/licenses/by/4.0/) Based on a work at www.jebas.org.



content in the leaves. The potential PGPBs were identified through 16S rRNA sequencing, as the two most effective strains, AFSI16 and ACSI02, belonged to thermo-alkaliphilic *Bacillus licheniformis* and *Burkholderia* sp., respectively. This study demonstrated the potential of these identified PGPB strains in enhancing crop performance, specifically in soilless cultivation systems.

1 Introduction

In the twenty-first century, the world's agricultural system confronts more challenges, including declining productivity and degradation of agroecosystem sustainability. According to United Nations projections, the global human population is anticipated to reach 9 billion by 2050, leading to a persistent rise in food demand coupled with a continuous shortage in supply and adverse changes in suitable climate for agriculture (Wood 2001; Alexandratos and Bruinsma 2012; Meena et al. 2017, Zeifman et al. 2022). Agricultural practices have undergone many important transformations worldwide, especially after the Green Revolution. To enhance plant productivity and crop yield, the use of new high-yielding seed varieties, synthetic fertilizers, pesticides, and other agrochemicals are being used for better agricultural practices, which have been posing serious risks to humans, ecosystems, and the environment at large (Kaushik et al. 2009; Pingali 2012; Basu et al. 2021). Scientists, farmers, and agricultural representatives are gradually focusing on new sustainable solutions for growing agriculture issues with minimal environmental footprint. Sustainable agriculture practices require products that can enhance crop health by improving nutrient uptake efficiency, mitigating biotic challenges, and reducing the support on fertilizers, including other benefits such as improving soil fertility by remediation of organic pollutants and heavy metals (Hirel et al. 2011; Singh and Ryan 2015).

Sustainable agriculture encourages reducing synthetic agrochemicals and emphasizing the utilization of natural materials biowaste obtained from biowaste and the inherent capabilities of microorganisms and plants to promote the health and productivity of crops (Fascella et al. 2018). In this context, chicken droppings manure (CDM) has the potential to enhance soil fertility through alterations in soil microbial dynamics, which helps nutrient cycling. Additionally, they offer a sustainable and cost-effective method for enhancing soil health (Liu et al. 2016; Minkina et al. 2023).

The plant rhizosphere is considered a significant region in the soil of the root zone point for microbial activity where the root system, microorganisms, and soil form an association to create a micro-ecosystem to support the plant's health at indirect levels (Li et al. 2019; De La Fuente Cantó et al. 2020). The rhizosphere microbial community varies among plant species, growth stages, and environmental habitat and often includes PGPB (Hayat et al. 2010;

Hussain et al. 2011). Some of the PGPB strains improve the resilience of plants to abiotic stresses such as drought and salinity (Baha and Bekki 2015; Delshadi et al. 2017). It is also crucial in heavy metal remediation and degrading organic pollutants under their enzymatic activities and metabolic pathways (El-Meihy et al. 2019). They assist in immobilizing, transforming, and detoxifying heavy metals in the soil, contributing significantly to environmental cleaning efforts (Arora 2020). In mitigating biotic stresses, PGPBs act as natural defenders for plants against pathogens, pests, and other stress-inducing agents. They stimulate the plant's immune responses, produce antimicrobial compounds, and enhance its tolerance to diseases and pests (Yu et al. 2022; Ranjan et al. 2023). Hence, these strains of PGPB are evident to serve as biological stimulants for increasing plant growth and development to support the United Nations Sustainable Development Goals (Bhardwaj et al. 2023a).

PGPBs can improve biological nitrogen fixation, increase phosphate solubility, produce phytohormones and other compounds, encourage beneficial mycorrhizal-plant interactions, and protect plants from pathogenic bacteria (Di Benedetto et al. 2017). PGPB, which include well-studied genera like *Azospirillum*, *Azotobacter*, and *Nitrobacter* (although only a few are highly capable at root colonization), along with other genera such as *Bacillus*, *Pseudomonas*, *Bradyrhizobium*, *Acinetobacter*, *Klebsiella*, *Mesorhizobium*, and *Rhizobium*, have demonstrated capabilities in colonizing the root surface, surviving, and competing with other microbiota (Ahemad and Kibret 2014; Walker et al. 2003). Implementing rhizobacteria is one of the best approaches to enhance phytoremediation efficiency (Rajput et al. 2022).

Plants and microorganisms form different relationships that accelerate beneficial (both symbiotic and non-symbiotic) and pathogenic interactions. As plants grow, microorganisms inhabit the rhizosphere and connect with roots, producing substances controlling plant growth. Conversely, plants differentiate compounds derived from microbes and adjust their defence and growth mechanisms in response to the specific type of microorganism (Ortíz-Castro et al. 2009; Walker et al. 2003).

In agricultural practices, hydroponics involves cultivating plants in soilless systems, carrying essential nutrients through a water-based solution. Hydroponic systems yield substantially more than soil-based systems and encourage quicker growth (Touliatos et al.

2016). This might be due to the more accessible nutrient supply and the deficiency of inhibitions to root growth from soil-related systematic factors (Lee and Lee 2015; Sharma et al. 2018). Using PGPB presents an innovative solution for some of the major challenges in hydroponic cultivation. They prevent pathogen outbreaks, increase plants' strength to environmental stress, and strengthen crop yield per square meter. These combined benefits lead to a reduced benefits period for the initial capital investment (Stegelmeier et al. 2022).

In this study, bacterial strains were isolated from diverse soil types and evaluated for their ability to promote plant growth under hydroponic conditions. The research also highlights the application of the identified PGPB on hydroponically grown *Oryza sativa* growth. The study emphasizes sustainable agriculture and explains isolated bacterial strains' plant growth-promoting (PGP) potential, offering a promising way for eco-friendly and resilient agricultural practices.

2 Materials and Methods

All the chemicals used in the extraction and characterization stages were high purity (analytical research grade). The seeds of *Oryza sativa* were procured from the Indian Agriculture Research Institute (IARI), New Delhi, India.

2.1 Sample collection

The soil samples were collected from 0-20 cm depths from five different locations Delhi-NCR region, India. The collected soil samples varied in nature and included forest soil, soil from agricultural fields, riverbank soil, soil from landfill sites, and clayey soil. The soil from the forest area near Gwal Pahadi, Gurugram, Haryana, India (Aravalli Hills), has remained untouched by human activities, leading to its classification as an 'undisturbed' soil and was located 17 km from Gurugram. The soil from the agricultural field was located 20 km from Gautam Buddha Nagar, Uttar Pradesh, India. The soil from the riverbank was collected from the River Yamuna bank at Kalindi Kunj, Delhi, India. Soil from the landfill region was collected near the Ghazipur landfill site, Ghaziabad, Uttar Pradesh, India. The clayey soil was near the soil of a pond in the Bulandshahr District, Uttar Pradesh,

India. These collected samples were designated as AFSI (Amity Forest Soil Isolates), AASI (Amity Agriculture Soil Isolates), AYSI (Amity Yamuna Soil Isolates), ALSI (Amity Landfill Soil Isolates), and ACSI (Amity Clayey Soil Isolates) respectively. Table 1 contains the comprehensive sampling particulars, while Figure 1 illustrates the sampling locations.

Five specific sampling sites were selected due to their significant variations in paedogenetic factors, including parent material, landform, land use, and management practices. Additionally, molecular-level diversity in soil samples was suspiciously considered during the selection process.

Several sub-samples were collected from the same locations, air-dried, and sieved through a 2 mm mesh for chemical analysis. All experiments were carried out at 25±1°C and atmospheric pressure. The glassware used was cleaned properly with neutral washing reagents and distilled water.

2.2 Physicochemical properties of the soil samples

Soil samples were assessed for estimation of organic carbon (OC), nitrogen (N), available phosphorus (P), potassium (K), pH, and temperature of the soil by standard methodology. The Walkley and Black approach assessed OC (Walkley and Black 1934; Xiao et al. 2021). The available N, P and K were estimated using the Kjeldahl method, Bray's P-1 method and ammonium acetate (C₂H₇NO₂) extraction method, respectively (Richer and Holben 1950; Bray and Kurtz 1945; Ashworth and Mrazek 1995). The pH of the compost samples was analyzed with a digital pH measuring device (Labman, LMPH-10) by making soil-to-water suspension in 1:2 (w/v) (Behera and Shukla 2015).

2.3 Quantification and isolation of bacterial population from soil samples

To determine the bacterial population per gram of soil, a 1 mL sample was taken from each prepared dilution and streaked onto nutrient agar (NA) plates for multiple streak isolations. The count of colonies, distinguished by their morphological features, was conducted using a digital colony counter. To calculate the number of colonies, the equation of Chauhan and Jindal (2020) was

Table 1 Sampling locations for the soil sample collection sites

S. No.	Sample Codes	Sampling Regions	Latitude	Longitude
1	AFSI	Forest soil	28.457523	77.026344
2	AASI	Agricultural field soil	28.411331	77.848434
3	AYSI	River Yamuna bank soil	28.545267	77.306092
4	ALSI	Soil near landfill	28.625242	77.327989
5	ACSI	Clayey soil	28.514580	77.377594

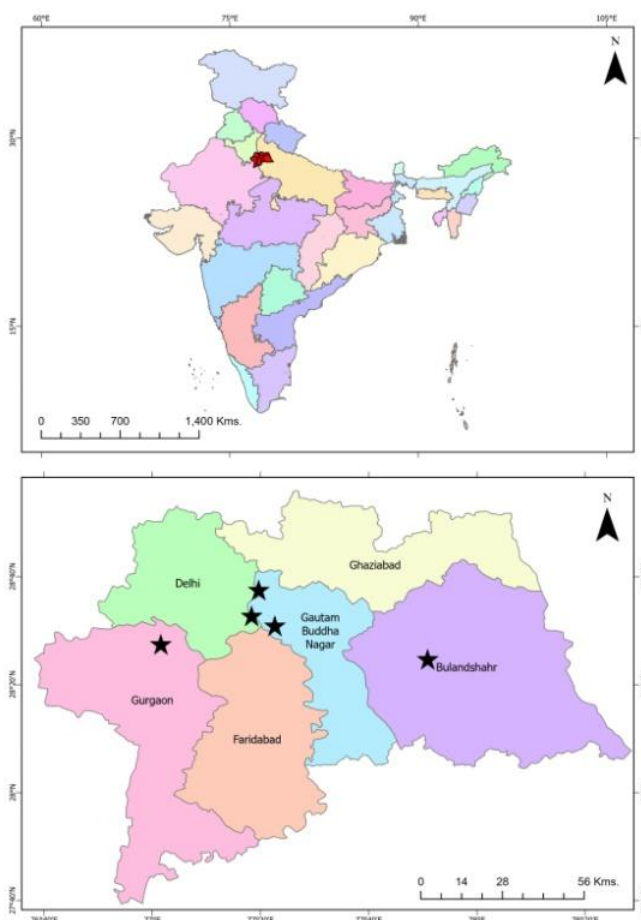


Figure 1 Sampling locations map of Delhi-NCR region

employed to express the count in Colony Forming Units per gram (CFU g⁻¹) of soil:

$$N = \frac{\Sigma C}{(n_1 + 0.1n_2)d} \times \frac{10}{\text{weight of sample taken}}$$

In this context, N represents the total colony-forming units within 1 mL of the sample, where 'd' signifies the dilution factor used for the initial counts, 'n1' and 'n2' denote the count of plates considered for the first and second dilutions, and ΣC sums up all the colonies observed across the plates. Upon microscopic examination, identical colonies were isolated and transferred onto NA plates to cultivate pure cultures. These cultures were subsequently assessed for their plant growth-promoting traits, as Chauhan and Jindal (2020) described.

The bacterial isolates were obtained through the pour-plate technique, using NA as the growth medium. The procedure involved serial 10-fold dilutions. Initially, 10 g of the sample was mixed with 90 mL of 0.9% saline solution. To evaluate the PGP potential of these isolates, distinct agar media were employed. The spread-plate cultures were sealed using parafilm and incubated in a

dark chamber at a controlled temperature of 25±1°C until the bacterial colonies became visible. This process was carried out in triplicate for each dilution. Subsequently, the colonies were differentiated based on morphological characteristics, isolated, and purified using the streak plate method. Based on their source of isolation, each isolate was assigned a unique code, and further subculturing was undertaken to ensure the isolation of pure colonies, which were then cultured on NA slants and stored at a temperature of 4°C for short-term usage (Chauhan and Jindal 2020).

2.4 Inoculum preparation

The selected bacterial isolates were aseptically inoculated into the nutrient broth and placed in an incubator at 30°C for 48 hours while shaking at 150 rpm. Centrifugation was carried out at 5000 rpm for 12 minutes to separate the cells. The resulting cell pellets were then resuspended in sterilized normal saline to attain an optical density of 1.0, corresponding to approximately 7 × 10⁸ CFU mL⁻¹. These prepared cultures served as a 1.0% (v/v) inoculum for investigating PGP attributes (Bhardwaj et al. 2023b).

2.5 Screening of bacterial isolates for PGP attributes

Using standard methods, the selected bacterial isolates were screened for various PGP attributes such as IAA production, siderophore production, PO_4^{2-} solubilization, NH_3 , and HCN production.

2.5.1 Indole acetic acid production

IAA production by bacterial isolates was assessed using the Salkowski reagent method. Bacterial cultures were grown in tryptophan-containing nutrient broth and subjected to centrifugation after 48 hours of incubation at $30 \pm 0.5^\circ\text{C}$ and 180 rpm in the dark to obtain the supernatants for testing IAA production (Gang et al. 2019). Two groups of 2 mL supernatants from nutrient broth cultures (one with tryptophan and one without) were incubated with 1 mL of Salkowski reagent for 30 minutes in the dark. The emergence of a pink colour confirmed IAA production, and its presence was further confirmed by measuring absorbance at 530 nm (Ehmann 1977).

2.5.2 Siderophore production

Siderophore production was assessed using the Chrome Azurol S (CAS) agar plate method (Schwyn and Neilands 1987). In this procedure, 48-hour-aged bacterial cultures were individually placed on CAS agar plates and then incubated for 48 hours at $28 \pm 1^\circ\text{C}$. These bacteria were cultured in nutrient broth for 72 hours at 28°C with continuous shaking at 150 rpm. The absence of the blue colour on the CAS agar plates indicated the presence of siderophores.

2.5.3 Phosphate solubilization

The assessment of PO_4^{2-} -solubilizing activity relied on observing clear halo zones surrounding bacterial colonies with the ability to solubilize calcium phosphate. Following the established protocol by Mehta and Nautiyal (2001), the qualitative examination of PO_4^{2-} -solubilization was conducted using Pikovskaya media. Each bacterial isolate was subjected to three replicates on these media plates, which were subsequently incubated at 30°C for 7 days. The formation of halo zones around the bacterial colonies was then examined as an indicator of PO_4^{2-} -solubilization.

2.5.4 Ammonia production

To assess NH_3 production by the isolates, they were initially cultivated in Ashby's N-free liquid medium for 24 hours at 37°C . Subsequently, these cultures were streaked and incubated on Ashby's N-free agar plates at the same temperature for 24 hours. NH_3 production was observed using the standard method (Kumar et al. 2012). The liquid medium-grown cultures underwent centrifugation for 10 minutes at 3000 rpm, and 0.2 mL of the supernatant was mixed with 1 mL of Nessler's reagent, with the

final volume adjusted to 8.5 mL using NH_3 -free distilled water. A colour change from brown to yellow indicated NH_3 production, while test tubes with no colour change were considered negative.

2.5.5 Hydrogen cyanide production

HCN production by the bacteria was examined using the method outlined by Lahlali et al. (2020). The bacteria were cultured on solid Luria Bertani (LB) medium supplemented with 4.4 gL^{-1} glycine. Each box's lid was lined with Whatman paper soaked in alkaline picrate and incubated for four days at 30°C . The presence of a red-orange colour indicated the production of HCN.

2.6 Evaluation of the potential effects of bacterial isolates on the growth of *O. sativa*

2.6.1 Seed procurement

The seeds of *O. sativa* were procured from National Seeds Corporation, IARI, Pusa, New Delhi, India, and were tested for germination potential. The seeds were sanitized for one minute with 70% ethanol (v/v), then for 20 min with 2.5% sodium hypochlorite with three washes with sterilized distilled water (Bhardwaj et al. 2023b).

2.6.2 Effects of Isolates on the seed germination rate (GR)

Sterilized square filter paper was placed in petri dishes and loaded with 45 seeds. Subsequently, 5 mL of sterilized distilled water and 0.1 mL of each bacterial isolate were added. The petri plates were sealed and incubated at $20 \pm 5^\circ\text{C}$ for 20 days. Control petri dishes contained uninoculated seeds (without bacterial isolates). Each day, the total number of germinated seeds was tallied, and the GR was calculated after 20 days using the provided equation (Islam et al. 2016).

$$\text{Germination rate \%} = \frac{\text{Germinated seeds}}{\text{Total seeds}} \times 100$$

2.6.3 Plant materials and growth conditions

Rice seeds (*Oryza sativa* L.) were procured from IARI, Delhi, India. Before use, seeds of consistent size underwent surface sterilization using a 10% (v/v) sodium hypochlorite solution for 10 minutes. Following this, they were thoroughly rinsed with distilled water and soaked for 4 hours. Subsequently, the healthy and uniformly sized seeds were placed in 150 mm petri plates, lined with Whatman no. 1 filter paper, and moistened with half-strength Hoagland's solution (pH 6.5) as described by Arditti and Dunn (1969). The bacterial inoculum was added in 10^8 CFU mL^{-1} . The seeds were then germinated in darkness at a temperature of $28 \pm 2^\circ\text{C}$ for 4 days. The ensuing seedlings were cultivated under a photon flux density (PFD) of $150 \mu\text{mol photons m}^{-2}\text{s}^{-1}$ and

maintained at a relative humidity range of 50–60%. This environment followed a 12-hour day/night cycle at a consistent temperature of $28 \pm 2^\circ\text{C}$ and humidity of 50% for 8 days within a growth chamber. Following this period, seedlings of uniform size were selected and transferred into half-strength Hoagland's solution for a 7-day acclimatization period. Subsequently, the leaves were carefully stored at -86°C until further analyses. After the 7-day treatment period, root and shoot samples were collected from both control and treated seedlings, and various parameters were analyzed (Arditti and Dunn 1969).

2.6.4 Morphological and Biochemical Characterization

The bacterial isolates exhibiting potential plant growth-promoting activity were subjected to morphological identification and biochemical tests. Colony morphology for colour, size, shape, margin, and elevation was observed under a compound microscope. Biochemical tests like oxidase, citrate, catalase, nitrate, starch, Indole, and Voges-Proskauer were performed (Chauhan and Jindal 2020).

2.6.5 Inoculation effects on growth parameters

The study assessed plant growth by measuring fresh and dry root and shoot weights. For each sample, ten randomly chosen seedlings underwent measurements. Dry weight was obtained by wrapping root and shoot sections in butter paper and oven-drying at $65\text{--}75^\circ\text{C}$ for 48 hours. Chlorophyll and carotenoid levels were determined by extracting 25 mg of fresh leaves with 80% acetone, using methods by Arnon (1949) and Ikan (1991).

The growth response was observed, focusing on chlorophyll content, shoot and root dry weight, and fresh weight. Measurements involved using a vernier calliper, manual counting, and spectrophotometric methods. Weight variations were determined using a standard balance during harvesting. Photosynthetic pigment analysis included harvesting the top leaf of matured plants, mixing a 0.2 g leaf sample with 80% acetone, and measuring absorbance at 652 nm using a UV-visible spectrophotometer (Lau et al. 2020).

2.7 DNA Isolation, PCR amplification, and phylogenetic assessment

DNA extraction process employed the use of GenElute™ Bacterial Genomic DNA kit. A 1.5 kbp 16S-rDNA segment was PCR-amplified with high-fidelity polymerase and the primers 16S forward (GGATGAGCCCGCGCCTA) and 16S reverse (CGGTGTGTACAAGGCCCGG). The PCR product was purified, visualized on agarose gel, and then subjected to bi-directional sequencing. NCBI's Blast software was used for the identification of the bacterium and to list its close relatives. Based on maximum identity scores, the top ten sequences were subjected to multiple

alignment software, Clustal W, where homologous nucleotide sequences were aligned. A phylogenetic tree was constructed using the neighbour-joining algorithm in MEGA 10 software, with tree-clade stability assessed through a 1000-replication bootstrap analysis (Kumar et al. 2018).

2.8 Statistical analysis

The gathered data experienced statistical analysis through IBM SPSS Statistics 23. An independent t-test was utilized to identify significant differences among the physicochemical properties of the 12 isolates. For assessing multiple comparisons between isolates and their impacts on plants, ANOVA Tukey's tests (T-test) were utilized. Germination results were compared against a control group, and all findings were visually presented using graphs created with MS Excel 2021.

3 Results

3.1 Soil physicochemical analysis

The soil physicochemical analysis unveiled notable variations in key parameters across the distinct soil samples. Organic carbon content exhibited a gradient, with AASI showcasing the highest at 4.2%, followed by AFSI at 3.2%, AYSI at 0.7%, ALSI at 0.2%, and ACSI at 2.6%. Nitrogen levels were highest in AFSI at 42 mgkg^{-1} , with AASI and ACSI recording intermediate values of 39 and 38 mgkg^{-1} , respectively. AYSI demonstrated a moderate nitrogen content of 26 mgkg^{-1} , while ALSI had the lowest at 21 mgkg^{-1} . Available phosphorus content followed a similar trend, with AFSI leading at 623 mgkg^{-1} , closely trailed by AASI at 611 mgkg^{-1} . AYSI exhibited a moderate level at 563 mg kg^{-1} , whereas ALSI and ACSI displayed lower values at 495 and 587 mgkg^{-1} , respectively. Further, the pH values varied distinctly, with ALSI characterized by a highly alkaline pH of 8.5 ± 0.4 , while AYSI and AFSI had pH values of 7.9 ± 0.2 and 7.8 ± 0.2 , respectively. ACSI samples were almost with a neutral pH of 7.2 ± 0.1 . Temperature differences were observed, with AFSI experiencing the highest at 48°C , while the lowest at 36°C with ACSI and AASI, AYSI, and ALSI exhibiting intermediate temperatures of 39, 38, and 40°C , respectively. These findings underscore the diverse soil characteristics (Table 2).

3.2 Quantification and isolation of bacteria

The forest area exhibited a total bacterial population of $1.9 \times 10^9\text{ CFUg}^{-1}$, while the agricultural area, Yamuna region, and disposal site displayed bacterial populations of $3.1 \times 10^6\text{ CFUg}^{-1}$, $1.6 \times 10^6\text{ CFUg}^{-1}$, and $1.1 \times 10^6\text{ CFUg}^{-1}$, respectively. Clayey soil recorded a bacterial population of $2.8 \times 10^7\text{ CFUg}^{-1}$. Subsequently, based on observed colony morphology on NA during the enumeration process, 51 isolates with identical colonies were specifically chosen for further screening to identify potential PGP strains (Figure 2).

Table 2 Physicochemical analysis of soil samples

S. No.	Parameters	AFSI	AASI	AYSI	ALSI	ACSI
1	Organic carbon	3.2%	4.2%	0.7%	0.2%	2.6%
2	Nitrogen (mgkg ⁻¹)	42	39	26	21	38
3	Available phosphorus (mgkg ⁻¹)	623	611	563	495	587
5	pH	7.8 ± 0.2	7.6 ± 0.1	7.9 ± 0.2	8.5 ± 0.4	7.2 ± 0.1
6	Temperature (°C)	48	39	38	40	36

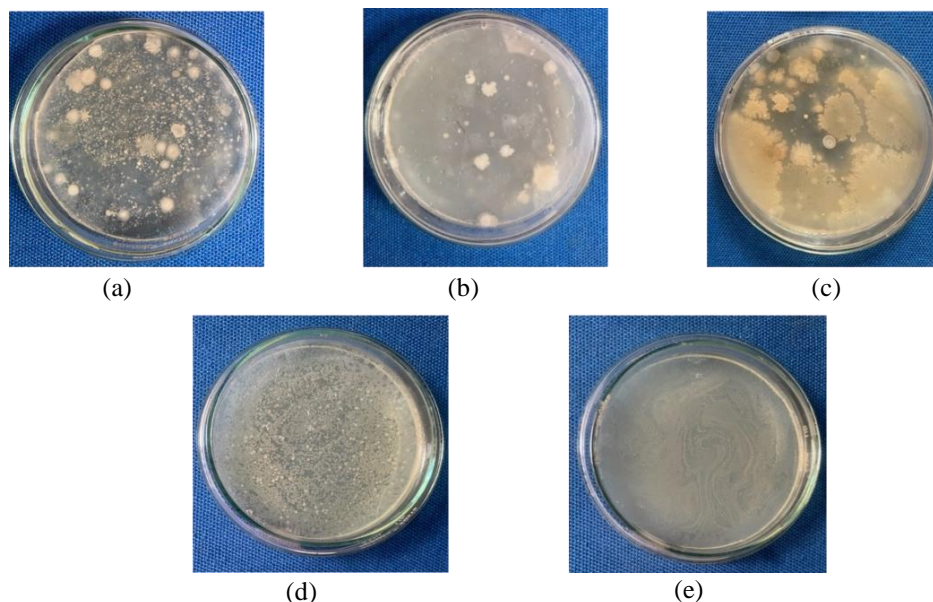


Figure 2 Bacterial Isolates from the five sampling sites: (a) Forest soil, (b) Agricultural field soil, (c) River Yamuna bank soil, (d) Soil near the landfill, and (e) Clayey soil

3.3 Screening of bacterial isolates for PGP attributes

In this study, 51 bacterial strains were isolated from various soil samples and their PGP attributes were evaluated. Twelve isolates were confirmed to be positive for IAA and siderophore production and the formation of HCN and NH₃, along with phosphate solubilization. IAA production was determined by a colour change from pale yellow to pink in Salkowski treatments; among the isolated bacterial strains, AFSI16 was identified as the highest IAA producer among the 51 isolates. Siderophore production was evidenced by a colour change from blue to orange in CAS medium for all 12 isolates. Clear zones surrounding bacterial colonies on Pikovskaya's agar confirmed the ability to solubilize phosphate. Among the isolates, only 12 demonstrated efficient emission of a high ammonia concentration, as indicated by a deep yellow colour in nesslerized spent broth. Additionally, HCN production was observed in the 12 isolates, evidenced by a colour change from pale yellow to red-orange in the LB medium. Thus, the twelve strains, namely AFSI06, AFSI07, AFSI10, AFSI16, AFSI19, AASI03, AASI07, AASI13, ACSI02, ACSI06, ACSI08, ACSI09,

and control were identified as exhibiting all PGP attributes and were selected for further experiments in a hydroponic setup.

3.4 The effect of PGPB isolates on the growth of *O. sativa* seedlings

In the current study, 12 bacterial strains were selected after a preliminary study, and it demonstrated that the inoculation of isolates had an impact on SFW, RFW, root length, shoot length, chlorophyll content, protein content, and carotenoid content of *O. sativa*. Significantly enhanced SFM was observed in AFSI16 (0.795 ± 0.012) and ACSI024 (0.795 ± 0.020), and it was found to be 23.27% higher compared to the control T0 (0.645 ± 0.020) (p<0.05). Concurrently, RFM showed substantial elevation in AFSI16 (0.321 ± 0.005) and AASI14 (0.322 ± 0.005), rising by 45.45% and 46.8%, respectively, compared to the control (0.221 ± 0.007) (p<0.05). However, except for AFSI16 and ACSI02, the other treatments did not exhibit significant changes (p<0.05) following the inoculation of PGP isolates on rice seedlings (Figure 3).

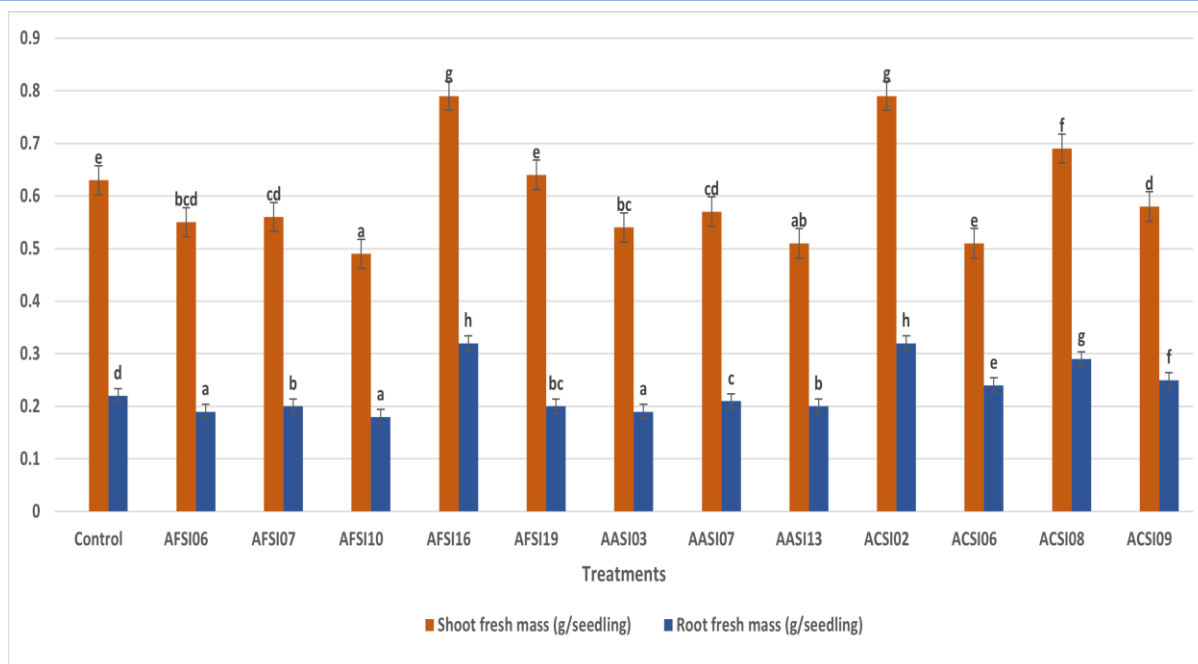


Figure 3 Effects of 12 isolates inoculated in the *O. sativa* crop in the Hydroponics system on shoot fresh mass and root fresh mass of plants. Error bars represent the mean \pm S.D of three replicates. Different letters above columns indicate statistically significant differences at $p \leq 0.05$

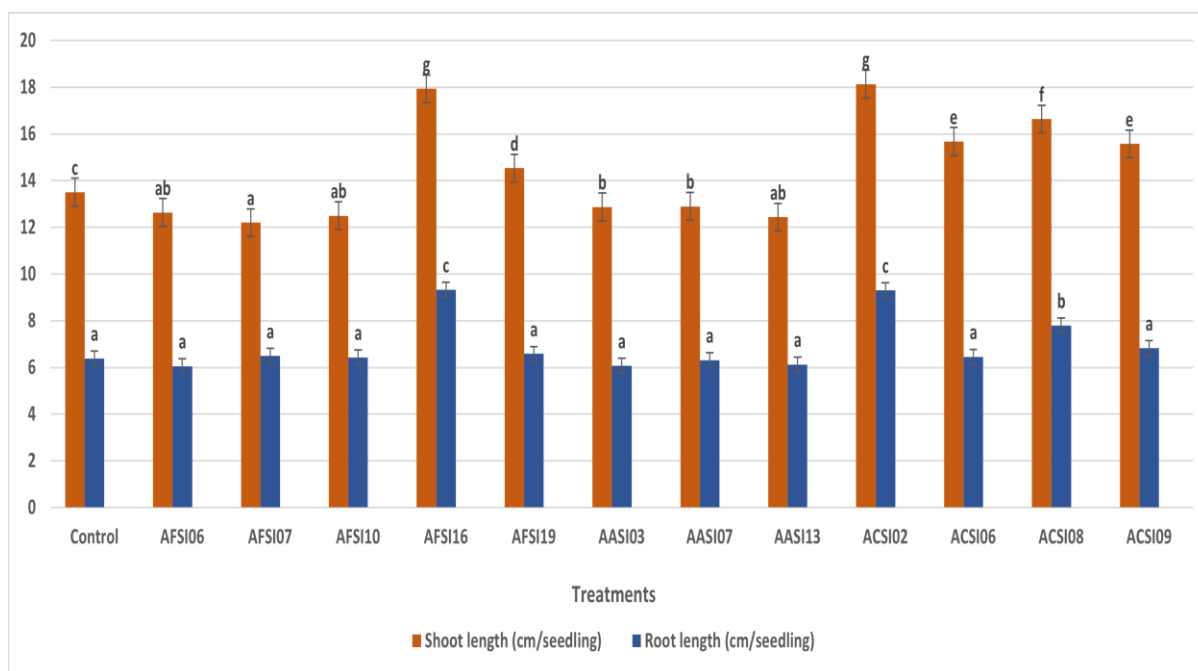


Figure 4 Effects of 12 isolates inoculated in the *O. sativa* crop in the Hydroponics system on plants' shoot and root length. Error bars represent the mean \pm S.D of three replicates. Different letters above columns indicate statistically significant differences at $p \leq 0.05$

Like shoot and root mass, significant improvements were observed in SL for AFSI16 (17.93 ± 0.145) and ACSI02 (18.13 ± 0.12) and it is demonstrating increases of 32.5% and 34.07%, respectively, compared to the control (13.5 ± 0.23) ($p < 0.05$). Meanwhile, RL exhibited significant enhancements in AFSI16 (9.32 ± 0.023) and

ACSI02 (9.3 ± 0.03), rising by 46.08% and 45.76%, respectively, in comparison to the control (6.38 ± 0.31) ($p < 0.05$). However, except for AFSI16 and ACSI02, the remaining treatments did not exhibit significant changes ($p < 0.05$) after the inoculation of PGP isolates on rice seedlings (Figure 4).

Significant improvements were observed in TP; among the tested 12 strains, bacterial strain AFSI16 (17.44 ± 0.76) displayed a 4.94% increase compared to the control (16.58 ± 0.46) ($p < 0.05$). Similarly, TC exhibited significant increases in AFSI16 (1.79 ± 0.18) and ACSI02 (1.73 ± 0.15), rising by 23.44% and 19.31%, respectively, compared to control (1.45 ± 0.05) ($p < 0.05$). Additionally, carotenoid

content significantly increased in AFSI16 (481.48 ± 15.74) and ACSI02 (493.66 ± 26.57), showing increments of 23.44 and 19.31%, respectively, compared to the control (435 ± 12.68) ($p < 0.05$). However, apart from AFSI16 and ACSI02, the other treatments did not exhibit significant changes ($p < 0.05$) after the inoculation of PGP isolates on rice seedlings (Figure 5).

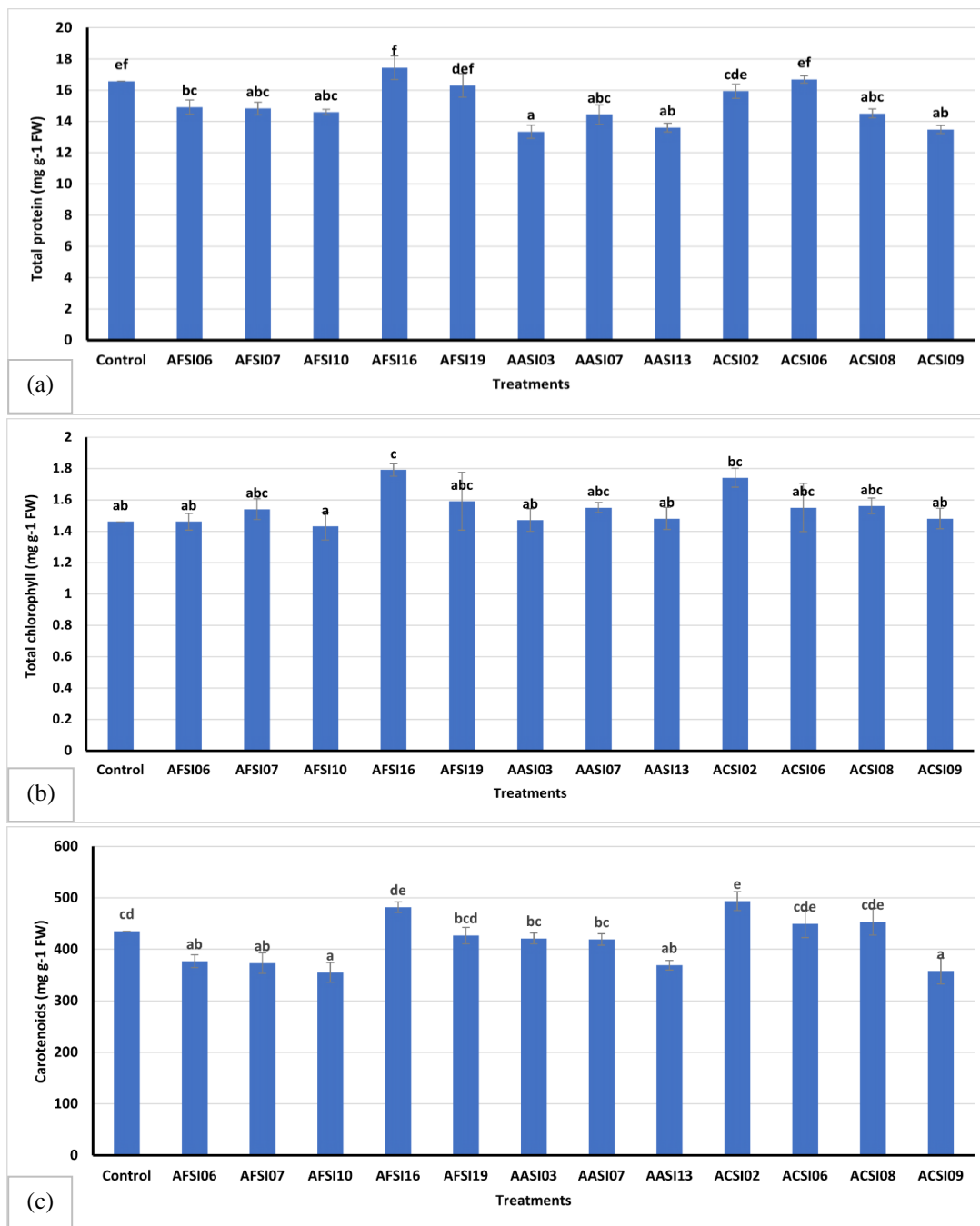


Figure 5 Effects of 12 isolates inoculated in the *O. sativa* crop in the Hydroponics system on (a) total protein, (b) total chlorophyll, and (c) carotenoid content of plants. Error bars represent the mean \pm S.D. of three replicates. Different letters above columns indicate statistically significant differences at $p \leq 0.05$

Table 3 Percentage growth promotion of PGP isolates on rice seedlings as compared to control

Treatments	Shoot fresh mass %	Root fresh mass %	Shoot length %	Root length %	Total protein %	Total Chlorophyll %	Carotenoid %
AFSII6	23.27	45.45	32.5	46.08	4.94	23.44	10.68
ACSI02	23.25	46.8	34.07	45.76	4.1	19.31	13.48

3.5 Efficacy of PGP isolates on the growth promotion of rice seedlings

Among the various treatments applied to rice seedlings, distinctive outcomes were observed. Treatment AFSII6 and ACSI02 exhibited the highest increase in shoot fresh mass by 23.27% and 23.25%. In a similar pattern, treatment ACSI02 resulted in the greatest surge in root fresh mass at 46.8%, followed by 45.5% of treatment AFSII6. Moreover, treatment ACSI02 has remarkably enhanced shoot length by 34.07% and treatment AFSII6 by 32.5%. The highest root length was observed in AFSII6 treatment (46.08%), followed by treatment ACSI02 (45.76%). Treatment AFSII6 exhibited the highest total protein content of 4.94%, while it was reported 4.1% in treatment ACSI02. Regarding chlorophyll content, 23.44% was the highest total chlorophyll content value observed in treatment AFSII6, while this % was reported 19.31% in treatment ACSI02. Carotenoid percentage of 13.48% was the maximum percentage reported in treatment ACSI02, followed by 10.68% in treatment AFSII6 (Table 3).

In general, two of the twelve bacterial isolates used in this study improved the growth parameter of rice seedlings as compared to the control; however, the AFSII6 isolate showed better enhancement (Table 3).

3.6 Morphological and Biochemical Characterization

Among the isolated bacterial strains, AFSII6 is characterized by irregular colonies with an undefined margin and demonstrates adaptability with a shiny, moist surface and pale colouration. Gram

staining revealed a positive result, which indicated the presence of a robust peptidoglycan layer. The rod-shaped, endospore-forming bacterium is actively motile, enhancing its exploration capabilities. Biochemically, it thrives aerobically and facultative anaerobically, showing positive catalase and citrate production. Negative results in Indole, oxidase, and urease tests contrast with positive nitrate reduction. These combined traits depict AFSII6 as a versatile and resilient bacterium adapted for diverse environments with potential clinical significance.

On the other hand, ACSI02 was characterized by circular colonies with entire margins (2-5 mm), presenting a convex, opaque surface that is white and glistening. Gram staining is negative, revealing curved rod-shaped vegetative cells without endospore formation. Despite the absence of endospores, ACSI02 is actively motile. Biochemically, it prefers aerobic growth and displays negative indole production. Positive catalase and citrate production highlights its ability to break down hydrogen peroxide and utilize citrate as a carbon source. ACSI02 is oxidase-positive, lacking urease activity and nitrate reduction. Importantly, it shows no haemolysis on blood agar, signifying non-destructive behaviour towards red blood cells. This collective profile defines ACSI02 as a motile, non-endospore-forming bacterium with specific colony morphology and metabolic traits (Table 4 and 5).

3.7 16SrRNA sequencing

A total of 168 ng and 172 ng of DNA were successfully extracted from the AFSII6 and ACSI02 strains, respectively. Subsequent 16S rRNA sequencing revealed that AFSII6 exhibited an impressive

Table 4 Morphological tests of *Bacillus licheniformis* (AFSII6) and *Burkholderia* sp. (ACSI02)

Morphological characteristics	AFSII6	ACSI02
Colony shape	Irregular	Circular
Margin	Irregular	Entire
Size of colony	-	2-5 mm
Elevation	Flat	Convex
Surface	Shiny and moist	Opaque
Colour	Pale	White and glistening
Odour	Yes	-
Gram staining	Positive	Negative
Shape of vegetative cells	Rod shaped	Curved rods
Endospore formation	Yes	No
Motility	Actively motile	Actively motile

Table 5 Biochemical tests of *Bacillus licheniformis* (AFSII6) *Burkholderia* sp. (ACSI02)

Biochemical tests	AFSII6	ACSI02
Growth	Aerobic and facultative anaerobic growth	Aerobic growth
Indole production	Negative	Negative
Catalase production	Positive	Positive
Citrate production	Positive	Positive
Oxidase production	Negative	Positive
Urease test	Negative	Negative
Nitrate reduction test	Positive	Negative
Haemolysis on blood agar plate	β -haemolytic	Negative

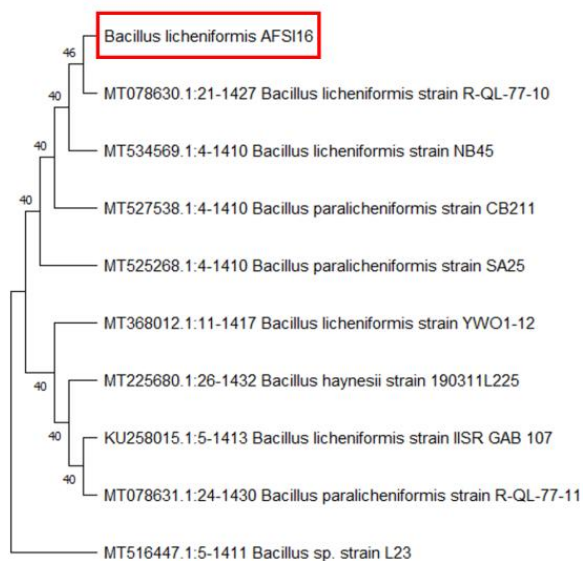


Figure 6 Phylogenetic tree of the selected isolates AFSII6 with its nearest neighbours

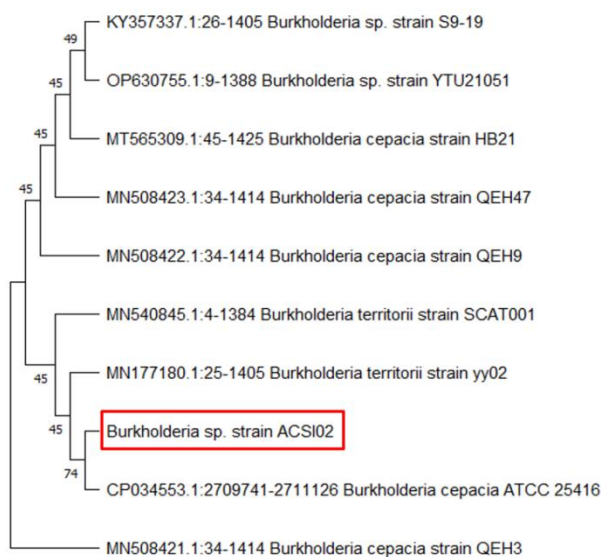


Figure 7 Phylogenetic tree of the selected isolate ACSI02 with its nearest neighbours

99.86% genetic similarity with *Bacillus licheniformis* strain IISR GAB 107, while ACSI02 demonstrated a 97.40% similarity to *Burkholderia* sp. strain S9-19. The 16S rRNA phylogenetic tree analysis further substantiated these findings, confirming that AFSI16 aligns with *B.licheniformis* (Figure 6) and ACSI02 corresponds to *Burkholderia* sp. (Figure 7).

4 Discussion

Holistic understanding is essential for informed agricultural strategies, promoting environmentally intentional approaches for sustainable crop health and enhanced productivity in diverse ecosystems. In this study, diverse soil samples from Delhi-NCR exhibited significant variations in organic carbon (OC), nitrogen (N), phosphorus (P), pH, and temperature. Among the collected soil samples, AASI had the highest organic carbon (4.2%), ALSI had the lowest (0.2%), and the nitrogen and phosphorus levels followed similar trends. pH values varied from highly alkaline in ALSI to slightly acidic in AYSI and AFSI. Temperature differences were observed, with AFSI experiencing the highest (48°C). Bacterial quantification showed varying populations, with the forest area having the highest at 1.9×10^9 CFUg⁻¹ and the disposal site the lowest at 1.1×10^6 CFUg⁻¹. Further screening of 51 isolates for PGP attributes added depth to microbial exploration. These findings align with research emphasizing the influence of soil physicochemical properties on microbial activities and community composition. For instance, the study by Chen et al. (2003) on *Burkholderia pseudomallei* highlighted the importance of soil pH and temperature in microbial growth, reflecting parallels with the Delhi-NCR soil variations. Sharma et al. (2019) demonstrated the correlation between physicochemical properties and soil microbial diversity, reinforcing that soil conditions drive microbial community shifts. Similarly, Mhete et al. (2020) investigated bacterial abundance and diversity under different land-use regimes, connecting these variations to soil properties, which resonates with the observed variations in Delhi-NCR soils. The study by Sapkota et al. (2020) on antimicrobial-producing *Actinomyces* further emphasizes the impact of diverse soil conditions on microbial functional capabilities.

In the current study, the results obtained from the hydroponics experiments, wherein isolates AFSI16 and ACSI02 exhibited a substantial enhancement in the growth parameters of *O. sativa*, align closely with other studies highlighting the favourable influence of *Bacillus* sp. and various other plant growth-promoting bacteria on a wide range of crops. Especially the results align with studies investigating the growth promotion effects of *Bacillus* sp. on rice seedlings, tomato plants, and paddy plants (Awlachev and Mengistie 2022; De O. Nunes et al. 2023; Kumari et al. 2022). The observed improvements in shoot and root parameters, as well as the promotion of root exudation of essential metabolites, parallel the positive effects reported in the hydroponics experiments

(Rekha et al. 2020). The study by Arimurti et al. (2022), focusing on bacteria isolated from hydroponic rock wool, aligns with our hydroponics results, showcasing positive influences on total protein, chlorophyll, and carotenoid content in *O. Sativa*. The concept of using specific bacterial isolates to enhance nutrient availability and alleviate stress demonstrated in this study is similar to the Wang et al. (2023) and Khan et al. (2021) studies. The similarity between our study and these diverse investigations provides additional context and highlights the key role of specific bacterial isolates in promoting plant growth, nutrient uptake, and stress tolerance across various crops.

Our study revealed that AFSI16, characterized as *Bacillus licheniformis*, and ACSI02, identified as *Burkholderia* sp., exhibit growth-promoting attributes in hydroponic *O. sativa* cultivation. In comparison, Mohammad et al. (2017) emphasize thermophilic *Bacillus licheniformis* enzyme production, while Pande et al. (2017) and O'Hair et al. (2020) explore *Burkholderia cepacia-related* strains for phosphate solubilization and biochemical production. The findings of this study contribute unique insights into the specific growth-related features of *B. licheniformis* and *Burkholderia* sp. in hydroponic rice systems.

Thermo-alkalophilic bacteria represent a fascinating group of microorganisms renowned for their ability to thrive in extreme conditions of both high temperature and alkalinity. These resilient bacteria have adapted to environments characterized by elevated temperatures, often exceeding 50° C, and alkaline pH levels ranging from 8-10 or higher; therefore, they could be categorized as thermos-alkalophilic bacteria as reported in previous studies (Brock 1978; Perry and Staley 1997; Souza and Martins 2001; Olsson et al. 2003). The genus *Bacillus* is adaptable to high-temperature settings and resilient in harsh environmental conditions (Connor et al. 2010; Kawasaki et al. 2011; Aanniz et al. 2015). Furthermore, Manachini et al. (1998) identified three distinct groups within 182 isolated *B. licheniformis* strains. Similarly, this strain has been found in various hot springs across the globe (Manachini et al. 1998).

Earlier studies in Jordan recognized the isolation of thermophilic bacteria categorized under the genus *Bacillus* (Mohammad et al. 2017). Thermo-alkalophilic bacteria play pivotal roles in bioremediation efforts and the production of enzymes and bioactive compounds. Their exceptional capacity to flourish and function well in demanding settings makes them different subjects for scientific investigation and raises the intriguing potential for various sectors (Tizazu et al. 2022). The unique contributions of *B.licheniformis* and *Burkholderia* sp. in hydroponic rice systems illuminate a path for eco-friendly practices, resonating with the broader movement towards environmentally conscious agricultural approaches for heightened productivity and improved crop health.

Conclusion

This study investigated the potential of two different species as plant growth-promoting bacteria (PGPB) in soilless cultivation: thermo-alkaliphilic *B. licheniformis* (AFSI16) and *Burkholderia* sp. (ACSI02). Following a rigorous screening procedure, 12 isolates with various PGP characteristics were identified and isolated, which suggested their potential to boost plant development. Among these twelve strains, AFSI16 and ACSI02 have remarkably impacted *O. sativa* (rice) growth in the hydroponics cultural system, especially by greatly enhancing root and shoot development. Two PGPB strains, AFSI16 and ACSI02, helped encourage crucial components essential for plant health. They particularly amplified the root length, possibly due to their capacity to stimulate root proliferation and elongation. Additionally, the presence of these strains led to heightened levels of proteins, carotenoid, and chlorophyll content within the plants, indicating their role in enhancing physiological processes vital for growth, possibly through nutrient uptake facilitation or enhanced metabolic activities. The conclusive identification of these PGPB strains through 16S rRNA sequencing further solidifies their significance in soilless cultivation. This discovery presents an exciting opportunity for sustainable and resource-efficient vegetable production in systems without traditional soil and offers a pathway to maximize growth and nutrition.

References

- Aanniz, T., Ouadghiri, M., Melloul, M., Swings, J., Elfahime, E., et al. (2015). Thermophilic bacteria in Moroccan hot springs, salt marshes and desert soils. *Brazilian Journal of Microbiology*, *46*(2), 443–453. <https://doi.org/10.1590/S1517-838246220140219>
- Ahemad, M., & Kibret, M. (2014). Mechanisms and applications of plant growth promoting rhizobacteria: Current perspective. *Journal of King Saud University - Science*, *26*(1), 1–20. <https://doi.org/10.1016/j.jksus.2013.05.001>
- Alexandratos, N., & Bruinsma, J. (2012). World agriculture towards 2030/2050: the 2012 revision.
- Arditti, J., & Dunn, A. (1969). *Experimental plant physiology: experiments in cellular and plant physiology*. Holt, Rinehart and Winston publication.
- Arimurti, A. R. R., Rohmayani, V., Romadhon, N., Rahmani, T. P. D., Watson, L. J., Wahyuni, K. S., & Ulumiya, N. (2022). The potency of bacteria isolated from the hydroponic rockwool of field mustard (*Brassica rapa* L.) for nitrogen fixation and indole acetic acid (IAA) production. *Biogenesis: Jurnal Ilmiah Biologi*, *10*(1), 112–120. DOI: <https://doi.org/10.24252/bio.v10i1.28451>.
- Arnon, D. I. (1949). Copper enzymes in isolated chloroplasts. Polyphenoloxidase in *Beta vulgaris*. *Plant Physiology*, *24*(1), 1–15. <https://doi.org/10.1104/pp.24.1.1>
- Arora, P. K. (Ed.). (2020). *Microbial technology for health and environment* (Vol. 22). Springer Singapore. <https://doi.org/10.1007/978-981-15-2679-4>
- Ashworth, J., & Mrazek, K. (1995). "Modified Kelowna" test for available phosphorus and potassium in soil. *Communications in Soil Science and Plant Analysis*, *26*(5–6), 731–739. <https://doi.org/10.1080/00103629509369331>
- Awlachew, Z. T., & Mengistie, G. Y. (2022). Growth promotion of rice (*Oryza sativa* L.) seedlings using plant growth-promoting rhizobacteria (Pgpr) isolated from northwest Ethiopia. *Advances in Agriculture*, *2022*, 1–8. <https://doi.org/10.1155/2022/1710737>
- Baha, N., & Bekki, A. (2015). An approach of improving plant salt tolerance of lucerne (*Medicago sativa*) grown under salt stress: Use of bio-inoculants. *Journal of Plant Growth Regulation*, *34*(1), 169–182. <https://doi.org/10.1007/s00344-014-9455-8>
- Basu, A., Prasad, P., Das, S. N., Kalam, S., Sayyed, R. Z., Reddy, M. S., & El Enshasy, H. (2021). Plant growth promoting rhizobacteria (Pgpr) as green bioinoculants: Recent developments, constraints, and prospects. *Sustainability*, *13*(3), 1140. <https://doi.org/10.3390/su13031140>
- Behera, S. K., & Shukla, A. K. (2015). Spatial distribution of surface soil acidity, electrical conductivity, soil organic carbon content and exchangeable potassium, calcium and magnesium in some cropped acid soils of India. *Land Degradation & Development*, *26*(1), 71–79. <https://doi.org/10.1002/ldr.2306>
- Bhardwaj, P., Chauhan, A., Ranjan, A., Mandzhieva, S. S., Minkina, T., Mina, U., Rajput, V. D., & Tripathi, A. (2023b). Assessing growth-promoting activity of bacteria isolated from municipal waste compost on *Solanum lycopersicum* L. *Horticulturae*, *9*(2), 214. <https://doi.org/10.3390/horticulturae9020214>
- Bhardwaj, P., Sharma, R. K., Chauhan, A., Ranjan, A., Rajput, V. D., et al. (2023a). Assessment of heavy metal distribution and health risk of vegetable crops grown on soils amended with municipal solid waste compost for sustainable urban agriculture. *Water*, *15*(2), 228. <https://doi.org/10.3390/w15020228>
- Bray, R. H., & Kurtz, L. T. (1945). Determination of total, organic, and available forms of phosphorus in soils. *Soil Science*, *59*(1), 39–46. <https://doi.org/10.1097/00010694-194501000-00006>
- Brock, T. D. (Ed.) (1978). *Thermophilic microorganisms and life at high temperatures*. Springer New York. <https://doi.org/10.1007/978-1-4612-6284-8>
- Chauhan, A., & Jindal, T. (2020). Microbiological Methods for Water, Soil and Air Analysis. In A. Chauhan, & T. Jindal (Eds.),

- Microbiological Methods for Environment, Food and Pharmaceutical Analysis* (pp. 93-196). Springer, Cham. https://doi.org/10.1007/978-3-030-52024-3_7
- Chen, Y. S., Chen, S. C., Kao, C. M., & Chen, Y. L. (2003). Effects of soil pH, temperature and water content on the growth of *Burkholderia pseudomallei*. *Folia Microbiologica*, 48(2), 253–256. <https://doi.org/10.1007/BF02930965>
- Connor, N., Sikorski, J., Rooney, A. P., Kopac, S., Koepfel, A. F., et al. (2010). Ecology of speciation in the genus *Bacillus*. *Applied and Environmental Microbiology*, 76(5), 1349-1358.
- De La Fuente Cantó, C., Simonin, M., King, E., Moulin, L., Bennett, M. J., Castrillo, G., & Laplaze, L. (2020). An extended root phenotype: The rhizosphere, its formation and impacts on plant fitness. *The Plant Journal*, 103(3), 951–964. <https://doi.org/10.1111/tpj.14781>
- De O. Nunes, P. S., De Medeiros, F. H. V., De Oliveira, T. S., De Almeida Zago, J. R., & Bettiol, W. (2023). *Bacillus subtilis* and *Bacillus licheniformis* promote tomato growth. *Brazilian Journal of Microbiology*, 54(1), 397–406. <https://doi.org/10.1007/s42770-022-00874-3>
- Delshadi, S., Ebrahimi, M., & Shirmohammadi, E. (2017). Effectiveness of plant growth promoting rhizobacteria on *Bromus tomentellus* Boiss seed germination, growth and nutrients uptake under drought stress. *South African Journal of Botany*, 113, 11–18. <https://doi.org/10.1016/j.sajb.2017.07.006>
- Di Benedetto, N. A., Corbo, M. R., Campaniello, D., Cataldi, M. P., Bevilacqua, A., Sinigaglia, M., & Flagella, Z. (2017). The role of plant growth promoting bacteria in improving nitrogen use efficiency for sustainable crop production: a focus on wheat. *AIMS microbiology*, 3(3), 413.
- Ehmann, A. (1977). The van URK-Salkowski reagent—A sensitive and specific chromogenic reagent for silica gel thin-layer chromatographic detection and identification of indole derivatives. *Journal of Chromatography A*, 132(2), 267–276. [https://doi.org/10.1016/S0021-9673\(00\)89300-0](https://doi.org/10.1016/S0021-9673(00)89300-0)
- El-Meihy, R. M., Abou-Aly, H. E., Youssef, A. M., Tewfike, T. A., & El-Alkshar, E. A. (2019). Efficiency of heavy metals-tolerant plant growth promoting bacteria for alleviating heavy metals toxicity on sorghum. *Environmental and Experimental Botany*, 162, 295–301. <https://doi.org/10.1016/j.envexpbot.2019.03.005>
- Fascella, G., Montoneri, E., & Francavilla, M. (2018). Biowaste versus fossil sourced auxiliaries for plant cultivation: The Lantana case study. *Journal of Cleaner Production*, 185, 322–330. <https://doi.org/10.1016/j.jclepro.2018.02.242>
- Gang, S., Sharma, S., Saraf, M., Buck, M., & Schumacher, J. (2019). Analysis of indole-3-acetic acid (Iaa) production in *Klebsiella* by LC-MS/MS and the Salkowski method. *Bio-Protocol*, 9(9). <https://doi.org/10.21769/BioProtoc.3230>
- Hayat, R., Ali, S., Amara, U., Khalid, R., & Ahmed, I. (2010). Soil beneficial bacteria and their role in plant growth promotion: A review. *Annals of Microbiology*, 60(4), 579–598. <https://doi.org/10.1007/s13213-010-0117-1>
- Hirel, B., Tétu, T., Lea, P. J., & Dubois, F. (2011). Improving nitrogen use efficiency in crops for sustainable agriculture. *Sustainability*, 3(9), 1452–1485. <https://doi.org/10.3390/su3091452>
- Hussain, Q., Liu, Y., Zhang, A., Pan, G., Li, L., Zhang, X., Song, X., Cui, L., & Jin, Z. (2011). Variation of bacterial and fungal community structures in the rhizosphere of hybrid and standard rice cultivars and linkage to CO₂ flux: Rice cultivars effect on microbial communities and CO₂ flux. *FEMS Microbiology Ecology*, 78(1), 116–128. <https://doi.org/10.1111/j.1574-6941.2011.01128.x>
- Ikan, R. (1991). *Natural products: A laboratory guide* (2nd ed). Academic Press.
- Islam, S., Akanda, A. M., Prova, A., Islam, Md. T., & Hossain, Md. M. (2016). Isolation and identification of plant growth promoting rhizobacteria from cucumber rhizosphere and their effect on plant growth promotion and disease suppression. *Frontiers in Microbiology*, 6. <https://doi.org/10.3389/fmicb.2015.01360>
- Kaushik, P., Abhishek, C., & Pankaj, G. (2009). Screening of *Lyngbya majuscula* for potential antibacterial activity and HPTLC analysis of active methanolic extract. *Journal of Pure and Applied Microbiology*, 3(1), 169-174.
- Kawasaki, Y., Aoki, M., Makino, Y., Sakai, H., Tsuboi, Y., et al. (2011). Characterization of moderately thermophilic bacteria isolated from saline hot spring in Japan. *Microbiology Indonesia*, 5(2), 2-2.
- Khan, M. A., Hamayun, M., Asaf, S., Khan, M., Yun, B.-W., Kang, S.M., & Lee, I.J. (2021). Rhizospheric bacillus *Bacillus* spp. Rescues plant growth under salinity stress via regulating gene expression, endogenous hormones, and antioxidant system of oryza *Oryza sativa* l. *Frontiers in Plant Science*, 12, 665590. <https://doi.org/10.3389/fpls.2021.665590>
- Kumar, A., Kumar, A., Devi, S., Patil, S., Payal, C., & Negi, S. (2012). Isolation, screening and characterization of bacteria from Rhizospheric soils for different plant growth promotion (PGP) activities: an in vitro study. *Recent research in science and technology*, 4(1), 1-5.

- Kumar, S., Stecher, G., Li, M., Knyaz, C., & Tamura, K. (2018). Mega x: Molecular evolutionary genetics analysis across computing platforms. *Molecular Biology and Evolution*, 35(6), 1547–1549. <https://doi.org/10.1093/molbev/msy096>
- Kumari, M., Swarupa, P., & Kumar, A. (2022). Validation and evaluation of plant growth promoting potential of rhizobacteria towards paddy plants. *Journal of Pure and Applied Microbiology*, 16(2), 1209–1225. <https://doi.org/10.22207/JPAM.16.2.50>
- Lahlali, R., Mchachtii, O., Radouane, N., Ezrari, S., Belabess, Z., Khayi, S., Mentag, R., Tahiri, A., & Barka, E. A. (2020). The potential of novel bacterial isolates from natural soil for the control of brown rot disease (*Monilinia fructigena*) on apple fruits. *Agronomy*, 10(11), 1814. <https://doi.org/10.3390/agronomy10111814>
- Lau, E. T., Tani, A., Khew, C. Y., Chua, Y. Q., & Hwang, S. S. (2020). Plant growth-promoting bacteria as potential bio-inoculants and biocontrol agents to promote black pepper plant cultivation. *Microbiological Research*, 240, 126549. <https://doi.org/10.1016/j.micres.2020.126549>
- Lee, S., & Lee, J. (2015). Beneficial bacteria and fungi in hydroponic systems: Types and characteristics of hydroponic food production methods. *Scientia Horticulturae*, 195, 206–215. <https://doi.org/10.1016/j.scienta.2015.09.011>
- Li, X., Cai, Y., Liu, D., Ai, Y., Zhang, M., et al. (2019). Occurrence, fate, and transport of potentially toxic metals (Ptms) in an alkaline rhizosphere soil-plant (Maize, *zea Zea mays* l.) system: The role of *Bacillus subtilis*. *Environmental Science and Pollution Research*, 26(6), 5564–5576. <https://doi.org/10.1007/s11356-018-4031-6>
- Liu, J., Ma, K., Ciais, P., & Polasky, S. (2016). Reducing human nitrogen use for food production. *Scientific Reports*, 6(1), 30104. <https://doi.org/10.1038/srep30104>
- Manachini, P. L., Fortina, M. G., Levati, L., & Parini, C. (1998). Contribution to phenotypic and genotypic characterization of *Bacillus licheniformis* and description of new genomovars. *Systematic and applied microbiology*, 21(4), 520-529.
- Meena, V. S., Mishra, P. K., Bisht, J. K., & Pattanayak, A. (Eds.). (2017). *Agriculturally important microbes for sustainable agriculture: volume 2: applications in crop production and protection*. Springer Singapore.
- Mehta, S., & Nautiyal, C. S. (2001). An efficient method for qualitative screening of phosphate-solubilizing bacteria. *Current Microbiology*, 43(1), 51–56. <https://doi.org/10.1007/s002840010259>
- Mhete, M., Eze, P. N., Rahube, T. O., & Akinyemi, F. O. (2020). Soil properties influence bacterial abundance and diversity under different land-use regimes in semi-arid environments. *Scientific African*, 7, e00246. <https://doi.org/10.1016/j.sciaf.2019.e00246>
- Minkina, T., Sushkova, S., Delegan, Y., Bren, A., Mazanko, M., et al. (2023). Effect of chicken manure on soil microbial community diversity in poultry keeping areas. *Environmental Geochemistry and Health*, 45(12), 9303–9319. <https://doi.org/10.1007/s10653-022-01447-x>
- Mohammad, B. T., Al Daghistani, H. I., Jaouani, A., Abdel-Latif, S., & Kennes, C. (2017). Isolation and Characterization of Thermophilic Bacteria from Jordanian Hot Springs: *Bacillus licheniformis* and *Thermomonas hydrothermalis* Isolates as Potential Producers of Thermostable Enzymes. *International journal of microbiology*, 2017, 6943952. <https://doi.org/10.1155/2017/6943952>
- O'Hair, J., Jin, Q., Yu, D., Poe, N., Li, H., Thapa, S., Zhou, S., & Huang, H. (2020). Thermophilic and alkaliphilic *Bacillus licheniformis* ynp5-tsu as an ideal candidate for 2,3-butanediol production. *ACS Sustainable Chemistry & Engineering*, 8(30), 11244–11252. <https://doi.org/10.1021/acssuschemeng.0c02759>
- Olsson, K., Keis, S., Morgan, H. W., Dimroth, P., & Cook, G. M. (2003). Bioenergetic properties of the thermoalkaliphilic *Bacillus* sp. Strain ta2. A1. *Journal of Bacteriology*, 185(2), 461–465. <https://doi.org/10.1128/JB.185.2.461-465.2003>
- Ortiz-Castro, R., Contreras-Cornejo, H. A., Macías-Rodríguez, L., & López-Bucio, J. (2009). The role of microbial signals in plant growth and development. *Plant Signaling & Behavior*, 4(8), 701–712. <https://doi.org/10.4161/psb.4.8.9047>
- Pande, A., Pandey, P., Mehra, S., Singh, M., & Kaushik, S. (2017). Phenotypic and genotypic characterization of phosphate solubilizing bacteria and their efficiency on the growth of maize. *Journal of Genetic Engineering and Biotechnology*, 15(2), 379–391. <https://doi.org/10.1016/j.jgeb.2017.06.005>
- Perry, J. J., & Staley, J. T. (1997). Taxonomy of eubacteria and archaea. *Microbiology: Diversity and Dynamics*, 388-413.
- Pingali, P. L. (2012). Green Revolution: Impacts, limits, and the path ahead. *Proceedings of the National Academy of Sciences*, 109(31), 12302–12308. <https://doi.org/10.1073/pnas.0912953109>
- Rajput, V. D., MiNkiNa, T., Kumari, A., Shende, S. S., Ranjan, A., et al. (2022). A review on nanobioremediation approaches for restoration of contaminated soil. *Eurasian Journal of Soil Science*, 11(1), 43–60. <https://doi.org/10.18393/ejss.990605>
- Ranjan, A., Rajput, V. D., Prazdnova, E. V., Gurnani, M., Bhardwaj, P., et al. (2023). Nature's antimicrobial arsenal: Non-ribosomal

- peptides from pgbp for plant pathogen biocontrol. *Fermentation*, 9(7), 597. <https://doi.org/10.3390/fermentation9070597>
- Rekha, K., Ramasamy, M., & Usha, B. (2020). Root exudation of organic acids as affected by plant growth-promoting rhizobacteria *Bacillus subtilis* RR4 in rice. *Journal of Crop Improvement*, 34(4), 571–586. <https://doi.org/10.1080/15427528.2020.1746719>
- Richer, A. C., & Holben, F. J. (1950). Preliminary report of the yeast fermentative procedure for the estimation of available soil nitrogen and general fertility level. *Soil Science Society of America Journal*, 14(C), 223–225. <https://doi.org/10.2136/sssaj1950.036159950014000C0051x>
- Sapkota, A., Thapa, A., Budhathoki, A., Sainju, M., Shrestha, P., & Aryal, S. (2020). Isolation, characterization, and screening of antimicrobial-producing actinomycetes from soil samples. *International Journal of Microbiology*, 2020, 1–7. <https://doi.org/10.1155/2020/2716584>
- Schwyn, B., & Neilands, J. B. (1987). Universal chemical assay for the detection and determination of siderophores. *Analytical Biochemistry*, 160(1), 47–56. [https://doi.org/10.1016/0003-2697\(87\)90612-9](https://doi.org/10.1016/0003-2697(87)90612-9)
- Sharma, N., Acharya, S., Kumar, K., Singh, N., & Chaurasia, O. P. (2018). Hydroponics as an advanced technique for vegetable production: An overview. *Journal of Soil and Water Conservation*, 17(4), 364. <https://doi.org/10.5958/2455-7145.2018.00056.5>
- Sharma, R., Singh, N. S., & Singh, D. K. (2019). Soil microbial diversity of peri-urban agricultural field and riverbank along Yamuna river in Delhi, India. *SN Applied Sciences*, 1(1), 22. <https://doi.org/10.1007/s42452-018-0024-9>
- Singh, B., & Ryan, J. (2015). Managing fertilizers to enhance soil health. *International Fertilizer Industry Association, Paris, France, 1*.
- Souza, A. N. D., & Martins, M. L. L. (2001). Isolation, properties and kinetics of growth of a thermophilic *Bacillus*. *Brazilian Journal of Microbiology*, 32, 271–275.
- Stegelmeier, A. A., Rose, D. M., Joris, B. R., & Glick, B. R. (2022). The use of pgbp to promote plant hydroponic growth. *Plants*, 11(20), 2783. <https://doi.org/10.3390/plants11202783>
- Tizazu, S., Tesfaye, G., Andualem, B., Wang, A., & Guadie, A. (2022). Evaluating the potential of thermo-alkaliphilic microbial consortia for azo dye biodegradation under anaerobic-aerobic conditions: Optimization and microbial diversity analysis. *Journal of Environmental Management*, 323, 116235. <https://doi.org/10.1016/j.jenvman.2022.116235>
- Touliatos, D., Dodd, I. C., & McAinsh, M. (2016). Vertical farming increases lettuce yield per unit area compared to conventional horizontal hydroponics. *Food and Energy Security*, 5(3), 184–191. <https://doi.org/10.1002/fes3.83>
- Walker, T. S., Bais, H. P., Grotewold, E., & Vivanco, J. M. (2003). Root exudation and rhizosphere biology. *Plant Physiology*, 132(1), 44–51. <https://doi.org/10.1104/pp.102.019661>
- Walkley, A., & Black, I. A. (1934). An examination of the degtjareff method for determining soil organic matter, and a proposed modification of the chromic acid titration method. *Soil Science*, 37(1), 29–38. <https://doi.org/10.1097/00010694-193401000-00003>
- Wang, G., Zhang, L., Zhang, S., Li, B., Li, J., et al. (2023). The combined use of a plant growth promoting *Bacillus* sp. Strain and GABA promotes the growth of rice under salt stress by regulating antioxidant enzyme system, enhancing photosynthesis and improving soil enzyme activities. *Microbiological Research*, 266, 127225. <https://doi.org/10.1016/j.micres.2022.127225>
- Wood, N. T. (2001). Nodulation by numbers: The role of ethylene in symbiotic nitrogen fixation. *Trends in Plant Science*, 6(11), 501–502. [https://doi.org/10.1016/S1360-1385\(01\)02128-8](https://doi.org/10.1016/S1360-1385(01)02128-8)
- Xiao, L., Zhang, W., Hu, P., Xiao, D., Yang, R., Ye, Y., & Wang, K. (2021). The formation of large macroaggregates induces soil organic carbon sequestration in short-term cropland restoration in a typical karst area. *Science of The Total Environment*, 801, 149588. <https://doi.org/10.1016/j.scitotenv.2021.149588>
- Yu, Y., Gui, Y., Li, Z., Jiang, C., Guo, J., & Niu, D. (2022). Induced systemic resistance for improving plant immunity by beneficial microbes. *Plants*, 11(3), 386. <https://doi.org/10.3390/plants11030386>
- Zeifman, L., Hertog, S., Kantorova, V., & Wilmoth, J. (2022). A world of 8 billion. United Nations Department of Economic and Social Affairs. Retrieved from https://www.un.org/development/desa/pd/sites/www.un.org.development.desa.pd/files/undesa_pd_2022_pb_140.pdf.



Journal of Experimental Biology and Agricultural Sciences

<http://www.jebas.org>

ISSN No. 2320 – 8694

Phytotoxicity and genotoxicity assessment of organic and inorganic contaminants detected in pharmaceutical industrial wastewaters using *Vigna radiata* and *Allium cepa*

Km Jyoti , Kuldeep Soni , Ram Chandra* 

Department of Environmental Microbiology, School for Environmental Sciences, Babasaheb Bhimrao Ambedkar University (A Central University), Lucknow-226025, Uttar Pradesh, India

Received – September 04, 2023; Revision – December 24, 2023; Accepted – February 25, 2024

Available Online – March 15, 2024

DOI: [http://dx.doi.org/10.18006/2024.12\(1\).76.92](http://dx.doi.org/10.18006/2024.12(1).76.92)

KEYWORDS

Pharmaceutical industrial wastewater

Phytotoxicity

Genotoxicity

Chromosomal aberration

Mitotic index

GC-MS

ABSTRACT

The discharged effluent of pharmaceutical industrial wastewater treatment plants (PIWWTPs) exhibits substantial environmental toxicity due to the intricate combination of organic and inorganic pollutants. This study assessed the phytotoxicity, genotoxicity, and cytotoxicity of untreated and treated pharmaceutical industrial wastewater (PIWW). Most of the physicochemical parameters viz. COD, BOD, EC, sulfide, sulfate, nitrate, phosphate, grease, phenols, and metal concentrations viz. B, Cr, Ca, Cd, Cu, Zn, Pb, Hg, and As in untreated wastewater (UTW) were noted beyond the permissible limit and remained higher in treated wastewater (TW). The findings revealed that the performance of PIWWTP was woefully inadequate. The GC-MS spectra of UTW and TW revealed the presence of various organic contaminants. The toxicological studies showed that the UTW had a high degree of phytotoxicity, which persisted even after the treatment as it inhibited the seed germination in *Vigna radiata*. The seed germination was inhibited up to 70% and 50% tested at 50% concentration of UTW and TW respectively. Genotoxicity was measured by determining mitotic index and chromosomal aberrations in *Allium cepa* root apex grown in untreated and treated PIWW. Compared to the negative control, the mitotic index dropped to 85% and 75% at the 50% concentrations of UTW and TW, respectively. Chromosomal aberrations were also found in the cellular mass of root apex growing in both UTW and TW. According to the findings, it is unsafe for the environment to release PIWW that has not been properly treated, as this could pose serious risks to environmental health.

* Corresponding author

E-mail: prof.chandrabbau@gmail.com (Chandra R)

Peer review under responsibility of Journal of Experimental Biology and Agricultural Sciences.

Production and Hosting by Horizon Publisher India [HPI]
(<http://www.horizonpublisherindia.in/>).
All rights reserved.

All the articles published by [Journal of Experimental Biology and Agricultural Sciences](#) are licensed under a [Creative Commons Attribution-NonCommercial 4.0 International License](#) Based on a work at www.jebas.org.



1 Introduction

Wastewater production due to anthropogenic activities is an inevitable practice. Numerous sources, like households, industries, hospitals, agricultural runoff, etc, can generate such wastewater. Among these sources, the pharmaceutical industry is the most significant because its effluent consists of numerous residual pharmaceutical compounds and metabolites. Over the past few years, the pharmaceutical industries have expanded rapidly, contributing to substantial global economic growth (Gros et al. 2019; Ramirez-Morales et al. 2021). Approximately three thousand compounds are used as pharmaceuticals, with hundreds of tonnes produced yearly to meet global demand (Grenni et al. 2018). India is among the world's leading manufacturers of pharmaceuticals, with over 10,500 pharmaceutical industries (Ray et al. 2019). The pharmaceutical industry's expansion coincided with an increase in wastewater output. Large-cap pharmaceutical industries have effluent treatment plants (ETPs) to treat wastewater, whereas small-sized industries use a common effluent treatment plant (CETP). The CETP in the pharmaceutical industrial area collects wastewater from a cluster of industries that manufacture different pharmaceutical products. As a result, the effluent from this CETP contains a range of water-soluble, non-biodegradable pharmaceutical residues. Among the various types of wastewater, the equity of effluent generated by the PIWWTP is very low, but its composition is quite enough to upset the equilibrium of receiving environmental bodies. The effluent comprises a substantial quantity of recalcitrant organic pollutants discharged from the pharmaceutical industry, mainly drug residues, animal and plant steroids, personal care products and heavy metals (Babaahmadi et al. 2017; Patel et al. 2019).

The introduction of pharmaceutically active chemicals in the environment has sparked worldwide concern. The pharmaceutical industry uses various treatment strategies to treat and repurpose wastewater to reduce environmental damage. The majority of these treatment plants are incapable of properly treating PIWW and are unable to meet the acceptable range of physicochemical characteristics and metal concentrations suggested by the World Health Organization (WHO) and Central Pollution Control Board, India (CPCB) (Rana et al. 2017). As a result, the effluent of the PIWWTP contains an abundance of pollutants. The amalgamation of such wastewater into the environment may have hazardous implications for human and environmental health. The antibiotics and metals present in the effluent can generate a selective pressure for antibiotic and metal resistance (Soni et al. 2022). Additionally, it could promote the growth of specific kinds of biotic communities and adversely affect the biodiversity index.

The pharmaceutical metabolites found in the PIWW can disrupt biogeochemical cycles and cause a variety of toxicities, including

phytotoxicity, genotoxicity, cytotoxicity, and mutagenicity (Pashaei et al. 2022; Samal et al. 2022). Kumari and Tripathi (2019) investigated the genotoxic effects of PIWW using the growing root apex of *A. cepa*. The mitotic index (MI) and chromosomal aberrations (CAs) were used to analyze the toxicity of PIWW, which demonstrated that it can cause a drop in the MI and can induce various CAs such as chromosome loss, c-mitosis, fragile chromosomes, and micro-nucleated conditions (Kumari and Tripathi 2019). Sharif et al. (2016) used a bacterial reverse mutation test and an Ames test to determine the mutagenic and genotoxic impact of PIWW. The mutagenic index of both examined *Salmonella typhimurium* strains (TA-100 and TA-102) decreased dose-dependent. The Ames test of wastewater revealed a drop-in frequency of chromosomal damage as wastewater concentration decreased. These findings suggested that PIWW, an intricate mixture of various organic-metallic contaminants, may have potent mutagenic and genotoxic implications on the exposed biotic community. Therefore, immediate action is needed to halt the spread of this global menace. Government regulatory bodies must act quickly to prevent the spread of PIWW without proper treatment. There is also a need to develop novel treatment strategies for adequately treating pharmaceutical metabolites.

Previous studies have looked into the occurrences of phytotoxicity, genotoxicity, and cytotoxicity caused by effluent from various treatment plants (Roy et al. 2015; Yadav et al. 2019; Haq and Kalamdhad 2021). To the best of our knowledge, limited studies have looked into the toxicity of the PIWW treatment plant's influent and effluent, and the topic is data-deficient. No study has evaluated the performance of PIWWTP based on PIWW toxicity. The novelty of this study was the performance evaluation of the PIWWTP by comparing data of physicochemical parameters, metal concentrations, and GC-MS analysis of influent and effluent, as well as assessment of its phytotoxic, genotoxic, and cytotoxic consequences.

2 Materials and methods

2.1 Sample collection

The wastewater samples were collected from a CETP located at the Integrated Industrial Estate (IIE), State Infrastructure Development Corporation Uttarakhand Limited (SIDCUL), Haridwar, Uttarakhand, India (29.9671° N, 78.0596° E). This CETP collected the PIWW from a cluster of industries. CETP has a treatment capacity of 4.5 MLD and uses a fully biological process, particularly a moving bed biofilm reactor (MBBR) (Ali et al. 2021). The untreated (UTW) and treated (TW) wastewater samples of PIWWTP were collected at the end of March 2023. For the assessment of physicochemical parameters, GC-MS, FTIR, genotoxicity and phytotoxicity the samples of wastewater were collected in a sterilized 2L glass container. For metal analysis, the samples were collected in a 500 ml food-grade plastic container preadded with 4-5 ml

concentrated HCl to avoid saltation of metals. Samples were brought to the lab in the icebox, stored at 4°C, and then filtered with Whatman filter paper for further analysis.

2.2 Analysis of physicochemical parameters and heavy metal

The methodologies applied to assess the physicochemical characteristics and metal concentration were based on the APHA 23rd edition, 2017 (Rice 2012). The physicochemical characteristics of UTW and TW studied in this study were pH, temperature, TDS, TSS, COD, BOD, EC, sulfide, sulfate, nitrate, phosphate, chloride, oil, grease, and phenols. The metal concentration was evaluated using an Inductively Coupled Plasma Mass Spectrometry (ICP-MS) instrument (ThermoFisher Scientific- ICAP Qnova Series). In this investigation, the concentrations of eleven metals were determined, viz., B, Cr, Ca, Cd, Cu, Ni, Zn, Fe, Pb, Hg, and As.

2.3 Estimation of organic contaminant

2.3.1 Preparation of samples and extraction of organic pollutant

Organic contaminants were extracted using ethyl acetate at pH 2.0 from untreated wastewater (UTW) and treated wastewater (TW) samples of effluent treatment plant (ETP) (Singh et al. 2023). A 500 ml separating funnel was filled with the 50 ml acidified sample. An equal quantity of ethyl acetate was added to the sample and agitated thoroughly for four to five hours. After proper shaking, the ethyl acetate extract was isolated and dried at 40°C using a rotatory evaporator (Rotavapor® R-300, BUCHI). The dried extracts of each sample were separately dissolved in 5 ml of ethyl acetate and passed through a syringe filter (0.22 µm; Sigma-Aldrich, USA). For further FTIR spectroscopy and GC-MS analysis, the filtrate of both samples was kept at 4°C.

2.3.2 FTIR spectroscopy analyses

The extract of wastewater samples was initially utilized to determine the functional groups of organic contaminants using Fourier Transform Infrared (FTIR) spectroscopy (Nicolet 6700, Thermo Scientific, USA). The method of FTIR analysis was based on a previous study by Kumar and Chandra (2020). Using an infrared spectrophotometer, infrared spectra of samples were obtained in the scanning range of 4000 to 500 cm⁻¹ (wave number) at 25°C and a resolution of 0.15 cm⁻¹.

2.3.3 Derivatization of extracted samples and GC-MS analysis

For silylation (Derivatization), 250 µl of extracted samples were put in GC vials and evaporated in the presence of N₂ gas. After adding 40 µl of C₅H₅N (pyridine) to the dried samples, silylation was conducted at 70°C for half an hour in the presence of N, O-trimethylchlorosilane (TMCS) and N, O-bis (trimethylsilyl) trifluoroacetamide (BSTFA). Derivatization of organic compounds

was performed in full scan mode with low mass (m/z): 50 amu to high mass (m/z): 800 amu.

The 1.5 µl silylated solution was introduced into a GC-MS column and segregated in a capillary tube (Thermo Fisher Scientific GC Ultra XLS Mass Spectrometer, America). The analytical GC capillary tube was filled with an inert carrier gas (Helium gas) at 300°C temperature and a flow rate of 1 ml·min⁻¹. The mass spectrum of electron ionization (EI) was recorded at 40 to 70 eV, covering a range of 50 to 800 m/z ratio. The resulting GC-MS spectra contain peaks representing distinct chemical compounds at certain retention times (RTs). Such compounds were identified by accessing the National Institute of Standards and Technology (NIST) library, USA (Babushok et al. 2007; Koo et al. 2016).

2.4 Toxicological implications of UTW and TW for environmental safety estimation

The toxicological impacts of untreated and treated PIWW were estimated using mung bean (*V. radiata*) seeds and onion bulbs (*A. cepa*). *V. radiata* was used to test the phytotoxicity, while *A. cepa* was used to test the cytotoxicity and genotoxicity.

2.4.1 Phytotoxicity assessment using mung bean (*V. radiata*) seeds

The method of seed germination experiments on mung bean (*V. radiata*) was based on a previous study by Salian et al. (2018). Mung bean seeds were obtained from a verified seed-selling outlet and superficially sterilized with 0.3% (*W/V*) HgCl₂ solution. By adding the required amount of distilled water, five test solutions of untreated and treated PIWW were prepared with concentrations (*V/V*) of (15%, 25%, 50%, 75%, and 100%). Petri plates (90 mm × 15 mm) containing 10 seeds were watered with 8 ml of test solutions, while tap water-irrigated seeds served as negative controls. The petri plates were incubated in a BOD incubator (Bionics Scientific, India) at 30 ±1°C. After 48 hours, the number of germinated seeds was noted and displayed as a percentage (%) of germination. After 5 days of treatment, seedling development variables (root and shoot length) were evaluated (Salian et al. 2018; Kumari and Tripathi 2019). The experiments were carried out in triplicate.

2.4.2 Genotoxicity estimation

Chromosomal aberrations in the root apex cells of *A. cepa* were used to determine the genotoxicity of both UTW and TW. Three test solutions (*V/V*) of 15%, 25%, and 50% of UTW and TW were used in this experiment. Above this concentration, there was almost no visible development in the root apex. To complete the cell cycle, the dividing cells of the root apex of onion bulbs were first rooted in tap water for 48 hours or until the length of the roots reached 1-2 cm. After that, the bulbs were transferred to test solutions for 24 hours. To determine the genotoxicity, the root apex was fixed in a CH₃COOH (glacial acetic acid) and alcohol

(1:3) for 12 hours at 65°C. The root apex was cleaned with distilled water and then hydrolyzed for five minutes at 65°C using 1N HCl. Following appropriate washing, hematoxylin was used as the stain during the processing of the root apex for slide preparation (Haq et al. 2017). About 4000 cells (400–1200 cells per slide) were scored to determine the MI. The CAs and MI were analyzed by using a phase contrast microscope (Nikon Eclipse Ci, Japan) and calculated by using the given formula:

$$\text{Mitotic Index (MI)(\%)} = \frac{\text{Number of dividing cells}}{\text{Number of total cells}} \times 100$$

$$\begin{aligned} \text{Chromosomal Aberrations (CA)(\%)} \\ = \frac{\text{Number of aberrant cells}}{\text{Number of total cell}} \times 100 \end{aligned}$$

2.5 Statistical analysis

The standard deviation of triplicate data of physicochemical parameters, metal concentrations, phytotoxicity, and genotoxicity was determined on Microsoft Excel 2019.

3 Results

3.1 Physicochemical parameters and metal concentration

The value of all the physicochemical parameters, the concentration of metals, the permissible limit of CPCB (2020) and the treatment efficiencies of PIWWTP are listed in Table 1. The pH and temperature of the UTW and TW were within an acceptable range of CPCB (2020). The values of TDS and TSS in UTW were

Table 1 Physicochemical characteristics and metal content in the untreated and treated wastewater of WWTP of pharmaceutical industrial area

Physicochemical Analysis	UTW	TW	Permissible limits (CPCB 2020)	Treatment Efficiency (%)
pH	6.68 ±0.28	7.29 ±0.26	6.0-8.5	-
Temperature (°C)	33.08 ±0.04	30.45 ±0.06	34	-
TDS (mg/L)	2822.56 ±26.22	1543.34 ±18.16	2100	45.32
TSS (mg/L)	2080.06 ±18.28	483.48 ±7.42	1500	76.75
COD (mg/L)	3819.86 ±15.70	3196.62 ±18.16	100	16.31
BOD (mg/L)	1190.72 ±8.18	664.67 ±7.12	250	44.17
EC (mS/L)	380.0 ±4.42	183 ±4.22	ND	51.84
Sulfide(mg/L)	124.60 ±2.80	28.06 ±0.92	2	77.47
Sulfate(mg/L)	400.81 ±3.62	100.82 ±1.58	NS	74.84
Nitrate (mg/L)	44.07 ±1.86	30.04 ±0.68	NS	31.83
Phosphate (mg/L)	600.65 ±9.46	240.54 ±4.95	5	59.95
Chloride (mg/L)	280.73 ±4.12	210.04 ±3.45	15	25.18
Oil and grease (mg/L)	709.66 ±11.46	412.60 ±8.78	10	41.85
Phenols (mg/L)	10.03 ±0.64	5.02 ±0.02	1.0	49.95
Metals Analyses (mg/L)	UTW	TW	Permissible limits (CPCB, 2020)	Treatment Efficiency (%)
B	14.56 ±1.45	9.19 ±0.62	2.0	36.88
Cr	5.09 ±0.23	3.23 ±0.01	2	36.54
Ca	120.07 ±0.02	105.03 ±0.07	ND	12.52
Cd	9.09 ±0.01	4.05 ±0.001	1.0	55.44
Cu	7.83 ±0.78	3.85 ±0.10	3	50.83
Ni	3.73 ±0.20	2.27 ±0.05	3.0	39.14
Zn	8.98 ±17.12	5.76 ±0.91	5	35.85
Fe	15.57 ±1.02	12.82 ±1.04	15	17.66
Pb	1.44 ±0.08	0.9 ±0.009	0.1	37.50
Hg	0.43 ±0.07	0.04 ±0.02	0.01	90.69
As	7.49 ±0.16	2.47 ±0.04	0.2	67.02

UTW- Untreated wastewater; TW- Treated wastewater; CPCB- Central Pollution Control Board; COD- Chemical oxygen demand; BOD- Biological oxygen demand; TSS- Total suspended solids; TDS- Total dissolved solids; EC- Electrical conductivity; ND- Not determined; ± - Standard deviation

2822.56 \pm 26.22 mg/L and 2080.06 \pm 18.28 mg/L, respectively, which was substantially higher than the permissible limit of CPCB (2020). Although both parameters were remediated after treatment (TW), the values of TDS and TSS fell below the threshold. The values of COD, BOD, EC, sulfide, sulfate, nitrate, phosphate, chloride, oil, grease and phenols remained higher than the CPCB (2020) permitted limit in the UTW and TW (Table 1). The PIWWTP's best treatment efficacy (77.47%) was observed for sulfide, whilst the lowest efficiency (16.31%) was noted for COD.

The UTW and TW samples included eleven metals and heavy metals viz. B, Cr, Ca, Cd, Cu, Ni, Zn, Fe, Pb, Hg, and As. All metals and heavy metals in the UTW sample were considerably higher than the CPCB (2020) acceptable range (Table 1). Following treatment, the levels of Ni and Fe dropped below the CPCB (2020) permitted limit, with respective treatment

efficiencies of 17.66% and 39.14%. The highest and lowest treatment efficiency was shown for Hg (90.69%) and Ca (12.52%), respectively.

3.2 FTIR spectroscopy

The FTIR spectra of the UTW and TW samples revealed several peaks corresponding to various wave numbers. These peaks indicated the presence of multiple contaminants with distinct functional groups. The UTW and TW have infrared wave numbers ranging from 4000 to 500 cm^{-1} . Figure 1 shows the infrared spectra of UTW and TW, which are interpreted in Table 2. The FTIR analysis was employed to compare the change in bond pattern and functional groups in the influent and effluent during the wastewater treatment process for the supporting data of compound characterization (Yang et al. 2015).

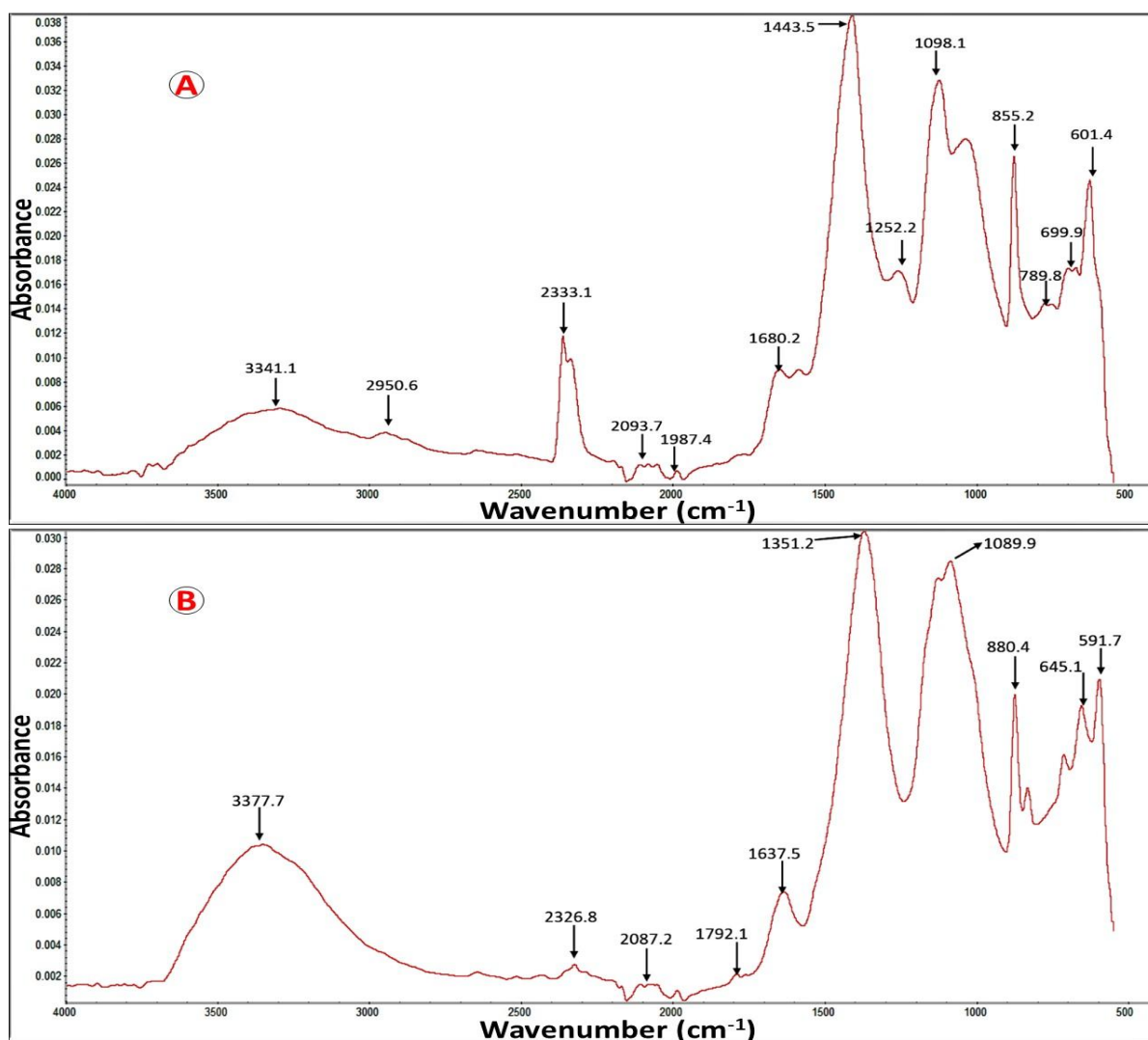


Figure 1 Fourier transform infrared (FTIR) spectroscopy analysis of ethyl acetate extract obtained from wastewater samples, A= UTW (Untreated wastewater); B= TW (Treated wastewater)

Table 2 Fourier-transform infrared (FTIR) spectroscopy analyses of ethyl acetate extract of untreated and treated wastewater samples

S. No.	Wavenumber (cm ⁻¹)	Functional group	UTW	TW
1.	3341.1	OH carbohydrates proteins and polyphenols	+	-
2.	3377.7	OH carbohydrates proteins and polyphenols	-	+
3.	2950.6	CH and CH ₂	+	-
4.	2333.1	C=C conjugated and C≡C	+	-
5.	2326.8	C=C conjugated and C≡C	-	+
6.	2093.7	CH and CH ₂	+	-
7.	2087.2	CH and CH ₂	-	+
8.	1987.4	CH and CH ₂	+	-
9.	1792.8	C=O ester fatty acid group	-	+
10.	1680.2	C=O group of quinone compounds	+	-
11.	1443.5	Stretching -C=O inorganic carbonate	+	-
12.	1351.2	C-N amide III band	-	+
13.	1252.2	C-N amide III band	+	-
14.	1098.9	C-O carbohydrate	+	-
15.	880.4	Bending -C=O inorganic carbonate	-	+
16.	855.2	Bending -C=O inorganic carbonate	+	-
17.	789.8	CH out of plane aromatic band	+	-
18.	699.9	CH out of plane aromatic band	+	-
19.	645.1	CH out of plane aromatic band	-	+
20.	601.4	CH out of plane aromatic band	+	-
21.	591.7	CH out of plane aromatic band	-	+

UTW: Untreated wastewater; TW: Treated wastewater; + : Present; - : Absent

3.3 GC-MS data analysis

The GC-MS chromatogram of ethyl acetate extract of UTW and TW samples displayed many major and minor peaks at different RTs (Figure 2; Table 3). The major peaks in the UTW extract were recorded at RT 7.49, 10.37, 12.35, 13.23, 16.04, 19.49, 22.03, 26.30, 27.95, 28.55, 37.31, and 37.56 minutes. These peaks corresponded to 2-Methyl-1,3-propanediol 2TMS; Silane, trimethyl (phenylmethoxy); 1-tert-Butyl-2,5-dimethoxybenzene; Ethyl isopropylaminoacetate; Pentanedioic acid, bis(trimethylsilyl) ester, 4-Bromo-5-methyl-2-phenylthiazole; 2-(5-acetyl-2-thienyl)-1,4-naphthoquinone; 5-Bromo-2-hydroxy-N'-(3-pyridinylmethylene) benzohydrazideditms; 6-methoxy-7-methyl-2,3-diphenyl-5,8-quinoxalinedione; Garcinixanthone F; n-Hexadecyloxy(triethyl)silane; (2R,3R)-2,3-Diacetoxy-a,a-carotene; and 2-methyl-3-acetyl-1a,3a,5,6-tetra(trimethylsiloxy)-benzofuran-4,7-dione, respectively.

The primary peaks in TW were found at RTs of 8.05, 14.04, 16.04, 24.62, 26.48, 27.60, 30.47, 33.64, 39.80 and 42.80 minutes. These

peaks were interpreted as 2-Trimethylsilylmethylcyclopentanone; Disiloxane, hexamethyl; Pentanedioic acid, bis(trimethylsilyl) ester, 4-Bromo-5-methyl-2-phenylthiazole; 2-Bromoethyl 3-bromotetrahydrofuron-2yl ether; 1,2-Benzenedicarboxylic acid, dibutyl ester; Hexadecanoic acid, trimethylsilyl ester; octadecanoic acid, trimethylsilyl ester; 1,2-Benzenedicarboxylic acid, dioctyl ester; Silane, [[[3a,5a)-cholestan-3-yl]oxy]triethyl; and 3,5-di-tert-butylstilbenyl phenyl ketone, respectively. Peaks at RT 16.04 minutes were detected in the chromatograms of both samples.

3.4 Phytotoxicity of pharmaceutical industrial wastewater

Table 4 shows the impact of UTW and TW on the early phase of seedling growth (5-seedling) after five days of incubation. On increasing the wastewater concentrations, seed germination efficiency (%), shoot growth, root growth, and biomass of germinating seed all reduced (Table 4; Figure 3). Maximum seed germination rate (%), shoot and root length growth, and increase in biomass were observed when the negative control (tap water) was used.

Table 3 Organic compounds detected by GC-MS analysis of untreated and treated wastewater samples collected from WWTP of pharmaceutical industrial area

RT	Compound Name	UTW	TW	Toxicity
6.43	1,2-Bis(trimethylsiloxy)ethane	-	+	Dermal and ophthalmic irritation
7.49	2-Methyl-1,3-propanediol 2TMS	+	-	Diarrhea, yellow nasal discharge
8.05	2-Trimethylsilylmethylcyclopentanone	-	+	Neurotoxicity
8.26	Docosane	+	-	ND
10.37	Silane, trimethyl(phenylmethoxy)	+	-	Dermal and ophthalmic irritation
11.05	Ethanol, 2-(2-ethoxyethoxy)	-	+	Neurotoxin - Acute solvent syndrome
12.35	1-tert-Butyl-2,5-dimethoxybenzene	+	-	Acute toxicity (Oral), Carcinogenicity
13.23	Ethyl isopropylaminooximinoacetate	+	-	Gastrointestinal irritation, rashes, and photosensitization
14.04	Disiloxane, hexamethyl	-	+	Low acute inhalation toxicity
14.43	bis(trimethylsilyl) methylmalonate	-	+	Respiratory tract and eye irritation
15.02	Sym-tetramethyl(diisopropyl)disiloxane	+	-	ND
16.04	Pentanedioic acid, bis(trimethylsilyl) ester, 4-Bromo-5-methyl-2-phenylthiazole	+	+	Endocrine disrupting chemical
16.93	(4-(Ethynyl-2,3 dinitrophenylethynyl)trimethylsilane	+	-	Dermal and ophthalmic irritation
18.32	1-(Trimethylsilylmethyl)dimethylsilyloxy-pentane	+	-	ND
19.49	2-(5-acetyl-2-thienyl)-1,4-naphthoquinone	+	-	Cellular toxicity
20.38	4-Acetyl-2-methoxy-trimethylsiloxy-benzene	+	-	ND
22.03	5-Bromo-2-hydroxy-N'-(3-pyridinylmethylene) benzohydrazideditms	+	-	Dermal and ophthalmic irritation
24.22	1-Pentamethyldisilyloxy-2-phenylethane	+	-	Affects the gastrointestinal and respiratory tract
24.62	2-Bromoethyl 3-bromotetrahydrofuron-2yl ether	-	+	ND

RT	Compound Name	UTW	TW	Toxicity
26.30	6-methoxy-7-methyl-2,3-diphenyl-5,8-quinoxalinedione	+	-	Chronic health effects- acute bronchospasm, hives (urticaria), deep dermal wheals (angioneurotic edema), running nose (rhinitis) and blurred vision
26.48	1,2-Benzenedicarboxylic acid, dibutyl ester	-	+	Skin and eye irritation
27.60	Hexadecanoic acid, trimethylsilyl ester	-	+	Endocrine disrupting chemical
27.95	Garciniaxanthone F	+	-	Neurotoxic and phenylketonuria
28.55	n-Hexadecyloxy(triethyl)silane	+	-	ND
30.47	Octadecanoic acid, trimethylsilyl ester	-	+	Endocrine-disrupting chemical, reproductive toxicity
31.20	Octadecanoic acid, trimethylsilyl ester	+	-	Endocrine-disrupting chemical, reproductive toxicity
32.16	1,1-Diisobutoxy-isobutane	-	+	Carcinogenic
32.36	Octadecanoic acid, butyl ester	+	-	Inflammation and skin irritation
33.64	1,2-Benzenedicarboxylic acid, dioctyl ester	-	+	Gastrointestinal irritation, rashes, and photosensitization
33.80	n-Hexadecyloxy(triethyl)silane	+	-	Skin and eye irritation
34.33	3-(4-nitrophenyl)quinazolin-4(3h)-one	+	-	Ulcerative colitis
34.52	Dirithromycin	-	+	Overdose causes nausea, vomiting, epigastric distress, and diarrhea.
37.31	(2R,3R)-2,3-Diacetoxy-a,a-carotene	+	-	Chronic vitamin A toxicity
37.56	2-methyl-3-acetyl-1a,3a,5,6-tetra(trimethylsiloxy)-benzo-furan-4,7-dione	+	-	ND
38.12	(4S)-2,2,4-tribenzyl-5,5-dimethyl-3-[(5R)-3-phenyl-2-isoxazoline-5-carbonyl]oxazolidine	-	+	LD50-Oral-Rat, LC50-Inhalation-Rat and carcinogen
39.80	Silane, [[(3a,5a)-cholestan-3-yl]oxy]triethyl	-	+	ND
41.23	4-ethyl-1,2,3,9,10-pentamethoxybenzo[a]heptalene	-	+	Eye and skin irritation
42.80	3,5-di-tert-butylstilbenyl phenyl Ketone	-	+	Burning sensation in the throat and chest. Abdominal pain
45.32	Dibutyl 2-bromovinylphosphonate	-	+	Irritation

RT- Retention time; UTW- Untreated wastewater; TW- Treated wastewater; + Present; - Absent; ND- Not determined

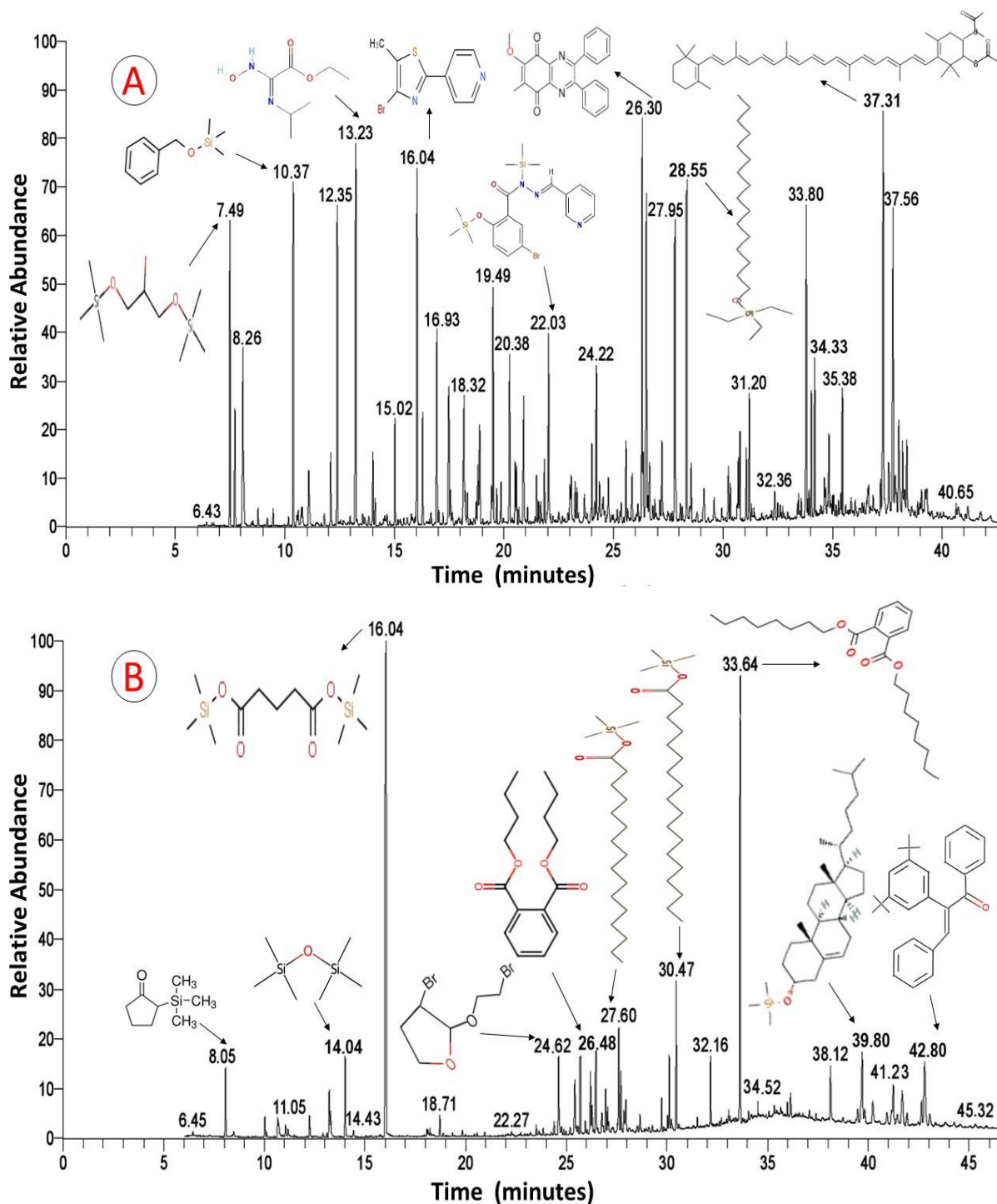


Figure 2 Chromatogram obtained during GC-MS analysis of ethyl acetate extract of wastewater samples showing the presence of various residual organic pollutants (ROPs), A= UTW (Untreated wastewater); B= TW (Treated wastewater).

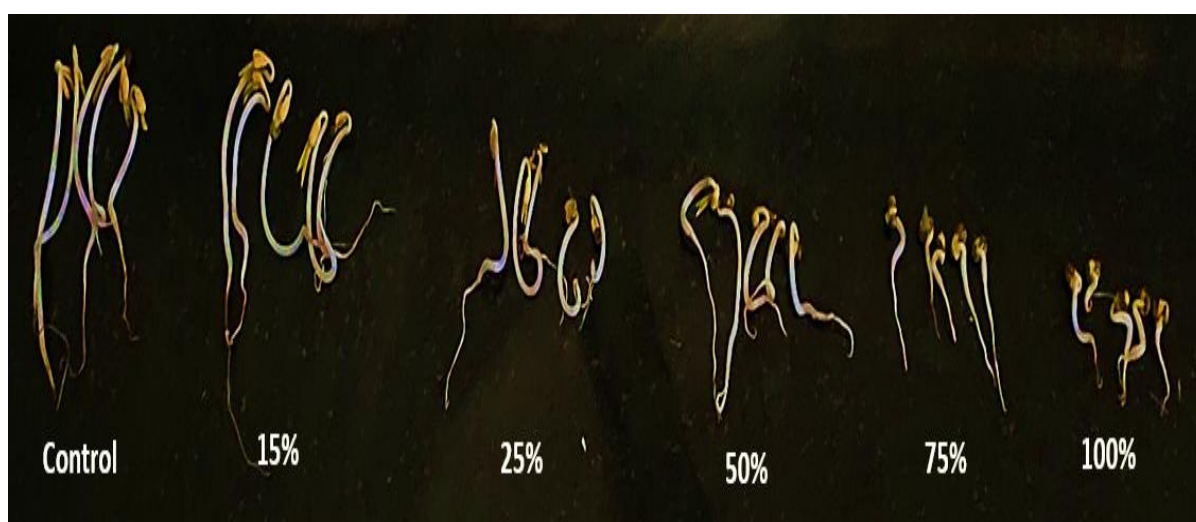
The seed germination was noticed till 50% UTW test solution, but above this concentration, it was not significant (Figure 3). However, seed germination was detected in all the five tested solutions of TW, though the magnitude of germination reduced

with each step. When using 100% UTW, there was no significant increase in shoot length, root length, or biomass. For 100% TW, a just-reverse trend was seen, indicating the higher toxicity of UTW (Table 4).

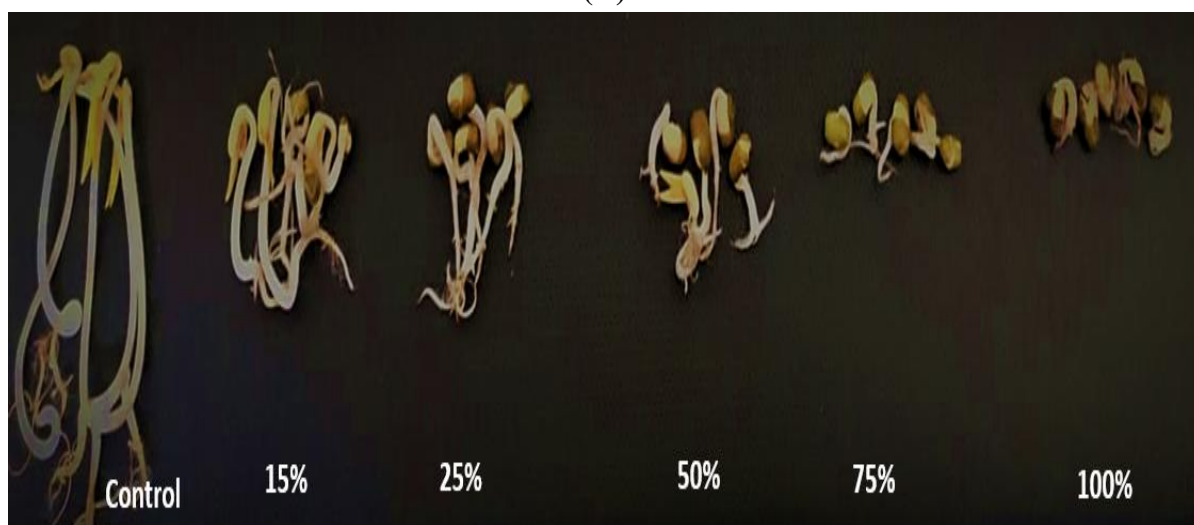
Table 4 Effect of different concentrations of pharmaceutical treated wastewater on seed germination, root length, shoot length and biomass in mung bean (*Vigna radiata*) plants

Wastewater (%)	Germination (%)		Shoot length (cm)		Root Length (cm)		Biomass (gm)	
	UTW	TW	UTW	TW	UTW	TW	UTW	TW
15	80	100	8.4 ±0.38	10.6 ± 0.41	1.2 ±0.02	1.8 ±0.05	1.0 ±0.002	1.9 ±0.004
25	60	80	5.7 ±0.23	9.6 ±0.26	1.1 ±0.9	1.6 ±0.11	0.9 ±0.001	1.4 ±0.002
50	30	50	2.5 ±0.06	7.9 ±0.03	0.7 ±0.18	1.5 ±0.02	0.4 ±0.04	0.8 ±0.17
75	0	5	0.2 ±0.02	4.3 ±0.03	0.2 ±0.009	1.4 ±0.08	0.0	0.3 ±0.02
100	0	4	0.0	2.3 ±0.04	0.0	1.1 ±0.06	0.0	0.2 ±0.04
Negative Control	100		12.2 ±0.15		2.8 ±0.05		3.23 ±0.057	

UTW- Untreated wastewater; TW- Treated wastewater; ± - Standard Deviation; Negative Control- Tap water



(A)



(B)

Figure 3 Effect of different concentrations of pharmaceutical industrial wastewater on early seedling growth of mung bean (*Vigna radiata*), A= UTW (Untreated wastewater); B= TW (Treated wastewater)

3.5 Cytotoxicity and genotoxicity of pharmaceutical industrial wastewater

The cytotoxicity and genotoxicity of untreated and treated PIWW were assessed in growing cells of the root apex of *A. cepa* using the MI and CA.

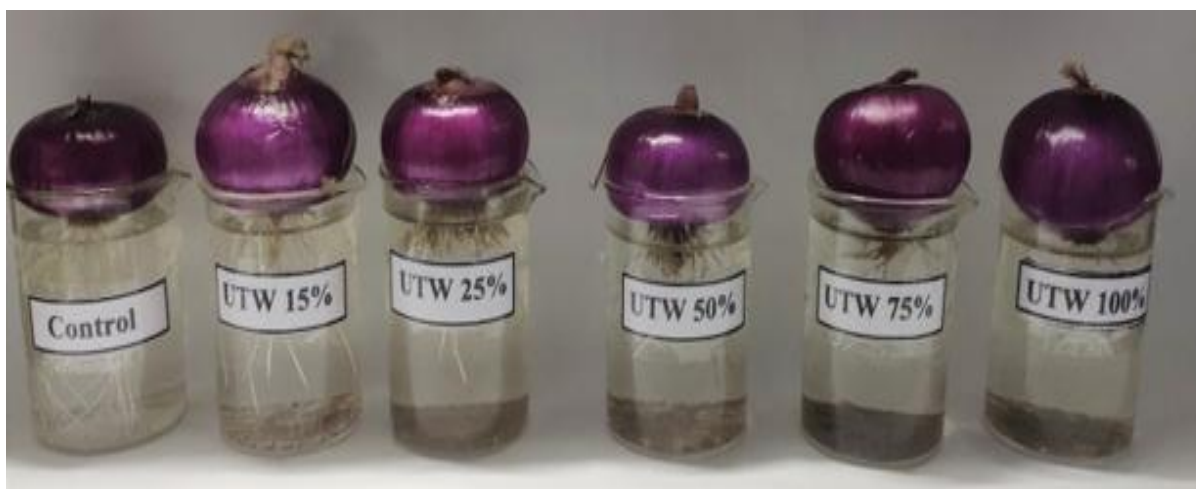
3.5.1 Mitotic index (MI)

The MI is a useful research tool for measuring the cytotoxic effects of various pollutants on cell division. MI quantifies the fraction of cells in the division phase as a percentage of the total cell population (Mercado et al. 2020). Table 4 highlights the cytotoxic effects of untreated and treated PIWW on *A. cepa* roots. The results showed that the mitotic index (MI%) value of the plant root apex was in the order of 37.62 (UTW 15%), 30.86% (UTW 25%), and 13.20 (UTW 50%) for untreated wastewater, and 44.92 (TW

15%), 38.18 (TW 25%), and 21.34 (TW 50%) for treated wastewater. The MI% for the negative control (tap water) was 85.54%. The MI% fell significantly with increasing UTW and TW concentrations, showing the presence of numerous cytotoxic residual contaminants in untreated and treated PIWW. The magnitude of the MI% decrease of the UTW test solution was greater than that of the TW test solution, indicating the PIWWTP's treatment efficiency.

3.5.2 Chromosomal aberrations

The results demonstrated that chromosomal and nuclear configurations remain wild-type in cells treated with negative control (tap water). However, treatment with increasing concentrations of untreated and treated PIWW caused an array of aberrations in the chromosome (Table 5; Figure 4). The detected aberrations were sticky metaphase (chromosomal clumping in the metaphase stage),



(A)



(B)

Figure 4 Effect of different concentrations of pharmaceutical industrial wastewater on root growth of onion bulb (*Allium cepa*); Control= Tap water; A= UTW (Untreated wastewater); B= TW (Treated wastewater)

Table 5 Assessment of different chromosomal abnormalities in *A. cepa* root apex cells. The root apex was subjected to various concentrations of untreated and treated wastewater of ETP for 24 hours

	Negative Control	UTW			TW		
	Tap Water	UTW (15%)	UTW (25%)	UTW (50%)	TW (15%)	TW (25%)	TW (50%)
Total cell	332	319	311	303	423	419	403
Dividing cell	284	120	96	40	190	160	86
Mitotic Index (%)	85.54 ±2.50	37.62 ±1.26	30.86 ±0.62	13.20 ±0.07	44.92 ±1.07	38.18 ±0.22	21.34 ±1.06
Chromosomal aberration							
Sticky metaphase	0.00	5.3 ±0.78	8.0 ±0.25	11 ±0.42	4.3 ±0.23	6.0 ±0.27	9.0 ±0.28
Vagrant chromosome	0.00	3 ±1.34	4 ±1.28	6 ±1.76	2 ±0.86	3 ±0.94	4 ±1.37
Chromosomal loss	0.00	2.6 ±.22	4.2 ±0.46	6.4 ±0.48	2.1 ±0.42	3.8 ±0.25	4.7 ±0.26
C-mitosis	0.00	4.2 ±0.98	5.2 ±1.14	7.1 ±2.01	2.8 ±0.83	3.4 ±1.04	5.5 ±1.02
Binucleated	0.00	1.9 ±0.8	7.0 ±1.02	9.0 ±1.26	1.3 ±0.48	5.0 ±0.88	8.0 ±1.00
Micronuclei	0.00	6 ±1.00	8 ±1.5	9.5 ±2.50	3 ±1.00	5 ±1.00	7.5 ±1.50
Aberrant cells (%)	0.00	13 ±1.50	18 ±2.00	22 ±2.40	7 ±1.00	12 ±1.60	14 ±1.8

UTW- Untreated wastewater; TW- Treated wastewater; ± - Standard Deviation

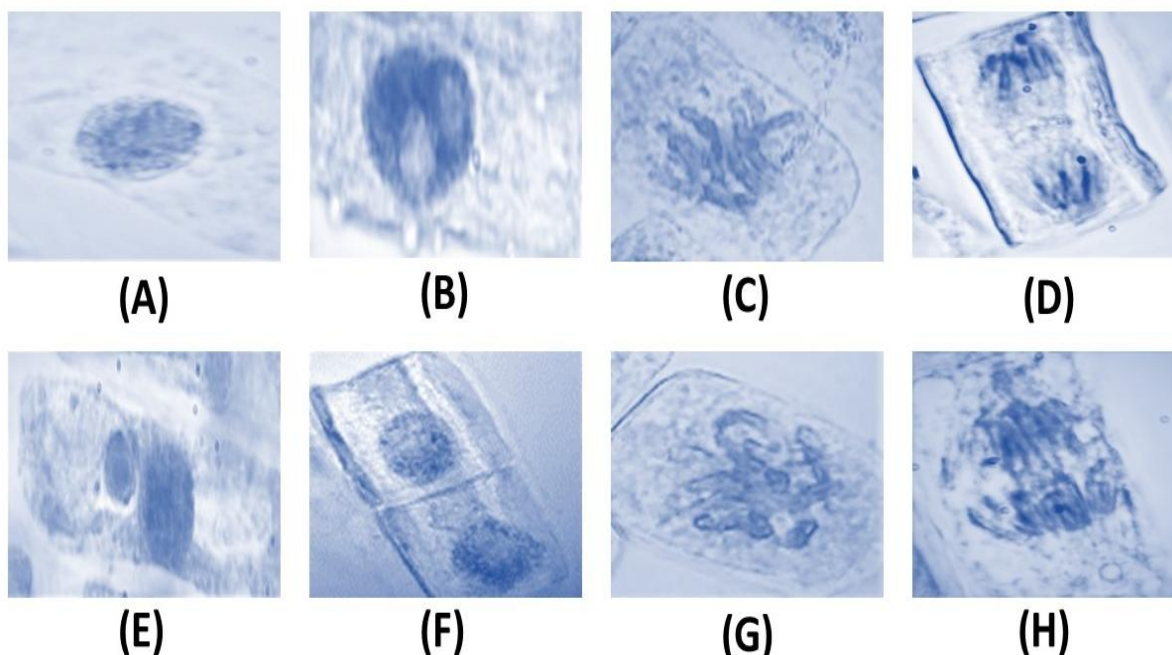


Figure 5 Chromosomal aberrations observed in root apex cells of *A. cepa* exposed to different concentrations of pharmaceutical wastewater (A) Disrupt prophase (B) C-mitosis (C) Sticky metaphase (D) lagged anaphase (E) Micronucleate (F) Binucleate (G) Chromosomal loss (H) vagrant

chromosome (unspecified wandering chromosome), chromosomal loss, c-mitosis (induced abortive division of nuclear material resulting in the doubling of chromosome), binucleated (cell with two nuclei), micronuclei (a smaller nucleus formed when a chromosome or its part fails to merge into one of the dividing nuclei during mitosis) and frequency of aberrant cells. The CAs were

detectable at all concentrations of test solutions for both UTW and TW. The frequency of aberrations was higher in UTW test solutions. The most common aberrations at all the wastewater concentrations studied were micronuclei, sticky metaphase, and c-mitosis. The highest frequency of abnormal cells was reported at a 50% UTW concentration (Table 5; Figure 5).

4 Discussion

TDS and TSS values were substantially reduced after treatment, but other metrics remained high, indicating the inability of PIWWTP. Such high physicochemical parameter values can have an array of environmental hazards (Hamaidi and Brahim 2019). The high turbidity is caused by inorganic and organic substances in wastewater received at ETPs (Theoneste et al. 2020), whereas TDS represents dissolved organic and inorganic compounds and a range of minerals and salts viz., Na, Ca, Cl, bicarbonates, and sulfates (Chen et al. 2021). TDS's inorganic and organic pollutants raise the wastewater's COD and BOD value. Singh and Singh (2018) define COD and BOD as the total amount of organic compounds and their constituents in wastewater. The high levels of COD, BOD, TDS, TSS, and turbidity in wastewater indicate a significant load of inorganic and organic chemicals. Such settings may be breeding grounds for clinical bacterial strains (Soni et al. 2024).

In this study, the physicochemical parameters BOD and COD of the effluent (TW) were 664.67 ± 7.12 mg/L and 3196.62 ± 18.16 mg/L, respectively. Kumari and Tripathi (2019) reported that PIWW's BOD and COD values were 7253.34 mg/L and 765.67 mg/L, respectively, substantially higher than this study. Further, the BOD value was much lower, and the COD value was significantly greater in this investigation. This comparison shows that TW contained a significant concentration of inorganic components susceptible to oxidation by the oxidant. Bakare et al. (2009) determined that the COD, BOD, TDS, phosphate, chloride, and nitrate concentrations were 147.04 mg/L, 48.13 mg/L, 336 mg/L, 61.3 mg/L, 5240 mg/L, and 42 mg/L, respectively. Comparing this study (Table 1), the COD, BOD, TDS, and phosphate values revealed by Bakare et al. (2009) were much lower, whereas chloride and nitrate values were significantly higher.

Most of the metal concentrations in the TW were many folds greater than the CPCB (2020) permissible limit (Table 1). When such effluent is exposed to the environment, it can cause phytotoxicity, cytotoxicity, and genotoxicity (Zhu et al. 2024). Mehrarad et al. (2016) reported that the effluent of PIWWTP had extremely high concentrations of heavy metals, including Pb (25.89 mg/L), Cd (12.34 mg/L), Zn (26.12 mg/L), Cr (17.46 mg/L), Mn (10.21 mg/L), Cu (18.34 mg/L), and Fe (43.22 mg/L). All of the metal concentrations in this investigation were substantially lower than those reported by Mehrarad et al. (2016) (Table 1). A just-reverse trend for metal concentration was seen when comparing this study's findings to those of Kumari and Tripathi (2019).

The FTIR spectra of the UTW extract showed more peaks than TW throughout a range of wave numbers (Figure 1). These peaks

imply that UTW absorbed more FTIR energy due to its high concentration of functional groups (Nandiyanto et al. 2019). According to the FTIR study (Figure 1), the peaks at 3341.1 cm^{-1} in the UTW extract and 3377.7 cm^{-1} in the TW extract correspond to OH carbohydrates and polyphenols. Mecozzi et al. (2012) revealed peaks in a similar range in the FTIR spectra of PIWWTP's effluent. Peaks 789.8 to 591.7 cm^{-1} correspond to C-H outside the aromatic band plane (Table 2).

Organic pharmaceutical compounds in wastewater can have many phytotoxic, genotoxic, and cytotoxic effects (Chowdhary et al. 2022). The GC-MS spectra of UTW and TW revealed various peaks at different RTs, corresponding to different pharmaceutical components. The peak at RT 16.04 minutes corresponded to Pentanedioic acid, bis(trimethylsilyl) ester, 4-Bromo-5-methyl-2-phenylthiazole showed in both samples. The number of peaks in the UTW was more than TW which indicates that there was vigorous treatment of wastewater was facilitated. Several pharmacological and therapeutic chemical metabolites were found in the UTW and TW, including 2-Trimethylsilylmethylcyclopentanone (RT- 8.05), Disiloxane, hexamethyl (RT- 14.04), Pentanedioic acid, bis(trimethylsilyl) ester, 4-Bromo-5-methyl-2-phenylthiazole (RT- 16.04), 2-(5-acetyl-2-thienyl)-1,4-naphthoquinone (RT- 19.49), 5-Bromo-2-hydroxy-N'-(3-pyridinyl methylene) benzohydrazideditms (RT- 22.03), Garciniaxanthone F (RT- 27.95), 3-(4-nitrophenyl)quinazolin-4(3h)-one (RT- 34.33) and Dirithromycin (RT- 34.52).

2-Trimethylsilylmethylcyclopentanone is a cyclopentanone derivative used to manufacture rubber products, medications, and insecticides (Li et al. 2019). Disiloxane hexamethyl, an ingredient in liquid bandages (sprayers on plasters) such as pavilion spray, is meant to protect wounded skin irritation occurs due to other bodily fluids (Gowtham et al. 2022). 2-(5-acetyl-2-thienyl)-1,4-naphthoquinone, a naphthoquinone derivative, has anti-tumor, antimicrobial, and antiproliferative activity. Discharging it into the environment can potentially disrupt the microflora and microfauna (Umar et al. 2023). 5-Bromo-2-hydroxy-N'-(3-pyridinyl methylene) benzo hydrazide ditms inhibit the development of hepatic cancer by reducing the activity of TGF- β (transforming growth factor- β) (Tseng et al. 2021). Garciniaxanthone F is a bioactive Xanthone isolated from *Garcinia mangostana* and used to treat injuries, dermal infections, cystitis, dysentery, and gonorrhoea. It induces quinone reductase (QR) and inhibits P⁴⁵⁰ activity (Ong et al. 2020; Shan et al. 2011). 3-(4-nitrophenyl) quinazolin-4(3h)-one a derivative of quinoxalin, while Dirithromycin is a derivative of erythromycylamine and both these are antimicrobial (Adel et al. 2021; Patel and Patel 2010). Its free dissemination into the environment may promote the evolution of antibiotic-resistant bacterial populations (Soni et al. 2022).

The determined physicochemical parameters, metal concentration, and organic pollutants revealed that the collected samples were highly contaminated (Table 1; Table 2). These pollutants may have various phytotoxic implications, including suppressing seed germination, shoot growth, root growth, and biomass development (Wadaan et al. 2023). In this investigation, the seed germination frequency was 100% when a negative control (tap water) was used, but it decreased substantially when the concentration of wastewater was increased (Table 4). The UTW had less potential to promote seed germination and growth than the TW, indicating that the UTW was more hazardous (Figure 3). Antibiotics are present in PIWW (Dias et al. 2023). These antibiotics can potentially impair nitrogen metabolism in nitrogen-fixing organisms, resulting in phytotoxicity (Fiaz et al. 2023).

To investigate the harmful effect on the root growth of onion bulbs, test solutions of different concentrations of UTW and TW were utilized. Significant differences were found when the root length data were compared to the negative control (tap water). Root development was not substantial in onions grown at 50% UTW concentrations (Figure 4). The MI for the negative control, UTW (50%) and TW (50%) observed in this investigation was 85.54 ± 2.50 , 13.20 ± 0.07 , and 21.34 ± 1.06 respectively, indicating a potent cytotoxic impact of PIWW. The MI for 25% of TW observed in this study was 38.18, greater than the value (9.6) detected in Kumari and Tripathi (2019) study at the same concentration of test solution. This comparative study shows that the cytotoxic impact of effluent calculated in this study is lower than in the study of Kumari and Tripathi (2019). The study of Drzymaa and Kalka (2023) revealed a similar trend. They calculated the toxicity of diclofenac and sulfamethoxazole on *Vicia faba* and observed that both pharmaceuticals reduced the MI by 46% and 22% in soil cultures and 45% and 47% in hydroponic cultures, respectively. The cellular mass of the root apex was treated with negative control (tap water) and revealed no chromosomal abnormalities, but in the test solutions CAs were observed (Figure 5; Table 5). Moreover, the magnitude of the aberration increased with increasing wastewater contents. Other researchers have also reported many CAs in their studies (Kumari and Tripathi 2019; James et al. 2015). The maximum CA obtained in this investigation was aberrant cells, 22 ± 2.40 at a 50% UTW concentration. The presence of CA in the cellular mass of the root apex of *A. cepa* may be due to the cumulative impact of many contaminants like heavy metals, therapeutic compounds, phenols and other organic contaminants in the PIWW. These studies demonstrated that heavy metals, therapeutic compounds, phenols and other organic contaminants in the pharmaceutical wastewater are primarily responsible for the cytotoxic and genotoxic consequences.

Conclusions

WWTPs, responsible for promising everyone access to clean water, sanitary conditions, and good health, are essential to

achieving the UN Sustainable Development Goals (SDGs), particularly SDGs 3 and 6. In comparison to effluents of other WWTP, the PIWWTP's effluent contains high levels of BOD, COD, nitrate, phosphate, metal concentration, pharmaceutical metabolites, and so on. The inability of PIWWTPs to completely remove pharmaceutical metabolites has been widely overlooked. The amalgamation of this effluent with the recipient environmental bodies may have several detrimental effects. It can potentially cause phytotoxicity and chromosomal aberrations and disrupt MI and other cytological processes. Due to these grave implications, immediate action is required to limit the propagation of this worldwide hazard. Public regulatory agencies must act quickly to prevent PIWWTPs from discharging hazardous effluent. The scientific community must develop more efficient, cost-effective methods for treating the PIWW.

Reference

- Adel, K., Amor, M., Alaeddine, R., Emira, N., Mousa, A., et al. (2021). Comparative Computational Analysis of Dirithromycin and Azithromycin in Search for a Potent Drug against COVID-19 caused by SARS-CoV-2: Evidence from molecular docking and dynamic simulation. *Cellular and Molecular Biology*, 67(5), 371-386.
- Ali, M., Almohana, A. I., Alali, A. F., Kamal, M. A., Khursheed, A., Khursheed, A., & Kazmi, A. A. (2021). Common effluent treatment plants monitoring and process augmentation options to conform non-potable reuse. *Frontiers in Environmental Science*, 9, 741343.
- Babaahmadi, F., Dobaradaran, S., Pazira, A., Eghbali, S. S., Khorsand, M., & Keshtkar, M. (2017). Data on metal levels in the inlet and outlet wastewater treatment plant of hospitals in Bushehr province, Iran. *Data in brief*, 10, 1-5.
- Babushok, V. I., Linstrom, P. J., Reed, J. J., Zenkevich, I. G., Brown, R. L., Mallard, W. G., & Stein, S. E. (2007). Development of a database of gas chromatographic retention properties of organic compounds. *Journal of Chromatography A*, 1157(1-2), 414-421.
- Bakare, A. A., Okunola, A. A., Adetunji, O. A., & Jenmi, H. B. (2009). Genotoxicity assessment of a pharmaceutical effluent using four bioassays. *Genetics and Molecular Biology*, 32, 373-381.
- Central Pollution Control Board, India (2020). <https://cpcb.nic.in/openpdffile.php?id=UmVwb3J0RmlsZXMTQWwM18xNjU1MzU0NzIxX21lZGlhcGhvdG8xNjQ>
- Chen, S., Xie, J., & Wen, Z. (2021). Microalgae-based wastewater treatment and utilization of microalgae biomass. *Advances in Bioenergy*, 6(1), 165-198.

- Chowdhary, P., Singh, A., Chandra, R., Kumar, P. S., Raj, A., & Bharagava, R. N. (2022). Detection and identification of hazardous organic pollutants from distillery wastewater by GC-MS analysis and its phytotoxicity and genotoxicity evaluation by using *Allium cepa* and *Cicer arietinum* L. *Chemosphere*, 297, 134123.
- Dias, I. M., Mourão, L. C., Andrade, L. A., Souza, G. B., Viana, J. C., Oliveira, S. B., & Alonso, C. G. (2023). Degradation of antibiotic amoxicillin from pharmaceutical industry wastewater into a continuous flow reactor using supercritical water gasification. *Water Research*, 234, 119826.
- Drzymala, J., & Kalka, J. (2023). Assessment of genotoxicity, mutagenicity, and cytotoxicity of diclofenac and sulfamethoxazole at environmental concentrations on *Vicia faba*. *International Journal of Environmental Science and Technology*, 21, 1-16.
- Fiaz, M., Ahmed, I., Hassan, S. M. U., Niazi, A. K., Khokhar, M. F., Farooq, M. A., & Arshad, M. (2023). Antibiotics induced changes in nitrogen metabolism and antioxidative enzymes in mung bean (*Vigna radiata*). *Science of The Total Environment*, 873, 162449.
- Gowtham, K., Kar, A., Rout, S. R., Sheikh, A., Talegaonkar, S., Kesharwani, P., & Dandela, R. (2022). Hybrid chitosan-based nanoparticulate systems for drug delivery. In *Hybrid Nanomaterials for Drug Delivery* (pp. 129-164). Woodhead Publishing. <https://doi.org/10.1016/B978-0-323-85754-3.00007-1>.
- Grenni, P., Ancona, V., & Caracciolo, A. B. (2018). Ecological effects of antibiotics on natural ecosystems: A review. *Microchemical Journal*, 136, 25-39.
- Gros, M., Marti, E., Balcázar, J. L., Boy-Roura, M., Busquets, A., et al. (2019). Fate of pharmaceuticals and antibiotic resistance genes in a full-scale on-farm livestock waste treatment plant. *Journal of hazardous materials*, 378, 120716.
- Hamaidi-Chergui, F., & Brahim Errahmani, M. (2019). Water quality and physicochemical parameters of outgoing waters in a pharmaceutical plant. *Applied Water Science*, 9(7), 165.
- Haq, I., & Kalamdhad, A. S. (2021). Phytotoxicity and cytogenotoxicity evaluation of organic and inorganic pollutants containing petroleum refinery wastewater using plant bioassay. *Environmental Technology & Innovation*, 23, 101651.
- Haq, I., Kumar, S., Raj, A., Lohani, M., & Satyanarayana, G. N. V. (2017). Genotoxicity assessment of pulp and paper mill effluent before and after bacterial degradation using *Allium cepa* test. *Chemosphere*, 169, 642-650.
- James, O., Oluwaleye, S., Olufunmilayo, A., & Adebisi, O. (2015). Cytotoxic effects and genotoxic screening of pharmaceutical effluents using onion bulbs (*Allium cepa* L.). *Journal of Advances in Biology & Biotechnology*, 2(1), 51-58.
- Koo, I., Kim, S., Shi, B., Lorkiewicz, P., Song, M., McClain, C., & Zhang, X. (2016). Elder: A compound identification tool for gas chromatography mass spectrometry data. *Journal of Chromatography A*, 1448, 107-114.
- Kumar, V., & Chandra, R. (2020). Metagenomics analysis of rhizospheric bacterial communities of *Saccharum arundinaceum* growing on organometallic sludge of sugarcane molasses-based distillery. *3 Biotech*, 10(7), 316.
- Kumari, V., & Tripathi, A. K. (2019). Characterization of pharmaceuticals industrial effluent using GC-MS and FT-IR analyses and defining its toxicity. *Applied Water Science*, 9, 1-8.
- Li, X., Deng, Q., Zhang, L., Wang, J., Wang, R., Zeng, Z., & Deng, S. (2019). Highly efficient hydrogenative ring-rearrangement of furanic aldehydes to cyclopentanone compounds catalyzed by noble metals/MIL-MOFs. *Applied Catalysis A: General*, 575, 152-158.
- Mecozzi, M., Pietroletti, M., Scarpiniti, M., Acquistucci, R., & Conti, M. E. (2012). Monitoring of marine mucilage formation in Italian seas investigated by infrared spectroscopy and independent component analysis. *Environmental Monitoring and Assessment*, 184, 6025-6036.
- Mehrarad, F., Ziarati, P., & Mousavi, Z. (2016). Removing heavy metals from pharmaceutical effluent by plarganium grandiflorum. *Biomedical and Pharmacology Journal*, 9(1), 151-161.
- Mercado, S. A. S., & Caleño, J. D. Q. (2020). Cytotoxic evaluation of glyphosate, using *Allium cepa* L. as bioindicator. *Science of the total environment*, 700, 134452.
- Nandiyanto, A. B. D., Oktiani, R., & Ragadhita, R. (2019). How to read and interpret FTIR spectroscopy of organic material. *Indonesian Journal of Science and Technology*, 4(1), 97-118.
- Ong, Y. S., Murugaiyah, V., Goh, B. H., & Khaw, K. Y. (2020). Bioactive xanthenes from *Garcinia mangostana*. *Plant-derived Bioactives: Chemistry and Mode of Action* (pp 281-300). Springer, Singapore. https://doi.org/10.1007/978-981-15-2361-8_13
- Pashaei, R., Zahedipour-Sheshglani, P., Dzingelevičienė, R., Abbasi, S., & Rees, R. M. (2022). Effects of pharmaceuticals on

- the nitrogen cycle in water and soil: a review. *Environmental Monitoring and Assessment*, 194(2), 105.
- Patel, M., Kumar, R., Kishor, K., Mlsna, T., Pittman Jr, C. U., & Mohan, D. (2019). Pharmaceuticals of emerging concern in aquatic systems: chemistry, occurrence, effects, and removal methods. *Chemical reviews*, 119(6), 3510-3673.
- Patel, N. B., & Patel, J. C. (2010). Synthesis and Antimicrobial Activity of 3-(1, 3, 4-Oxadiazol-2-yl) quinazolin-4 (3H)-ones. *Scientia pharmaceutica*, 78(2), 171-194.
- Ramirez-Morales, D., Masis-Mora, M., Beita-Sandi, W., Montiel-Mora, J. R., Fernandez-Fernandez, E., et al. (2021). Pharmaceuticals in farms and surrounding surface water bodies: Hazard and ecotoxicity in a swine production area in Costa Rica. *Chemosphere*, 272, 129574.
- Rana, R. S., Singh, P., Kandari, V., Singh, R., Dobhal, R., & Gupta, S. (2017). A review on characterization and bioremediation of pharmaceutical industries' wastewater: an Indian perspective. *Applied water science*, 7, 1-12.
- Ray, A., Tripathi, S., & Rai, A. (2019). Pharmaceuticals Export and Market Evolution in India and Thailand. *Trends in Biosciences*, 12(1), 1-20.
- Rice, E.W. (Ed.) (2012). *Standard methods for the examination of water and wastewater (Vol. 10)*. Washington, DC: American public health association.
- Roy, S., Nagarchi, L., Das, I., Mangalam Achuthananthan, J., & Krishnamurthy, S. (2015). Cytotoxicity, Genotoxicity, and Phytotoxicity of Tannery Effluent Discharged into Palar River Basin, Tamil Nadu, India. *Journal of toxicology*, 2015, 504360. <https://doi.org/10.1155/2015/504360>.
- Salian, R., Wani, S., Reddy, R., & Patil, M. (2018). Effect of brewery wastewater obtained from different phases of treatment plant on seed germination of chickpea (*Cicer arietinum*), maize (*Zea mays*), and pigeon pea (*Cajanus cajan*). *Environmental Science and Pollution Research*, 25, 9145-9154.
- Samal, K., Mahapatra, S., & Ali, M. H. (2022). Pharmaceutical wastewater as Emerging Contaminants (EC): Treatment technologies, impact on environment and human health. *Energy Nexus*, 6, 100076.
- Shan, T., Ma, Q., Guo, K., Liu, J., Li, W., Wang, F., & Wu, E. (2011). Xanthenes from mangosteen extracts as natural chemopreventive agents: potential anticancer drugs. *Current molecular medicine*, 11(8), 666-677.
- Sharif, A., Ashraf, M., Anjum, A. A., Javeed, A., Altaf, I., et al. (2016). Pharmaceutical wastewater being composite mixture of environmental pollutants may be associated with mutagenicity and genotoxicity. *Environmental Science and Pollution Research*, 23, 2813-2820.
- Singh, K., Tripathi, S., & Chandra, R. (2023). Bacterial assisted phytoremediation of heavy metals and organic pollutants by *Cannabis sativa* as accumulator plants growing on distillery sludge for ecorestoration of polluted site. *Journal of Environmental Management*, 332, 117294.
- Singh, R.L., Singh, R.P. (2018). Introduction. In: R.L. Singh, R.P. Singh (Eds.), *Advances in Biological Treatment of Industrial Waste Water and Their Recycling for a Sustainable Future* (pp. 1–11). Springer Nature Singapore. <https://doi.org/10.1007/978-981-13-1468-1>.
- Soni, K., Jyoti, K., Chandra, H., & Chandra, R. (2022). Bacterial antibiotic resistance in municipal wastewater treatment plant; mechanism and its impacts on human health and economy. *Bioresource Technology Reports*, 19, 101080.
- Soni, K., Kothamasi, D., & Chandra, R. (2024). Municipal wastewater treatment plant showing a potential reservoir for clinically relevant MDR bacterial strains co-occurrence of ESBL genes and integron-integrase genes. *Journal of Environmental Management*, 351, 119938.
- Theoneste, S., Vincent, N. M., & Xavier, N. F. (2020). The effluent quality discharged and its impacts on the receiving environment case of kacyiru sewerage treatment plant, Kigali, Rwanda. *International Journal of Agriculture and Environmental Research* 6(11), 20-29.
- Tseng, T. H., Lee, H. J., Lee, Y. J., Lee, K. C., Shen, C. H., & Kuo, H. C. (2021). Ailanthoidol, a neolignan, suppresses TGF- β 1-induced HepG2 hepatoblastoma cell progression. *Biomedicine*, 9(9), 1110.
- Umar, H., Aliyu, M. R., Usman, A. G., Ghali, U. M., Abba, S. I., & Ozsahin, D. U. (2023). Prediction of cell migration potential on human breast cancer cells treated with *Albizia lebbek* ethanolic extract using extreme machine learning. *Scientific Reports*, 13(1), 22242.
- Wadaan, M. A., Baabbad, A., Khan, M. F., Shanmuganathan, R., & Daniel, F. (2023). Phytotoxicity and cytotoxicity attributes of immobilized *Bacillus cereus* treated and untreated textile effluents on *Vigna mungo* seeds and *Artemia franciscana* larvae. *Environmental Research*, 231, 116111.
- Yadav, A., Raj, A., Purchase, D., Ferreira, L. F. R., Saratale, G. D., & Bharagava, R. N. (2019). Phytotoxicity, cytotoxicity and genotoxicity evaluation of organic and inorganic pollutants rich

- tannery wastewater from a Common Effluent Treatment Plant (CETP) in Unnao district, India using *Vigna radiata* and *Allium cepa*. *Chemosphere*, 224, 324-332.
- Yang, L., Han, D. H., Lee, B. M., & Hur, J. (2015). Characterizing treated wastewaters of different industries using clustered fluorescence EEM-PARAFAC and FT-IR spectroscopy: Implications for downstream impact and source identification. *Chemosphere*, 127, 222-228.
- Zhu, D., Ge, C., Sun, Y., Yu, H., Wang, J., & Sun, H. (2024). Identification of organic pollutants and heavy metals in natural rubber wastewater and evaluation its phytotoxicity and cytogenotoxicity. *Chemosphere*, 349, 140503.



Journal of Experimental Biology and Agricultural Sciences

<http://www.jebas.org>

ISSN No. 2320 – 8694

Ethnopharmacological study of medicinal plants used in the treatment of skin diseases in the Western Middle Atlas region (Morocco)

Fatiha El Azzouzi^{1*} , Soukaina Chaouqi² , Meryem Makkaoui³ ,
Hanae Briguiche¹ , Lahcen Zidane¹ 

¹Plant, Animal Productions and Agro-industry laboratory, Sciences Faculty, Ibn Tofail University, B.P.133 14000, Kenitra, Morocco

²Organic Chemistry, Catalysis and Environment Laboratory, Sciences Faculty, Ibn Tofail University, BP 242, 14000, Kenitra, Morocco

³Microbiology and Molecular Biology Laboratory, Faculty of Sciences, Mohamed V University, PO Box 1014, Rabat, Morocco

Received – September 04, 2023; Revision – December 21, 2023; Accepted – January 22, 2024

Available Online – March 15, 2024

DOI: [http://dx.doi.org/10.18006/2024.12\(1\).93.105](http://dx.doi.org/10.18006/2024.12(1).93.105)

KEYWORDS

Ethnopharmacology

Medicinal plants

Skin diseases

Western Middle Atlas

ABSTRACT

An investigation was conducted among 360 people from the local population of the Western Middle Atlas of Morocco to identify medicinal plants used for treating skin diseases. Various parameters, including Relative Frequency of Citation (RFC), Family Use Value (FUV), Plant Part Value (PPV), Informant Consensus Factor (ICF), and Fidelity Level (FL), were used for data collection and assessment. During the investigation, 45 medicinal plant species belonging to 33 families were documented, with the most important family being Euphorbiaceae (FUV = 0.292). The highest ICF value (ICF=0.991) was mentioned for skin cancer. The poultice was found to be the primary method for preparing the majority of remedies (51%). Leaves were the most commonly used plant part (PPV = 0.476), and *Allium sativum* L. was the most widely used species (RFC = 0.302). These findings are a preliminary step towards conserving and popularising these plant species, promoting sustainable practices in traditional medicine, safeguarding biodiversity, and integrating these valuable botanical resources into modern healthcare systems.

* Corresponding author

E-mail: azzouzi.fatiha89@gmail.com (Fatiha El Azzouzi)

Peer review under responsibility of Journal of Experimental Biology and Agricultural Sciences.

Production and Hosting by Horizon Publisher India [HPI]
(<http://www.horizonpublisherindia.in/>).
All rights reserved.

All the articles published by [Journal of Experimental Biology and Agricultural Sciences](#) are licensed under a [Creative Commons Attribution-NonCommercial 4.0 International License](#) Based on a work at www.jebas.org.



1 Introduction

Plant species are highly diverse and abundant, and they play a crucial role in maintaining ecosystem balance and providing essential natural resources for human survival and development (Spichiger et al. 2000). Medicinal plants, in particular, are an invaluable inheritance for mankind, especially for underprivileged societies in developing countries that rely on them for their main healthcare needs and sustenance (Salhi et al. 2010). According to the World Health Organization (WHO), around 80% of populations in developing countries, including African countries, depend on traditional medicine as their primary source of medicines (World Health Organization 2019; SasiPriya 2020). In Morocco, the Mediterranean climate promotes the growth of approximately 4800 plant species of vascular flora (Fennane and Rejdali 2018), giving rise to a long tradition of utilizing medicinal plants derived from diverse civilizations, including Africans, Arabs, Andalusians, and Berbers (Bellakhdar 2006).

Skin diseases are a significant public health issue, encompassing a range of pathologies. Over the past 30 years, the frequency of these diseases has significantly increased worldwide, including in emerging countries (Stambouli 2018; Grenez 2019). Skin diseases are common across all age groups, and they hold a significant place in the consultation profile in Africa, encompassing mycotic, parasitic, bacterial, and viral infections (Orion and Wolf 2014). The biological properties of plants for treating dermatological ailments are promising, with some highlighted through various

studies, while others are still the subject of research worldwide. Several studies have identified medicinal plant species with beneficial properties in treating skin diseases. In Turkey, Erarslan et al. (2020) identified 191 medicinal species with properties useful for skin diseases. Similarly, Tsioutsiou et al. (2022) reported the utilization of 967 taxa with various medicinal properties in the South Balkan and East Mediterranean regions. Makgobole et al. (2023) identified 211 plant species implicated in treating multiple skin conditions in West Africa. Ajjoun et al. (2022) documented a total of 401 plants in Morocco. This study aims to conduct an ethnopharmacological survey on the medicinal plants traditionally used for managing skin diseases in various regions of the Western Middle Atlas of Morocco. The study seeks to record and analyze the range of medicinal plants used in treating skin diseases in the study region, to preserve valuable herbal knowledge acquired by the local population, and to contribute to various scientific fields, including phytochemical and pharmacological research.

2 Materials and Methods

2.1 Study area description

The study sites are situated in the Beni Mellal-Khenifra region, located at the center of Morocco. This region is known for its diverse geographical, cultural, and economic aspects. The study region comprises various provinces, such as Beni Mellal, Khenifra, Azilal, Fquih Ben Salah, and Khouribga (HCP 2017) (Figure 1).

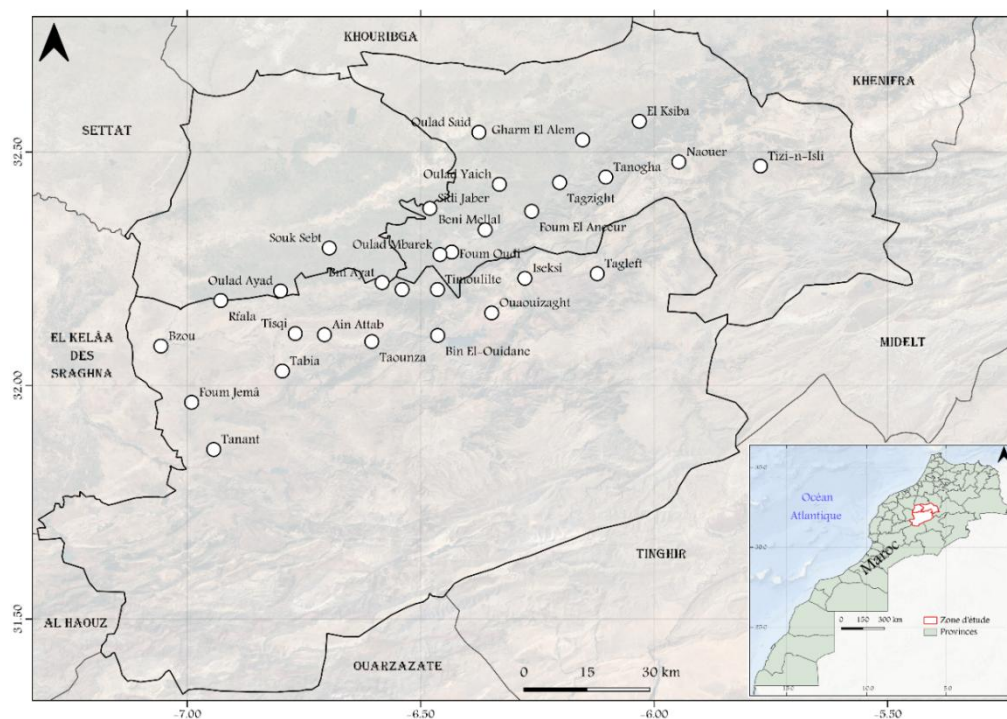


Figure 1 The map of the study area showing the locations of the survey points

The Beni Mellal-Khenifra region in Morocco is home to the important Oued OumErrabia River and covers a large part of its upstream catchment area. The region experiences varying levels of rainfall and temperatures, with different climates across the plain and mountain areas. The vegetation in the region reflects the Mediterranean bioclimatic staging, but traditional agro-pastoral practices and forest management have greatly influenced the landscape (Taïbi et al. 2015). The region's population is estimated to be 2,520,776 people, which is 7.45% of the overall population (HCP 2017). The region has great tourism potential, with popular sites such as Ain Asserdoun, the panoramic castle of Beni Mellal, the summering centre of Elksiba, the waterfalls of Ouzoud, Tamga Cathedral, the AitBougamaz valley, and various mountain trails attracting many tourists every year (Direction Régionale de Beni Mellal-Khenifra 2019).

2.2 Methodology

An ethnobotanical examination was conducted between 2013-2014 in the Western Middle Atlas to collect and document traditional practices associated with medicinal plants used to treat skin diseases. The survey involved 360 participants who were interviewed using a pre-determined questionnaire. The survey was carried out using random stratified sampling, allowing for a comprehensive floristic inventory to be obtained and ethnobotanical surveys to be conducted across various regions within the specified area. During the interviews, discussions were conducted in local languages and Arabic. The survey recorded information such as the gender, age, academic level, and marital status of the participants, as well as the local names of the plants used, the plant parts utilized, the preparation methods, the method of administration, and the ailments treated. Several field trips were organized to the research areas, which successfully captured digital photographs and assigned local names to the medicinal plants for producing herbarium sheets. The taxonomic identification was carried out using Moroccan floras T1, T2, and T3, and herbarium specimens (Fennane et al. 1999; Fennane et al. 2007; Fennane et al. 2014) and catalogues (Bellakhdar 1997; Hmamouchi 2001). The obtained results were analyzed using descriptive statistics in the form of percentages through computer software (SPSS Statistics 21 and Excel 2016). The participants' demographic data were analyzed using simple descriptive statistical methods using frequencies and percentages. The ethnopharmacological data were analyzed using various methods, including Family Use Value (FUV), Relative Citation Frequency (RFC), Fidelity Level (FL), Informant Consensus (ICF), and Plant Part Value (PPV).

2.2.1 Family Use Value (FUV)

The FUV index measures the significance of a plant family in a community by considering the number of species utilized from that

family. FUV is calculated using the formula $FUV = UVs/Ns$, as described in Sreekeesoon and Mahomoodally (2014), where UVs use values of the species, and Ns: total number of species within each family.

2.2.2 Relative Frequency of Citation (RFC)

The RFC index measures how often a plant is identified as a remedy by people providing information. It is calculated by dividing the number of informants who mention a particular plant by the total number of informants. This formula is expressed as $RFC = FC / N$ ($0 < RFC < 1$), where FC is the number of informants mentioning the use of the species, and N is the number of informants participating (Tardío and Pardo-De-Santayana 2008).

2.2.3 Fidelity Level (FL)

The FL is a classification system used to determine the effectiveness of collected plant species in treating specific disorders. It was calculated by finding the percentage of people who suggest using a particular plant for a specific purpose. The calculation uses the formula $FL = (Ip / Iu) \times 100$. Where Ip represents the number of informants who mentioned using a particular plant for a particular purpose, and Iu represents the total number of informants who mentioned the plant for any use (Alexiades and Sheldon 1996; Sreekeesoon and Mahomoodally 2014).

2.2.4 Informant Consensus Factor (ICF)

This index ascertains the extent of community agreement regarding the utilization of a specific plant (Heinrich et al. 1998); it was computed based on the formula $ICF = Nur - Nt / Nur - 1$, where Nur is represented as the number of illnesses used in each category, and Nt is the full sum of species mentions reported within each category.

2.2.5 Plant Part Value (PPV)

The PPV is a metric that we employed to indicate the usage prevalence. Its calculation was conducted as follows: $PPV = RU_{\text{plant part}} / RU$, where $RU_{\text{plant part}}$ is the sum of utilizations for each plant component, and RU is the total instances of plant part utilization (Gomez-Beloz 2002).

3 Results and Discussion

3.1 Participant demographic details

A total of 360 participants, consisting of 220 females and 140 males, were interviewed for this study. The results indicated that herbs effectively treat health issues of both genders in the Western Middle Atlas region. However, women showed more knowledge of

plant species and their usage, accounting for 61.11% of the respondents compared to 38.89% for men. The prevalence of women in this study is explained by their careful attention to disease prevention and adherence to traditional practices. It is worth noting that women traditionally provide food and healthcare to their families during times of illness. These findings are consistent with other ethnobotanical studies conducted on a national level (Benknigie et al. 2010; Salhi et al. 2010; El Hafian et al. 2014; Khenissi and Rouabhia 2021; Bentabet et al. 2022).

A significant percentage of the respondents in the research site were over the age of 60 (39.72%), followed by those aged between 40-60 years (31.11%) and between 20-40 years (23.33%). Only a small percentage of respondents were under the age of 20 (5.83%) (Table 1). The higher involvement of elderly respondents may be because they possess traditional knowledge and understanding passed down through generations. However, there is a decline in the transmission of knowledge about medicinal plants, which can be attributed to younger people's disbelief in the efficacy of herbal medicine. This disbelief is influenced by modernization and foreign cultural influences. As a result, traditional medical wisdom is unlikely to disappear as there is no consistent intergenerational exchange between older and younger individuals. These observations are consistent with findings from other regions in Morocco (Anyiam 1995; Benlamdini et al. 2014; El Hafian et al. 2014; Bounoua and Djoudi 2022; Chaachouay et al. 2022).

According to the gathered data, married individuals (72.77%) use medicinal plants more than singles (27.22%). This trend can be attributed to the fact that married people can avoid or reduce the costs associated with seeing doctors and buying pharmaceuticals. In addition, those who live in rural areas (81.88%) are more familiar with using plants to manage skin diseases. These findings are consistent with El Hilah et al. (2015) and Chaachouay et al. (2022) research. Regarding the education level

of the participants, more than half of them (59.72%) were uneducated. 28.33% had attended primary school, while 9.89% had completed secondary school education. Interestingly, interviewees with advanced educational backgrounds showed minimal use of medicinal plants (3.05%). Therefore, the utilization of medicinal plants decreases with an increase in educational achievement. This conclusion is consistent with the findings of studies conducted by Lahsissene et al. (2009), El Hilah et al. (2015), Bouzid et al. (2017), and Achour et al. (2022).

3.2 Quantitative analysis

3.2.1 Predominant families and their FUV

The study in the area revealed that people used 45 different plant species from 33 families to treat skin disorders. The study included scientific names, local names, the parts of plants used, the method of preparation, local medicinal uses and various details like FC, RFC, FL, and FUV particulars, all mentioned in Table 2.

The Solanaceae family had the highest number of species represented (5 species), followed by Asteraceae and Lamiaceae (3 species each). Other families, such as Cucurbitaceae, Amaryllidaceae, Rhamnaceae, and Poaceae (2 species each), were also well-represented. The remaining families had only one species represented (Figure 2). Among the reported families, Euphorbiaceae (FUV=0.292), Verbenaceae (FUV=0.275), and Cupressaceae (FUV=0.272) were the three most frequently enumerated families based on the FUV index. This notable prevalence can be explained by the extensive presence of these families in the Western Middle Atlas region owing to ecological conditions. These findings contradict the results of Ajjoun et al. (2022) and Nasab et al. (2022), where Asteraceae and Lamiaceae were found to be the most frequently cited families for treating skin disorders.

Table 1 Demographic characteristics of interviewees in the Western Middle Atlas of Morocco

Variables	Category	Total	Percentages (%)
Gender	Female	220	61.11
	Male	140	38.89
Age groups	< 20	21	5.83
	[20-40]	84	23.33
	[40-60]	112	31.11
	>60	143	39.72
Marital status	Married	262	72.77
	Single	98	27.22
Academic level	Illiterate	215	59.72
	Primary	102	28.33
	Secondary	32	8.89
	University	11	3.05
Living environment	Rural	289	81.88
	Urban	71	19.72

Table 2 Summary of medicinal flora for treating skin diseases in the Western Middle Atlas region (Morocco)

Family	Scientific name	Vernacular name	Part used	Preparation	Local medicinal uses	FC	RFC	FL	FUV
Amaryllidaceae	<i>Allium cepa</i> L	Lbesla	Bulb	Poultice	The bulb is ground with leaves of <i>lawsonia inermis</i> L. and olive oil to remove burn scars.	51	0.141	100	0.221
	<i>Allium sativum</i> L	Touma	Bulb	Poultice	Poultices of garlic triturated with olive oil are used to grow hair and treat eczema.	109	0.302	73.4	
Aizoaceae	<i>Aizoon canariense</i> L	El-ghassoule	Leaves	Poultice	A mixture of powder and olive oil paste is used to cure Eczema.	23	0.064	100	0.064
Anacardiaceae	<i>Pistacia atlantica</i> Desf	L-Btem	Bark	-	The resin is applied externally to heal wounds	22	0.061	100	0.061
Apiaceae	<i>Ammi majus</i> L	Trillan	Seeds	Poultice	Paste of seeds mixed with roots of <i>Anacyclus pyrethrum</i> L. and honey is applied against vitiligo	89	0.247	100	0.247
Apocynaceae	<i>Nerium oleander</i> L	Ddefla	Leaves/ Bark	Powder/ Poultice	Powder of leaves is used to cure burns and eczema. Bark is crushed to paste and applied externally in case of alopecia.	77	0.214	51.5	0.214
Arecaceae	<i>Chamaerops humilis</i> L	El-Ghaz/ Doum	Roots	Powder	The roots heated with fire are used in local application against warts.	12	0.033	100	0.033
Asparagaceae	<i>Agave americana</i> L	Ssabra/ Sayber	Leaves	Powder	Powder of leaves associated to <i>Agave americana</i> , <i>Lepidium sativum</i> , <i>Opuntia ficus-indica</i> (L.) Mill., is used against skin cancer	79	0.219	100	0.219
Asteraceae	<i>Anacyclus pyrethrum</i> L	Taqendicht/ Iguntas	Roots	Powder	Powder of <i>Anacyclus pyrethrum</i> L. blended with honey is used to heal vitiligo.	42	0.116	100	0.162
	<i>Artemisia herba-alba</i> Asso.	Chih/ Ifzi	Leaves	Poultice	Fresh leaves are crushed to paste and applied externally in case of pimples	39	0.108	100	
	<i>Carlina gummifera</i> (L) Less.	Addad	Roots	Poultice	The roots macerated in water are used against vitiligo.	94	0.261	100	
Cistaceae	<i>Cistus ladanifer</i> L	Touzalt	Leaves	Poultice	Paste of leaves mixed with <i>Lawsonia inermis</i> L. is used to moisturize dry hair.	19	0.052	100	0.052
Cucurbitaceae	<i>Citrullus colocynthis</i> (L) Schrad	El-hdej	Fruit	Poultice	Paste of cooked fruit mixed with tar is used to cure eczema.	22	0.061	100	0.133
	<i>Cirtullus vulgaris</i> (L) Schrad	Dellah	Fruit	Crude	The water of watermelon is used to cure burns.	74	0.205	100	
Cupressaceae	<i>Tetraclinis articulata</i> (Vahl) Masters	El Ârâr	Leaves/ Roots	Poultice	Powder of leaves blended with Castor oil is applied to arrest hair fall. Roots are used as antifungal. Thick tar is used against eczema.	98	0.272	54.1	0.272

Family	Scientific name	Vernacular name	Part used	Preparation	Local medicinal uses	FC	RFC	FL	FUV
Fabaceae	<i>Ceratonia siliqua</i> L	Kharroub/ Tikida	Leaves/ Fruit	Crude/ Powder	Fresh leaf is applied externally on warts. Powder from fruit is applied externally in case of eczema.	36	0.100	100	0.100
Fagaceae	<i>Quercus suber</i> L	Dbagh/ Tûnwat/ El Ballût	Bark/ Fruit	Poultice	A paste made from a combination of powder and olive oil is applied externally for wounds. Paste of Powder mixed with the leaves of <i>Rosmarinus officinalis</i> L. is used to cure burns.	37	0.103	64.8	0.103
Juglandaceae	<i>Juglans regia</i> L	L-Gergaâ/ Sswak	Bark	Powder	Powder of barks is used against inflammatory dermatosis.	68	0.189	100	0.189
Lamiaceae	<i>Lavandula dentata</i> L	Lkhzama	Leaves	-	Its essential oil is applied to cure cracked heels.	12	0.033	100	0.068
Linaceae	<i>Marrubium vulgare</i> L	Merriwta/ Ferkizout	Leaves	Poultice	Fresh leaves are crushed to paste and applied externally in case of wounds.	32	0.089	100	0.080
	<i>Rosmarinus officinalis</i> L	Yazir	Leaves	Decoction	Decoction of fresh leaves is used to strengthen the hair.	30	0.083	100	
	<i>Linum usitatissimum</i> L	Zerri't El-Kettan	Seeds	Poultice	The seeds macerated in olive oil are used as a poultice to stimulate hair growth.	29	0.080	100	
Lythraceae	<i>Lawsonia inermis</i> L	El-henna	Leaves	Poultice	Powdered leaves mixed with crushed bulbs of <i>Allium cepa</i> L., and olive oil are used to treat burn scars.	56	0.155	100	0.155
Moraceae	<i>Ficus carica</i> L	Karmous	Fruit	Latex	Latex is applied externally to treat warts.	21	0.058	100	0.058
Musaceae	<i>Musa x paradisiaca</i> L	Banane	Fruit	Crude	Peels are recommended to cure warts.	19	0.053	100	0.053
Myrtaceae	<i>Myrtus communis</i> L	Rayhane	Leaves	Poultice	Fresh leaves, mixed with alum powder and tar of <i>Cedrus atlantica</i> , are applied externally against eczema.	23	0.064	100	0.064
Nitrariaceae	<i>Peganum harmala</i> L	L-Harmel	Seeds	Poultice	Combined with the seeds of <i>Lepidium sativum</i> and the leaves of <i>Tetraclinis articulata</i> , powdered and crushed in olive oil, are used to heal wounds. A mixture of powder and olive oil paste is used to enhance hair growth and make it shinier.	64	0.178	67.1	0.178
Oleaceae	<i>Olea europaea</i> L	Zitoun	Leaves	Powder	Powder from Leaves is applied externally in case of wounds.	17	0.047	100	0.047
Pinaceae	<i>Pinus pinaster</i> Aiton	Tayda/ Dbibigha	Bark	Powder	Powder of barks associated to <i>Lawsonia inermis</i> L. is used to cure burns.	62	0.172	100	0.172

Family	Scientific name	Vernacular name	Part used	Preparation	Local medicinal uses	FC	RFC	FL	FUV
Plantaginaceae	<i>Plantago major</i> L	El-messassa	Leaves	Crude	Fresh leaf is applied externally on boils.	59	0.164	100	0.164
Plumbaginaceae	<i>Plumbago europeae</i> L	Timrabdine	Leaves	Crude	Fresh leaves are applied externally on warts and alopecia.	69	0.192	55.1	0.192
Poaceae	<i>Hordeum vulgare</i> L	Ch'ir	Seeds	Poultice	Paste of powder mixed with rose water is applied against acne.	12	0.033	100	0.036
	<i>Triticum durum</i> Desf	Zraâ	Seeds	Poultice	Powder of <i>Triticum durum</i> and <i>Prunus amygdalus</i> stokes var. amara DC. mixed with honey is used to lighten the skin.	21	0.058	100	
Rhamnaceae	<i>Rhamnus alaternus</i> L	Tisknane	Bark	Poultice	Paste of powder mixed with milk is applied to cure burns.	24	0.067	100	0.069 0.042
	<i>Ziziphus lotus</i> (L.) Lam	Nnbeg/ Ssedra	Leaves	Crude	Fresh leaves are applied externally against eczema.	26	0.072	100	
Rosaceae	<i>Prunus amygdalus</i> stokes var. amara DC	Luz Harr	Fruit	Poultice	The mixture of powder and olive oil paste is employed to moisturize the face, strengthen the hair, and thicken eyebrows.	15	0.042	100	
Solanaceae	<i>Capsicum annuum</i> L	Felflahlouwa / Tehmira	Fruit	Powder	Powder of fruits is used against burns and wounds.	35	0.098	51.4	0.095
	<i>Capsicum frutescens</i> L	Soudaniya	Fruit	Poultice	<i>Capsicum frutescens</i> L. and <i>Allium sativum</i> L. are crushed together and applied against Alopecia areata.	41	0.114	100	
	<i>Nicotiana tabacum</i> L	Tabac	Leaves	Powder	Powder from leaves is applied externally against skin disorders.	47	0.130	100	
	<i>Solanum elaeagnifolium</i> Cav	El-Âwssage	Leaves	Poultice	A blend of powder and water paste is utilized to heal eczema.	20	0.055	100	
	<i>Solanum nigrum</i> L	Bouqnini	Leaves	Crude	Fresh leaves are applied externally against eczema.	29	0.080	100	
Theacea	<i>Camellia thea</i> Link	Atây	Leaves	Powder	Paste of powder mixed with honey is applied externally to cure burns and wounds.	37	0.103	64.8	0.103
Thymelaeaceae	<i>Daphne gnidium</i> L	Lezzâz	Leaves	Poultice	Powder of leaves blended with Castor oil is applied to arrest hair fall.	48	0.133	100	0.133
Verbenaceae	<i>Verbena officinalis</i> L	Baymout	Leaves	Poultice, powder, squash	Leaves associated to <i>Mentha rotundifolia</i> Ehrh. are crushed to paste and then applied externally to cure wounds. Combined with <i>Cynara humilis</i> L., <i>Camellia thea</i> Link. and the chicken bone in powder are used against burns. Crushed leaf is applied to cure foot corn.	99	0.275	44.4	0.275
Zygophyllaceae	<i>Zygopgyllumgaetulum</i>	El-Aggaya	Seeds	Powder	Powder of seeds blended with olive oil is applied against acne	12	0.033	100	0.036

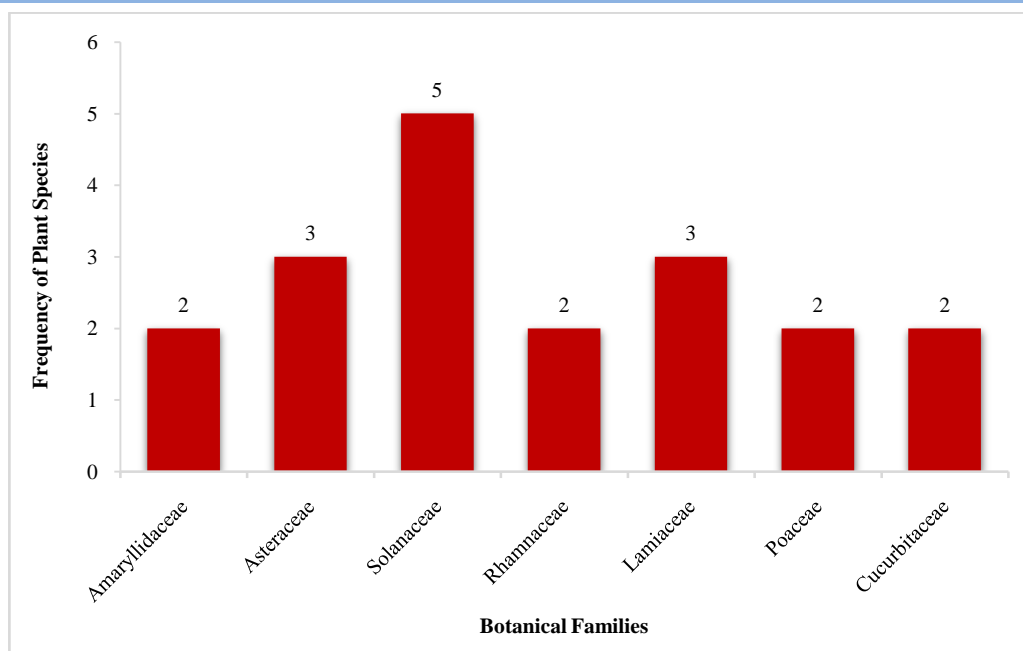


Figure 2 shows the prevalence of plant families that effectively treat skin disorders. Only families with more than one species are shown

3.2.2 Spectrum of medicinal flora and their RFC values

The study calculated each plant species' Relative Frequency of Citation (RFC) to determine their local importance. The RFC values ranged between 0.033 and 0.302. The highest RFC value was recorded for *A. sativum* (0.302), followed by *E. resinifera* Berg. (RFC=0.292) and *V. officinalis* L. (RFC=0.272). On the other hand, the lowest RFC values (RFC=0.033 each) were found for three plant species, namely *Chamaerops humilis* L., *Lavandula dentata* L., and *Hordeum vulgare*. These plants were cited by a significant number of informants, indicating their high RFC. Further analysis through phytochemical and pharmaceutical research is required to explore the active constituents of these plant species, which could be utilized for drug extraction (Vitalini et al. 2013). The study also highlights the importance of conservation initiatives for these plant species, as their prevalent use may pose a threat of overharvesting and endanger their populations.

3.2.3 Fidelity Level Index (FL)

Data assessment revealed that the FL value ranged from 40.9% to 100%. Among the collected plant species, 35 demonstrated an FL value of 100%. These plant species are used for managing inflammatory skin disorders and are distributed among 16 species, including *Aizoon canariense* L., *Chamaerops humilis* L., *Artemisia herba-alba* Asso., *Citrullus colocynthis* (L.) Schrad., *Ceratonia siliqua* L., and *Juglans regia* L. Four other species, namely *Allium cepa* L., *Lawsonia inermis* L., *Pinus pinaster* Aiton, and *Rhamnus alaternus* L., are used for treating burns, while three species, namely *Ammi majus* L., *Anacyclus pyrethrum* L., and *Carlina*

gummifera (L.) Less are used for treating vitiligo. Additionally, *Pistacia atlantica* Desf., *Marrubium vulgare* L., and *Olea europaea* L. are used for treating wounds. During the survey, the use of *Agave americana* L. in treating skin cancer and *Capsicum frutescens* L. in treating alopecia was also recorded (Table 2). These findings can be attributed to these plant species' medicinal usefulness and indigenous value. The lowest FL value was noted for *Euphorbia resinifera* Berg., which could be because the populace widely utilizes it due to its numerous therapeutic effects. This species is exclusive to Morocco. Many researchers have documented the pharmacological activity of *Euphorbia resinifera* extracts, including antioxidant (Boutoub et al. 2020; Benrahou et al. 2022), antitumoral (Talbaoui et al. 2020; Hmidouche et al. 2023), antibacterial (Moujanni et al. 2017; Talbaoui et al. 2020; Benjamaa et al. 2020), and antifungal activities (Ourhizif et al. 2022).

3.2.4 Categories of diseases and their ICF values

The research has identified seven categories of diseases: inflammatory skin diseases, wounds, burns, vitiligo, scalp disorders, skin cancer, and cosmetic care. The ICF values range from 0.963 to 0.991. The categories with high ICF values are skin cancer (0.991), vitiligo (0.988), burns (0.976), scalp disorders (0.975), inflammatory skin diseases (0.972), cosmetic care (0.968), and wounds (0.963) (Table 3). This indicates that the traditional utilization of medicinal plants is reliably known among respondents (Lin et al. 2002). Furthermore, it shows that there is widespread sharing of traditional insights into managing skin diseases and alleviating chemotherapy side effects in skin cancer cases among people within the study area.

Table 3 Ethnobotanical ICF values by skin disease category

Category	Plant species used and number of citations	Total number of		
		Species	Use citations	ICF
Inflammatory skin diseases (warts, eczema, acne, pimples, boils)	<i>Allium sativum</i> L. (80), <i>Aizoon canariense</i> L. (23), <i>Nerium oleander</i> L. (32), <i>Citrullus colocynthis</i> (L.) Schrad. (22), <i>Tetralinis articulata</i> (Vahl) Masters. (45), <i>Euphorbia resinifera</i> Berg. (43), <i>Ceratonia siliqua</i> L. (36), <i>Myrtus communis</i> L. (23), <i>Ziziphus lotus</i> (L.) Lam. (26), <i>Solanum elaeagnifolium</i> Cav. (20), <i>Solanum nigrum</i> L. (29), <i>Quercus suber</i> L. (22), <i>Verbena officinalis</i> L. (62), <i>Chamaerops humilis</i> L. (12), <i>Ficus carica</i> L. (21), <i>Musa x paradisiaca</i> L. (19), <i>Plumbago europeae</i> L. (38), <i>Artemisia herba-alba</i> Asso. (39), <i>Juglans regia</i> L. (68), <i>Lavandula dentata</i> L. (12), <i>Plantago major</i> L. (59), <i>Hordeum vulgare</i> L. (12), <i>Nicotiana tabacum</i> L. (47), <i>Verbena officinalis</i> L. (25)	24	815	0.972
Wounds	<i>Pistacia atlantica</i> Desf. (22), <i>Quercus suber</i> L. (24), <i>Marrubium vulgare</i> L. (32), <i>Peganum harmala</i> L. (21), <i>Olea europaea</i> L. (17), <i>Capsicum annuum</i> L. (17), <i>Camellia thea</i> Link. (13), <i>Verbena officinalis</i> L. (44).	8	190	0.963
Burns	<i>Allium cepa</i> L. (51), <i>Nerium oleander</i> L. (23), <i>Citrullus vulgaris</i> (L.) Schrad. (74), <i>Quercus suber</i> L. (13), <i>Lawsonia inermis</i> L. (56), <i>Pinus pinaster</i> Aiton. (62), <i>Rhamnus alaternus</i> L. (24), <i>Capsicum annuum</i> L. (18), <i>Camellia thea</i> Link. (24), <i>Verbena officinalis</i> L. (30).	10	378	0.976
Cosmetic care	<i>Cistus ladanifer</i> L. (19), <i>Linum usitatissimum</i> L. (29), <i>Peganum harmala</i> L. (43), <i>Triticum durum</i> Desf. (21), <i>Prunus amygdalus stokes</i> var. <i>amara</i> DC. (15).	5	127	0.968
Vitiligo	<i>Ammi majus</i> L. (89), <i>Anacyclus pyrethrum</i> L. (42), <i>Carlina gummifera</i> (L.) Less. (94), <i>Euphorbia resinifera</i> Berg. (32)	4	257	0.988
Scalp disorders	<i>Allium sativum</i> L. (29), <i>Nerium oleander</i> L. (22), <i>Euphorbia resinifera</i> Berg. (30), <i>Plumbago europeae</i> L. (31), <i>Capsicum frutescens</i> L. (41), <i>Tetralinis articulata</i> (Vahl.) Masters. (53), <i>Rosmarinus officinalis</i> L. (30), <i>Daphne gnidium</i> L. (48)	8	284	0.975
Skin cancer	<i>Agave americana</i> L. (79), <i>Euphorbia resinifera</i> Berg. (31)	2	110	0.991

3.3 Plant parts used in remedy formulation

According to the survey, people living in the Western Middle Atlas region use different parts of medicinal plants to cure ailments. The most commonly used parts are leaves (PPV=0.476), followed by fruits (PPV = 0.122), barks (PPV = 0.108), seeds (0.105), roots (PPV= 0.084), and bulbs (0.078) (Figure 3). The reason for the preference for leaves is their easy availability, simple preparation, and the fact that they contain secondary metabolites responsible for the plant's bio-properties. Leaves are also important for photosynthesis. Similar findings have been observed in studies conducted in Morocco (El Azzouzi et al. 2018; Chaachouay et al. 2023; Idm'hand et al. 2023) and across Africa (Yetein et al. 2013; Etienne et al. 2021; Falana et al. 2023) where leaves are the primary part of the plant used for preparing herbal remedies.

3.4 Cure preparations practices

Various preparation methods, such as infusion, decoction, cataplasm, powder, and maceration, are used to enhance the ease of administration of the active compounds in plants. Details about the modes of preparation for each plant have been integrated into Table 2. The study found that the majority of cures were prepared through poultice (51%), followed by powder (27%) and crude (13%). The combined percentage of other preparation methods did

not exceed 9% (Figure 4). Numerous ethnobotanical surveys have documented diverse methods of preparing medicinal plants for treating skin disorders, including powders, pastes, and decoctions (Begum and Nath 2000; Malik et al. 2019; Chaachouay et al. 2022). The most widely used method of preparation among patients in this study was the poultice, which could be attributed to its convenient preparation method for treating skin ailments. This finding aligns with the results of a prior study conducted by Saising et al. (2022).

3.5 Origin of information regarding medicinal plants

During the ethnobotanical survey, 69% of the interviewees stated that they relied on the advice and experiences of their immediate surroundings to obtain knowledge about the healing properties of plants. This highlights the importance of the intergenerational transfer of folk practices. A smaller percentage (23%) obtained knowledge from herbalists, while 7% gained information through personal experiences. Only 1% sought information from doctors. The surroundings and shared experiences of others remain the primary influential channels for conveying information about the healing properties of plants. Therefore, it is important to consider the curative power of plants not just as a tradition but as a field of science that should be studied and improved to be applied safely and effectively by healthcare professionals.

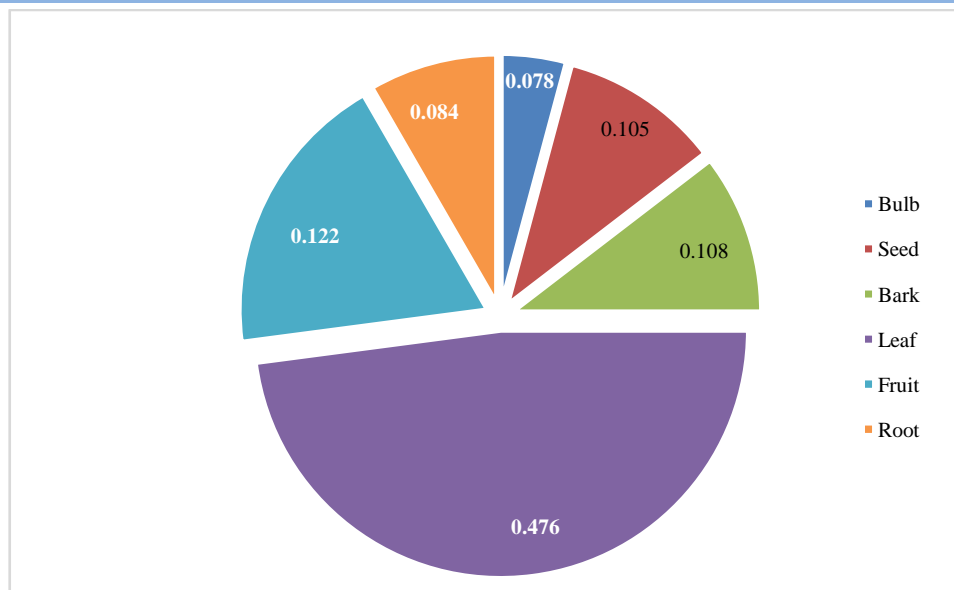


Figure 3 Parts used in the skin disease treatment (PPV index)

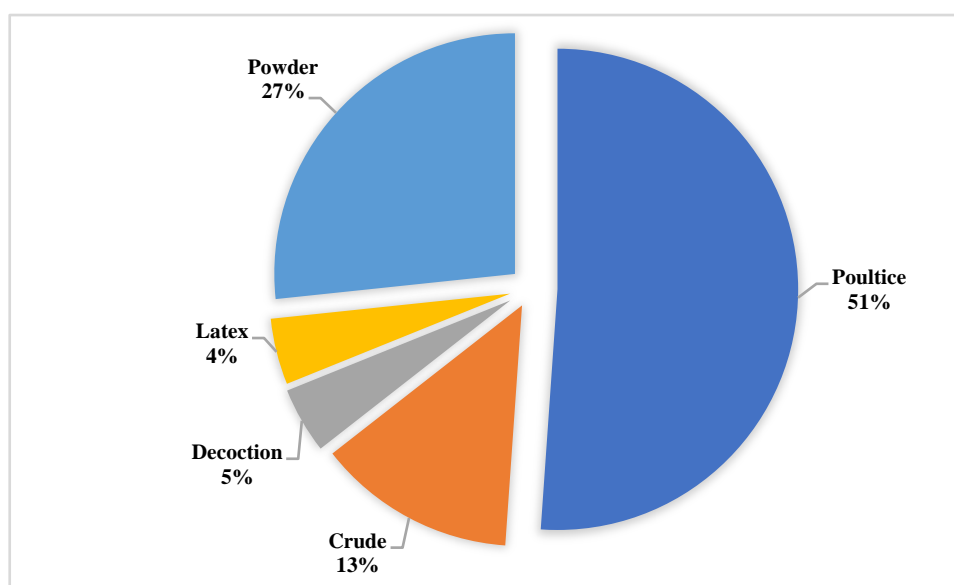


Figure 4 Incidence of different types of medicines used for treating skin disorders

Conclusion

This study documents the use of traditional medicinal plants by the people of the Western Middle Atlas region for treating various skin diseases. The research identified 45 plant species from 33 families, with Solanaceae, Lamiaceae, and Asteraceae being the most commonly used. *Allium sativum* L. (RFC = 0.302) and *Euphorbia resinifera* Berg were the plants with the highest citation rates. (RFC = 0.292), and *Verbena officinalis* L. (0.275). The most commonly used part of the plant was the foliage (PPV of 0.476), and the most frequently used preparation method was a poultice (51%). The majority (69%) of the informants learned about the

medicinal use of plants for skin diseases through the experiences of others. This study highlights the importance of utilizing Moroccan natural resources and traditional knowledge. The findings can serve as a foundation for future studies on the listed plants' biological and phytochemical properties to manage skin diseases.

Acknowledgments

We are indebted to all the habitats of our study area for their help during the ethnobotany field surveys. Please accept our sincere thanks and gratitude to all those who helped in our work.

Conflict of interest

No financial or competing interests were disclosed by the authors.

References

- Achour, S., Chebaibi, M., Essabouni, H., Bourhia, M., Ouahmane, L., et al. (2022). Ethnobotanical study of medicinal plants used as therapeutic agents to manage diseases of humans. *Evidence-Based Complementary and Alternative Medicine*, 2022. DOI: <https://doi.org/10.1155/2022/4104772>.
- Ajjoun, M., Kharchoufa, L., Merrouni, I. A., & Elachouri, M. (2022). Moroccan medicinal plants traditionally used for the treatment of skin diseases: from ethnobotany to clinical trials. *Journal of Ethnopharmacology*, 297, 115532. DOI: 10.1016/j.jep.2022.115532.
- Alexiades, M. N., & Sheldon, J.W. (1996). Selected Guidelines for ethnobotanical research: A field Manual. The New York Botanical Garden, Bronx. NY 99-133.
- Anyinam, C. (1995). Ecology and ethnomedicine: exploring links between current environmental crisis and indigenous medical practices. *Social science & medicine*, 40(3), 321-329. DOI: [https://doi.org/10.1016/1277-9536\(94\)E0098-D](https://doi.org/10.1016/1277-9536(94)E0098-D).
- Begum, D., & Nath, S. C. (2000). Ethnobotanical review of medicinal plants used for skin diseases and related problems in Northeastern India. *Journal of herbs, spices & Medicinal plants*, 7(3), 55-93. DOI : https://doi.org/10/1300/J044v07n03_07.
- Bellakhdar, J. (1997). La pharmacopée marocaine traditionnelle. Médecine arabe ancienne et Savoirs populaires. Editions Le Fennec, Casablanca/ Ibis Press. 764 p. Paris.
- Bellakhdar, J. (2006). Plantes médicinales au Maghreb et soins de base: précis de phytothérapie moderne. Éditions le Fennec.
- Benjamaa, R., Moujanni, A., Terrab, A., Eddoha, R., Benbachir, M., et al. (2020). Relationship among antibiotic residues and antibacterial activity of the endemic spurge honey (*Euphorbia resinifera* O. Berg) from Morocco. *Emirates Journal of Food and Agriculture*, 32(11), 795-807. DOI: 10.9755/ejfa.2020.V32.i11.2190.
- Benkhniq, O., Zidane, L., Fadli, M., Elyacoubi, H., Rochdi, A., & Douira, A. (2010). Etude ethnobotanique des plantes médicinales dans la région de Mechraâ Bel Ksirri (Région du Gharb du Maroc). *Acta Botanica Barcinonensia*, 53, 191-216.
- Benlamdini, N., Elhafian, M., Rochdi, A., & Zidane, L. (2014). Etude floristique et ethnobotanique de la flore médicinale du Haut Atlas oriental (*Haute Moulouya*). *Journal of applied biosciences*, 78, 6771-6787. DOI: 10.4314/jab.v78i0.17.
- Benrahou, K., El Guourami, O., Mrabti, H. N., Cherrah, Y., & Faouzi, M. E. A. (2022). Investigation of antioxidant, hypoglycemic and anti-obesity effects of *Euphorbia Resinifera* L. *Journal of Pharmacopuncture*, 25(3), 242. DOI: 10.3831/KPI.2022.25.3.242.
- Bentabet, N., Rajaa, R., & Sakina, N. (2022). Enquête ethnobotanique et inventaire des plantes médicinales utilisées dans le traitement des maladies dermatologiques dans la ville d'Ain Temouchent. *Journal of Applied Biosciences*, 170(1), 17704-17719.
- Bounoua, A., & Djoudi, Y. (2022). *Etude ethnobotanique, phytochimique et activités biologiques de l'extrait méthanolique d'une plante médicinale* (Master dissertation).
- Boutoub, O., El-Guendouz, S., Estevinho, L. M., Paula, V. B., et al. (2020). Antioxidant activity and enzyme inhibitory potential of *Euphorbia resinifera* and *E. officinarum* honeys from Morocco and plant aqueous extracts. *Environmental Science and Pollution Research*, 28, 503-517. DOI: 10.1007/s11356-020-10489-6.
- Bouزيد, A., Chadli, R., & Bouزيد, K. (2017). Étude ethnobotanique de la plante médicinale *Arbutus unedo* L. dans la région de Sidi Bel Abbés en Algérie occidentale. *Phytothérapie*, 15(6), 373-378. DOI : 10.1007/s10298-016-1027-6.
- Chaachouay, N., Benkhniq, O., & Zidane, L. (2022). Ethnobotanical and Ethnomedicinal study of medicinal and aromatic plants used against dermatological diseases by the people of Rif, Morocco. *Journal of Herbal Medicine*, 32, 100542. DOI : <https://doi.org/10.1016/j.hermed.2022.100542>.
- Chaachouay, N., Belhaj, S., El Khomsi, M., Benkhniq, O., & Zidane, L. (2023). Herbal remedies used to treat digestive system ailments by indigenous communities in the Rif region of northern Morocco. *Vegetos*, 1-18. DOI: <https://doi.org/10.1007/s42535-023-00606-4>.
- Direction Régionale de Beni Mellal-Khenifra. (2019). Monographie Régionale sur le secteur de l'Habitat et de la Politique de la ville au niveau de la Région de Beni Mellal-Khenifra. Pp. 87.
- El Azzouzi, F., Asserar, N., Zaouai, F., Benkhniq, O., Hachi, M., & Zidane, L. (2018). Ethnomedicinal evaluation of medicinal plants used against gastrointestinal disorders in the western middle atlas region (Morocco). *Annual Research & Review in Biology*, 1-11. DOI: 10.9734/ARRB/2018/43599.
- El Hafian, M., Benlandini, N., Elyacoubi, H., Zidane, L., & Rochdi, A. (2014). Etude floristique et ethnobotanique des plantes médicinales utilisées au niveau de la préfecture d'Agadir-Ida-

- Outanane (Maroc). *Journal of Applied Biosciences*, 81(2014), 7198-7213.
- El Hilah, F., Ben Akka, F., Dahmani, J., Belahbib, N., et al. (2015). Etude ethnobotanique des plantes médicinales utilisées dans le traitement des infections du système respiratoire dans le plateau central marocain. *Journal of Animal & Plant Sciences*, 25(2), 3886-3897.
- Erarslan, Z. B., Ecevit-Genç, G., & Kültür, Ş. (2020). Medicinal plants traditionally used to treat skin diseases in Turkey—eczema, psoriasis, vitiligo. *Journal of Faculty of Pharmacy of Ankara University*, 44(1), 137-166. DOI: <https://doi.org/10.33483/jfpau.586114>.
- Etienne, O. K., Dabé, D. O. G. A., Bernadine, O. B. A. M., & Noël, Z. G. (2021). Plantes médicinales utilisées dans le traitement des maladies microbiennes dans la région du hambol, nord de la Côte d'Ivoire. *Journal of Animal & Plant Sciences*, 47(1), 8412-8425. DOI: <https://doi.org/10.35759/JAnmPLSci.v47-1.6>.
- Falana, M. B., Nurudeen, Q. O., Salimon, S. S., & Abubakar, I. B. (2023). Ethnopharmacological Survey of Medicinal Plants Used in the Management of Skin-Related Conditions in Ilorin, North-Central, Nigeria. *Traditional and Integrative Medicine*, 8(1), 56-76. DOI: <https://doi.org/10.18502/tim.v8i1.12404>.
- Fennane, M., Tattou, M. I., Mathez, J., Ouyahya, A., et al. (1999). Flore pratique du Maroc: manuel de détermination des plantes vasculaires. Volume 1: Pteridophyta, *Gymnospermae*, *Angiospermae* (*Lauraceae-Neuradaceae*). Travaux de l'Institut Scientifique, série botanique, 36, Rabat, pp. 588.
- Fennane, M., Ibn Tattou, M., Outahya, A., & El Oualidi, J. (2007). Flore pratique du Maroc, manuel de détermination des plantes vasculaires. Volume 2: Angiosperme (*Leguminosae-Lentibulariaceae*). Travaux de l'Institut Scientifique, série botanique, 36, Rabat, pp. 636.
- Fennane, M., Ibn Tattou, M., & El Oualidi, J. (2014). Flore pratique du Maroc, Manuel de détermination des plantes vasculaires. Volume 3: (*Leguminosae-Lentibulariaceae*). Travaux de l'Institut Scientifique, série botanique, N°40, Rabat, 794p.
- Fennane, M., & Rejdali, M. (2018). Moroccan vascular plant Red Data Book: A basic tool for plant conservation. *Flora Mediterranea*, 28(1), 339-350. DOI: [10.7320/FIMedit28.339](https://doi.org/10.7320/FIMedit28.339).
- Gomez-Beloz, A. (2002). Plant use knowledge of the Winikina Warao: the case for questionnaires in ethnobotany. *Economic Botany*, 56(3), 231-241.
- Grenez, E. P. (2019). Phytothérapie-exemples de pathologies courantes à l'officine: Fatigue, Insomnie, Stress, Constipation, Rhume, Douleur et Inflammation. Mémoire de diplôme de docteur en pharmacie. Université de Lille Faculté de Pharmacie de Lille.
- Haut-Commissariat au plan. (2017). Monographie Régionale Beni Mellal-Khenifra, pp. 221.
- Heinrich, M., Ankli, A., Frei, B., Weimann, C., & Sticher, O. (1998). Medicinal plants in Mexico: Healers' consensus and cultural importance. *Social Science & Medicine*, 47(11), 1859-1871.
- Hmamouchi, M. (2001). Les plantes médicinales et aromatiques marocaines. 2^{ème} Edition. Impri Fédala (Mohammadia), pp. 108-109.
- Hmidouche, O., Bouftini, K., Chafik, A., Khouri, S., Rchid, H., Rahimi, A., et al. (2023). Ethnomedicinal Use, Phytochemistry, Pharmacology, and Toxicology of *Euphorbia resinifera* O. Berg.(B): A Review. *Journal of Zoological and Botanical Gardens*, 4(2), 364-395. DOI: <https://doi.org/10.3390/jzbg4020029>.
- Idm'hand, E., Msanda, F., & Cherifi, K. (2023). Medicinal plants used for gastrointestinal disorders in Morocco. *Ethnobotany Research and Applications*, 26(1), 1-29. DOI: <http://dx.doi.org/10.32859/era.26.70.1-29>
- Khenissi, I., & Rouabhia, C. (2021). Etude ethnobotanique des plantes médicinales dans quelques communes de Tébessa (Master dissertation, Université Laarbi Tebessi Tebessa).
- Lahsissene, H., Kahouadji, A., & Hseini, S. (2009). Catalogue des plantes médicinales utilisées dans la région de Zaër (Maroc Occidental). *Lejeunia*, revue de botanique.
- Lin, J., Puckree, T., & Mvelase, T. P. (2002). Anti-diarrheal evaluation of some medicinal plants used by Zulu traditional healers. *Journal of Ethnopharmacology*, 79(1), 53-56. DOI: [10.1016/s0378-8741\(01\)00353-1](https://doi.org/10.1016/s0378-8741(01)00353-1).
- Makgobole, M. U., Mpfana, N., & Ajao, A. A. N. (2023). Medicinal Plants for Dermatological Diseases: Ethnopharmacological Significance of Botanicals from West Africa in Skin Care. *Cosmetics*, 10(6), 167. DOI: <https://doi.org/10.3390/cosmetics10060167>
- Malik, K., Ahmad, M., Zafar, M., Ullah, R., et al. (2019). An ethnobotanical study of medicinal plants used to treat skin diseases in northern Pakistan. *BMC Complementary and Alternative Medicine*, 19(1), 1-38. DOI: <https://doi.org/10.1186/s12906-019-2605-6>.
- Moujanni, A., Partida, L., Essamadi, A. K., Hernanz, D., et al. (2017). Physicochemical characterization of unique unifloral honey: *Euphorbia resinifera*. *CyTA-Journal of Food*, 16(1), 27-35. DOI: [10.1080/19476337.2017.1333529](https://doi.org/10.1080/19476337.2017.1333529).

- Nasab, F. K., Zare, M., Mehrabian, A., & Ghotbi-Ravandi, A. A. (2022). Ethnopharmacological survey of medicinal plants used to treat skin diseases among herbal shops in Jahrom, Iran. *Collectanea Botanica*, *41*, e001. DOI : 10.3989/collectbot.2022.v41.001.
- Orion, E., & Wolf, R. (2014). Psychologic consequences of facial dermatoses. *Clinics in Dermatology*, *32*(6) :767-71. DOI: <https://doi.org/10.1016/j.clindermatol.2014.02.016>.
- Ourhzif, E. M., Ricelli, A., Stagni, V., Cirigliano, A., Rinaldi, T., et al. (2022). Antifungal and Cytotoxic Activity of Diterpenes and Bisnorses quiterpenoides from the Latex of *Euphorbia resinifera* Berg. *Molecules*, *27*(16), 5234. DOI: <https://doi.org/10.3390/molecules27165234>.
- Saising, J., Maneenoon, K., Sakulkeo, O., Limsuwan, S., et al. (2022). Ethnomedicinal Plants in Herbal Remedies Used for Treatment of Skin Diseases by Traditional Healers in Songkhla Province, Thailand. *Plants*, *11*(7), 880. DOI: 10.3390/plants11070880.
- Salhi, S., Fadli, M., Zidane, L., & Douira, A. (2010). Floristic and ethnobotanical study of medicinal plants of Kénitra (Maroc). *Lazaroa*, *31*(1), 133-146.
- Sasi Priya, S. (2020). Maeruaoblongifolia—What do we really know? Overview, Progress and Perspectives. *Journal of Peer Scientist*, *2*(1), e1000012.
- Spichiger, R. E., Savolainen, V. V., Figeat, M., & Jeanmonod, D. (2002). Botanique systématique des plantes à fleurs. Presses Polytechniques et Universitaires Romandes. Francia.
- Stambouli, O. B. (2018). La maladie dermatophytique : Une affection immunogénétique. *Revue Française d' Allergologie*, *58*(3), 254.
- Sreekeesoon, D. P., & Mahomoodally, M. F. (2014). Ethnopharmacological analysis of medicinal plants and animals used in the treatment and management of pain in Mauritius. *Journal of Ethnopharmacology*, *157*, 181-200. DOI: 10.1016/j.jep.2014.09.030.
- Taïbi, A. N., El Khalki, Y., & El Hannani, M. (2015). Atlas régional de la région du Tadla-Azilal. Maroc, Université d'Angers (France) et Université du Sultan Moulay Slimane Béni Mellal.
- Talbauoui, A., El Hamdaoui, L., Bouyahya, A., El Moussaouiti, M., et al. (2020). Chemical composition, in vitro cytotoxic, and antibacterial activities of Moroccan medicinal plants *Euphorbia resinifera* and *Marrubium vulgare*. *Biointerface Research in Applied Chemistry*, *10*(6), 7343-7355. DOI: 10.33263/BARIAC106.73437355.
- Tardío, J., & Pardo-de-Santayana, M. (2008). Cultural importance indices: a comparative analysis based on the useful wild plants of Southern Cantabria (Northern Spain). *Economic Botany*, *62*, 24-39. DOI : 10.1007/s12231-007-9004-5.
- Tsioutsiou, E. E., Amountzias, V., Vontzalidou, A., Dina, E., Stevanović, Z. D., Cheilari, A., & Aligiannis, N. (2022). Medicinal Plants Used Traditionally for Skin Related Problems in the South Balkan and East Mediterranean Region—A Review. *Frontiers in Pharmacology*, *13*, 936047. DOI: <https://doi.org/10.3389/fphar.2022.936047>.
- Vitalini, S., Iriti, M., Puricelli, C., Ciuchi, D., et al. (2013). Traditional knowledge on medicinal and food plants used in Val San Giacomo (Sondrio, Italy)—An alpine ethnobotanical study. *Journal of Ethnopharmacology*, *145*(2), 517-529. DOI : 10.1016/j.jep.2012.11.024.
- World Health Organization. (2019). WHO global report on traditional and complementary medicine.
- Yetein, M. H., Houessou, L. G., Lougbégnon, T. O., Teka, O., et al. (2013). Ethnobotanical study of medicinal plants used for the treatment of malaria in plateau of Allada, Benin (West Africa). *Journal of Ethnopharmacology*, *146*(1), 154-163. DOI: <https://doi.org/10.1016/j.jep.2012.12.022>.



Journal of Experimental Biology and Agricultural Sciences

<http://www.jebas.org>

ISSN No. 2320 – 8694

Effects of Elicitation on *Invitro* Regeneration of two Tomato (*Solanum lycopersicum* L.) Cultivars in Tissue Culture

Alhagie K. Cham^{1,3*}, Ma del Carmen Ojeda Zacarías^{1*}, Héctor Lozoya Saldaña², Rigoberto E. Vázquez Alvarado¹, Emilio Olivares Sáenz¹, Omar Guadalupe Alvarado Gómez¹

¹Autonomous University of Nuevo León, Faculty of Agronomy, Street Francisco Villa S/N, Col. Ex Hacienda El Canada, Gral. Escobedo, Nuevo León. P.C. 66054. Mexico

²Autonomous University of Chapingo, Phytotechnics Department, Mexico-Texcoco highway Km 38.5, 56230 Chapingo, P.C 56230. Mexico

³Department of Entomology and Plant Pathology, University of Tennessee, Knoxville, TN, USA

Received – July 21, 2023; Revision – January 10, 2024; Accepted – January 31, 2024

Available Online – March 15, 2024

DOI: [http://dx.doi.org/10.18006/2024.12\(1\).106.123](http://dx.doi.org/10.18006/2024.12(1).106.123)

KEYWORDS

Concentration

Explant

Growth

Propagation

Tissue culture

ABSTRACT

Exploring alternative avenues, *in vitro* culture emerges as a promising option for potential bioactive compound sources. However, compared to intact plants, only a few cultures demonstrate efficient synthesis of secondary metabolites. Elicitors have gained prominence as stress agents for enhancing *in vitro* micropropagation in specific tissues, organs, and cells. Recent advancements in plant tissue culture involve elicitors, opening new possibilities for *in vitro* production of crucial food crops. This research aimed to investigate the impact of three elicitors (Activane®, Micobiol®, and Stemicol®) on germination and *in vitro* multiplication of two tomato cultivars explants, employing both direct and indirect *in vitro* organogenesis. Among the tested elicitors, Micobiol® emerged as a successful elicitor, promoting optimal seed germination, survival, and 100% growth compared to the 80% in the control group. Further, Activane® exhibited a favourable induction response and achieved 96%, 95%, and 100% in weight and diameter of callus, yet various elicitor concentrations did not exert significant influence across treatments. In conclusion, an effective disinfection and *in vitro* implantation of tomato seeds ensured successful germination, promoting seedling survival and growth. Various elicitors positively impacted *in vitro* organogenesis, particularly in root induction, with higher survival percentages in acclimatized plants. The study guides future research on elicitor treatments for large-scale tomato *in vitro* propagation, emphasizing the need to identify optimal elicitor concentrations.

* Corresponding author

E-mail: chamalhagiek@gmail.com (Alhagie K. Cham)

Peer review under responsibility of Journal of Experimental Biology and Agricultural Sciences.

Production and Hosting by Horizon Publisher India [HPI]
(<http://www.horizonpublisherindia.in/>).
All rights reserved.

All the articles published by [Journal of Experimental Biology and Agricultural Sciences](#) are licensed under a [Creative Commons Attribution-NonCommercial 4.0 International License](#) Based on a work at www.jebas.org.



1 Introduction

Tomato (*Solanum lycopersicum* L.) stands out as a vital perennial crop within the Solanaceae family, holding immense economic and cultural significance globally. Renowned for its nutritional value, it serves as a crucial source of vitamin C, essential minerals like phosphorus and potassium, and carotenoids such as lycopene and β -carotene (SIAP 2020; Aldubai et al. 2022; Liu et al. 2022). Leading tomato-producing nations include China, the United States, India, Turkey, Egypt, Italy, Iran, Spain, Brazil, Mexico, Uzbekistan, and Russia (Peralta and Spooner 2006). In Mexico, the cultivation of tomatoes spans 43,903 hectares, yielding 63,116 tonnes/ha, distributed across various regions. Noteworthy production zones encompass the Northwest (Sinaloa, Sonora, and Baja California), the Pacific coast (Nayarit, Jalisco, Michoacán, Guerrero, and Oaxaca), the Central North Zone (San Luis Potosí and Coahuila), and Las Huastecas (Tamaulipas, Veracruz, San Luis Potosí, and Hidalgo), contributing significantly to meet domestic market demands throughout the year. While traditional open-field and greenhouse cultivation historically dominated tomato production in Mexico, recent trends indicate a growing adoption of innovative farming technologies by Mexican tomato growers (SIAP 2020; Aznar-Sánchez et al. 2020; Maureira et al. 2022).

Today, the genetic transformation of tomatoes requires an efficient micropropagation and regeneration *in vitro* system. Thus, biotechnological methods have played a pivotal role in facilitating the propagation of commercially significant fruit species. These methods enable the selection of elite plant material, mitigate phytosanitary issues, and require minimal space while independent of traditional agricultural inputs (Hussain et al. 2012; Hasnain et al. 2022). Plant tissue culture has emerged as a promising alternative for the sustainable production of various plant species affected by environmental or geographical constraints. Successful application of plant tissue culture relies on establishing efficient culture systems that address key challenges encountered by plants *in vitro*. Direct organogenesis has been widely adopted, a method allowing the regeneration of complete seedlings from plant tissues without dedifferentiation stages like callus or somatic embryo formation. Inducers and elicitors have been employed in this approach to enhance the production of numerous plant species (Hussain et al. 2012; Baenas et al. 2014; Al-Khayri and Naik, 2020; Xu et al., 2023). *In vitro* plant cultures present an appealing and economically viable alternative to traditional methods for producing agriculturally important crops. Notably, they offer the only sustainable and ecological system for obtaining complex chemical structures biosynthesized by rare or endangered plant species resistant to domestication. The *in-vitro* propagation of tomato crops is influenced by various biotic and abiotic conditions (Ramirez-Estrada et al. 2016; Munim et al. 2019).

Moreover, the regeneration of plants through tissue culture techniques is a crucial aspect of biotechnological research and the genetic manipulation of plants. Cultures are meticulously maintained in aseptic environments to ensure the production of disease-free plants and are also free from the risk of reinfection. Achieving high-frequency plant regeneration from *in-vitro* tissue culture is essential for successfully applying tissue culture techniques in crop improvement. Inducing direct organogenesis in tomato plants is a valuable alternative for the clonal propagation of disease-free plants and is particularly useful for genetic transformation. Therefore, there is an urgent need for technological and biotechnological interventions to enhance the *in vitro* regeneration of tomato plants (Karim and Kayum 2007; Holmes et al. 2021; Ozyigit et al. 2023).

While regeneration systems for different tomato varieties, organogenesis has been widely documented using various explants such as hypocotyls, leaves, or cotyledons. Evidence of achieving higher *in-vitro* regeneration using elicitors in tomatoes is limited. Numerous elicitors have been studied for their response in *in-vitro* germination, micropropagation, growth, and crop production in various crops including *S. lycopersicum* (García-Osuna et al. 2015; Murillo-Gómez et al. 2017; Cham et al. 2021; Cham et al. 2022), *Stevia rebaudiana* (Bayraktar et al. 2016), and *Hypericum perforatum* in shoot cultures (Gadzovska et al. 2014). Elicitors are actively being explored as a biotechnological strategy in studying processes related to plant material production, as they enable the rapid generation of healthy crops that can be propagated on a large scale to meet commercial demand. Hence, the objective of this research was to assess the impact of three elicitors (Activane[®], Micobiol[®], and Stemicol[®]) on the germination and multiplication of *in vitro* explants from two tomato cultivars through both direct and indirect *in vitro* organogenesis.

2 Materials and Methods

2.1 Plant Material and Growth Conditions

The plant materials utilized for the two tomato cultivars were "Semilla Hortaflor Jitomate Bola" and "Semilla Hortaflor Jitomate Saladete." In the case of seeds, they were disinfected using a solution of Sodium Hypochlorite (NaOCl) at concentrations of 15% (v/v Cloralex[®]). Explants from *in vitro* plants did not undergo disinfection, as they originated from aseptic plants. The leaf and petiole explants were sourced from *in vitro* plants of the selected two tomato cultivars. All experiments were conducted during the summer-spring period of 2020-2021 at the Laboratory of Tissue Culture (LCT) within the Faculty of Agronomy at the Autonomous University of Nuevo León (UANL). The laboratory is situated at the Campus of Agricultural Sciences in the municipality of Gral. Escobedo, NL, Mexico.

Table 1 Evaluated treatments with different concentrations of elicitors for the experiments *in vitro*

Treatment	Elicitor	Doses
T1(Cntl)	Control	0.00
T2(Act*)	Activane®	0.20, 0.40, 0.60 mL L ⁻¹
T3(Micb1*)	Micobiol®	0.20, 0.40, 0.60 mL L ⁻¹
T4(Stml*)	Stemicol®	0.20, 0.40, 0.60 mL L ⁻¹

2.2 Preparation of Elicitors

Three elicitors (Activane®, Micobiol®, and Stemicol®) were individually dissolved in 25 mL of distilled water across three required concentrations (0.2, 0.4, & 0.6 mL L⁻¹). Prior to this, stock solutions of Activane®, Micobiol®, and Stemicol® were incorporated into the media (MS) at the desired concentrations after autoclaving at 121°C for 15 minutes. In the current study, the elicitors (Activane®, Micobiol®, and Stemicol®) at three distinct concentrations (0.2, 0.4, & 0.6 mL L⁻¹) were individually added to the media (MS) as elicitors (Table 1).

2.3 Preparation of Culture Medium

The culture medium employed consisted of the fundamental salts of the Murashige-Skoog 1962 (MS) medium, supplemented with 30g L⁻¹ sucrose and 4.4g L⁻¹ phytigel. The pH was adjusted to 5.8 using NaOH and 1N HCl. This medium was dispensed into Magenta® boxes measuring 7 x 9 cm, each containing 30 mL medium. Subsequently, the boxes were sterilized in an autoclave at 121°C under 15 pounds of pressure for 15 minutes.

2.4 Evaluation of Sterilization Treatments

The plant materials, specifically tomato seeds, underwent surface sterilization through a multi-step process. Initially, they were immersed in 70% ethanol for 60 seconds, followed by three washes with sterile distilled water. Subsequently, the seeds were placed in a solution of Sodium Hypochlorite (NaOCl) at concentrations of 15% and 20% (v/v Cloralex®), supplemented with 0.02% Tween 20, for 15 minutes. This sterilization process was reiterated for thorough disinfection. Following the treatment, the seeds were washed thrice with sterile distilled water, following the protocol outlined by Espinosa (2005).

The sterilized tomato seeds were then introduced into the culture medium (MS) with doses of Sodium Hypochlorite (NaOCl) at 15% and 20% (v/v Cloralex®), with ten repetitions for each treatment. The experimental units were arranged under a photoperiod of 16 hours of light and eight hours of darkness at a temperature of 24 ± 2 °C. The experimental design employed was a completely randomized design with a factorial arrangement (2 X 2), incorporating ten repetitions for each factor: (a) cultivar and (b) doses of the sterilizing agent. Data collection occurred every three

days over a month, focusing on evaluating the percentage of germination, contamination, and oxidation at this stage.

2.5 Evaluation of *In Vitro* Seed Germination and Growth

The materials utilized comprised tomato seeds from the two cultivars, namely "Bola and Saladette". The seeds underwent a disinfection process described earlier to eliminate surface contaminants, conducted under a laminar flow hood. Subsequently, the tomato seeds were introduced into the culture medium (MS) with four treatments (Control, Activane®, Micobiol®, and Stemicol®) at three different doses, with 15 repetitions per treatment. After sowing, the experimental units were maintained under photoperiod conditions of 16 hours of light and eight hours of darkness at a temperature of 24 ± 2 °C. The experimental design employed was a completely randomized design with a factorial arrangement (2 x 3 x 3) incorporating fifteen repetitions, considering factor (a) cultivars, factor (b) elicitors, and factor (c) doses of elicitors. Finally, data collection occurred every three days over 8 weeks. At this stage, the evaluation encompassed parameters such as the percentage of germination, oxidation, viability, number of leaves, and plant height.

2.6 Preparation of Explants for *in-vitro* culture

The explants employed in the study were segments of nodes measuring 1.5 to 2.0 cm in length, sourced from both branches and leaves of the mother plants belonging to the tomato cultivars. These mother plants were previously propagated and housed in transparent glass bottles approximately 15-20 cm in length. The propagated plants were incubated at the Laboratory of Tissue Culture (LCT) for 21 days. Under controlled conditions, with a photoperiod of 16 hours of light and eight hours of darkness and at a temperature of 24 ± 2 °C, the explants were allowed to acclimate before being utilized in the experiments (Figure 1).

2.7 Direct and Indirect *in-vitro* Organogenesis or Callogenesis (callus formation)

Two-week-old seedlings (derived from the previous stage) measuring 2.0 cm in height were utilized for the subsequent stage of the experiment. These seedlings were established in a medium (DM) consisting of basic salts, vitamins, 100 mg L⁻¹ of myo-inositol, and three concentrations of each elicitor: Activane®

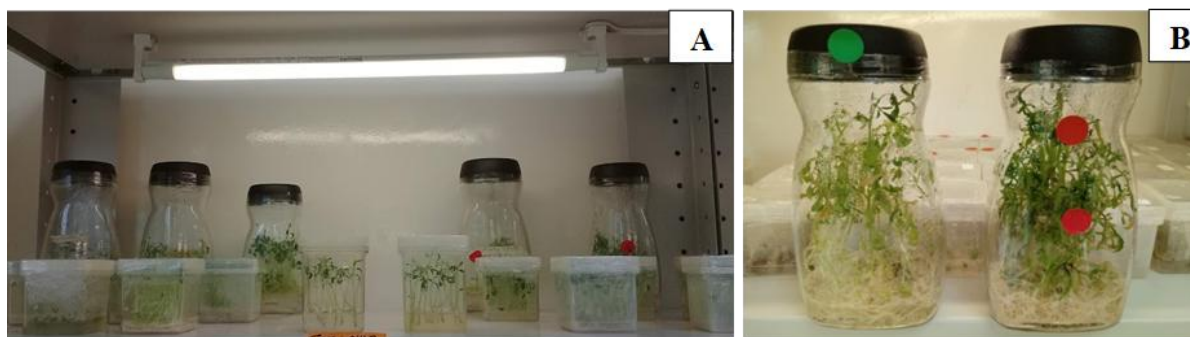


Figure 1 The mother plants used as explants for the *in vitro* culture; the explants consist of segments of 1.5 to 2.0 cm in length from branches and leaves of the two tomato cultivars (B) Saladette (Green tag) and Bola (Red tag).

(0.2, 0.4, 0.6 mL L⁻¹), Micobiol® (0.2, 0.4, 0.6 mL L⁻¹), and Stemicol® (0.2, 0.4, 0.6 mL L⁻¹). The medium also included 30 g L⁻¹ of sucrose and 4.3 g L⁻¹ of phytigel, and four explants were placed per experimental unit. The experiment followed a completely randomized design with a factorial arrangement of (2 x 3 x 3) and incorporated five repetitions for each treatment. The experimental units were subjected to controlled conditions of photoperiod and temperature, comprising 16 hours of light (54 μmol m⁻² s⁻¹) and 8 hours of darkness at 24 ± 2 °C. After three months, the following variables were assessed for direct organogenesis: asepsis percentage, growth, oxidation, viability, and the number of leaves. For indirect organogenesis, the flasks were incubated in the dark, and the assessment included asepsis percentage, induction, oxidation, viability, days to first callus formation, callus diameter, and weight.

2.8 Root Induction

In the subsequent phase, regenerated shoots from the previous stage were isolated and transplanted into a new medium containing Murashige-Skoog 1962 (MS) medium. This medium was supplemented with various concentrations of IBA (0 or 1.5 mg L⁻¹), NAA (0, 0.5, 1, or 1.5 mg L⁻¹), putrescine (160 mg L⁻¹), and/or AgNO₃ (2, 4, or 6 mg L⁻¹). Additionally, three concentrations of each elicitor were added: Activane® (0.2, 0.4, 0.6 mL L⁻¹), Micobiol® (0.2, 0.4, 0.6 mL L⁻¹), and Stemicol® (0.2, 0.4, 0.6 mL L⁻¹) to induce root development. The experimental units were subjected to controlled photoperiod and temperature conditions, involving 16 hours of light (54 μmol m⁻² S⁻¹) and 8 hours of darkness at 24 ± 2 °C. After six weeks, rooting indices were recorded for each treatment, including rooting percentage, root number, and root length. The data recorded encompassed the root initiation response (%), root length (cm), and the number of roots per shoot.

2.9 Acclimatization

The best-rooted plantlets from each treatment were selected and acclimatized in pots containing a mixture of peat moss and

vermiculite (1:1 v/v). The agar was thoroughly washed off with distilled water before transplanting. The pots were covered with clear plastic bags with a few holes and were consistently watered to maintain high humidity for three weeks. Subsequently, the hardened plantlets were transferred to a greenhouse set at a day temperature of approximately 25 °C, with a relative humidity of about 85%. Frequent daily watering was continued to keep the soil consistently moist. After 2 weeks in the greenhouse, assessments were made for plant survival, plant height (cm), and the number of leaves.

2.10 Statistical analysis

The data obtained from the aforementioned experiments were subjected to statistical analysis using SPSS STATISTIC software version 21.0, a program designed for Windows. The analysis involved Analysis of Variance (ANOVA), and Tukey means multiple comparisons analysis was performed with a significance level set at P≤0.05.

3 Results and Discussion

3.1 Impact of Various Sterilization Methods on *in-vitro* micropropagation

The aim is to evaluate how various sterilization procedures impact the *in vitro* germination, contamination, and oxidation of tomato seeds. Sterilization treatments using two concentrations i.e., 15% and 20% (v/v) of sodium hypochlorite (bleach) applied for 15 minutes. The results, based on a thirty-day evaluation of two sterilization treatments using a solution of Sodium Hypochlorite (NaOCl) at 15 and 20% (v/v Cloralex®), indicate superior outcomes for the treatment with a 15% NaOCl solution. This observation holds across all evaluated variables for both tomato cultivars in *in-vitro* conditions. However, no significant statistical difference was observed between the two treatments (Figure 2).

Sodium hypochlorite is widely employed as a seed and explant sterilization agent in various plant species, with bleach concentration and exposure varying between species. Sterilization

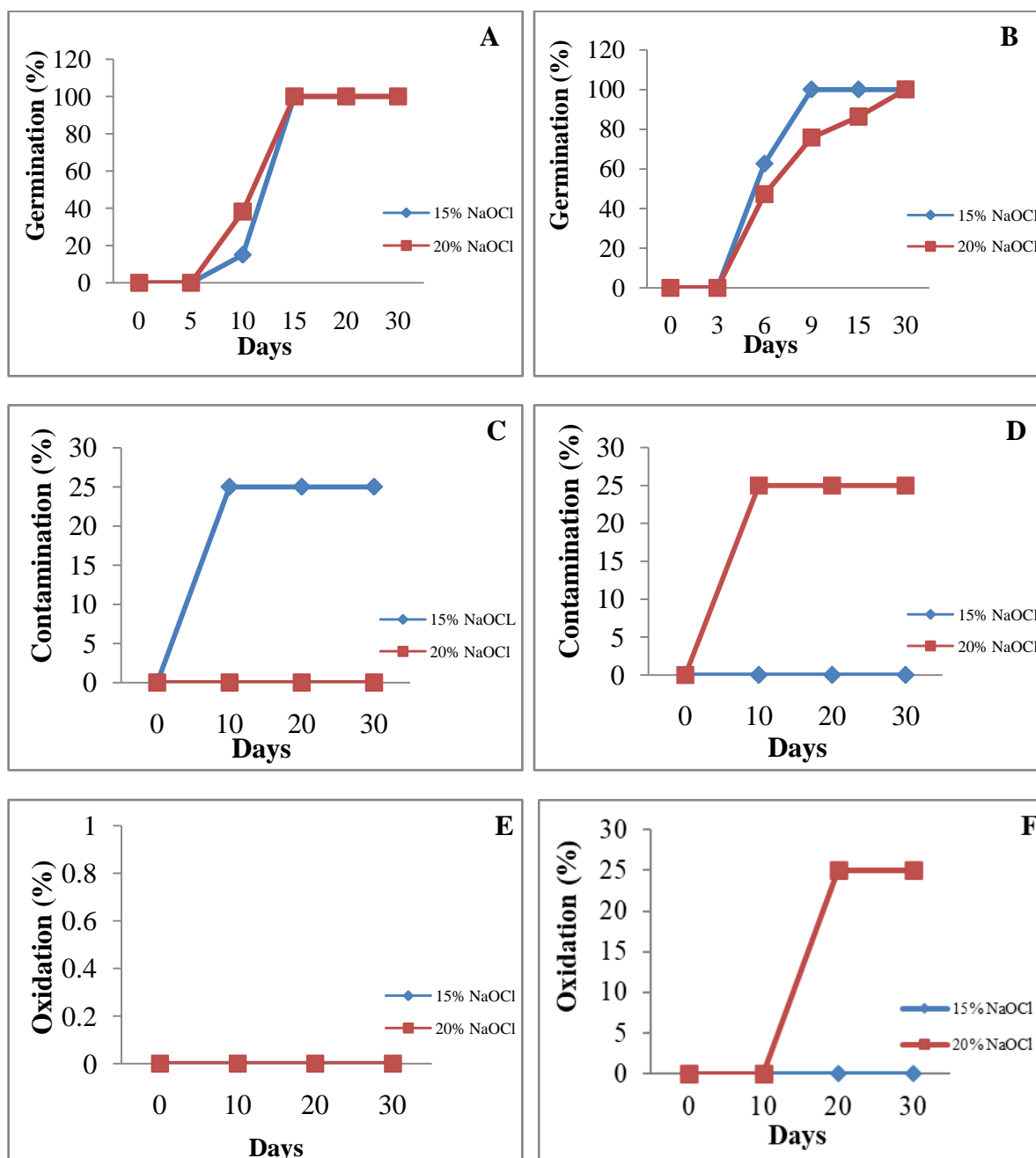


Figure 2 Impact of diverse sterilization methods on germination percentage (A) Saladette experimental materials and (B) Bola experimental materials; (C) contamination in Saladette and (D) contamination in Bola and (E) oxidation of Saladette and (F) oxidation of Bola tomato seeds.

protocols often include a combination of bleach and a 70% ethanol rinse (Espinosa 2005; Barampuram et al. 2014; Calaña-Janeiro et al. 2019). In this study, combined protocols were applied to sterilize seeds of two tomato cultivars using different bleach treatments. The highest germination rates, 80% and 65%, were achieved with Sodium Hypochlorite (NaOCl) concentrations of 15% and 20% (v/v Cloralex[®]), respectively.

The Saladette cultivar achieved a 75% contamination-free rate with NaOCl at 15%, while the Bola cultivar attained a 75% contamination-free rate with NaOCl at 20%. Additionally, oxidation-free seeds were obtained from the Saladette cultivar, while only 25% oxidation was observed in the treatment with NaOCl at 20% for the Bola cultivar. Across all evaluated variables, NaOCl at 15% proved the most efficient, providing good results

for tomato seeds. This concentration induced greater responses for both cultivars at the experiment's conclusion, aligning with Espinosa's findings (2005).

It is noteworthy that the study's results highlight sodium hypochlorite's efficacy at 15% for surface sterilization of contaminated tomato seeds and promoting their germination. These findings are consistent with prior studies, such as using sodium hypochlorite for surface sterilization of cotton seeds in *in vitro* culture (Barampuram et al. 2014).

3.2 Effect of Elicitors on *in vitro* Seed Germination and Shoot growth

In this study, the application of elicitors significantly enhanced shoot growth after 4 weeks of *in vitro* culture. Notably, elicitor-treated plants exhibited the highest shoot length, although the various concentrations did not show a discernible effect on the treatments across the two tomato cultivars (Figure 3).

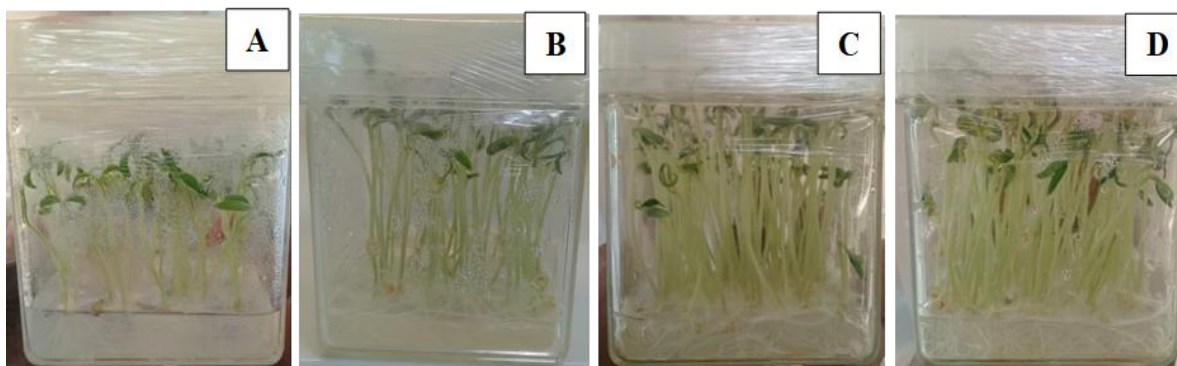
The assessment of *in vitro* seed germination, height, number of leaves, and viability in the Saladette and Bola cultivars revealed a positive impact of various types and concentrations of elicitors on

the studied variables. The statistical analysis conducted under the study conditions indicated significant differences ($P \leq 0.05$) for the number of leaves and height variables in both cultivars. Specifically, the Saladette cultivar exhibited noteworthy variations in the number of leaves and height, with the highest values observed in the T3 treatment (Micobiol®) (Table 2).

While the studied elicitors demonstrated a positive impact on the variables of leaf number, growth, as well as the germination and viability percentages of explants, the varied concentrations of elicitors did not yield a significant effect on the outcomes. The germination percentage of seeds in both tomato cultivars showed a slight influence from the elicitors, increasing explant viability. Simply, the application of elicitors in this study led to substantially higher values in treated plants than those without elicitors.

These findings align with previous reports on *Stevia rebaudiana*, *Physalis peruviana*, *Fagonia indica*, and *Ajuga bracteosa*. In these instances, the *in vitro* use of elicitors, including salicylic acid (SA), chitosan (CHI), and methyl jasmonate (Me-J), had a positive impact on suppressing germination and plant growth in cultured tissues (Bayraktar et al. 2016; Ali et al. 2018; Khan et al. 2018).

Saladette:



Bola:

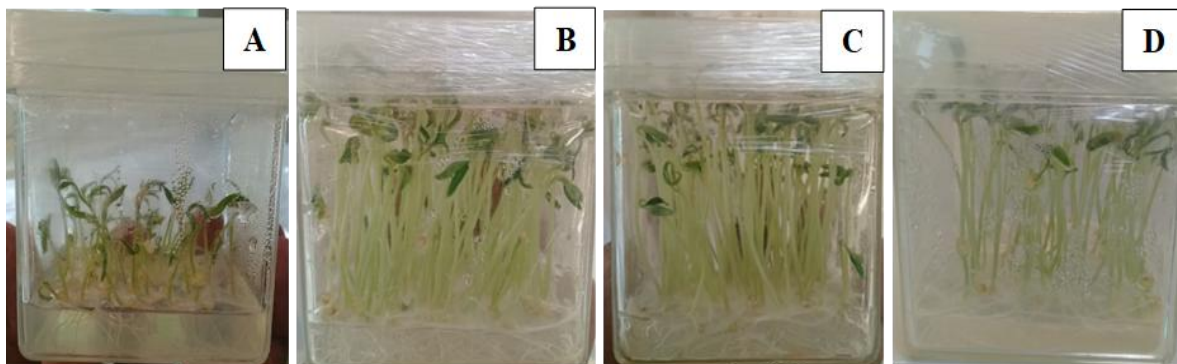


Figure 3 Effect of different types of elicitors on *in vitro* shoot growth and percentage of germination from the seeds of the two tomato cultivars after 4 weeks of culture, the treatments were (A) T₁-Control, (B) T₂-Activane®, (C) T₃-Micobiol® and (D) T₄-Stemicol®.

Table 2 Impact of various types and concentrations of elicitors on the number of leaves, growth, germination percentage, and *in vitro* viability of two cultivars of *S. lycopersicum* L. after an 8-week culture period

Concentration of Elicitors (mL/L ⁻¹)	Number of Leaves	Height (cm)	Germination (%)	Viability (%)
Tomato Saladette:				
Cntl				
D ₀ = 0.00	5.13 ^{ab}	5.67 ^b	80	80
Act [®]				
D ₁ = 0.20	5.33 ^a	7.67 ^a	100	90
D ₂ = 0.40	5.47 ^a	7.57 ^a	80	85
D ₃ = 0.60	5.60 ^a	7.44 ^a	100	100
Micbl [®]				
D ₁ = 0.20	5.60 ^a	7.77 ^a	100	85
D ₂ = 0.40	6.00 ^a	7.47 ^a	100	100
D ₃ = 0.60	6.00 ^a	7.23 ^a	100	100
Stml [®]				
D ₁ = 0.20	6.00 ^a	7.83 ^a	80	100
D ₂ = 0.40	5.60 ^a	7.73 ^a	100	100
D ₃ = 0.60	5.60 ^a	7.50 ^a	100	80
Tomato Bola:				
Cntl				
D ₀ = 0.00	4.23 ^{ab}	4.10 ^b	70	90
Act [®]				
D ₁ = 0.20	5.37 ^a	7.30 ^a	80	88
D ₂ = 0.40	5.10 ^a	6.20 ^{ab}	80	98
D ₃ = 0.60	5.30 ^a	6.93 ^a	80	95
Micbl [®]				
D ₁ = 0.20	5.50 ^a	6.90 ^a	80	100
D ₂ = 0.40	5.63 ^a	7.30 ^a	80	100
D ₃ = 0.60	5.57 ^a	7.30 ^a	80	96
Stml [®]				
D ₁ = 0.20	5.37 ^a	7.23 ^a	100	95
D ₂ = 0.40	4.13 ^b	7.77 ^a	100	90
D ₃ = 0.60	5.43 ^a	6.27 ^{ab}	80	100

Doses one (1) = D₁, Doses two (2) = D₂ and Doses three (3) = D₃, the different letters are significantly different ($P \leq 0.05$) according to Tukey's multiple range test.

3.3 Effect of Elicitors on *in vitro* Direct Organogenesis

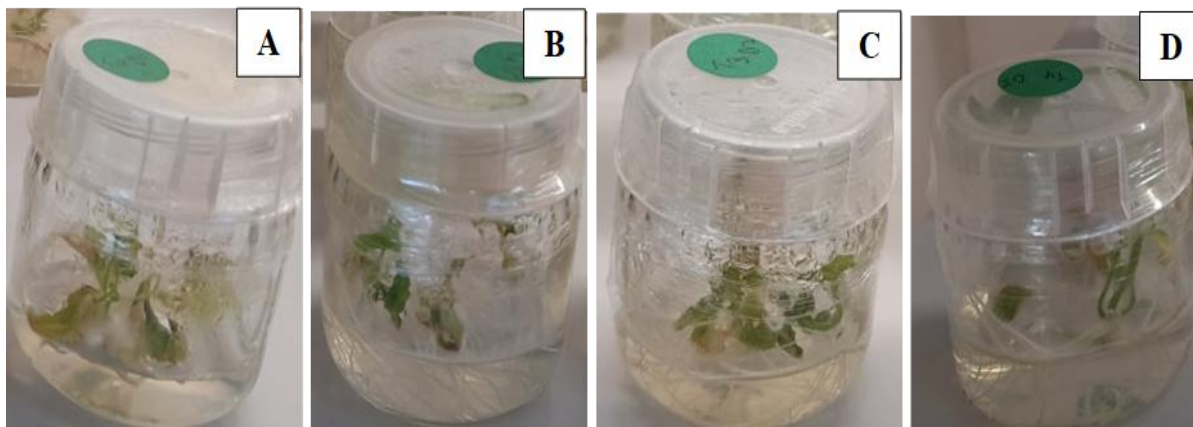
The explants cultivated in the preceding stage displayed uniform growth, exhibiting similar patterns across the two tomato cultivars. The overall health of the explants was notably robust, owing to the optimal environmental conditions maintained during the two-week preparation period. This ensured their suitability for the subsequent developmental stage. Direct and callus induction initiation involved using a medium incorporating elicitation treatments. Following explant induction, direct organogenesis became evident. The elongation of shoots and subsequent leaf development accompanied shoot regeneration. Additionally, leaves exhibited the generation of new shoots originating from the base of the petiole, while stems demonstrated elongation and the emergence of new leaves from the axillary bud (Figure 4).

Following direct organogenesis in the two tomato cultivars, the applied elicitors positively impacted bud growth while concurrently reducing phenolic oxidation. This contributed to the

overall enhancement of explant viability. The findings presented in Table 3 indicate that concerning the number of buds and bud growth variables, no significant effects were observed for the concentration of elicitors or the different types of elicitors individually. However, a noteworthy outcome emerged as the interaction between both variables proved significant ($P \leq 0.05$).

In the case of leaf explants, the comparison of mean tests revealed significant differences ($P \leq 0.05$) in the response of elicitors, with the highest average observed in the treated explants for the variable total growth. Specifically, elicitor T3-Micobiol[®] induced greater responses across all three concentrations (D1=21.45, D2=21.50, and D3=22.50 mL L⁻¹). Interestingly, the three concentrations of the elicitors evaluated did not exhibit any significant differences ($P \leq 0.05$) across all treatments. These results suggest that the application of elicitors not only influences the growth of shoots/buds but also enhances the percentage of oxidation, minimizes contamination, and improves the *in vitro* viability of the explants.

Saladette:



Bola:

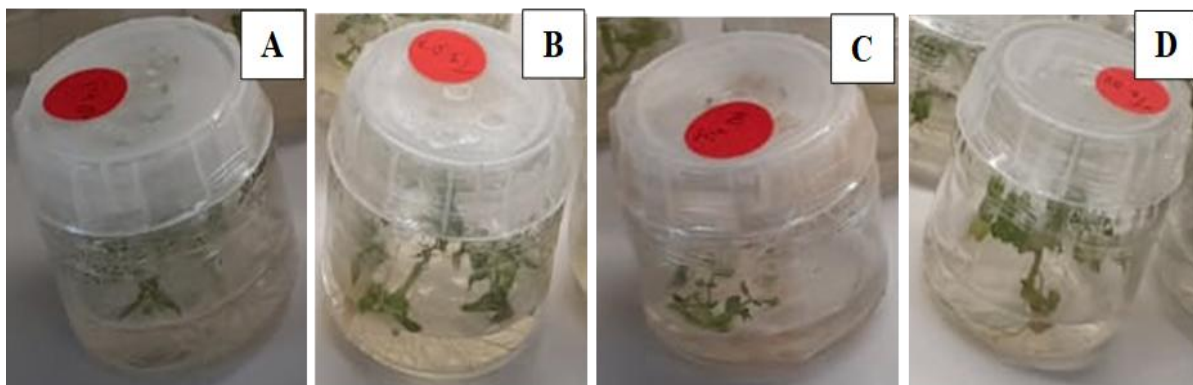


Figure 4 Effect of different types of elicitors on direct *in vitro* shoot organogenesis of the two tomato cultivars after 4 weeks of culture, the treatments were (A) T1-Control, (B) T2-Activane[®], (C) T3-Micobiol[®] and (D) T4-Stemicol[®].

Table 3 Impact of different types and concentrations of elicitors on bud number, growth, oxidation percentage, and *in vitro* viability in two cultivars of *S. lycopersicum* L. over a 12-week culture period

Concentration of Elicitors (mL/L ⁻¹)	Number of Buds	Bud Growth	Length/Total Growth	Viability (%)	Oxidación (%)
Tomato Saladette					
Cntl					
D = 0.00	3.25	5.00	18.50 ^b	83	50
Act [®]					
D ₁ = 0.20	3.00	5.50	16.50 ^c	100	100
D ₂ = 0.40	3.00	6.00	18.50 ^b	89	100
D ₃ = 0.60	3.00	6.00	18.00 ^b	100	100
Micbl [®]					
D ₁ = 0.20	3.00	6.00	18.00 ^b	100	100
D ₂ = 0.40	4.00	5.66	22.32 ^a	100	100
D ₃ = 0.60	3.50	5.83	20.16 ^{ab}	98	100
Stml [®]					
D ₁ = 0.20	4.75	4.62	20.90 ^{ab}	99	100
D ₂ = 0.40	3.50	5.42	18.82 ^b	97	100
D ₃ = 0.60	3.50	5.62	19.87 ^b	100	100
Tomato Bola					
Cntl					
D = 0.00	3.20	4.25	14.12 ^b	100	100
Act [®]					
D ₁ = 0.20	3.50	5.08	17.83 ^{ab}	100	100
D ₂ = 0.40	3.25	5.12	16.50 ^{ab}	100	100
D ₃ = 0.60	3.10	5.37	16.12 ^{ab}	100	100
Micbl [®]					
D ₁ = 0.20	4.00	5.32	21.45 ^a	100	100
D ₂ = 0.40	3.75	5.75	21.50 ^a	100	100
D ₃ = 0.60	3.75	6.00	22.50 ^a	100	100
Stml [®]					
D ₁ = 0.20	3.00	4.62	13.87 ^{ab}	100	100
D ₂ = 0.40	3.25	5.37	17.37 ^{ab}	100	100
D ₃ = 0.60	3.50	5.75	20.00 ^{ab}	100	100

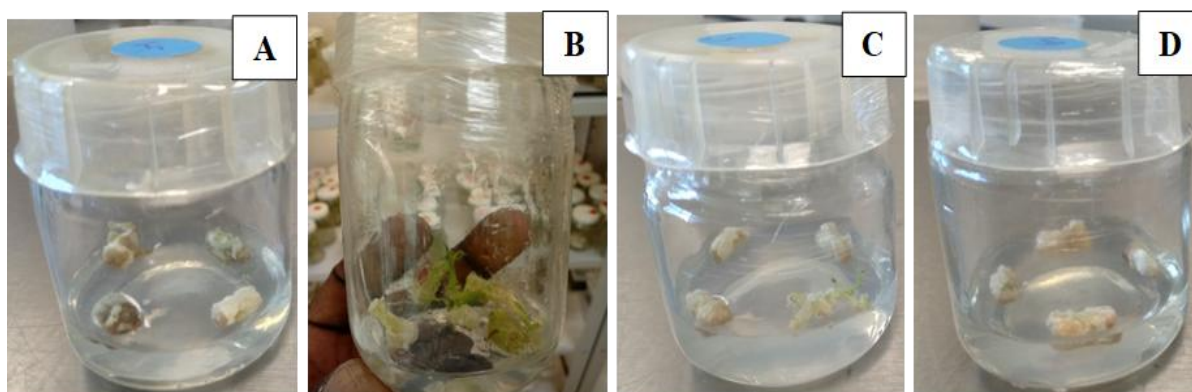
Doses one (1) = D₁, Doses two (2) = D₂ and Doses three (3) = D₃; the different letters are significantly different ($P \leq 0.05$) according to Tukey's multiple range test.

3.4 Effect of Elicitors on *in vitro* Indirect Organogenesis (Callus Formation)

To stimulate *in vitro* indirect organogenesis in two cultivars of *S. lycopersicum*, the impact of three elicitors was assessed concerning callus formation and induction in the explants (Figure 5). In both cultivars, the explants exhibited the highest induction rates in elicitor-treated callus, with values reaching 97% and 95.66% for treatments T2-Activane® and T3-Micobiol®, respectively. Notably, a superior induction rate was observed in T2-Activane®, with no significant differences identified among the various concentrations of the elicitors even 12 weeks after the explant inoculation (Table 4).

The intensity of callus formation and induction in explants changed under the influence of elicitation. Leaf explants from two tomato cultivars were subjected to incubation in MS nutrient medium containing various elicitors concentrations, and the callus formation processes were subsequently assessed. The treatment with T2-Activane® yielded the highest average callus-forming densities (97), closely followed by T3-Micobiol® (95.66). In most elicitor treatments, the first signs of callus were observed by day 6.

Saladette:



Bola:

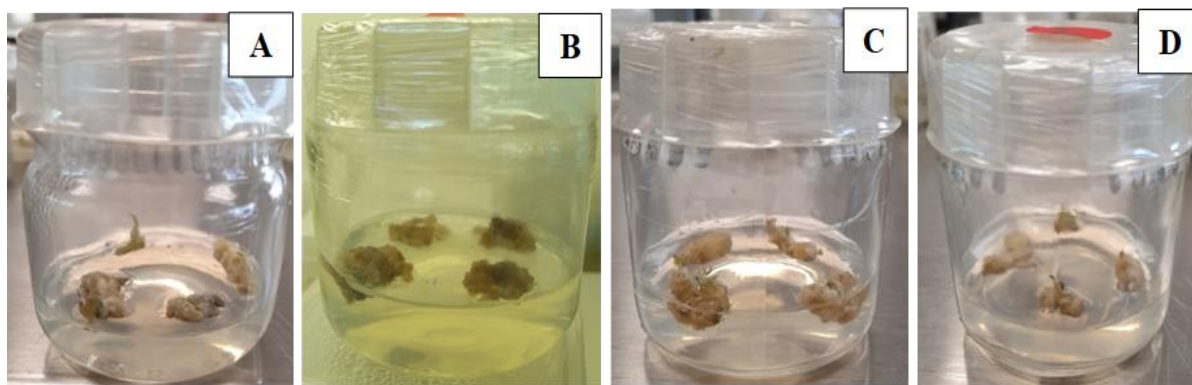


Figure 5 Effect of different types of elicitors on indirect *in vitro* organogenesis on the explants callus formation and induction of the two tomato cultivars after 12 weeks of culture; the treatments were (A) T₁-Control, (B) T₂-Activane®, (C) T₃-Micobiol® and (D) T₄-Stemicol®

Explants in the T1-Control treatment exhibited low-density callus, attributed to a high presence of oxidation and reduced viability. Despite viability being compromised by elevated contamination levels, some explants demonstrated lower averages of callus formation. Earlier studies have shown that employing a two-stage culture system with a combined treatment of mannitol (2mM) and JA (40µM) led to the optimal accumulation of resveratrol in the callus biomass of *Vitis vinifera* (Raluca et al., 2011).

3.5 Root Induction

Root induction and development on regenerated shoots were observed after three weeks into the culture in MS medium supplemented with elicitors (Figure 6). The highest percentage of root initiation responses was observed in explants treated with the elicitors. Our findings also revealed that the highest average root length was observed in treatments T2-Activane® (2.0 cm) and T4-Stemicol® (2.4 cm) for the Saladette cultivar. Similarly, for the Bola cultivar, the highest average root lengths were observed in T2-Activane® (2.2 cm) and T3-Micobiol® (2.3 cm) (Table 5).

Table 4 Impact of varied types and concentrations of elicitors on callus presence, initial callus appearance, callus induction, oxidation, and in vitro viability in two cultivars of *S. lycopersicum* L. over a 12-week culture period

Concentration of Elicitors (mL/L ⁻¹)	First Callus Formation (day)	Callus Weight (gram)	Callus Diameter (mm)	Callus Induction (%)	Viability (%)	Oxidation (%)
Tomato Saladette						
Cntl						
D = 0.00	7	0.4 ^d	2.20 ^e	90 ^b	83	50
Act [®]						
D ₁ = 0.20	7	0.84 ^b	8.30 ^a	96 ^a	100	100
D ₂ = 0.40	6	1.06 ^a	7.20 ^{ab}	95 ^a	89	100
D ₃ = 0.60	7	0.67 ^c	5.10 ^c	100 ^a	100	100
Micbl [®]						
D ₁ = 0.20	6	0.42 ^d	6.35 ^b	97 ^a	100	100
D ₂ = 0.40	6	0.15 ^e	1.60 ^e	90 ^b	100	100
D ₃ = 0.60	6	0.41 ^d	4.35 ^{cd}	100 ^a	98	100
Stml [®]						
D ₁ = 0.20	7	0.21 ^e	3.55 ^d	88 ^b	99	100
D ₂ = 0.40	7	0.54 ^d	4.90 ^c	87 ^c	97	100
D ₃ = 0.60	6	0.20 ^e	2.15 ^e	96 ^a	100	100
Tomato Bola						
Cntl						
D = 0.00	8	0.40 ^e	4.85 ^f	88 ^{bc}	90	80
Act [®]						
D ₁ = 0.20	7	1.00 ^{cd}	9.10 ^{bc}	91 ^b	99	90
D ₂ = 0.40	7	1.07 ^c	7.55 ^{de}	93 ^b	95	95
D ₃ = 0.60	7	1.32 ^b	9.45 ^{abc}	96 ^{ab}	90	100
Micbl [®]						
D ₁ = 0.20	7	0.92 ^d	7.00 ^e	98 ^a	100	100
D ₂ = 0.40	8	1.37 ^b	8.35 ^{cd}	91 ^b	99	95
D ₃ = 0.60	7	0.49 ^e	5.45 ^f	98 ^a	97	100
Stml [®]						
D ₁ = 0.20	8	1.58 ^a	10.7 ^a	90 ^b	100	98
D ₂ = 0.40	7	1.62 ^a	10.2 ^{ab}	95 ^{ab}	95	100
D ₃ = 0.60	6	1.26 ^b	9.85 ^{ab}	94 ^{ab}	99	95

Doses one (1) = D₁, Doses two (2) = D₂ and Doses three (3) = D₃, the different letters are significantly different ($P \leq 0.05$) according to Tukey's multiple range test.

Table 5 Impact of different types and concentrations of elicitors on the number of roots, root length, contamination, oxidation, and in vitro viability of two cultivar of *Solanum lycopersicum*

Concentration of elicitors (mL/L ⁻¹)	Number of roots	Root length (cm)	Contamination Free (%)	Viability (%)	Oxidation (%)
Tomato Saladette					
Cntl					
D ₀ = 0.00	8	1.68 ^c	92	90	68
Act [®]					
D ₁ = 0.20	11	2.09 ^b	98	99	100
D ₂ = 0.40	12	2.01 ^b	100	100	100
D ₃ = 0.60	11	2.0 ^b	100	100	100
Micbl [®]					
D ₁ = 0.30	12	2.02	99	100	100
D ₂ = 0.50	11	1.78 ^c	100	100	98
D ₃ = 0.70	11	2.0 ^b	100	100	100
Stml [®]					
D ₁ = 0.60	10	2.40 ^a	100	99	100
D ₂ = 0.80	13	2.38 ^a	99	96	100
D ₃ = 0.100	11	2.29 ^a	100	100	99
Tomato Bola					
Cntl					
D ₀ = 0.00	7	1.78 ^d	88	98	88
Act [®]					
D ₁ = 0.20	11	2.28 ^b	100	100	100
D ₂ = 0.40	10	2.29 ^b	100	100	100
D ₃ = 0.60	11	2.36 ^a	100	100	100
Micbl [®]					
D ₁ = 0.30	10	2.28 ^b	100	100	100
D ₂ = 0.50	10	2.29 ^b	98	100	100
D ₃ = 0.70	11	2.36 ^a	100	100	100
Stml [®]					
D ₁ = 0.60	11	2.10 ^c	98	100	100
D ₂ = 0.80	10	2.38 ^a	100	100	100
D ₃ = 0.100	11	2.10 ^c	100	100	100

Doses one (1) = D₁, Doses two (2) = D₂ and Doses three (3) = D₃; **The different letters are significantly different ($P \leq 0.05$) according to Tukey's multiple range test

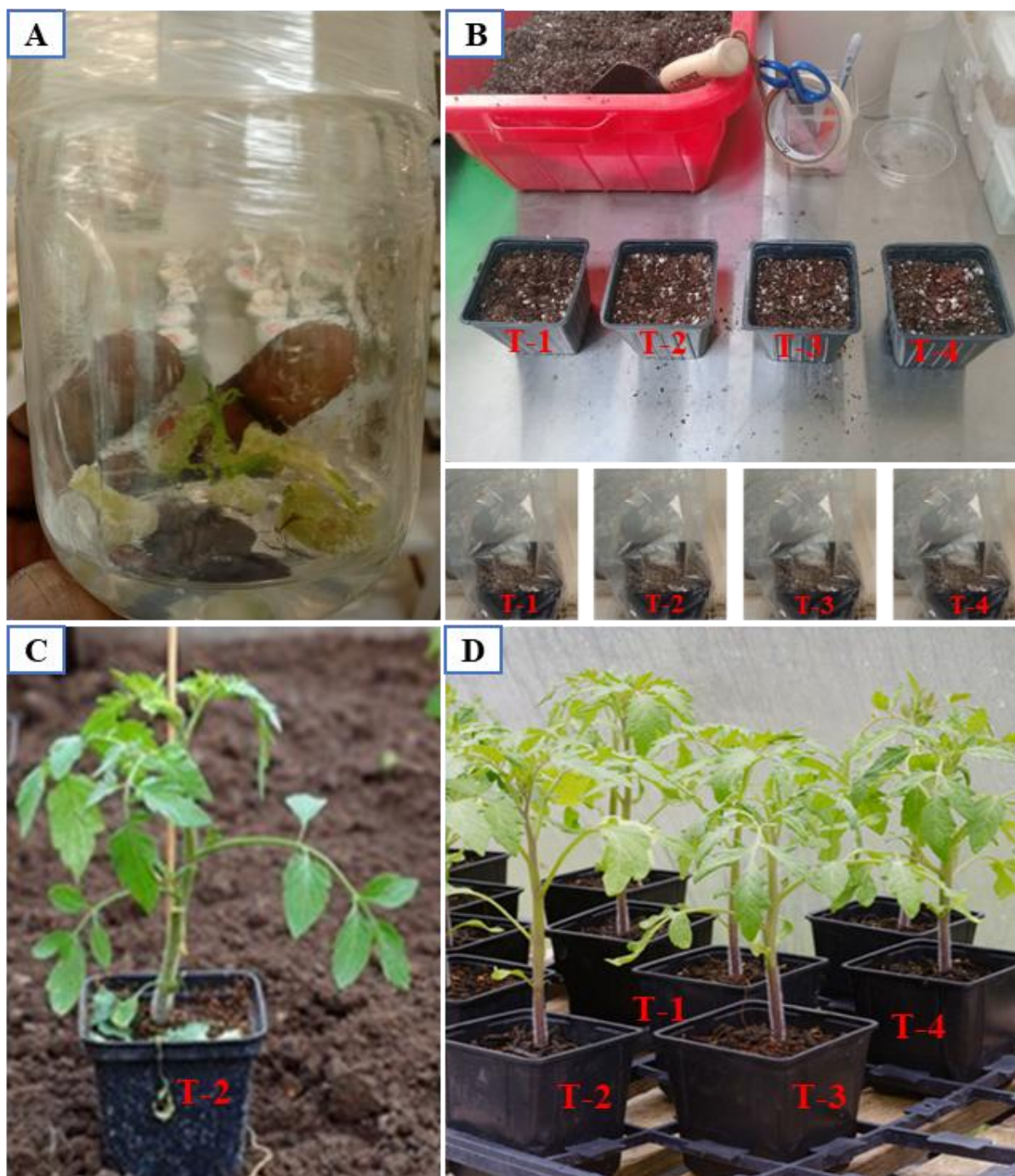


Figure 6 *In vitro* callus formation, root induction and acclimatization in the greenhouse of the two tomato cultivars (A) Callus, root and shoot induction, (B) Pots containing peat moss and vermiculite for the acclimatization, (C) Fully developed plantlets with adaptation in the greenhouse and (D) Developed individual plant continuing growth.

3.6 Acclimatization

The acclimatization of the plantlets was successfully achieved by providing a favourable environment across all treatments. *In vitro* rooted plantlets from each treatment were subsequently

transplanted into a natural and well-maintained greenhouse condition. The gathered data revealed a 100% survival rate for all treatments in the Saladette cultivar. In the case of the Bola cultivar, treatments with elicitors exhibited an average survival rate of 99.7%, compared to 96% for the control (Table 6).

Table 6 Effect of elicitors on the acclimatization of the plantlets for the two tomato cultivars

Concentration of Elicitors (mL/L ⁻¹)	Plant height (cm)	Number of Leaves	Survival Rate (%)
Tomato Saladette:			
Cntl			
D ₀ = 0.00	18.6	14 ^b	100
Act [®]			
D ₁ = 0.20	19.4	15 ^{ab}	100
D ₂ = 0.40	20.3	17 ^a	100
D ₃ = 0.60	21.5	17 ^a	100
Micbl [®]			
D ₁ = 0.20	20.4	16 ^a	100
D ₂ = 0.40	20.0	16 ^a	100
D ₃ = 0.60	19.8	14 ^b	100
Stml [®]			
D ₁ = 0.20	21.1	16 ^a	100
D ₂ = 0.40	18.9	13 ^{bc}	100
D ₃ = 0.60	19.0	13 ^{bc}	100
Tomato Bola:			
Cntl			
D ₀ = 0.00	17.8	11 ^c	96
Act [®]			
D ₁ = 0.20	19.2	14 ^{ab}	100
D ₂ = 0.40	18.0	13 ^b	98
D ₃ = 0.60	18.3	13 ^b	100
Micbl [®]			
D ₁ = 0.20	19.5	15 ^a	100
D ₂ = 0.40	19.0	15 ^a	100
D ₃ = 0.60	19.0	15 ^a	100
Stml [®]			
D ₁ = 0.20	17.9	11 ^c	100
D ₂ = 0.40	18.3	13 ^b	100
D ₃ = 0.60	18.6	12 ^{bc}	100

Doses one (1) = D₁, Doses two (2) = D₂ and Doses three (3) = D₃; **The different letters are significantly different ($P \leq 0.05$) according to Tukey's multiple range test

Contrastingly, the outcomes indicated significant differences in the number of leaves per plant among the two tomato cultivars originating from different explant sources and subjected to varying concentrations of elicitors. However, no significant difference was observed in the plant height (cm) across the treatments. The plants exhibited robust and sturdy growth, achieving full rigidity after 2 weeks in the greenhouse, and continued their subsequent growth and development.

In the current study, the sterilization protocols utilizing 15% Sodium Hypochlorite (NaOCl) in Cloralex[®] have demonstrated effectiveness in achieving oxidation and contamination-free seeds, leading to 100% seed germination within two weeks in the tomato cultivars (Espinosa 2005; Barampuram et al. 2014; Calaña-Janeiro et al. 2019). The investigation delved into the effects of elicitation on *in vitro* seed germination, as well as direct and indirect *in vitro* organogenesis in the explants. These elicitors are commonly employed as potential additives alongside plant growth regulators during different *in vitro* plant propagation stages, aiming to enhance plant quality, regeneration rates, and overall process efficiency. Elicitation stands out as one of the most effective methods for promoting plant growth and elevating the production of *in vitro* secondary metabolites (Zhao et al. 2005).

Biotic elicitors, derived from living organisms, are recognized by specific receptors bound to the cell membrane. This stimulus is then transmitted to the cell through a signal transduction system, leading to changes that ultimately result in the formation of phytoalexins (Baenas et al. 2014). On the other hand, abiotic elicitors are substances of non-biological origin, often inorganic compounds like salts or physical factors. These can be utilized to produce bioactive compounds by modifying plant secondary metabolism across various plant species in culture systems (Verpoorte et al. 2002; Namdeo 2007; Gorelick and Bernstein 2014; Ramirez-Estrada et al. 2016). In a study by Bayraktar et al. (2018), all the elicitors (MeJA, SA, and CHI) demonstrated a positive impact, resulting in an increase in the number of leaves, shoot growth, and biomass accumulation when compared to untreated *in vitro* plantlets.

In this study, plants treated with elicitors exhibited the highest levels of callus formation, weight, diameter, and callus induction in the two *S. lycopersicum* cultivars. However, varying concentrations of elicitors did not yield significant differences in the treatments. Elicitor treatments also enhanced shoot growth after 4 weeks of *in vitro* culture, with the highest shoot length achieved in plants treated with elicitors. Elicitors have been reported to be effective in various plant developmental processes, including seed germination and seedling growth (Bayraktar et al. 2016; Ali et al. 2018; Khan et al. 2018; Li et al. 2018).

Among various treatments applied to callus cultures of *Fagonia indica*, AlCl₃ (0.1 mM concentration) was reported to improve biomass accumulation (fresh weight) to the highest extent compared to the control (Khan et al. 2021). As abiotic elicitors, heavy metals have been widely used in several plant species to enhance growth, biomass, phytochemical accumulation, and antioxidant potential (Kurz et al. 1987; Khan et al. 2021). Various salts of cadmium (Cd²⁺) and aluminium chloride (AlCl₃) have been reported to increase the production of compounds in callus cultures of *Rauvolfia serpentina*, *Melissa officinalis* L., and cell cultures of *Vitis vinifera* (Cai et al. 2013; Urdová et al. 2015; Zafar et al. 2017).

Previously, elicitors were also employed to improve plant propagation in various *in-vitro* cultures, including callus and adventitious root cultures of *F. indica* (Saeed et al. 2017), shoot growth and development, callus, and cell suspension cultures in *Hypericum perforatum* L. explants (Gadzovska et al. 2013). Elicitation in callus cultures of *Stevia rebaudiana* stimulated callus induction response and callus physiology, resulting in good callus texture at lower concentrations (Javed et al. 2017).

Conclusions

An effective disinfection methodology was employed for the *in vitro* implantation of tomato seeds in the two cultivars, ensuring successful seed germination (explants) and promoting the adequate survival and growth of the seedlings. The application of various elicitors in direct and indirect *in vitro* organogenesis on the explants positively affected the evaluated variables. However, different concentrations of elicitors did not yield significant differences in the treatments. Root induction was successful, with a greater response in root initiation and higher survival percentages observed after acclimatization in plants treated with elicitors. The results obtained from this study can guide future research endeavours aimed at expanding the use of elicitor treatments in large-scale *in vitro* propagation of tomatoes, focusing on identifying the most effective concentrations for optimal results.

Acknowledgements

The authors express their gratitude for the support provided by the National Council of Science and Technology (CONACyT), the Faculty of Agronomy of the Autonomous University of Nuevo Leon (FAUANL), and Lida de México SA DE CV.

Compliance with Ethical Standards

The authors declare no conflicts of interest associated with this publication. Additionally, there are no ethical issues infringed upon in this study. The authors have adhered to the principles of ethical and professional conduct. No funding was secured for this research, and no humans or animals were involved.

References

- Aldubai, A. A., Alsadon, A. A., Migdadi, H. H., Alghamdi, S. S., Al-Faifi, S. A., & Afzal, M. (2022). Response of Tomato (*Solanum lycopersicum* L.) Genotypes to Heat Stress Using Morphological and Expression Study. *Plants*, *11*, 615. <https://doi.org/10.3390/plants11050615>.
- Ali, H., Khan, M. A., Ullah, N., & Khan, R. S. (2018). Impacts of hormonal elicitors and photoperiod regimes on elicitation of bioactive secondary volatiles in cell cultures of *Ajuga bracteosa*. *Journal of Photochemistry and Photobiology Biology*, *183*, 242-250.
- Al-Khayri, J. M., & Naik, P. M. (2020). Elicitor-Induced Production of Biomass and Pharmaceutical Phenolic Compounds in Cell Suspension Culture of Date Palm (*Phoenix dactylifera* L.). *Molecules*, *25*(20), 4669.
- Aznar-Sánchez, J. A., Velasco-Muñoz, J. F., López-Felices, B., & Román-Sánchez, I. M. (2020). An Analysis of Global Research Trends on Greenhouse Technology: Towards a Sustainable Agriculture. *International Journal of Environmental Research and Public Health*, *17* (2), 664.
- Baenas, N., Garcia-Viguera, C., & Moreno, D. A. (2014). Elicitation: A tool for enriching the bioactive composition of foods. *Molecules*, *19*, 13541–13563.
- Barampuram, S., Allen, G., & Krasnyanski, S. (2014). Effect of various sterilization procedures on the *in vitro* germination of cotton seeds. *Plant Cell, Tissue, and Organ Culture*, *118*(2), 179–185.
- Bayraktar, M., Naziri, E., Akgun, I. H., Karabey, F., Ilhan, E., Akyol, B., & Gurel, A. (2016). Elicitor induced stevioside production, *in vitro* shoot growth, and biomass accumulation in micropropagated *Stevia rebaudiana*. *Plant Cell, Tissue, and Organ Culture*, *127*(2), 289–300.
- Bayraktar, M., Naziri, E., Karabey, F., Akgun, I. H., Bedir, E., Röck-okuyucu, B., & Gürel, A. (2018). Enhancement of stevioside production by using biotechnological approach in *in vitro* culture of *Stevia rebaudiana*. *International Journal of Secondary Metabolite*, *5*(4), 362-374.
- Cai, Z., Kastell, A., Speiser, C., & Smetanska, I. (2013). Enhanced resveratrol production in *Vitis vinifera* cell suspension cultures by heavy metals without loss of cell viability. *Applied Biochemistry and Biotechnology*, *171*(1), 330–340.
- Calaña-Janeiro, V. M., Izquierdo-Oviedo, H., González-Cepero, M. C., Rodríguez-Llanes, Y., Rodríguez-Hernández, M., & Horta-Fernández, D. (2019). Disinfection of pepper seeds (*Capsicum annuum* L.) cultivar 'YAMIL' for *in vitro* implantation. *Cultivos Tropicales*, *40*(3), e07.
- Cham, A. K., Ojeda-Zacarías, M. C., Lozoya-Saldaña, H., Alvarado-Gómez, O. G., & Vázquez-Alvarado, R. E. (2022). Effects of Elicitors on the Growth, Productivity and Health of Tomato (*Solanum lycopersicum* L.) under Greenhouse Conditions. *Journal of Agricultural Science and Technology*, *24*(5), 1129–1142.
- Cham, A. K., Zacarías, M. del C. O., Saldaña, H. L., Vázquez Alvarado, R. E., Olivares Sáenz, E., Martínez-Ávila, G. C., & Alvarado Gómez, O. G. (2021). Potential elicitors on secondary metabolite production and antioxidant defense activity of two tomato (*Solanum lycopersicum* L.) cultivars. *Italian Journal of Agronomy*, *16*(3), 1883.
- Espinosa O., Trillos G., Hoyos S., Afanador K., & Correa L. (2005). Potencial de propagación *in vitro* para el tomate de árbol partenocárpico *Cyphomandra betacea* Cav. (Sendt). *Journal of the National Faculty of Agronomy*, *58* (1), 2685-2695.
- Gadzovska, S., Tusevski, O., Maury, S., Delaunay, A., Joseph, C., & Hagège, D. (2014). Effects of polysaccharide elicitors on secondary metabolite production and antioxidant response in *Hypericum perforatum* L. shoot cultures. *Scientific World Journal*, *10*, 609-649.
- Gadzovska, S., Maury, S., & Delaunay, A. (2013). The influence of salicylic acid elicitation of shoots, callus, and cell suspension cultures on production of naphthodianthrones and phenylpropanoids in *Hypericum perforatum* L. *Plant Cell, Tissue, and Organ Culture*, *113*(1), 25–39.
- García-Osuna, H., Escobedo Bocado, L., Robledo-Torres, V., Benavides Mendoza, A., & Ramírez Godina, F. (2015). Germination and micropropagation of tetraploid husk tomato (*Physalis ixocarpa*). *Revista Mexicana de Ciancia's Agrícola's*, *6*(spe12), 2301-2311.
- Gorelick, J., & Bernstein, N. (2014). Elicitation: An underutilized tool in the development of medicinal plants as a source of therapeutic secondary metabolites. *Advances in Agronomy*, *124*, 201 – 230.
- Hasnain, A., Naqvi, S. A. H., Ayesha, S. I., Khalid, F., Ellahi, M., et al. (2022). Plants *in vitro* propagation with its applications in food, pharmaceuticals, and cosmetic industries; current scenario and future approaches. *Frontiers in Plant Science*, *13*, 1009395. <https://doi.org/10.3389/fpls.2022.1009395>.
- Holmes, J. E., Lung, S., Collyer, D., & Punja, Z. K. (2021). Variables Affecting Shoot Growth and Plantlet Recovery in Tissue Cultures of Drug-Type *Cannabis sativa* L. *Frontiers in Plant Science*, *12*, 732-344.

- Hussain, A., Qarshi, I. A., Nazir, H., & Ullah, I. (2012). Plant tissue culture: Current status and opportunities. In Leva, A., & Rinaldi, L. M. R. (Eds.) Recent advances in plant *in vitro* culture. Intech, DOI: 10.5772/50568.
- Javed, R., Yucesan, B., Zia, M., & Gurel, E. (2017). Elicitation of Secondary Metabolites in Callus Cultures of *Stevia rebaudiana* Bertoni Grown Under ZnO and CuO Nanoparticles Stress. *International Journal of Sugar Crops and Related Industries*, 20(2), 194–201.
- Karim, M. A., & Kayum, M. A. (2007). In vitro regeneration of tomato plant from leaf and internode segments. *Journal of Bangladesh Agricultural University*, 5(2), 213-216.
- Khan, H., Khan, T., Ahmad, N., Zaman, G., Khan, T., Ahmad, W., & Abbasi, B. H. (2021). Chemical Elicitors-Induced Variation in Cellular Biomass, Biosynthesis of Secondary Cell Products, and Antioxidant System in Callus Cultures of *Fagonia indica*. *Molecules*, 26(21), 6340.
- Khan, T., Abbasi, B. H., & Khan, M. A. (2018). The interplay between light, plant growth regulators and elicitors on growth and secondary metabolism in cell cultures of *Fagonia indica*. *Journal of Photochemistry and Photobiology Biology*, 185, 153-160.
- Kurz, W. G. W., Constabel, F., Eilert, U., & Tyler, R. T. (1987). Elicitor treatment: a method for metabolite production by plant cell cultures in vitro. In: D.D. Breimer, P. Speiser (Eds.) Topics in pharmaceutical sciences 1987 (pp 283–290). Elsevier, Amsterdam New York.
- Li, Y. Y., Chan, C., Stahl, C., & Yeung, E. C. (2018). Recent advances in orchid seed germination and micropropagation. In: Y.I. Lee, & E.C. Yeung (Eds.) Orchid propagation: from laboratories to greenhouses methods and protocols (pp. 1-25). New York: Springer.
- Liu, W., Liu, K., Chen, D., Zhang, Z., Li, B., El-Mogy, M. M., Tian, S., & Chen, T. (2022). *Solanum lycopersicum*, a Model Plant for the Studies in Developmental Biology, Stress Biology and Food Science. *Foods*, 11(16), 2402. <https://doi.org/10.3390/foods11162402>.
- Maureira, F., Rajagopalan, K., & Stöckle C. O. (2022). Evaluating tomato production in open-field and high-tech greenhouse systems. *Journal of Cleaner Production*, 337, 130-459.
- Munim, T. B., Zena, H., Jazar, M., & Nazmul, H. (2019). The effects of elicitors and precursor on *in-vitro* cultures of *Trifolium resupinatum* for sustainable metabolite accumulation and antioxidant activity. *Biocatalysis and Agricultural Biotechnology*, 22, 101–337.
- Murashige, T., & Skoog, F. (1962). A revised medium for rapid growth and bioassays with tobacco tissue cultures. *Physiologia Plantarum*, 15(3), 473-497.
- Murillo-Gómez, P. A., Hoyos, S., Rodrigo M., & Chavarriaga, P. (2017). Organogénesis *in-vitro* using three tissue types of tree tomato [*Solanum betaceum* (Cav.)]. *Agronomía Colombiana*, 35(1), 5-11.
- Namdeo, A. G. (2007). Plant cell elicitation for production of secondary metabolites: A review. *Pharmacognosy Reviews*, 1, 69–79.
- Ozyigit, I. I., Dogan, I., Hocaoglu-Ozyigit, A., Yalcin, B., Erdogan, A., Yalcin, I. E., Cabi, E., & Kaya, Y. (2023). Production of secondary metabolites using tissue culture-based biotechnological applications. *Frontiers in Plant Science*, 14(1), 132-555.
- Peralta, I. E., & Spooner, D. M. (2006). History, Origin and Early Cultivation of Tomato (Solanaceae). In M.K. Razdan & A.K. Mattoo (Eds.) Genetic Improvement of Solanaceous Crops, Volume 2 tomato (pp. 24). Science Publisher.
- Raluca, M., Sturzoiu, C., Florenta, H., Aurelia, B., & Gheorghe, S. (2011). Biotic and abiotic elicitors induce biosynthesis and accumulation of resveratrol with antitumoral activity in the long-term *Vitis vinifera* L. callus cultures. *Romanian Biotechnological Letters*, 16(6), 6683–6689.
- Ramirez-Estrada, K., Vidal-Limon, H., Hidalgo, D., Moyano, E., Golenioswki, M., Cusidó, R. M., & Palazon, J. (2016). Elicitation, an Effective Strategy for the Biotechnological Production of Bioactive High-Added Value Compounds in Plant Cell Factories. *Molecules*, 21(2), 182.
- Saeed, S., Ali, H., Khan, T., Kayani, W., & Khan, M. A. (2017). Impacts of methyl jasmonate and phenyl acetic acid on biomass accumulation and antioxidant potential in adventitious roots of *Ajuga bracteosa* Wall ex Benth., a high valued endangered medicinal plant. *Physiology and Molecular Biology of Plants*, 23, 229–237.
- Servicio de Información Agroalimentaria y Pesquera (SIAP). (2020). Online: <https://www.gob.mx/siap/acciones-y-programas/produccionagricola-33119>.
- Urdová, J., Rexová, M., Mučaji, P., & Balažová, A. (2015). Elicitation A tool to improve secondary metabolites production in *Melissa officinalis* L. suspension cultures. *Acta Facultatis Pharmaceuticae Universitatis*, 62(Suppl. SIX), 46–50.

- Verpoorte, R., Contin, A., & Memelink, J. (2002). Biotechnology for the production of plant secondary metabolites. *Phytochemistry Reviews*, 1, 13–25.
- Xu, F., Valappil, A.K., Mathiyalagan, R., Tran, T.N.A., Ramadhania, Z.M., Awais, M., & Yang, D.C. (2023). *In Vitro* Cultivation and Ginsenosides Accumulation in *Panax ginseng*: A Review. *Plants*, 12(17): 3165.
- Zafar, N., Mujib, A., Ali, M., Tonk, D., & Gulzar, B. (2017). Aluminum chloride elicitation (amendment) improves callus biomass growth and reserpine yield in *Rauvolfia serpentina* leaf callus. *Plant Cell, Tissue, and Organ Culture*, 130, 357–368.
- Zhao, J., Davis, L. C., & Verpoorte, R. (2005). Elicitor signal transduction leading to production of plant secondary metabolites. *Biotechnology Advances*, 23, 283–333.



Journal of Experimental Biology and Agricultural Sciences

<http://www.jebas.org>

ISSN No. 2320 – 8694

ARTIFICIAL INTELLIGENCE IN TACKLING CORONAVIRUS AND FUTURE PANDEMICS

Shagufta Quazi¹ , Sampa Karmakar Singh² , Rudra Prasad Saha¹ ,
Arpita Das¹ , Manoj Kumar Singh^{1*} 

¹Department of Biotechnology, School of Life Science & Biotechnology, Adamas University, Kolkata India-700126

²The West Bengal National University of Juridical Sciences, Dr. Ambedkar Bhavan-12, LB Block, Sector III, Salt Lake City, Kolkata, India-700098

Received – October 31, 2023; Revision – December 31, 2023; Accepted – January 15, 2024

Available Online – March 15, 2024

DOI: [http://dx.doi.org/10.18006/2024.12\(1\).124.137](http://dx.doi.org/10.18006/2024.12(1).124.137)

KEYWORDS

AI

COVID-19

Artificial Intelligence

ML

Machine Learning

ABSTRACT

SARS-COV-2 (Severe Acute Respiratory Syndrome Coronavirus 2) was initially tested in Wuhan City, China, in December 2019 and had a devastating impact worldwide, exterminating more than 6 million people as of September 2022. It became the biggest worldwide health crisis since the 1918 influenza outbreak. Viruses generally mutate randomly, so predicting how SARS-CoV-2 will transform over the next few months or years and which forms will predominate is impossible. The possibilities for virus mutation, in theory, are practically endless. Enabling researchers to determine which antibodies have the potential to be most effective against existing and future variations could help machine learning to assist in drug discovery. In the COVID-19 pandemic, AI has benefited four key areas: diagnosis, clinical decision-making for public health, virtual assistance, and therapeutic research. This study conducted a discourse analysis and textual evaluation of AI (deep learning and machine learning) concerning the COVID-19 outbreak. Further, this study also discusses the latest inventions that can be very helpful in future pandemic detection. COVID-19 has already changed our lives, and in the future, we might be able to deal with pandemics like this with the help of AI. This review has also emphasized the legal implications of AI in the battle against COVID-19.

* Corresponding author

E-mail: manojitcb@yahoo.co.in (Manoj Kumar Singh)

Peer review under responsibility of Journal of Experimental Biology and Agricultural Sciences.

Production and Hosting by Horizon Publisher India [HPI]
(<http://www.horizonpublisherindia.in/>).
All rights reserved.

All the articles published by [Journal of Experimental Biology and Agricultural Sciences](#) are licensed under a [Creative Commons Attribution-NonCommercial 4.0 International License](#) Based on a work at www.jebas.org.



1 Introduction

The COVID-19 pandemic greatly impacted global politics and economy (Naudé 2020). It had a severe impact on people's lives all around the world and caused many deaths. Despite enormous vaccine advancements, outbreaks still occur in more than 200 nations. People in different countries must adopt new ways to combat COVID-19. It is critical to develop antiviral medications and treatment methods to manage COVID-19. After passing through the human respiratory system, the unique coronavirus severely damages the patient's lungs, leading to illnesses more severe than the commonly recognized case of pneumonia. Inflammation and swelling of the lungs resulted in regions of ground-glass opacity (GGO). We need to devise alternate ways to diagnose the condition because its symptoms are challenging to spot, and not many diagnostic instruments are available. Numerous researchers around the world are looking for solutions to these problems. Researchers are actively identifying several possible barriers and offering ways to stop the transmission of the virus in one of the study domains known as machine learning (ML) (Albalawi and Mustafa 2022). In this pandemic, AI has assisted with socioeconomics, clinical diagnosis and therapy, scientific research and drug discovery, demography, and other aspects of the crisis. A way to learn more about a novel viral strain's biology and control epidemics may be made possible by artificial intelligence (AI) with its growing capabilities (Davenport and Kalakota 2019).

Both doctors and hospitals have struggled during this major outbreak, resulting in increasing workloads that make it more difficult for them to identify and admit suspected patients to hospitals. According to previous reports, some patients with an early coronavirus infection tested negative on computed tomography, making it more challenging for radiologists to check out the infection conclusively. Due to inadequate resources to isolate COVID-positive patients from all the suspected cases, the infected individuals may transfer the virus to their close contacts while waiting for RT-PCR detection of the SARS-CoV-2 virus. Even this can happen while waiting 48 hours for COVID-positive confirmation (Khera et al. 2021). In the initial phase, SARS-CoV-2 underwent very little genetic change, except for the globally dominant variant D614G, which showed comparable severity but enhanced transmissibility. Since then, many other SARS-CoV-2 variations have been identified, and, as a result of their potential harm to public health, these are now referred to as variations of concern (VOCs). Five VOCs of SARS-CoV-2 have been reported till now: Alpha (B.1.1.7), Beta (B.1.351), Gamma (P.1), Delta (B.1.617.2), and Omicron (B.1.1.529). There is a greater affinity of the spike protein of the Delta variant towards ACE2 receptors in human cells, which boosts viral attachment to the cell and its subsequent attachment (Aleem et al. 2023). According to Davenport and Kalakota (2019) hospitals were responsible for

approximately 40% of cases. It is critical to swiftly validate patients' COVID-19 status because early false negative reports could raise the likelihood of viral transmission. AI can recognize patterns in big data sets, potentially among the most important tools for resolving this dilemma. AI uses speech recognition, advanced learning, ML, Natural Language Processing, and data evaluation to track contacts, create vaccinations, and improve biometric technology. The main objective of applications of AI in the health field is to examine relationships between patient care and clinical methods. The primary applications of AI systems include medicine, research, clinical decision-making for public health, virtual assistance, and diagnostics.

'Figure 1' depicts AI and its application in COVID-19 detection. There are three main categories for coronavirus diagnosis with the help of AI, and these include binary detection (whether the individual is coronavirus positive or negative), assessment of aberrant regions in lungs caused by COVID-19, and differentiation among the individuals who are COVID-19 positive, negative and pneumonia. The most thoroughly researched category was binary detection (Presence or absence of COVID-19). The most restricted research fields involve prognosis of acute respiratory illness, infectivity to patients from foreign countries, incorporation of imaging (Magnetic Resonance Imaging, Computed Tomography, X-rays) and medical reports, customizing chemotherapy, and fatality prognosis. Radiological scans are incorporated into machine learning exemplars to anticipate critical care unit hospitalization requirements by employing natural language processing for medical data (Summers 2021). This review article collected a discourse analysis and textual evaluation of AI (ML and Deep Learning) about the COVID-19 pandemic from NCBI, PubMed, PMC, Science Direct and ResearchGate. This was followed by summarising significant contributions and the latest AI technology advancements during the COVID-19 pandemic. While collecting personal data about people is necessary for disease control, breaching privacy remains a major challenge. Blockchain may be helpful in this situation to safeguard data integrity and protect consumers from online fraud. Nevertheless, hackers are still attacking individuals with malware, and the privacy of individuals is still being shared. With the growing advancements, there will be a time when the era of hackers will be over, and our information will stay private.

2 Application of AI in Combating COVID-19

AI can be used more frequently in the health sector due to the intricacy and expansion of data. Funders, healthcare providers, and biomedical research organizations use various AI technologies. The primary application areas are diagnosis, clinical decision-making for public safety, virtual assistance, therapeutics, and research.

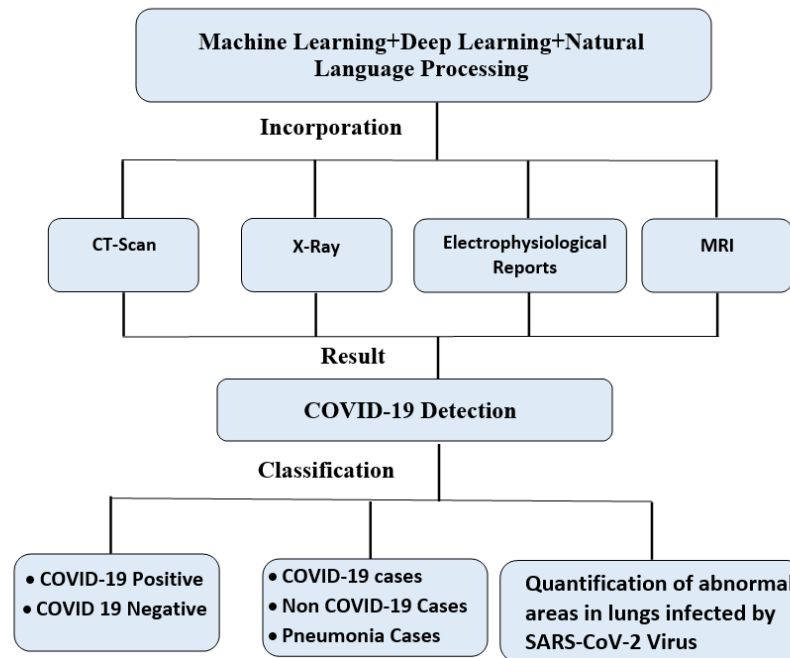


Figure 1 Schematic of AI application in COVID-19 management

2.1 Diagnosis

During the pandemic, AI algorithms are vital for quickly detecting patients who are COVID-19-positive. Most articles discuss using chest CT scans and AI algorithms to detect COVID-19. As a consequence, applications of AI in the early detection of COVID-19 using various medical research and their challenges and promises in COVID-19 have been analyzed in this study. In treating COVID-19 during the pandemic, medical imaging methods, including computed tomography (CT) scans and X-rays, are essential. These imaging tools are becoming more potent to recently created artificial intelligence (AI) technologies, which are also helping medical practitioners. When used by qualified radiologists, chest image analysis, mainly CT, shows early lung abnormalities and attains greater precision. Additionally, chest radiography, particularly chest X-ray (CXR), is affordable and widely accessible. Radiologists must make a visual diagnosis to diagnose chest CT with certain issues. For instance, diagnosing a chest CT requires a lot of time due to the large quantity of sections. Moreover, COVID-19, a recently identified lung condition, has symptoms similar to those of several pneumonias. For radiotherapists to function at a good detection level, particularly when distinguishing comparable diseases, they must acquire a significant amount of CT diagnostic expertise (Vaishya et al. 2020; Jin et al. 2020). Unlike other respiratory conditions, such as lesion detection, lung cancer diagnosis, and tuberculosis screening, distinguishing COVID-19 from other cases of pneumonia is challenging due to the high degree of similarity between

different types of pneumonia and the vast differences in different phases of the same kind. Therefore, an AI detection technique tailored to COVID-19 is required. Additional advantages of AI diagnostic methods are improved performance, high repeatability, and broad implementation (Jin et al. 2020). Panwar et al. (2020) discussed nCOVnet, which can identify a patient who is COVID-19 positive in less than 5 seconds with 97.62% accuracy with the limited available data. Similarly, Butt et al. (2020) demonstrated ResNet-18 and ResNet-23, which uses CT scans to build the model and show 86.7% efficiency. In this context, Apostolopoulos and Mpesiana (2020) described about VGG19 (Visual Geometric Group), which shows 98.75% accuracy. Singh and Gupta (2019) published an article regarding a deep learning technique based on Rectified Linear Units (ReLU), which can detect malignant lung cancer with an accuracy of 85.55%. Chen et al. (2020a) also described RF (Random Forest) with more than 95% accuracy in predicting COVID-19 severity. In a detailed study, Alqudah et al. (2020) demonstrated a “Support Vector Machine” (SVM), “K-Nearest Neighbor” (KNN), and “Random Forest” (RF) with the CNN using soft-maxcan to diagnose SARS-Cov-2 virus and found their accuracy is about 98% (Alqudah et al. 2020). Li et al. (2020) demonstrated XGBoost and reported that it can distinguish COVID-19 patients from influenza patients with more than 92% accuracy (Li et al. 2020). Guhathakurata et al. (2021) also described the Support vector machine (SVM), which can classify COVID cases into “Mildly infected”, “Severely infected”, and “Non-infected” with 87% accuracy (Table 1).

Table 1 AI Applications in Healthcare System and COVID-19 Management

AI Techniques	Role	Reference
Decision tree algorithm	Clinical decision making	Azar and El-Metwally 2013
DRUGSURV	Drug Repurposing	Amelio et al. 2014
Rectified Linear Unit (ReLU) based deep learning method	Diagnosis (85.55% accuracy)	Singh and Gupta 2019
MARIA and NetMHCpan4	Vaccine formulation	Fast and Chen 2019
“K-Nearest Neighbor” (KNN), “Random Forest” (RF), and “Support Vector Machine” (SVM) with the CNN using soft-max	Diagnosis (98% accuracy)	Alqudah et al. 2020
Visual Geometric Group (VGG19)	Diagnosis (98.75% accuracy)	Apostolopoulos and Mpesiana 2020; Panwar et al. 2020
ResNet-23 and ResNet-18	Diagnostic purpose (86.7% accuracy)	Butt et al. 2020
Random Forest (RF)	Diagnostic purpose (>95% accuracy)	Chen et al. 2020a
DrugBank using a gradient-boosted decision tree (GBDT) model	Drug Repurposing	Gao et al. 2020
XGBoost	Diagnosis (>92% accuracy)	Li et al. 2020
Vaxign reverse vaccinology platform	Vaccine formulation	Ong et al. 2020
nCOVnet	Diagnosis (97.62% accuracy)	Panwar et al. 2020
multi-layer neural network	Vaccine formulation	Prachar et al. 2020
3D protein exemplar of 3CLpro	Drug Repurposing	Zhang et al. 2020
AlphaFold created by Google DeepMind	Vaccine formulation	Zhavoronkov et al. 2020
Convolutional Neural Networks utilizing Tensorflow (CNN-TF)	Virtual Assistants	Alodat 2021
Support vector machine (SVM)	Diagnosis (87% accuracy)	Guhathakurata et al. 2021

2.2 Clinical Decision-Making for Public Safety

Supervised learning (SL), deep learning (DL) and Machine learning (ML) are three types of AI technologies that are particularly well adapted for use with healthcare data and impending problems. The difficult task of risk-classifying patients for medicines, identifying those at risk of imminent symptoms, and monitoring a variety of minor outcomes to optimize overall health outcomes can be made more accessible for clinicians with the aid of AI. Since there are many advanced AI methodologies, the ease with which doctors can understand and interpret the results will vary; the next paradigm shift in medical training will include integrating practitioners in model creation and teaching them this. Doctors frequently employ decision tree algorithms. However, they are fundamentally tied to the initial tree layout, making them less useful (Azar and El-Metwally 2013). Big data techniques are widely used in healthcare services to support scientific proof for clinical decision-making amid technological, sociological, and ethical challenges. The medical information is updated regularly with changing statistics and growing observations and includes numerous patient groups and a range of results (Santosh 2020). Theories and models of decompensation, mortality risk, or therapeutic approach developed for SARS-Cov-2 negative cohorts are not expected to uphold previous reports' effectiveness since COVID-19 has a different phenotype as compared to the typical

Acute Respiratory Distress Syndrome (ARDS) (Zampieri et al. 2019; Mousavizadeh and Ghasemi 2020). Few clinical algorithms have been implemented to identify COVID-19 infection in symptomatic patients or prioritized specific predictors, missing important data and thus restricting performance in extensive screens. Patients who move between different therapeutic environments (Emergency departments, outpatient departments, floor units, and Intensive care units) produce distinct individual data that represents their phenotypes, demand various therapeutic tools, and take part in a variety of choices that might be minor or possibly serious. Clinical staff, patients, and their family members can benefit from the fast performance of all existing data in such configurations and throughout each transformation. This will enable them to make well-informed, scientific-proof guidelines and participate in collective decision-making to decide on the most appropriate action (Debnath et al. 2020).

2.3 Virtual Assistance

AI employs natural language processing to respond to COVID-19-related questions, offer accurate information, provide straightforward suggestions, and deliver multi-lingual consultative services. It can also monitor symptoms and make recommendations about whether or not a person should be admitted to the hospital or place themselves in self-isolation at

home (Cury et al. 2021). It has been estimated that people worldwide are consulting doctors virtually since it is a better option than personal advice when the pandemic emerged in Wuhan (Webster 2020). The term "telemedicine," which was coined in 1970, means "healing from afar" and relates to the application of technology for communication and information to enhance societal well-being by facilitating access to medical data (WHO 2019). By implementing chatbots to answer patients' COVID-19 inquiries and providing virtual consultations and evaluations, telemedicine intends to keep patients at home while treating mild COVID-19 symptoms. As a result, fewer people will be exposed to COVID-19. This decreases the use of resources and the burden on the care system. Efficiency and strategic planning tools can produce initiatives based on regional infection counts to evaluate the number of patients requiring hospitalization, beds for intensive care, medicines and mechanical ventilation (Moore et al. 2020). To reduce the chances of transmission in clinical and non-clinical personnel caring for COVID-19 patients, research on the interactive telemedicine approach and computed tomography (CT) strategy was implemented (Miyake et al. 2021). Alodat (2021) used several deep learning-based technologies to power real-time telemedicine to respond to and manage the COVID-19 situation. According to research, the "Convolutional Neural Networks Using Tensorflow" (CNN-TF) system could differentiate between positive and negative COVID-19 situations. An Internet of Things (IoT) based wearable tracking device was created by Al Bassam et al. (2021) to evaluate several crucial parameters of COVID-19. By tracking the individuals' real-time geolocation data, the technology would immediately notify the appropriate medical officials regarding quarantine infringement for potentially infectious patients. This system uses three layers: an Android web layer for smartphones, a cloud layer with an application peripheral interface, and wearable IoT sensor layers (Al Bassam et al. 2021). New research suggests a computer-aided decision-making framework as a telemedicine component to aid practitioners in making the best choice. The design combines ML models that were designed using information from both clinical queries and patient symptoms. With an accuracy of 84.9%, the combination's outcome demonstrated enticing predictability, suggesting the model's ability to forebode the medical assessment of a potential patient's status based on the reported symptoms and potentially assisting clinicians in making the best choices (Faris et al. 2021)

2.4 Therapeutics and Research

Virus identification, mutation evaluation, recurrence prediction, biological assessment, tracking and isolation, vaccine research, and processes for controlling the virus are among the main SARS-CoV-2 concerns where AI can play a crucial role. Researchers have been motivated by the SARS-CoV-2 pandemic to create cutting-edge, rapid antiviral treatments. Innate

immunological responses to disease pathogenesis or host physiological machinery required for viral infections are targeted by host-based antiviral medicines. Utilizing proven methods for drug development might enhance it. A medicine or vaccine typically takes a long time to produce using conventional approaches, but multiple research has used AI techniques to find possible treatments and build efficient and secure vaccinations for COVID-19 to speed up the whole process (Regla-Nava et al. 2015). Molecular dynamics and molecular docking are two computational techniques widely used to find potential artificial and natural therapeutic options for SARS-CoV-2 target protein. The capacity of natural or artificial molecules to attach to the proper pharmacophore sited of the target protein may be examined using extensive chemical libraries of chemicals (Pinzi and Rastelli, 2019). Drug repurposing, defined as adapting current medications for novel treatment purposes, has been an effective drug development method for lowering expenses and streamlining drug authorization. It is possible to teach AI systems to search through the current pharmacological market for potential COVID-19 treatments (Amelio et al. 2014). Thirteen medicines with anti-feline infectious peritonitis (FIP) coronavirus activity were identified using AI. Additional research showed these medications inhibit SARS-CoV-2 (Ke et al. 2020). Forty-one drug candidates were analyzed with a high degree of certainty and a high "Area Under the Receiver Operating Characteristic" (AUROC) of 0.85 (Zeng et al. 2020). After screening 8,565 medications, DrugBank has been using a gradient-boosted decision tree (GBDT) model. Gao et al. (2020) discovered 20 FDA-approved treatments and 20 preclinical medicines that could be beneficial against SARS-CoV-2 (Gao et al. 2020). Zhang et al. (2020) found protein-ligand interaction pairings and constructed a 3D protein exemplar of 3CLpro. Then, they offered probable molecule and tripeptide lists for 3CLpro (Zhang et al. 2020). Batra et al. (2020) used accurate ensemble docking and machine learning to extract 75 FDA-approved and 100 additional ligands as possible COVID-19 chemotherapeutic drugs from data sets.

Researchers have identified several correlations between the SARS COV (2002) virus and SARS COV-2 (2019) virus, and based on the data already available, it is conceivable to create AI learning models that could help in predicting drug structures that could cure COVID-19 (Gns et al. 2019). During situations, the safest and genuinely required approach is to request this specific information about medicine so that the AI professionals can utilize their measurements to evaluate relevant attributes of the drug. To achieve this, governments and legislators throughout the world must take action to compel large pharmaceutical corporations and research facilities to collaborate with smaller test partnerships and share their knowledge. The repurposed medicine will reach the advanced testing phase without the first research and safety

evaluations (Mohanty et al. 2020). Any of the most promising work is based on identifying virus mutation before there is even a new virus. Software developed by the Salama community can determine nucleotide substitution of the Avian pneumoencephalitis (Newcastle virus) in primary RNA sequences using a “rough-set gene evolution theory” (Salama et al. 2016). “Rough set theory” is a data analysis theory that is considered a significant method for accessing incoherent and ambiguous information, particularly in the applications of AI (Zhang et al. 2016). Training data were made, with one-generation RNA sequences as inputs and next-generation RNA sequences as outputs. The system was introduced to estimate successive generations of RNA sequences, and after that, the results are applied to real sequences of RNA. They applied the algorithm to Avian pneumoencephalitis virus databases in China and South Korea and detected that the mutant nucleotides were approximately 70% accurate (Khan et al. 2020).

3 AI AND ML in Vaccine Preparation

The White House has appealed to AI researchers worldwide to deliver cutting-edge text and data mining tools to support COVID-19-related studies in partnership with academic institutions and tech enterprises. Scholarly reports based on COVID-19 have been updated weekly, and the Allen Institute for AI has published this data as open-source in partnership with top research institutions. This data is crucial for launching new research projects (Alimadadi et al. 2020). The taxonomic classification of COVID-19 genomes, the CRISPR (“Clustered Regularly Interspaced Short Palindromic Repeats”) based COVID-19 identification test, the safety assessment of serious COVID-19 patients, and the revelation of possible drug candidates against COVID-19 are all accomplished through the use of highly advanced machine learning techniques. A component of bacterial immune systems that cut DNA called CRISPR has been developed into a gene-editing tool. It is a precise tool for a restriction enzyme that can cut the DNA sequence by following a predefined track (Metsky et al. 2020; Ge et al. 2020; Yan et al. 2020; Randhawa et al. 2020). The previous finding, in which senior citizens are at a higher risk for COVID-19, is contradicted by a new report that the number of young adults suffers from serious COVID-19 symptoms, suggesting an immediate need for a systematic risk assessment focused on individual physiological and genetic properties. Biochemistry (expression degree of ACE2) and clinical details (respiratory history, ability to survive, virus load and age) of COVID-19 patients with implicit health issues may, therefore, be evaluated using machine learning methods to classify not just certain attributes (e.g. ACE2) for risk factors, but, existing portfolio and predictive analytics for the structured preparation of ongoing therapeutic strategies and COVID-19 defensive measures are also performed. It's been shown that ACE2 genetic polymorphism, expressed by various gene mutations in the human genome, affects

the virus-binding process, indicating a potential genetic vulnerability to COVID-19 (Cao et al. 2020). By studying genetic variations that are symptomless, moderate, or severe using COVID-19 patient data, it is now possible to determine and predict individuals based on their susceptibility or tolerance to contracting COVID-19 infections with the help of ML techniques. As a result, the ML algorithm can return specific target gene mutations, such as the ACE2 polymorphism, as important components for pragmatic and rationalistic analysis in its decision-making process. For instance, great sensitivity and efficiency have been proven for machine learning-driven testing of SARS-CoV-2 assay models utilizing a viral detection approach powered by CRISPR. Based on their unique breathing patterns, neural network classification techniques for the widespread screening of COVID-19 patients were developed (Wang et al. 2020). To identify and follow COVID-19 patients automatically over time, a deep learning-based categorization approach of thoracic CT scans was created (Gozes et al. 2020). A deep learning framework for drug development was used to create and manufacture novel drug-like substances targeting SARSCoV-2. AlphaFold, a deep learning technology created by Google DeepMind, has published expected COVID-19-related protein structures that can take months with conventional experimental methods and serve as useful knowledge for COVID-19 vaccine formulation (Zavoronkov et al. 2020). Prachar et al. (2020) found 174 SARS-CoV-2 biomarkers with better prognostic molecular docking and the ability to stably connect to 11 HLA allotypes using a multi-layer neural network. The fact that the authors assessed the peptide-HLA prediction model currently being utilized to identify SARS-CoV-2-related biomarkers is important. Fast and Chen (2019) used the MARIA and NetMHCpan4 artificial neural network approaches to identify SARS-CoV-2 T-cell and B-cell epitopes. The method found 2 putative neutralizing B-cell epitopes on the S protein and 405 T-cell epitopes with excellent presentation scores for both MHC-I and MHC-II. These findings will assist in the creation of effective COVID-19 vaccines and neutralizing antibodies. When compared to the S protein, they discovered that the largest non-structural protein, nsp3 (Coronaviridae family), which earned the highest protective immunogenicity score, emerged as the most promising vaccine option for COVID-19 (Fast and Chen 2019). In addition, Ong et al. (2020) designed a Vaxign reverse vaccinology platform combined with ML has been introduced for COVID-19 vaccine candidates. The overabundance of COVID-19 treatment reports in hospitals around the world also necessitates more developed AI methods to evaluate the tailored therapeutic potential for analyzing fresh patients, such as predicting the chances of hospitalization, that not only provide each patient with high-quality care but also helps the local hospital system set up and operation. The availability of COVID-19 clinical findings that can be regulated and maintained in conveniently accessible databases is a significant potential problem. Therefore, it is crucial to develop

cyberinfrastructure that will support global cooperation. The incorporation of COVID-19-related clinical findings with current biobanks, such as the UK Biobank, along with information already known about those patients, like physiological and genotypic attributes, can help us in the direction of a more expedient and practical approach by bioinformaticians and computational scientists for meaningful data analysis.

4 The Application of AI and Blockchain in the Covid-19 Pandemic

Point-of-care (POC) testing is carried out near the patient's location and provides fast results that enhance patient care. POC screening was developed and implemented in response to the COVID-19 pandemic to minimize the spread of the virus and relieve the strain on the health system. Emerging medical breakthroughs like blockchain and AI technology can be combined with POC diagnostics to enable patients to self-test during quarantine (Mashamba-Thompson and Crayton 2020). A sophisticated blockchain technology database system allows unrestricted data sharing inside a company's server. Blockchain technology can improve the procedures for clinical trials for vaccines and pharmaceuticals, publicly track donations and fundraising events, increase public awareness, and serve as a trustworthy data-tracking system (Agbo et al. 2019). The World Economic Forum brought attention to the fact that hackers are distributing malware through coronavirus map data. These hackers pretend to be real interactive maps that show the disease's distribution. By doing this, fraudsters deceive people into disclosing their private data, including Passwords, card details and usernames. The attackers then trade this confidential information on the dark web or use it to defraud individuals. The issues with centralized data systems can be solved by blockchain technology. It eliminates any failure in the system while introducing permanence and data integrity. Anyone with an internet connection can use a blockchain data tracking system to quickly and securely obtain updated data about the SARSCoV-2-virus (Marbough et al. 2020). In resource-limited environments, Smartphone-linked POC diagnoses and self-testing are effectively applied (Makhudu et al. 2019; Bervell and Al-Samarraie 2019). However, there isn't enough proof to support the use of blockchain technology for disease detection. All experiments are reported to the disease control authority by the blockchain and AI system, along with the proportion of positive and negative test reports (Braun et al. 2013). This will ensure appropriate patients are admitted to quarantine centres for treatment and analysis. The AI feature would allow powerful data collection (patient knowledge, patient geographic position, and medical reports), authentication, review, and blockchain systems to quickly extract modified data from fragmented medical data sources with high trust. Local manufacture of these remedies might assist in overcoming supply chain challenges (Kuupiel et al. 2017).

5 Cross Population Test Models in COVID-19 and the Role of Active Learning

AI is a new model for health care, offering alternatives to conventional practices and therapies. The core tenet of AI-driven products is that they require a lot of data on all known combinations for preparation. Traditional machine learning also promotes a positive collection of compiled data, making classifiers well-qualified within the supervised learning domain. Unfortunately, researchers failed to quantify the number of training sets that should be developed for a successful classifier and whether it is still acceptable to wait for reasonably large amounts of data to be collected. For instance, deep learning (DL) requires enormous training data (Guo et al. 2019; Chen et al. 2020b). Most AI-driven solutions can only create concrete evidence models for coronavirus cases. The severity of the coronavirus epidemic will spread restricted data, according to AI specialists. According to The Wall Street Journal, coronavirus exhibits flaws in AI health software. Given the paucity of current coronavirus data and the shortcomings of health services delivered as AI in the face of emergent, rapidly spreading illnesses, several testing app suppliers are avoiding equipment upgrades (Santosh 2020). In particular, online platforms, newspaper articles, healthcare articles, and conventional AI-driven tools may not provide the desired outcomes for real-world scenarios with less data.

Active learning is used in contrast to passive learning (standard ML classifiers) to solve a learning conundrum where the learner has some control over selecting the data to be learned (Sammut and Webb 2017). Exploiting real-time data is required since manual annotation and analysis cannot be done in real-time. It implies that rather than having a traditional collection of training, verification and testing sets, AI-driven resources are needed, and these can be trained over time without requiring full knowledge of the results, this is known as Active Learning (AL). Using Anomaly Detection (AD) techniques, the variations in data over time may be measured when studying. AD aids in locating and identifying unusual objects, incidents, or findings that give rise to concerns by varying dramatically from the rest of the data or a collection of standard data for that unique occurrence (Bouguelia et al. 2018).

Since there is a dearth of sufficient data from the essential regions, cross-population test models are further necessary in these situations. Parallel to this, the data collected over time can be used to train models depending on the choices. RNA sequences are the most common data type AI-driven tools utilized for coronaviruses (Ai et al. 2020). In addition, it considers and checks Data from chest X-rays, computerized tomography (CT) scans, electronic health records (EHRs), and other sources. Alibaba unveiled a brand-new AI-based tool that can accurately diagnose coronavirus illness using up to 96% of the time using CT scans. It may be

applied to various data types, including multidimensional data, vector data (1D array, signal, or pattern), and 2D matrices (images). Thus, it makes sense for AI researchers to use longitudinal and multimodal data to examine whether different types of data can help to give an accurate judgement over time regarding COVID-19 outbreaks rather than using machine learning models with one type of data and looking for clustering methods to incorporate outcomes (Fong et al. 2019).

6 Latest Inventions in the Use of AI in COVID-19

Prognostic computational techniques are being employed more often and have proven effective in delivering information that helps improve clinical management and policies. Such innovations are currently in their early phases; therefore, acceptance for meaningful policy evaluation at the national and global levels is only slowly progressing. Nevertheless, a recent instance shows that AI-powered computers are becoming more precise (Allam et al. 2020). COVID-19 induces a decrease in oxygen levels, which is challenging to diagnose because the patients do not show perceptible respiratory problems, which leads to a state of silent hypoxia. Therefore, it is essential to identify this silent version of hypoxia in COVID-19 individuals before they start to suffer from breathing difficulties (Teo 2020). This silent hypoxia can be detected via mobile phones acquired with medical-graded pulse oximeters to record the oxygen saturation values easily. Tayfur and Afacan (2019) evaluated pulse oximetry measurements against two diagnostic instruments often seen in emergency rooms with a Samsung Galaxy S8 mobile, which showed 96% to 99% similarity compared to standard procedure. The gadget's accuracy is very high when the users' oxygen saturation levels are over 90%. Healthy individuals have oxygen saturation levels between 95 and 100%, might use their cellphones to effortlessly measure their oxygen level on a routine basis at home and get in touch with their doctor right once if they see a noticeable drop below 95% (Tayfur and Afacan 2019).

A viable strategy for COVID-19 surveillance, identification, and prognosis is wearable Internet of Things (IoT) devices. Even for asymptomatic people, the sensor readings from wearable technology can warn patients of a possible COVID-19 disease as symptoms develop (Seshadri et al. 2020). A technique to detect coronavirus-affected patient from their breathing patterns via smartphone has been developed by Alkhodari and Khandoker (2022). To test this technique, 480 breathing sounds of people were acquired from the Coswara database (open data), out of which 240 voices were shallow and 240 voices were deep. Using a cellphone microphone and a web application, 120 COVID-19 patients' and 120 healthy individuals' voices were recorded with "Mel-frequency Cepstral Coefficients" (MFCC) attribute extraction from the voice data, and in-depth attributes were acquired using a mixture of "Convolutional Neural Network" (CNN) and "Bi-directional Long

Short-Term Memory units" (BiLSTM) to make up the deep learning tool. As a result, it showed 94.58% accuracy in differentiating between COVID-19-positive cases and normal cases. It also suggests using deep learning as a prior examination technique for such conditions before doing industry-standard RT-PCR analyses (Alkhodari and Khandoker 2022).

Wearable technology (Activity trackers and smartwatches) has generated significant attention due to its ability to measure our health. The focus of the pandemic has shifted to whether these wearable technologies may identify physiological abnormalities which might point to a COVID-19 infection. It might then assist with early testing and quarantine, halting the spread of the virus (Mishra et al. 2020). The effects of COVID have been mapped out on a larger scale using smartwatches. Fitbit is a smartwatch brand that showed variations in sleeping pattern data collected from thousands of customers during the outbreak. According to the data, people slept longer on average compared to the initial phase of the pandemic (Rezaei and Grandner 2021).

Wurzer et al. (2021) established a telemonitoring technique in which respiratory rate, temperature, oxygen saturation level and pulse rate can be monitored every 15 minutes via phone calls. With the help of the web or cellular phone, the Telecovid centre receives the information, and an experienced crew keeps track of it around the clock. The National Early Warning Score was adjusted to determine each person's specific risk. 153 (76 men and 77 women) patients older than 60 years of age or who fulfilled any one criteria like pregnancy, cancer, high blood pressure, diabetes, cardiovascular or lung diseases were included. The Telecovid crew recommended 20 COVID-19 individuals to the hospital. All patients acknowledged the ease of use of the gadget. Approximately 90% of the recommended patients were grateful for the research since they were admitted and treated at the right time.

In 2020, Dubai Police deployed AI-based smart helmets incorporated with IR (Infrared radiation) cameras, facial detection technology, and automobile plate number readers to quickly observe individuals and identify potential coronavirus cases using thermal scanning. The United Arab Emirates is the first country to employ this technique. These 'smart helmets' instantaneously obtain additional personal information about the home address and detect the body temperature of individuals on public transportation. In the meantime, a Chinese company, Hanwang Technology Ltd, claimed that they had created the nation's first facial detection system to detect people wearing or without masks (Ahlawat and Krishnamurthi 2022).

7 Overcoming Challenges

AI has several applications in the healthcare sector due to the development of sophisticated technology, but there are also

substantial disadvantages in this field that hinder AI from being fully absorbed into the current healthcare sector. To create good results, AI exemplars are getting increasingly complex. Due to its complexity, AI operates in a "black box," making it more challenging to understand how the model truly works (Wadden 2021). Healthcare professionals must understand how precisely AI produces specific discoveries to respond correctly. Lack of justification creates trustworthiness issues for both healthcare organizations and patients. Explainable AI (XAI) approaches can be used to tackle this issue and promote trust between humans and machines. Medical experts can apply complex but intelligible algorithms as more study is done in this area (Linardatos et al. 2020).

Finding high-quality medical data is a significant barrier to implementing AI in healthcare. Getting information about a patient's health is always challenging due to its sensitivity and moral obligations. Even automated processing is time-consuming and expensive because interpreting a particular model might take up to ten thousand pictures. By obtaining additional sets of data from a single image and drastically lowering the quantity of data required to train a system, new methods of diagnostic image interpretations are assisting in overcoming this obstacle (Kotter and Ranschaert 2021).

The medical error made by diagnostic tools is 60%, which causes 40,000–80,000 fatalities annually in US hospitals. Thus, the application of AI in various medical sectors can aid in minimizing judgment mistakes caused by humans. Organizations are hesitating to embrace AI in diagnostics, even though it can provide more precise results by reducing the chances of human error. To make sure the machine learning exemplar is applicable, it must be examined and confirmed, and the model must generalize effectively, avoiding overfitting or underfitting over the training set (Lee and Yoon 2021). A legal basis must be established for exchanging data and accessibility for AI technologies. To improve AI effectiveness in the healthcare sector, relevant data exchange and intelligence gathering are necessary. The accuracy of the information is crucial since the more confident users generate the output, the lower the danger of undesirable results (Moreno 2020).

8 Legal Implications of AI in Combating COVID-19

AI rapidly changes how we work and live and is viewed as the fourth industrial revolution ("Ministry of Electronics & Information Technology, Government of India, 2023"). To tackle global challenges like COVID-19, AI and ML are potent tools that may promote science and research and increase access to healthcare (Report of Committee – D on cyber security, safety, Legal and ethical issues, Ministry of Electronics & Information Technology, Government of India, 2018). Recently, to combat

COVID-19, the world has witnessed AI's vital role. However, it has also attracted concerns like privacy and anti-discrimination. 'The right to Privacy is a fundamental right' (Justice KS Puttaswamy (Retd.) & Anr. vs. UOI and Ors, 2017). AI can suffer from "*algorithmic bias*," which has striking implications for health care. Thus, the algorithms must be developed to not exacerbate social inequities in health care (Atherine 2021). Unfortunately, AI remains largely unregulated. The "Information Technology Act 2000" and the rules and regulations framed are India's primary statutes governing AI. In 2018, the "Ministry of Electronics and Information Technology" (MEITY) established the following four committees to advance AI initiatives and create a regulatory framework: (i) Committee on Platforms and Data for AI, (ii) Committee on Leveraging AI for Identifying National Missions in Key Sectors, (iii) Committee on Mapping Technological capabilities, Key Policy enablers required across sectors. Skilling and Re-skilling R & D, and (iv) Committee on Cyber Security, Safety, Legal and Ethical Issues. These Committees have provided various recommendations. It's high time to frame comprehensive guidelines based on these recommendations in consultation with all the stakeholders, including civil society.

9 Conclusion and Future Prospects

In recent times, Artificial intelligence has steadily moved beyond the laboratory into public and clinical concerns, including the early detection of outbreaks and the insightful analysis of vast healthcare records. AI has significantly raised our degree of diagnosis, prediction, and therapy in the COVID-19 battle. Through significant clinical data, AI was able to examine the epidemiological, medical, and pharmacological impacts of COVID-19. Diagnostic analysis, genetic analysis, patient hospitalization, healthcare, pharmaceutical research, and related medical and health services have been impacted by AI. "Table 1" depicts numerous AI, ML and DL applications in the healthcare system. In drug research, a cutting-edge approach to finding cures for illnesses rapidly and safely involves repurposing already-approved medications and finding new applications for AI. AI is beneficial in predicting virus propagation, relieving the pressure on medical professionals and the rush to develop a treatment for COVID-19. However, contemporary research has shown AI's flaws and drawbacks. Simple AI strategies have dominated research in COVID-19, and only a small amount of study is focused on creating novel AI technologies. The limitations are: a) minimal success in AI research toward creating medications and vaccinations against SARS-CoV-2 has been achieved. b) AI has not yet impacted COVID-19 since it is challenging to utilize due to a lack of data and an overflow of data. Thorough human-AI interaction and careful data privacy and public health balance would be required to overcome these limitations. Furthermore,

there hasn't been any cross-disciplinary AI study on COVID-19. AI has not yet impacted COVID-19. The disease outbreak and possible solutions may speed up the advancement of the economic system, including the automation of human workers, the outsourcing of manufacturing operations, and market dominance by a small number of new digital companies, even though the use of AI is limited. It can be concluded that AI scientists don't necessarily hesitate to prepare, validate and analyze the prototypes for the complete datasets; instead, AI-driven devices must be incorporated from the start of data gathering. Experts are concerned about AI because they believe that AI and ML technologies will replace workers in their current positions in the upcoming years. Even though such technologies are replacing humans in various work roles across industries, including marketing, banking, telecommunications, and more, this is not diminishing job chances. AI is creating a variety of new career openings that were not even possible a few decades ago. It is essential to the healthcare industry, which we have already discussed. There doesn't seem to be a direct link between exposure to AI and employment. However, more engagement with AI is associated with faster employment rates in jobs with substantial technology use.

References

- Agbo, C. C., Mahmoud, Q. H., & Eklund, J. M. (2019). Blockchain Technology in Healthcare: A Systematic Review. *Healthcare (Basel)*, 7(2), 56.
- Ahlawat, C., & Krishnamurthi, R. (2022). Internet of Things-based smart helmet to detect possible COVID-19 infections. *Cyber-Physical Systems*, 15–36. <https://doi.org/10.1016/B978-0-12-824557-6.00004-2>
- Ai, T., Yang, Z., Hou, H., Zhan, C., Chen, C., et al. (2020). Correlation of Chest CT and RT-PCR Testing for Coronavirus Disease 2019 (COVID-19) in China: A Report of 1014 Cases. *Radiology*, 296(2), E32–E40. <https://doi.org/10.1148/radiol.2020200642>
- Al Bassam, N., Hussain, S. A., Al Qaraghuli, A., Khan, J., Sumesh, E. P., & Lavanya, V. (2021). IoT based wearable device to monitor the signs of quarantined remote patients of COVID-19. *Informatics in medicine unlocked*, 24, 100588.
- Albalawi, U., & Mustafa, M. (2022). Current Artificial Intelligence (AI) Techniques, Challenges, and Approaches in Controlling and Fighting COVID-19: A Review. *International journal of environmental research and public health*, 19(10), 5901
- Aleem, A., Akbar Samad, A. B., & Vaqar, S. (2023). Emerging Variants of SARS-CoV-2 and Novel Therapeutics Against Coronavirus (COVID-19). In *StatPearls*. StatPearls Publishing.
- Alimadadi, A., Aryal, S., Manandhar, I., Munroe, P. B., Joe, B., & Cheng, X. (2020). Artificial intelligence and machine learning to fight COVID-19. *Physiological Genomics*, 52(4), 200–202.
- Alkhodari, M., & Khandoker, A. H. (2022). Detection of COVID-19 in smartphone-based breathing recordings: A pre-screening deep learning tool. *PLoS ONE*, 17(1), e0262448.
- Allam, Z., Dey, G., & Jones, D. S. (2020). Artificial Intelligence (AI) Provided Early Detection of the Coronavirus (COVID-19) in China and Will Influence Future Urban Health Policy Internationally. *AI*, 1(2), 156–165. <http://dx.doi.org/10.3390/ai1020009>.
- Alodat M. (2021). Using Deep Learning Model for Adapting and Managing COVID-19 Pandemic Crisis. *Procedia computer science*, 184, 558–564.
- Alqudah, A., M., Qazan, S., & Alqudah, A. (2020). Automated Systems for Detection of COVID-19 Using Chest X-ray Images and Lightweight Convolutional Neural Networks. *Research Square*. 47(1). <https://doi.org/10.21203/rs.3.rs-24305/v1>.
- Amelio, I., Gostev, M., Knight, R. A., Willis, A. E., Melino, G., & Antonov, A. V. (2014). DRUGSURV: a resource for repositioning of approved and experimental drugs in oncology based on patient survival information. *Cell death & disease*, 5(2), e1051.
- Apostolopoulos, I. D., & Mpesiana, T. A. (2020). Covid-19: automatic detection from X-ray images utilizing transfer learning with convolutional neural networks. *Physical and engineering sciences in medicine*, 43(2), 635–640.
- Atherine J. I. (2021). Algorithmic Bias in Health Care Exacerbates Social Inequities — How to Prevent It. Retrieved from <https://www.hsph.harvard.edu/ecpe/how-to-prevent-algorithmic-bias-in-health-care/> last accessed 24/01/2023
- Azar, A. T., & El-Metwally, S. M. (2013). Decision tree classifiers for automated medical diagnosis. *Neural Computing & Applications*, 23 (7/8), 2387. DOI: 10.1007/s00521-012-1196-7.
- Batra, R., Chan, H., Kamath, G., Ramprasad, R., Cherukara, M. J., & Sankaranarayanan, S. K. R. S. (2020). Screening of Therapeutic Agents for COVID-19 Using Machine Learning and Ensemble Docking Studies. *The journal of physical chemistry letters*, 11(17), 7058–7065.
- Bervell, B., & Al-Samarraie, H. (2019). A comparative review of mobile health and electronic health utilization in sub-Saharan African countries. *Social science & medicine (1982)*, 232, 1–16. <https://doi.org/10.1016/j.socscimed.2019.04.024>
- Bouguelia, M., Nowaczyk, S., Santosh, K. C., & Verikas, A. (2018). Agreeing to disagree: Active learning with noisy labels

- without crowdsourcing. *International Journal of Machine Learning & Cybernetics*, 9(8), 1307–1319.
- Braun, R., Catalani, C., Wimbush, J., & Israelski, D. (2013). Community health workers and mobile technology: a systematic review of the literature. *PLoS One*, 8(6), e65772.
- Butt, C., Gill, J., Chun, D., & Babu, B. A. (2020). Deep learning system to screen coronavirus disease 2019 pneumonia. *Applied Intelligence*, 53, <https://academicworks.medicine.hofstra.edu/articles/6359>.
- Cao, Y., Li, L., Feng, Z., Wan, S., Huang, P., Sun, X., Wen, F., Huang, X., Ning, G., & Wang, W. (2020). Comparative genetic analysis of the novel coronavirus (2019-nCoV/SARS-CoV-2) receptor ACE2 in different populations. *Cell discovery*, 6, 11. <https://doi.org/10.1038/s41421-020-0147-1>
- Chen, J., Wu, L., Zhang, J., Zhang, L., Gong, D., et al. (2020a). Deep learning-based model for detecting 2019 novel coronavirus pneumonia on high-resolution computed tomography. *Scientific reports*, 10(1), 19196. <https://doi.org/10.1038/s41598-020-76282-0>.
- Chen, Y., Ouyang, L., Bao, F. S., Li, Q., Han, L. et al. (2020b). An interpretable machine learning framework for accurate severe vs non-severe covid-19 clinical type classification. *Journal of Medical Internet Research* doi: 10.2196/23948.
- Cury, R. C., Megyeri, I., Lindsey, T., Macedo, R., Batlle, J., et al. (2021). Natural Language Processing and Machine Learning for Detection of Respiratory Illness by Chest CT Imaging and Tracking of COVID-19 Pandemic in the US. *Radiology Cardiothoracic imaging*, 3(1), e200596. <https://doi.org/10.1148/ryct.2021200596>.
- Davenport, T., & Kalakota, R. (2019). The potential for artificial intelligence in healthcare. *Future healthcare journal*, 6(2), 94–98. <https://doi.org/10.7861/futurehosp.6-2-94>
- Debnath, S., Barnaby, D. P., Coppa, K., Makhnevich, A., Kim, E. J., Chatterjee, S., et al. (2020). Machine learning to assist clinical decision-making during the COVID-19 pandemic. *Bioelectronic medicine*, 6, 14. <https://doi.org/10.1186/s42234-020-00050-8>
- Faris, H., Habib, M., Faris, M., Elayan, H., & Alomari, A. (2021). An intelligent multimodal medical diagnosis system based on patients' medical questions and structured symptoms for telemedicine. *Informatics in Medicine Unlocked*, 23, 100513. <https://doi.org/10.1016/j.imu.2021.100513>.
- Fast, E. & Chen, B. (2020). Potential T-cell and B-cell epitopes of 2019-nCoV. *bioRxiv*. Retrieved from 10.1101/2020.02.19.955484.
- Fong, S. J., Li, G., Dey, N., Crespo, R. G., & Herrera-Viedma, E. (2019). Finding an accurate early forecasting model from small dataset: A case of 2019-ncov novel coronavirus outbreak. *International Journal of Interactive Multimedia and Artificial Intelligence*, 6(1), 51–6.
- Gao, K., Nguyen, D. D., Chen, J., Wang, R., & Wei, G. W. (2020). Repositioning of 8565 Existing Drugs for COVID-19. *The journal of physical chemistry letters*, 11(13), 5373–5382.
- Ge, Y., Tian, T., Huang, S., et al. (2020). A data-driven drug repositioning framework discovered a potential therapeutic agent targeting COVID-19. *bioRxiv 986836* [Preprint]. Retrieved from <https://www.biorxiv.org/content/10.1101/2020.03.11.986836v1>
- Gns, H. S., Gr, S., Murahari, M., & Krishnamurthy, M. (2019). An update on Drug Repurposing: Re-written saga of the drug's fate. *Biomedicine & pharmacotherapy = Biomedecine & pharmacotherapie*, 110, 700–716. <https://doi.org/10.1016/j.biopha.2018.11.127>
- Gozes, O., Frid-Adar, M., Greenspan, H., Browning, P.D., Zhang, H., et al. (2020). Rapid AI Development Cycle for the Coronavirus (COVID-19) Pandemic: Initial Results for Automated Detection & Patient Monitoring using Deep Learning CT Image Analysis. *arXiv2003.05037*. Retrieved From: <https://arxiv.org/abs/2003.05037>
- Guhathakurata, S., Kundu, S., Chakraborty, A., & Banerjee, J. S. (2021). A novel approach to predict COVID-19 using support vector machine. *Data Science for COVID-19*, 351–364. <https://doi.org/10.1016/B978-0-12-824536-1.00014-9>
- Guo, Q., Li, M., Wang, C., Wang, P., Fang, Z., et al. (2019). Host and infectivity prediction of wuhan 2019 novel coronavirus using deep learning algorithm. *bioRxiv*, 914044 [Preprint]. Retrieved from https://www.researchgate.net/publication/338821819_Host_and_infectivity_prediction_of_Wuhan_2019_novel_coronavirus_using_deep_learning_algorithm.
- Jin, C., Chen, W., Cao, Y., Xu, Z., Tan, Z., et al. (2020). Development and evaluation of an artificial intelligence system for COVID-19 diagnosis. *Nature Communications*, 11, 5088. <https://doi.org/10.1038/s41467-020-18685-1>.
- Justice, K.S. Puttaswamy (Retd.) & Anr. vs. UOI & Ors [(2017) 10 SCC 1, https://main.sci.gov.in/supremecourt/2012/35071/35071_2012_Judgement_26-Sep-2018.pdf
- Ke, Y. Y., Peng, T. T., Yeh, T. K., Huang, W. Z., Chang, S. E., et al. (2020). Artificial intelligence approach fighting COVID-19 with repurposing drugs. *Biomedical journal*, 43(4), 355–362. <https://doi.org/10.1016/j.bj.2020.05.001>

- Khan, Z. H., Siddique, A., & Lee, C. W. (2020). Robotics Utilization for Healthcare Digitization in Global COVID-19 Management. *International journal of environmental research and public health*, 17(11), 3819. <https://doi.org/10.3390/ijerph17113819>
- Khera, R., Liu, Y., de Lemos, J. A., Das, S. R., Pandey, A., et al. (2021). Association of COVID-19 Hospitalization Volume and Case Growth at US Hospitals with Patient Outcomes. *The American journal of medicine*, 134(11), 1380–1388.e3. <https://doi.org/10.1016/j.amjmed.2021.06.034>
- Kotter, E., & Ranschaert, E. (2021). Challenges and solutions for introducing artificial intelligence (AI) in daily clinical workflow. *European radiology*, 31(1), 5–7.
- Kuupiel, D., Bawontuo, V., & Mashamba-Thompson, T. P. (2017). Improving the Accessibility and Efficiency of Point-of-Care Diagnostics Services in Low- and Middle-Income Countries: Lean and Agile Supply Chain Management. *Diagnostics (Basel, Switzerland)*, 7(4), 58. <https://doi.org/10.3390/diagnostics7040058>
- Lee, D., & Yoon, S. N. (2021). Application of Artificial Intelligence-Based Technologies in the Healthcare Industry: Opportunities and Challenges. *International journal of environmental research and public health*, 18(1), 271. <https://doi.org/10.3390/ijerph18010271>
- Li, W. T., Ma, J., Shende, N., Castaneda, G., Chakladar, J., Tsai, J. C., et al. (2020). Using machine learning of clinical data to diagnose COVID-19: a systematic review and meta-analysis. *BMC medical informatics and decision making*, 20(1), 247. <https://doi.org/10.1186/s12911-020-01266-z>
- Linardatos, P., Papastefanopoulos, V., & Kotsiantis, S. (2020). Explainable AI: A Review of Machine Learning Interpretability Methods. *Entropy (Basel, Switzerland)*, 23(1), 18. <https://doi.org/10.3390/e23010018>
- Makhudu, S.J., Kuupiel, D., Gwala, N., & Mashamba-Thompson, T. (2019). The Use of Patient Self-Testing in Low- and Middle-Income Countries: A Systematic Scoping Review. *Point of Care: The Journal of Near-Patient Testing & Technology*, 18, 9–16.
- Marbough, D., Abbasi, T., Maasmi, F., Omar, I. A., Debe, M. S., et al. (2020). Blockchain for COVID-19: Review, Opportunities, and a Trusted Tracking System. *Arabian journal for science and engineering*, 45(12), 9895–9911.
- Mashamba-Thompson, T. P. & Crayton, E. D. (2020). Blockchain and Artificial Intelligence Technology for Novel Coronavirus Disease-19 Self-Testing. *Diagnostics (Basel)*, 10(4), 198.
- Metsky, H. C., Freije, C. A., Kosoko-Thoroddsen, T. S. F., Sabeti, P. C. & Myhrvold, C. (2020). CRISPR-based surveillance for COVID-19 using genomically-comprehensive machine learning design. Biorxiv preprint. <https://doi.org/10.1101/2020.02.26.96702>
- Ministry of Electronics & Information Technology, Government of India, (2023). <https://www.meity.gov.in/artificial-intelligence-committees-reports> last accessed 24/01/2023
- Mishra, T., Wang, M., Metwally, A. A., Bogu, G. K., Brooks, A. W., Bahmani, A., et al. (2020). Pre-symptomatic detection of COVID-19 from smartwatch data. *Nature biomedical engineering*, 4(12), 1208–1220. <https://doi.org/10.1038/s41551-020-00640-6>
- Miyake, S., Higurashi, T., Kato, H., Yamaoka, Y., Kessoku, T., et al. (2021). Evaluation of a combination protocol of CT-first triage and active telemedicine methods by a selected team tackling COVID-19: An experimental research study. *Journal of infection and public health*, 14(9), 1212–1217. <https://doi.org/10.1016/j.jiph.2021.08.016>
- Mohanty, S., Harun Ai Rashid, M., Mridul, M., Mohanty, C., & Swayamsiddha, S. (2020). Application of Artificial Intelligence in COVID-19 drug repurposing. *Diabetes & metabolic syndrome*, 14(5), 1027–1031. <https://doi.org/10.1016/j.dsx.2020.06.068>
- Moore, J. H., Barnett, I., Boland, M. R., Chen, Y., Demiris, G., Gonzalez-Hernandez, G., et al. (2020). Ideas for how informaticians can get involved with COVID-19 research. *BioData mining*, 13, 3. <https://doi.org/10.1186/s13040-020-00213-y>
- Moreno, H. (2020). The Importance of Data Quality-Good, Bad or Ugly. Forbes. Retrieved from: <https://www.forbes.com/sites/forbesinsights/2017/06/05/the-importance-of-data-quality-good-bad-or-ugly/#614a247a10c4>
- Mousavizadeh, L., & Ghasemi, S. (2021). Genotype and phenotype of COVID-19: Their roles in pathogenesis. *Journal of microbiology, immunology, and infection = Wei mian yu gan ran za zhi*, 54(2), 159–163.
- Naudé, W. (2020). Artificial intelligence vs COVID-19: limitations, constraints and pitfalls. *AI & society*, 35(3), 761–765. <https://doi.org/10.1007/s00146-020-00978-0>
- Office Memorandum, Ministry of Electronics & Information Technology, Government of India (2018). https://www.meity.gov.in/writereaddata/files/constitution_of_four_committees_on_artificial_intelligence.pdf last accessed 24/01/2023
- Ong, E., Wong, M. U., Huffman, A., & He, Y. (2020). COVID-19 Coronavirus Vaccine Design Using Reverse Vaccinology and

- Machine Learning. *Frontiers in immunology*, *11*, 1581. <https://doi.org/10.3389/fimmu.2020.01581>
- Panwar, H., Gupta, P. K., Siddiqui, M. K., Morales-Menendez, R., & Singh, V. (2020). Application of deep learning for fast detection of COVID-19 in X-Rays using nCOVnet. *Chaos, solitons, and fractals*, *138*, 109944.
- Pinzi, L., & Rastelli, G. (2019). Molecular docking: Shifting paradigms in drug discovery. *International Journal of Molecular Sciences*, *20*(18), 4331.
- Prachar, M., Justesen, S., Steen-Jensen, D. B., Thorgrimsen, S., Jurgons, E., Winther, O., & Bagger, F. O. (2020). Identification and validation of 174 COVID-19 vaccine candidate epitopes reveals low performance of common epitope prediction tools. *Scientific reports*, *10*(1), 20465. <https://doi.org/10.1038/s41598-020-77466-4>
- Randhawa, G. S., Soltysiak, M. P. M., El Roz, H., de Souza, C. P. E., Hill, K. A., & Kari, L. (2020). Machine learning using intrinsic genomic signatures for rapid classification of novel pathogens: COVID-19 case study. *bioRxiv* 932350 [Preprint]. Retrieved from: <https://www.biorxiv.org/content/10.1101/2020.02.03.932350v3>.
- Regla-Nava, J. A., Nieto-Torres, J. L., Jimenez-Guardeño, J. M., Fernandez-Delgado, R., Fett, C., et al. (2015). Severe acute respiratory syndrome coronaviruses with mutations in the E protein are attenuated and promising vaccine candidates. *Journal of virology*, *89*(7), 3870–3887. <https://doi.org/10.1128/JVI.03566-14>
- Report of committee – D on cyber security, safety, Legal and ethical issues, Ministry of Electronics & Information Technology, Government of India (2023). Retrieved from https://www.meity.gov.in/writereaddata/files/Committees_D-Cyber-n-Legal-and-Ethical.pdf last accessed 24/01/2023
- Rezaei, N., & Grandner, M. A. (2021). Changes in sleep duration, timing, and variability during the COVID-19 pandemic: Large-scale Fitbit data from 6 major US cities. *Sleep Health*, *7*(3), 303–313.
- Salama, M. A., Hassanien, A. E., & Mostafa, A. (2016). The prediction of virus mutation using neural networks and rough set techniques. *EURASIP journal on bioinformatics & systems biology*, *2016* (1), 10. <https://doi.org/10.1186/s13637-016-0042-0>.
- Sammut, C., & Webb, G.I. (Eds.) (2017). *Encyclopedia of machine learning and datamining*. 2nd edn, Springer, Boston, MA.
- Santosh K. C. (2020). AI-Driven Tools for Coronavirus Outbreak: Need of Active Learning and Cross-Population Train/Test Models on Multitudinal/Multimodal Data. *Journal of medical systems*, *44*(5), 93. <https://doi.org/10.1007/s10916-020-01562-1>
- Seshadri, D. R., Davies, E. V., Harlow, E. R., Hsu, J. J., Knighton, S. C., Walker, T. A., Voos, J. E., & Drummond, C. K. (2020). Wearable Sensors for COVID-19: A Call to Action to Harness Our Digital Infrastructure for Remote Patient Monitoring and Virtual Assessments. *Frontiers in digital health*, *2*, 8. <https://doi.org/10.3389/fdgh.2020.00008>
- Singh, G.A.P., & Gupta, P. (2019). Performance analysis of various machine learning-based approaches for detection and classification of lung cancer in humans. *Neural Computing and Applications*, *31*(10), 6863–6877.
- Summers, R.M. (2021). Artificial Intelligence of COVID-19 Imaging: A Hammer in Search of a Nail. *Radiology*, *298* (3), E162-E164.
- Tayfur, İ., & Afacan, M. A. (2019). Reliability of smartphone measurements of vital parameters: A prospective study using a reference method. *The American journal of emergency medicine*, *37*(8), 1527–1530.
- Teo J. (2020). Early Detection of Silent Hypoxia in Covid-19 Pneumonia Using Smartphone Pulse Oximetry. *Journal of medical systems*, *44*(8), 134.
- Vaishya, R., Javaid, M., Khan, I. H., & Haleem, A. (2020). Artificial Intelligence (AI) applications for COVID-19 pandemic. *Diabetes & metabolic syndrome*, *14*(4), 337–339.
- Wadden J. J. (2021). Defining the undefinable: the black box problem in healthcare artificial intelligence. *Journal of medical ethics*, *48* (10),107529. <https://doi.org/10.1136/medethics-2021-107529>.
- Wang, Y., Hu, M., Li, Q., Zhang, X.P., Zhai, G., & Yao, N. (2020). Abnormal respiratory patterns classifier may contribute to large-scale screening of people infected with COVID-19 in an accurate and unobtrusive manner. *arXiv*2002.05534 [Preprint]. Retrieved From: <https://arxiv.org/abs/2002.05534>
- Webster P. (2020). Virtual health care in the era of COVID-19. *Lancet*, *395*(10231), 1180-1181.
- WHO. (2019). Telemedicine: Opportunities and Developments in Member State. <https://www.afro.who.int/publications/telemedicine-opportunities-and-developments-member-state>
- Wurzer, D., Spielhagen, P., Siegmann, A., Gercekcioglu, A., Gorgass, J., et al. (2021). Remote monitoring of COVID-19 positive high-risk patients in domestic isolation: A feasibility

- study. *PLoS one*, 16(9), e0257095. <https://doi.org/10.1371/journal.pone.0257095>
- Yan, L., Zhang, H-T., Xiao, Y., Wang, M., Guo, Y., et al. (2020). Prediction of survival for severe Covid-19 patients with three clinical features: development of a machine learning-based prognostic model with clinical data in Wuhan. *medRxiv* 20028027 [Preprint]. Retrieved from: <https://www.medrxiv.org/content/10.1101/2020.02.27.20028027v3>.
- Zampieri, F. G., Costa, E. L., Iwashyna, T. J., Carvalho, C. R. R., Damiani, L. P., Taniguchi, L. U., Amato, M. B. P., Cavalcanti, A. B., & Alveolar Recruitment for Acute Respiratory Distress Syndrome Trial Investigators (2019). Heterogeneous effects of alveolar recruitment in acute respiratory distress syndrome: a machine learning reanalysis of the Alveolar Recruitment for Acute Respiratory Distress Syndrome Trial. *British journal of anaesthesia*, 123(1), 88–95. <https://doi.org/10.1016/j.bja.2019.02.026>
- Zeng, X., Song, X., Ma, T., Pan, X., Zhou, Y., et al. (2020). Repurpose Open Data to Discover Therapeutics for COVID-19 Using Deep Learning. *Journal of proteome research*, 19(11), 4624–4636. <https://doi.org/10.1021/acs.jproteome.0c00316>.
- Zhang, H., Saravanan, K. M., Yang, Y., Hossain, M. T., Li, J., Ren, X., Pan, Y., & Wei, Y. (2020). Deep Learning Based Drug Screening for Novel Coronavirus 2019-nCov. *Interdisciplinary sciences, computational life sciences*, 12(3), 368–376. <https://doi.org/10.1007/s12539-020-00376-6>.
- Zhang, Q., Xie, Q., & Wang, G. (2016). A Survey on Rough Set Theory and Its Applications. *CAAI Transactions on Intelligence Technology*, 1(4), 323-333.
- Zhavoronkov, A., Aladinskiy, V., Zhebrak, A. et al. (2020). Potential COVID-2019 3C-like Protease Inhibitors Designed Using Generative Deep Learning Approaches. *In silico Med Hong Kong Ltd A*. 307, E1.



Journal of Experimental Biology and Agricultural Sciences

<http://www.jebas.org>

ISSN No. 2320 – 8694

Residue-specific orientation of arrestin in 5-HTR_{1B} (Serotonin Receptor)- βArrestin-1 interaction

Somdatta Bhattacharya¹ , Joydeep Paul¹ , Srijan Haldar³ , Kuntal Pal^{1,2*} 

¹Department of Biotechnology, School of Life Science and Biotechnology, Adamas University, Barasat-Barrackpore Road, Kolkata-700126, West Bengal, India.

²School of Biosciences and Technology (SBST), Vellore Institute of Technology, 632014, Vellore, Tamil Nadu, India

³Department of Biochemistry, School of Life Science and Biotechnology, Adamas University, Barasat-Barrackpore Road, Kolkata-700126.

Received – October 31, 2023; Revision – December 31, 2023; Accepted – January 15, 2024

Available Online – March 15, 2024

DOI: [http://dx.doi.org/10.18006/2024.12\(1\).138.144](http://dx.doi.org/10.18006/2024.12(1).138.144)

KEYWORDS

G protein-coupled receptor

Neurotensin receptor

β-Arrestin1, 5-HTR_{1B}

90 rotation

Tango assay

ABSTRACT

Physiologically G protein-coupled receptors (GPCRs) are an important class of cell surface proteins capable of sensing the exogenous signals across the cell membrane through G-protein-dependent and independent pathways. Activated GPCRs initiate diverse G-protein-independent signalling through interaction with arrestin. Arrestins comprise a family of four proteins that act as signal regulators of GPCRs. Arrestin specificity and assembly orientation with a particular GPCR depend on the finger loop's residues. Recent cryo-EM structural elucidation of neurotensin receptor-1(NTSR1)-β-arrestin1 complex reveals its striking difference from Rhodopsin-visual-Arrestin by a 90° rotation of β-Arrestin1 concerning the receptor. Alignment of neurotensin receptor 1(NTSR1)-β-Arrestin1 assembly with 5-HTR_{1B} (Serotonin receptor) structure shows an ionic interaction mediated complex formation between receptor binding cleft and finger loop of arrestin. Mutational analysis of finger loop residues R65, D67, and D69 of β-Arrestin1 by tango assay confirms its possible interaction with an electropositive pocket of K79 and R161 in 5-HTR_{1B}.

* Corresponding author

E-mail: kuntal.pal@vit.ac.in (Kuntal Pal)

Peer review under responsibility of Journal of Experimental Biology and Agricultural Sciences.

Production and Hosting by Horizon Publisher India [HPI]
(<http://www.horizonpublisherindia.in/>).
All rights reserved.

All the articles published by [Journal of Experimental Biology and Agricultural Sciences](#) are licensed under a [Creative Commons Attribution-NonCommercial 4.0 International License](#) Based on a work at www.jebas.org.



1 Introduction

The structural analysis of GPCRs are critical for innovative cell signalling process findings. The 5% of the human genome coding for GPCRs makes it one of the largest families of membrane-bound proteins (Yin et al. 2019). These molecules, being one of their kind, represent a giant class of receptors having more than 850 participants responsible for their multivarious roles in the physiology of the living world. Both endogenous and exogenous signals control these receptors. They are majorly responsive to hormones, metabolites, and even numerous neurotransmitters. GPCRs are controlled by two important regulators, the G-protein and the arrestins. GPCRs with seven membrane-spanning domains are convenient for the ligands to access and are important drug targets due to their functioning through downstream signalling (Yin et al. 2019; Yang et al. 2021). GPCRs signalling may occur via G-proteins or through Arr1 and Arr2. The activated GPCRs, upon initiating the G-proteins downstream pathways subsequently recruit some unique molecules such as G-receptor kinases (GRKs). GRKs add phosphate groups at specific Ser and Thr positions of GPCRs' cytoplasmic loops and tail, allowing them to bind specifically to the arrestins. As the receptors bind to arrestins, their interactions with G-proteins affect their deactivation. Interestingly, different G-protein-independent cellular signalling pathways are directed by the arrestins interaction with the GPCRs (Figure 1). The arrestin-mediated signalling is crucial for GPCR desensitization and recycling (Yang et al. 2021). GPCRs classification suggests the

presence of six different classes, segregated by sequence conservation. The biggest one is Class A, represented by Rhodopsin, the smallest one is Class B, such as the Secretin receptor, and others are classified as Class C or glutamate receptor, Class D or fungal mating pheromone receptor, Class E or cyclic AMP receptor and Class F of Frizzled receptors. The last decade witnessed a behemoth paradigm in GPCR structural biology and was considered the 'golden era' of GPCR research. The Class A type GPCR comprises the family of rhodopsin-like receptors with 719 members subdivided into subgroups like sensory receptors, orphan receptors and others including the peptide, protein, lipid, melatonin, nucleotide, alicarboxylic acid, aminergic, etc. which are the most physiologically active and are effective for targeting of drugs (Basith et al. 2018; Yang et al. 2021). The two major pathways, G-protein and arrestin, are found to operate exclusively through biased GPCR-based ligands, which specifically regulate either arrestin or G-protein-mediated pathways (Reiter et al. 2012). The GPCR ligands are biased and are a better alternative than unbiased activators and inhibitors, as they can induce the receptor to promote the binding of a group of selective partners, which might be therapeutically beneficial with negligible side effects. The research is found to progress more towards biased ligands, which turned out to be new-generation drugs targeting and moderating the function of GPCR- (Kenakin 2012). Furthermore, the role of GPCRs in cancer metastasis and angiogenesis via the efficacious crosstalk mechanism with receptor tyrosine kinases has also been thoroughly investigated (Mandal et al. 2021).

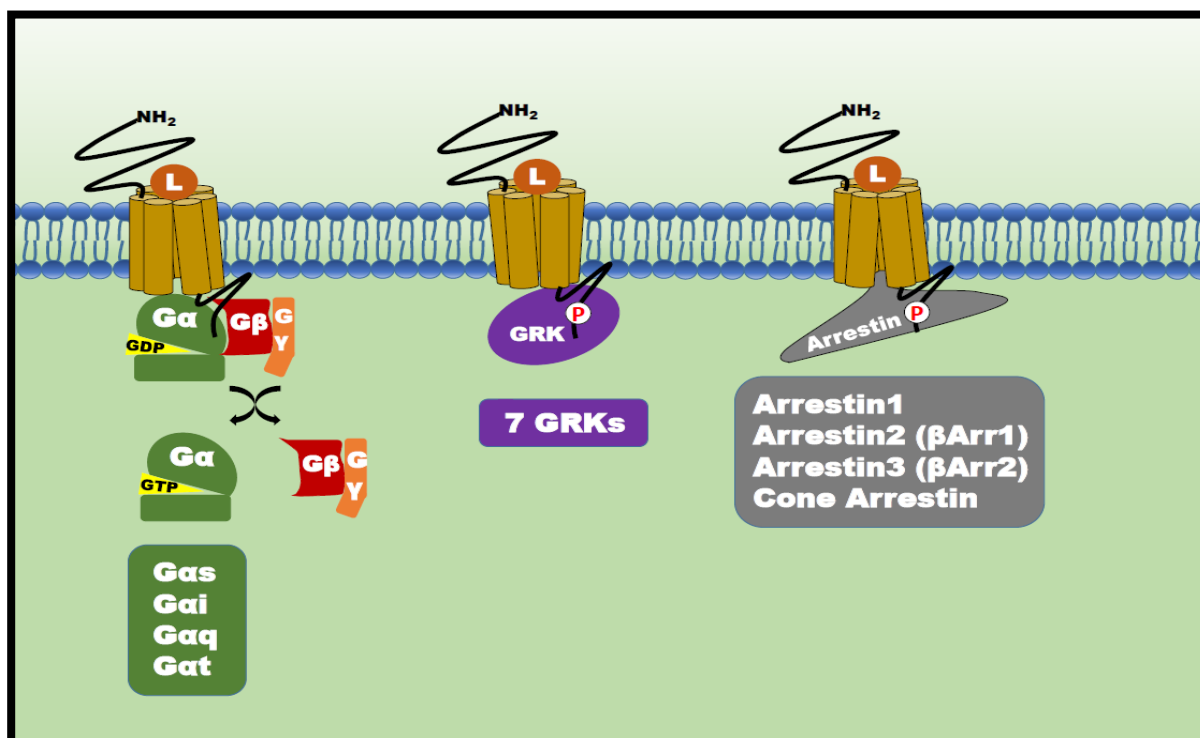


Figure 1 Detailed overview of GPCR Signalling mechanism with different binding partners

1.1 The Serotonin Receptor

The 5-HT (5-hydroxytryptamine) receptors, better known as serotonin receptors, are an important category of receptors that transmit signals across synaptic clefts and are abundant in the neurons. The neurotransmitter serotonin is released from the serotonergic neurons of the brain. It has been observed from various studies that their level rises considerably in neurological tissues that have undergone damage or injury (Sommer 2004). Serotonin and its receptors have been associated with multiple psychiatric and neurological disorders, from regular headaches and migraines to severe and complex consequences like schizophrenia and depression (Berger et al. 2009; McCorvy and Roth 2015). The serotonin receptors modify the secretion of many neurotransmitters, including acetylcholine, dopamine, glutamate, epinephrine/norepinephrine, etc. They are essential mediators of different hormones like oxytocin, vasopressin, prolactin, etc. The Serotonin receptors are the key regulators that influence some of the important neurological processes, and any impairment in its function may lead to disorders like depression, anxiety, cognition loss, etc. Thus, they constitute an important class of drug targets for various types of drugs, contributing to hallucinogens, antidepressants, antipsychotics and antimigraine agents. Being abundant in central and peripheral nervous systems, 14 types of receptors are being discovered, of which 13 are GPCRs targeting almost 40% of the FDA-approved drugs (McCorvy and Roth 2015; Jean-Charles et al. 2017). Due to the stressful lifestyle, people tend to suffer more from migraine and anxiety, leading to more consumption of non-specific medications, which may cause adverse health hazards and have been implicated in causing irreversible damage to the nervous system. A detailed investigation has become the need of the day to explore the structural details of the serotonin receptor- β -arrestin complex. The importance of the serotonin receptor as a potential drug target; hence, it is more

likely that this unique structural complex that has not been investigated to date might turn out to be a promising target for drug discovery.

1.2 The negative or positive regulators of GPCRS: Arrestins?

The Arrestins are in the important family of signal-regulating molecules for GPCRS. It includes four types of arrestins viz., Arrestin 1-4. The arrestins 1 and 4 (visual and cone arrestin) are usually more specifically functional to the rhodopsins, while the other two arrestins 2-3 (β Arr1 and β Arr2) are found to modulate the signalling of many non-visual GPCRS (Yin et al. 2019). GPCRS are cytosolic adaptor proteins previously known to restrain GPCR signalling initiated through G proteins. It has been further biochemically identified that the arrestins do not necessarily 'halt' the signal transduction of GPCRS. Instead, they facilitate endocytosis and kinase activation, which leads to other signalling pathways specific to its position in the endosomes. The signalling promoted by β -arrestins has been revealed as being independent of G-protein activation (Wang et al. 2013). Here, we tried elucidating the serotonin receptor conformation as a drug target through its interaction with β -Arrestin1.

1.3 The Structure of Ergotamine bound 5HTR_{1B}

The Serotonin receptor variant in our study is 5-HT_{1B}. This receptor is mainly found to be abundant in the basal ganglia and lesser numbers in the other regions of the nervous system like the amygdala, cerebral cortex, and hypothalamus. The axon terminals of neurons are sites for 5-HTR_{1B} receptors. This receptor is widely studied for its pivotal role in the development of aggression, cognition, memory, addiction, etc., making it an impeccable drug target. The previously solved structure of 5-HTR_{1B} with Ergotamine (PDB: 4IAQ) in the absence of the third intracellular loop ICL3 shown in Figure 2a was solved and published by Wang

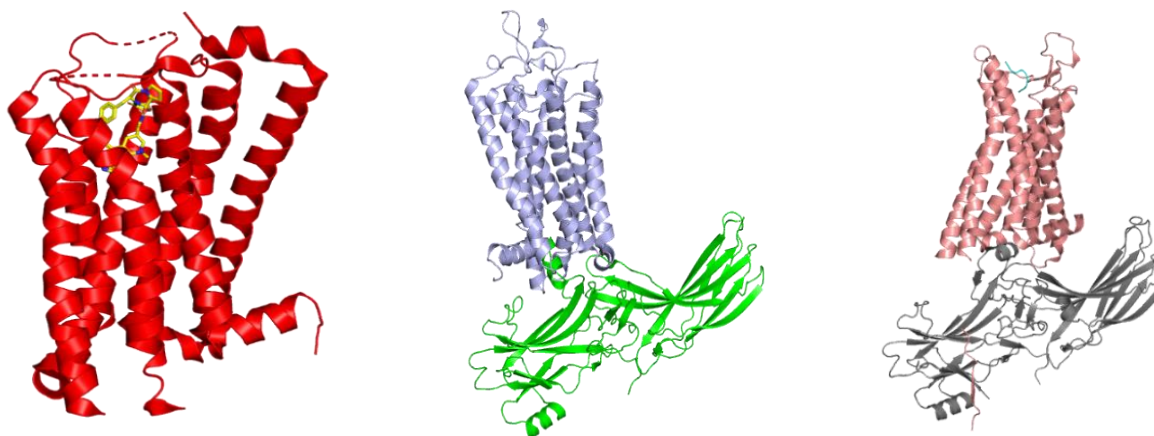


Figure 2 (a) The molecular state of Ergotamine bound 5HTR_{1B}, (PDB: 4IAQ), (b) The structural organization of Rhodopsin (Blue)- β -arrestin (Green) complex, (PDB: 4ZWJ), (c) The cryo-EM structure of NTSR-1(Salmon) - β -arrestin1 (Grey) complex, (PDB: 6PWC).

et al. (2013). This was the first structural insight of receptors that became crucial for all future biochemical studies and homology modelling. The structure revealed similar binding modes for the ligands Ergotamine and dihydroergotamine. These ligands were found to occupy orthosteric pockets, which have been created by the conserved residues of the 5-hydroxytryptamine receptor family, that provide evidence in support of family-wide agonist activity of 5-hydroxytryptamine (Wang et al., 2013; Kang et al., 2015).

1.4 The Structural organization of the Rhodopsin-visual Arrestin complex

Another breakthrough in the research of structural GPCR came in 2015 when Yang et al. (2015) published the structural state attained by Rhodopsin with visual arrestin solved by an X-ray laser light source shown in Figure 2b. An attractive feature of this structural complex was that arrestins bind asymmetrically to rhodopsin, hence found to be identical among four molecules in the asymmetric unit and that supports conformational uniqueness of rhodopsin-arrestin assembly. This work was the first to report the molecular state of a GPCR docked to arrestins, which further supports the investigation of structural plasticity associated with arrestin-biased signalling (Kang et al. 2015)

1.5 The molecular state of NTSR-1- β -arrestin1 Complex

In 2019, the same group unraveled the molecular state of Neurotensin Receptor occupied by β -Arrestin-1 by cryo-EM

method for the first time, as shown in Figure 2c. The same group associated with the experimental paper conducted an interesting experiment with the Rhodopsin-v-arrestin complex and NTSR-1- β -arrestin1 complex structures. The two structures were superposed to observe the relative orientation of the two types of arrestins. It showed that the arrestins were positioned at two significantly distinct orientations, which were about 90° rotated around the axis that was vertical to the plasma-membrane layer. Despite being similar kinds of molecules, the complexes revealed a marked difference in the orientation of arrestins to the receptors. The alignment of the transmembrane domains of these two complexes revealed the Arr2 orientation turned by 90° along the visual arrestin axis (Figure 3). Such a facsimile has conferred an overt range of dynamism. Moreover, the interaction of rhodopsin with v-arrestin and NTSR-1 with β -Arrestin1 opened a new avenue for GPCR research and confirmed that specific interaction is a significant aspect of drug designing.

1.6 The structural Alignment of NTSR-1- β -arrestin1 complex with 5HTR_{1B}

A structural alignment of Neurotensin receptor 1(NTSR1)- β -Arrestin1 assembly with Serotonin receptor (5-HTR_{1B}) was designed to understand the interaction between β -arrestin 1 and the serotonin receptor by visualizing in PyMOL as there is no known structure to date. Following the alignment, we deleted the NTSR-1 receptor from the NTSR-1-5HTR_{1B}- β -arrestin1 complex to investigate a closer interaction between 5HTR_{1B} and β -arrestin1

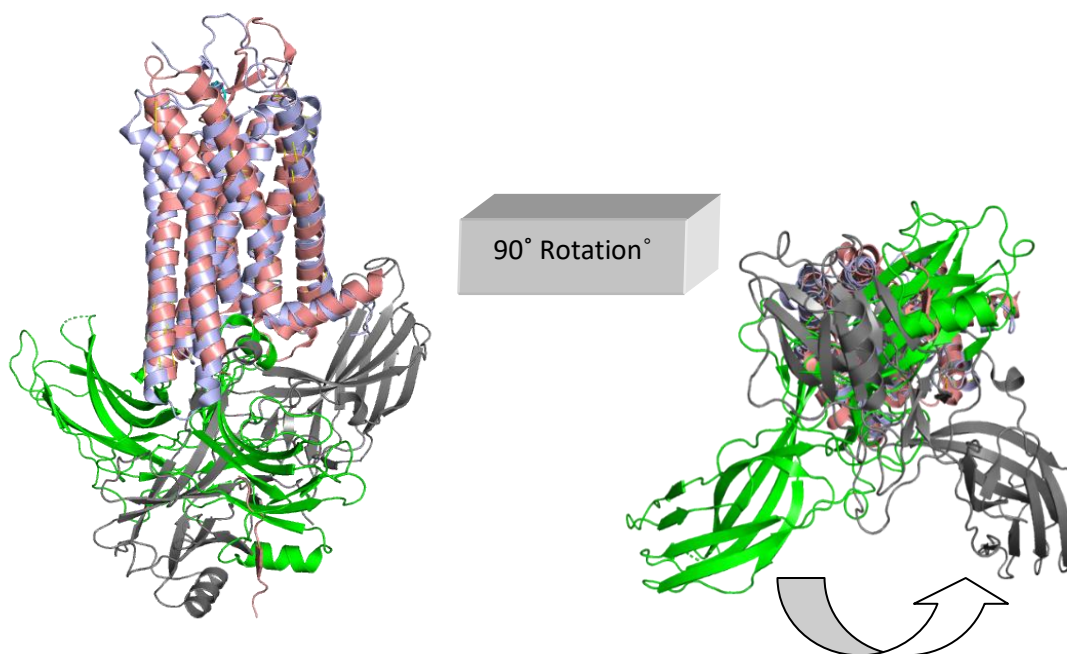


Figure 3 (a) Structural alignment of Rhodopsin (Blue) v-arrestin (green) with NTSR-1(Salmon), β -arrestin1 (Grey), (b) Cytoplasmic view of v arrestin vs. β -arrestin1 position after 90 ° rotation

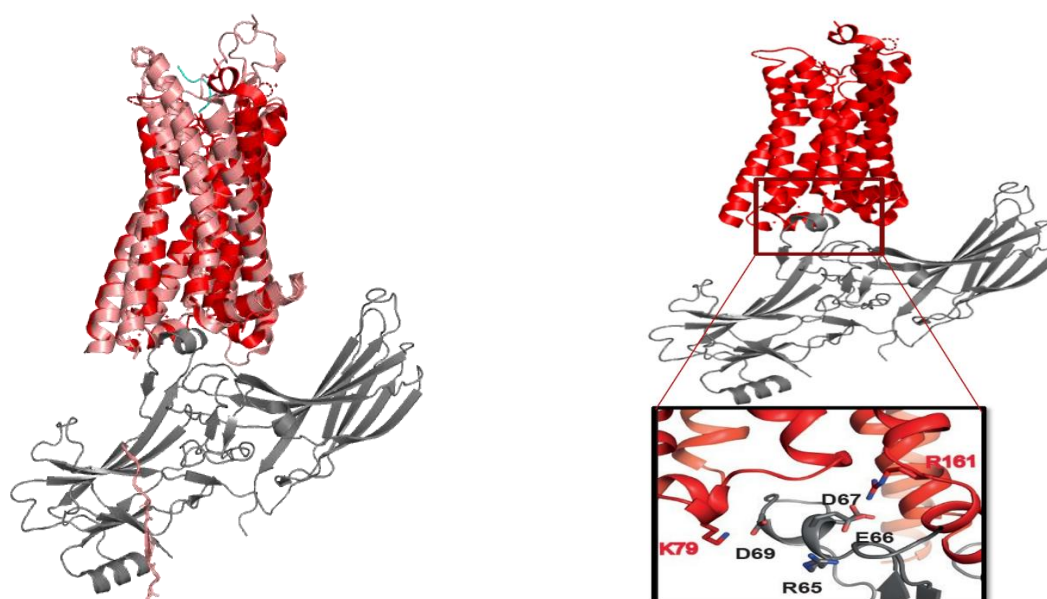


Figure 4 (a) Alignment and identification of residues participating in the 5HTR_{1B}-β-Arrestin 1 complex. 5HTR_{1B} (Red), NTSR-1 (Salmon), β-Arrestin1 (Grey); (b) A closed look at the participating residues in the 5HTR_{1B}-β-Arrestin1 complex

(Figure 4a and b). It has shown striking results, identifying specific and unique residues that are gravely engaged in the ligand-receptor interaction. Notably, such residues are not found in the NTSR-1 receptor but only in 5HTR_{1B}, confirming the stringent specificity of such interactions (Yin et al. 2019).

2 Materials and methods

2.1 Construct preparation

The complex formed by the Biological Resource Imaging Laboratory (BRIL), NTSR1-Arr2-Fab30, has been taken as a structural reference for our experimental studies. The structures referred for studies conducted for this paper are the human Neurotensin receptor 1 (NTSR1) (UniProtKB ID: P30989), the human Arrestin-2 with 3A mutations (residues 1-3334 I386A, V387A, F388A, UniProtKB ID: P49407), and the human Serotonin receptor (5HTR_{1B}) with UniProtKB ID: P28222. The Arr2 mutants were cloned into pcDNA6 vector, modified to encode 3× Flag tags at the C-terminal. The 5-HTR_{1B} receptor was PCR amplified and cloned into pcDNA6, previously modified to encode Hemagglutinin (3× HA) tags at the C-termini. The information from PDB structures (4IAQ, 4ZJW and 6PWC) and their sequence alignments were used to design the mutations to probe the receptor/arrestin interface (Kang et al. 2015; Yin et al. 2019).

2.2 Site-directed Mutagenesis

The finger loop mutations of β-Arrestin1 were designed by Site-directed mutagenesis. The mutation constructs were created by the

quick-change method (Agilent). The protein sequencing was performed to confirm all plasmid constructs before protein expression and protein interaction studies by Tango-Assay (Kang et al., 2015; Yin et al., 2019).

2.3 Tango Assay

The Tango Assay was performed with pcDNA6.1 vector carrying 5HTR_{1B} wild-type receptor (1-418). cDNA in the fusion of tobacco etch virus protease (TEV protease) cut site followed by transcriptional inducer tTa at the C-termini of vector in the expression cassette (pcDNA6-5HTR_{1B}-TEV site-tTA). Similarly, the Arr2(1-393, wild type) construct was prepared by fusing it with cDNA of TEV protease at C-termini (pcDNA-Arr2-TEV protease), which will be responsible for cleaving the reporter gene (Figure 5a,b). The possible interacting residues between 5HTR_{1B} and Arr2, if in proximity, will result in TA's separation by cutting at the TEV site, which activates the expression of reporter gene TA-dependent luciferase. Before conducting the assay in HTLA cells, a 24-hour culture of cells in a 24-well plate was done to a population of 5×10^4 cells/well. This was followed by cotransfection with Arr2-TEV protease (10 ng) plasmids, 5HTR_{1B}-TEVsite-tTA (10 ng) and phRG-tkRenilla luciferase-expressing plasmid (5 ng) utilizing Xtreme GENE 9 DNA Transfection Reagent (Roche). The cells were transfected for 24 hours and kept in 24 well plate overnight with PBS (vehicle), 50 μM Ergotamine, and 5 μM ML314, respectively. Then, luciferase assay was used to evaluate the interactions following the protocol provided by Dual-Luciferase Kit (Promega) (Kang et al. 2015; Yin et al. 2019).

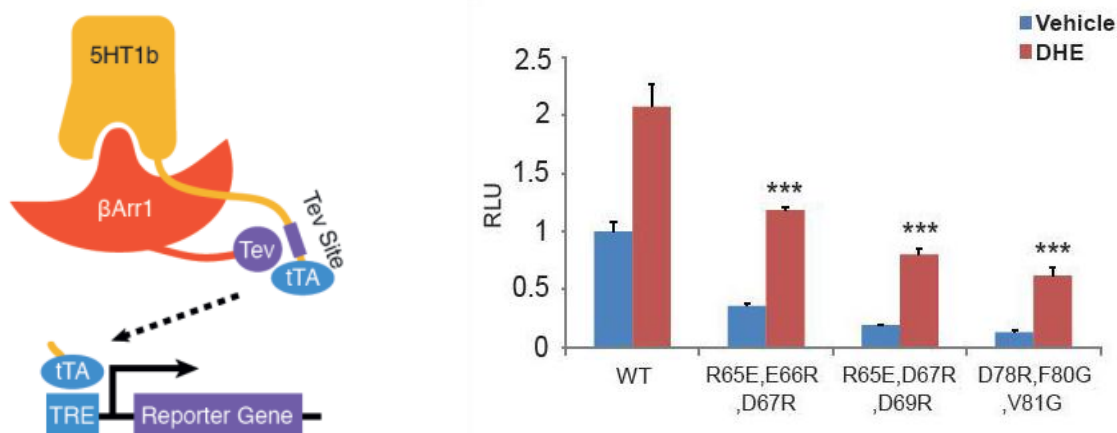


Figure 5 (a) The amino acid-mediated interaction between 5HTR_{1B}- β -arrestin1 by Tango Assay; (b) A detailed graphical depiction of the Ergotamine-bound serotonin receptor- β -arrestin1 interaction in the wild type and the mutant arrestin residues showing a gradual decrease in the interaction, confirming a specific interaction between them.

3 Results and Discussion

The amino acid-mediated interaction interface between the serotonin receptor and β -arrestin1. A remarkable GPCR analytical assay binds the receptor to arrestin, leading to GPCR desensitization. Our study was conducted with the Serotonin receptor and β -arrestin1. A successful receptor-ligand binding could be confirmed by Tango Assay, where β -arrestin1 has an attached Tev protease cassette, and the serotonin receptor has a Tev cleavage site. On successful interaction between the receptor binding cleft of serotonin receptor and the β -arrestin1 finger loop, cleavage of the protease site results, confirming the interactions leading to further cues for studying and identifying the residues participating in the 5HTR_{1B}- β -Arrestin1 complex formation. A detailed investigation of β -arrestin1 and 5-HTR_{1B} (Serotonin receptor) provided astounding findings. It was observed that some intricate ionic and hydrophobic interactions mediated complex formation between receptor binding cleft and finger loop of β -arrestin1. Some specific mutations were generated, R65, D67 and D69, in the finger loop of β -arrestin1 by Tango assay, confirming arrestin's possible interaction with the electropositive pocket of K79 and R161 in 5-HTR_{1B}. The interaction between the Ergotamine-bound serotonin receptor- β -arrestin1 complex showed well-ordered interaction.

In contrast, the various mutants generated in the finger loop of β -arrestin1 showed a decreased degree of interaction because serotonin possibly interacts specifically with β -arrestin1. The interaction seems to be mediated by the ionic and hydrophobic interactions. It is also important to understand the molecular conformation of long ICL3 of 5HTR_{1B} while in complex with arrestin. The exchanges are highly GPCR sequence-specific. Similarly, the role of phosphorylation sites in ICL3 was evaluated by biochemical studies (Gupta et al. 2023)

Conclusions

The mutations generated in the β -arrestin1 finger loop display a unique possibility of interaction between β -arrestin1 and 5HTR_{1B} receptors. This implication can be exploited for new research avenues and has been found to add another bright feather to the insurmountable progress in GPCR research. This development has rendered the serotonin receptor a vital drug target with options in the future direction. This paper contributes to the significance of the specificity of the interaction of the ligand-receptor complex. This study can also contribute to drug design, assist with virtual screening, and develop vaccines for treating cancer and other deadly diseases in the near future, which will be a boon to humanity.

Acknowledgement

Nil

Conflict of Interest

The authors declare that there is no conflict of interest.

Appendices

The protein structures have been prepared in PyMOL. (Reference: <https://pymol.org/2>). The notion of experimental design and sample preparation techniques were taken from the corresponding author's paper published in 2015 (Reference 1 and 12).

References

Basith, S., Cui, M., Macalino, S. J. Y., Park, J., Clavio, N. A. B., Kang, S., & Choi, S. (2018). Exploring G Protein-Coupled Receptors (GPCRs) Ligand Space via Cheminformatics

- Approaches: Impact on Rational Drug Design. *Frontiers in pharmacology*, 9, 128. <https://doi.org/10.3389/fphar.2018.00128>
- Berger, M., Gray, J. A., & Roth, B. L. (2009). The expanded biology of serotonin. *Annual review of medicine*, 60, 355–366. <https://doi.org/10.1146/annurev.med.60.042307.110802>
- Gupta, D.O., Karbat, I., & Pal, K. (2023). Understanding the Molecular Regulation of Serotonin Receptor 5-HTR_{1B}- β -Arrestin1 Complex in Stress and Anxiety Disorders. *Journal of molecular neuroscience : MN*, 73(7-8), 664–677. <https://doi.org/10.1007/s12031-023-02146-7>
- Jean-Charles, P. Y., Kaur, S., & Shenoy, S. K. (2017). G Protein-Coupled Receptor Signaling Through β -Arrestin-Dependent Mechanisms. *Journal of cardiovascular pharmacology*, 70(3), 142–158. <https://doi.org/10.1097/FJC.0000000000000482>
- Kang, Y., Zhou, X. E., Gao, X., He, Y., Liu, W., et al. (2015). Crystal structure of rhodopsin bound to arrestin by femtosecond X-ray laser. *Nature*, 523(7562), 561–567. doi:10.1038/nature14656
- Kenakin T. P. (2012). Biased signalling and allosteric machines: new vistas and challenges for drug discovery. *British journal of pharmacology*, 165(6), 1659–1669. <https://doi.org/10.1111/j.1476-5381.2011.01749.x>
- Mandal, S., Chakrabarty, D., Bhattacharya, A., Paul, J., Haldar, S., & Pal, K. (2021). miRNA regulation of G protein-coupled receptor-mediated angiogenic pathways in cancer. *Nucleus*, 64, 303–315. <https://doi.org/10.1007/s13237-021-00365-0>
- McCorvy, J. D., & Roth, B. L. (2015). Structure and function of serotonin G protein-coupled receptors. *Pharmacology & therapeutics*, 150, 129–142. <https://doi.org/10.1016/j.pharmthera.2015.01.009>
- Reiter, E., Ahn, S., Shukla, A. K., & Lefkowitz, R. J. (2012). Molecular mechanism of β -arrestin-biased agonism at seven-transmembrane receptors. *Annual review of pharmacology and toxicology*, 52, 179–197. <https://doi.org/10.1146/annurev.pharmtox.010909.105800>
- Sommer C. (2004). Serotonin in pain and analgesia: actions in the periphery. *Molecular neurobiology*, 30(2), 117–125. <https://doi.org/10.1385/MN:30:2:117>
- Wang, C., Jiang, Y., Ma, J., Wu, H., Wacker, D., et al. (2013). Structural basis for molecular recognition at serotonin receptors. *Science*, 340(6132), 610–614. doi:10.1126/science.1232807
- Yang, D., Zhou, Q., Labroska, V., Qin, S., Darbalaei, S., et al. (2021). G protein-coupled receptors: structure- and function-based drug discovery. *Signal transduction and targeted therapy*, 6(1), 7. <https://doi.org/10.1038/s41392-020-00435-w>
- Yang, L., Yang, D., de Graaf, C., Moeller, A., West, G.M., et al. (2015). Conformational states of the full-length glucagon receptor. *Nature Communications*, 6, 7859. <https://doi.org/10.1038/ncomms8859>
- Yin, W., Li, Z., Jin, M., Yin, Y. L., de Waal, P. W., et al. (2019). A complex structure of arrestin-2 bound to a G protein-coupled receptor. *Cell research*, 29(12), 971–983. <https://doi.org/10.1038/s41422-019-0256-2>



Journal of Experimental Biology and Agricultural Sciences

<http://www.jebas.org>

ISSN No. 2320 – 8694

Analyzing the antimicrobial efficacy of the economically important tree *Knema linifolia* (Roxb.) Warb

Ria Bhar¹, Arpita Das¹, Srijan Haldar^{2*}, Joydeep Paul^{1*} 

¹Department of Biotechnology, School of Life Science and Biotechnology, Adamas University, Kolkata, India

²Department of Biological Sciences, School of Life Science and Biotechnology, Adamas University, Kolkata, India

Received – October 31, 2023; Revision – December 31, 2023; Accepted – January 15, 2024

Available Online – March 15, 2024

DOI: [http://dx.doi.org/10.18006/2024.12\(1\).145.152](http://dx.doi.org/10.18006/2024.12(1).145.152)

KEYWORDS

Knema linifolia

Antibacterial

Crude extract

Phytochemical

Ethno-medicine

ABSTRACT

Knema linifolia is widely used for fuel wood, fodder and healthcare purposes. This plant treats various diseases in different parts of India, including Assam, Meghalaya, Alipurduar and Darjeeling districts of West Bengal. This study was carried out to determine the bactericidal properties of various parts of *K. linifolia* aqueous extract. The aqueous extract of the leaves, bark, stem and plant sap were tested against *Escherichia coli* (gram-negative bacteria) & *Staphylococcus aureus* (gram-positive bacteria). Among the tested extracts, both the leaf and bark extracts were found to have high bactericidal potential and can kill more than 60% of both bacterial strains with a concentration of 300µg/mL through an agar diffusion test. The MIC (Minimum Inhibitory Concentration) values for the leaf and bark extracts were recorded at ≤1000µg/mL & ≤500µg/mL, respectively. It has also been found that both the bark and leaf extracts contain high tannins, which might be essential for the antibacterial properties of *Knema* sp. There is currently a lack of proper documentation on using *K. linifolia*, which makes it challenging to conduct clinical or commercial research to support new uses in modern phototherapy. This study aims to fill this gap and provide significant information that could lead to changes in modern medicine.

* Corresponding author

E-mail: joydeppaul2009@gmail.com (J. Paul);

srijan.haldar@adamasuniversity.ac.in (S. Haldar)

Peer review under responsibility of Journal of Experimental Biology and Agricultural Sciences.

Production and Hosting by Horizon Publisher India [HPI]
(<http://www.horizonpublisherindia.in/>).
All rights reserved.

All the articles published by [Journal of Experimental Biology and Agricultural Sciences](#) are licensed under a [Creative Commons Attribution-NonCommercial 4.0 International License](#) Based on a work at www.jebas.org.



1 Introduction

Medicinal or herbal plants have always been considered an important source of antimicrobial drugs in various countries worldwide. Over the last few decades (almost 30 years), there has been a significant increase in the use of highly effective herbal ingredients for treating multiple diseases. It has been reported that about eighty percent of the global population started depending on phytomedicinal sources to support their basic healthcare needs (Chipinga et al. 2018). The reasons could be (i) people use these herbal medications as complementary therapy because healthcare costs have significantly increased in the last few decades and (ii) the use of herbal remedies or natural antidotes is a cultural trend due to the ineffectiveness or resistance issues with the conventional pharmaceuticals (Ndamba et al. 1994). A wide range of diseases has shown minimal response to pharmaceutical antidotes, and the plausible solution could be herbal supplements (Chipinga et al. 2018).

Herbal supplements are effectively utilized in treating the following conditions, such as anti-inflammation healing skin infections, to cure splenic problems & complications during pregnancy in different parts of India and have been popular in local cultures over many decades. Multiple reports have shown that natural compounds are highly effective as an alternative antimicrobial component, combating drug resistance against commercially available antimicrobials (Yang et al. 2022). In such a wide range of medicinal plants, *K. linifolia* is a valuable species, containing high amounts of bioactive compounds, and therefore, it becomes the area of research in this study (Steenkamp et al. 2004). Only a handful of literature has been explored to introduce this plant species briefly. *K. linifolia* (Knema tree) falls under the family Myristicaceae and is a deciduous plant mainly found within the tropical region of Assam and West Bengal (Barstow and Timberlake 2018). Different members of this genus show various benefits, especially as medicinal plants to treat various diseases. The diseases that the use of this plant can treat are chronic fever, jaundice, splenic problems, high inflammations, problems related to breathing trouble and compromised taste bud responses (Alen et al. 2000; Wiart et al. 2004; Dhawan 2012; Salleh and Ahmad 2017; Supriya and Sreekanth 2021; Saising et al. 2022). The tree has extensive medicinal properties, widely known among the locals of Assam and northern parts of West Bengal to treat various infections and rare illnesses. However, few research works have been published on the diversified use of the medicinal properties of *K. linifolia* and the other species of the genus *Knema*. Also, no or little work has been carried out on screening, assessment, and isolation of phytoconstituents and biological evaluation of the stem, leaf or bark extracts of *K. linifolia* for antimicrobial, anti-cancer, and anti-protozoan activities. Only two reports have been published so far, which discussed the presence of various phytochemicals like tannins, terpenes, flavonoids, steroids, etc., in

some other species of the genus *Knema* (Salleh and Ahmad 2017; Supriya and Sreekanth 2021). The absence of proper knowledge and documentation of the genus *Knema* and over-exploitation by the local people marked many species of the genus *Knema*, including *Knema linifolia*, as “decreasing” species in the IUCN red list of threatened species (Sheeja et al. 2013). Only a few *K. linifolia* trees have been reported alive in India, mainly in Assam, Meghalaya, Alipurduar & Darjeeling districts of West Bengal (Barstow and Timberlake 2018). To search for effective alternative therapy modalities, it is important to understand the adequacy and helpfulness of *K. linifolia*, which can be utilized to treat different bacterial and other contagious diseases commercially. Hence, this research was carried out to discover the microbicidal properties of *K. linifolia* plant extracts, which could add valuable facts to the existing information pool in developing new safe antimicrobial substances from natural products. Therefore, this study has been carried out to evaluate the antimicrobial efficacy of *K. linifolia* bark, leaf, stem and plant sap samples crude extracts against two bacterial strains, *E. coli* and *S. aureus*. Along with this, the phytochemical content present in these different parts of *K. linifolia* has also been measured using standard biochemical tests.

2 Materials and Methods

2.1 Plant Sample Collection & Extraction

The Samples (Leaf, Bark, Sap, Steam) of *K. linifolia* (Roxb.) Warb were collected from the Alipurduar district of West Bengal, India. The Botanical Survey of India (BSI), Kolkata, identified the species. The collected samples (leaf, bark, sap, and stem) were brought to the laboratory, cleaned thoroughly with a brush to remove dust and debris, then washed in running tap water (pH:7), followed by drying in a hot air oven (37°C) stored into tightly closed containers till extraction at room temperature. For extraction preparation, 200 ml of sterile water and 20g of each plant material (including bark, leaves, stems, and sap-derived compounds) were macerated in a mortar and pestle and left at room temperature for 48 hours with occasional shaking. This was followed by the filtration of the mixture through a Whatman channel paper no. 1 (7.0 cm). The same procedure has been repeated five times using water as the solvent to increase the yield. Then, the precipitates were kept at 50°C until completely dried into powder form. The dried materials of the leaf, bark, stem and sap extracts were finally held at 4°C for further experimental usage (Kamanula et al. 2017). The final concentration used in this study was 100 µg/ml.

2.2 Microorganisms and Microbial culture media

In the form of bacterial agents, *Escherichia coli* (*E. coli*; ATCC 35218) and *Staphylococcus aureus* (*S. aureus*; ATCC 25923) were used for the experiments. Mueller Hinton agar (Sigma) media was prepared as per company guidelines under aseptic conditions.

2.3 Antimicrobial Activity: Cup-plate Method

The antibacterial efficacies of different natural compounds have been regularly tested through the cup-plate method, using small holes as the reservoir of the experimental natural substances (Brantner et al. 1994). The method followed according to (Zaika 1988). In brief, 50 ml of Mueller Hinton agar has been used to prepare a standard Petri plate. After leaving the medium to settle down in the plate for 1 hour, holes/cups with a diameter of 7mm were made in the petri plates. 40 μ l of the sterilized molten medium was used to seal the bottom of each cup. The cups were then filled by adding three different concentrations (100, 200, 300 μ l) of the *K. linifolia* bark, leaf, stem & plant sap extract, while the sterilized distilled water was used as a negative control (1.0 mg/ml; data not shown). 100 μ g/ml of ampicillin was added as positive control to one of the cups. These plates were then kept at 37°C for the next 24 hours. The experiment had been replicated thrice. The zone of inhibition was measured in diameter (mm) for *E. coli* and *S. aureus* with a vernier calliper (Das et al. 2012).

2.4 Minimal inhibitory concentration (MIC) of Bark and Leaf Aqueous Extract

Minimal inhibitory concentration (MIC) tests were considered as measuring boundaries to find the impacts of antimicrobial compounds. MIC was done in a flat-bottomed 96 well microtitre plate against *E. coli* and *S. aureus* for 24 hours at 35-37°C as described by (Paul Bhattacharya et al. 2020). Each concentration of the aqueous extract from leaf, bark, stem, and plant sap was used, and the experiment was performed in triplicate. The final concentration of *K. linifolia* bark and stem extracts ranged from 3.9-1000 μ g/mL. Additional negative and positive controls were used for the experiment.

2.5 Quantitative Estimation of Phytochemicals

Phytochemicals are quantified from the leaf and bark-dried powder of *K. linifolia*. Subjective examinations were conducted for tannins, terpenoids, saponins, phenolic compounds and flavonoids. Standard chemicals used are tannic acid (SRL 92101), Linalool (Sigma-L2602), Diosgenin (TCI-D1474), Gallic acid (Sigma-G7384) & Quercetin (Sigma-Q4951) for the isolation and identification of tannins, terpenoids, saponins, phenolic compounds and flavonoids (Mandal et al. 2013; Mujeeb et al. 2014). To determine the total amount of tannins, 5g of *K. linifolia* leaf and bark powder was dissolved in 20 mL of 50% methanol and stirred for 1hr in the presence of heat. After filtration, the filtrate was mixed with 20mL of distilled water, 10ml of 17% sodium carbonate and 2.5mL of Folin-Denis reagent and left stranded for 20 minutes. The resulting bluish-green mixture was analyzed at 760nm wavelength, and the tannin content was calculated by comparing it with the respective standard.

Similarly, 5g of leaf and bark dried powder (wi) were dissolved in 9 mL of ethanol and kept for 24 hours before filtration to determine the total terpenoid amount. The filtrate was further extracted using 10mL of pet ether. The extracts were kept for complete evaporation and complete drying (wf), and the total yield was calculated by using the formula $(wi-wf/wi \times 100)$ (Malik et al. 2017).

To determine the total amount of saponins, 5g of finely powdered leaf and bark were dissolved in 100 mL of Isobutyl alcohol and stirred for 5 hours before adding 20 mL of 40% saturated magnesium carbonate solution. After filtration, 2 mL of 5% FeCl₃ solution and 50 mL of distilled water were supplemented to the filtrate and kept for 30 minutes until the colourless solution turned blood red. The resulting blood-red solution was measured at 380nm, and the saponin content was calculated by comparing it with the respective standard.

For determining the total amount of phenolic compounds, 5g of the leaf and bark-dried powder were boiled in the presence of 50 mL of ether, kept for 15 minutes, and further distributed in a ratio of 2:1 (distilled water: extract). The resulting solution was further supplemented with 2 mL of NH₄OH, followed by adding 5 mL of pentanol and incubated for 30 minutes at room temperature. The absorbance was recorded at 505 nm, and the total phenol content was calculated by comparing it with the respective standard.

5 g of finely powdered leaf and bark were boiled in 2M HCl for 30 minutes to determine the flavonoid amount. After filtration, an equal volume of ethyl acetate was added dropwise to the filtrate. The weight of precipitated flavonoids was determined and reported as mg/g.

2.6 Statistical Analysis

All the statistical analyses were done using a Paired two-tailed Student's t-test. Each experiment was repeated thrice, and data was presented as mean \pm standard deviation (SD) (Bhaumik et al. 2009).

3 Results

Freshly collected plant parts, viz, leaves, fruits, and seeds of the species *Knema linifolia* (Roxb.) Warbs were collected from the Jaldapara National Park, Alipurduar, West Bengal, during the summer. The Herbarium leaves, fruit and seed samples (Figure 1) were submitted at the National Herbarium of India, Indian Botanical Garden of Calcutta and Unique Species ID and certificate provided by BSI office, Kolkata (Specimen No.:RB-01 Specimen Name: *Knema linifolia* (Roxb.)Warb).

3.1 Antibacterial Effect of Different Parts Aqueous Extract of *Knema linifolia*

The inhibitory activities of the aqueous leaf, bark, stem and sap extracts of *K. linifolia* were evaluated against gram-positive bacteria

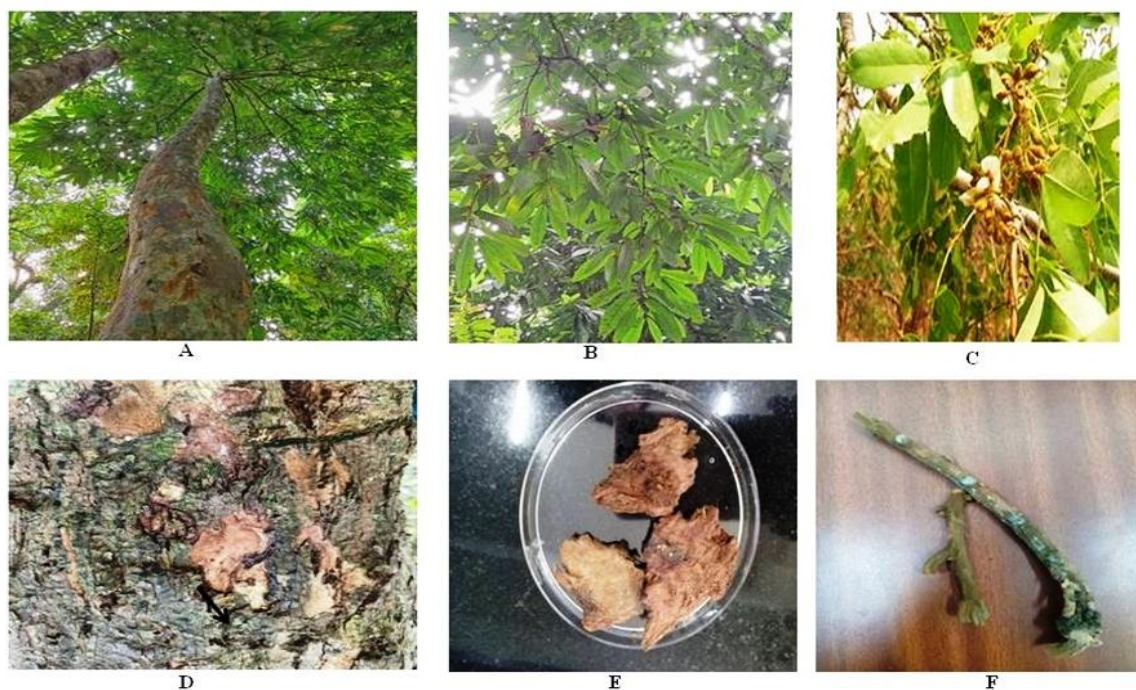


Figure 1 *K. linifolia* (Roxb.) Warb A) Tree, B) Leaf, C) Leaf twig and mature fruits, D) Plant Sap ,E) Bark, F) Stem. Pictures of different parts of *Knema linifolia* (Roxb.) Warb taken at the Jaldapara national park, West Bengal (26.6960° N, 89.2855° E) on 25th April, 2022.

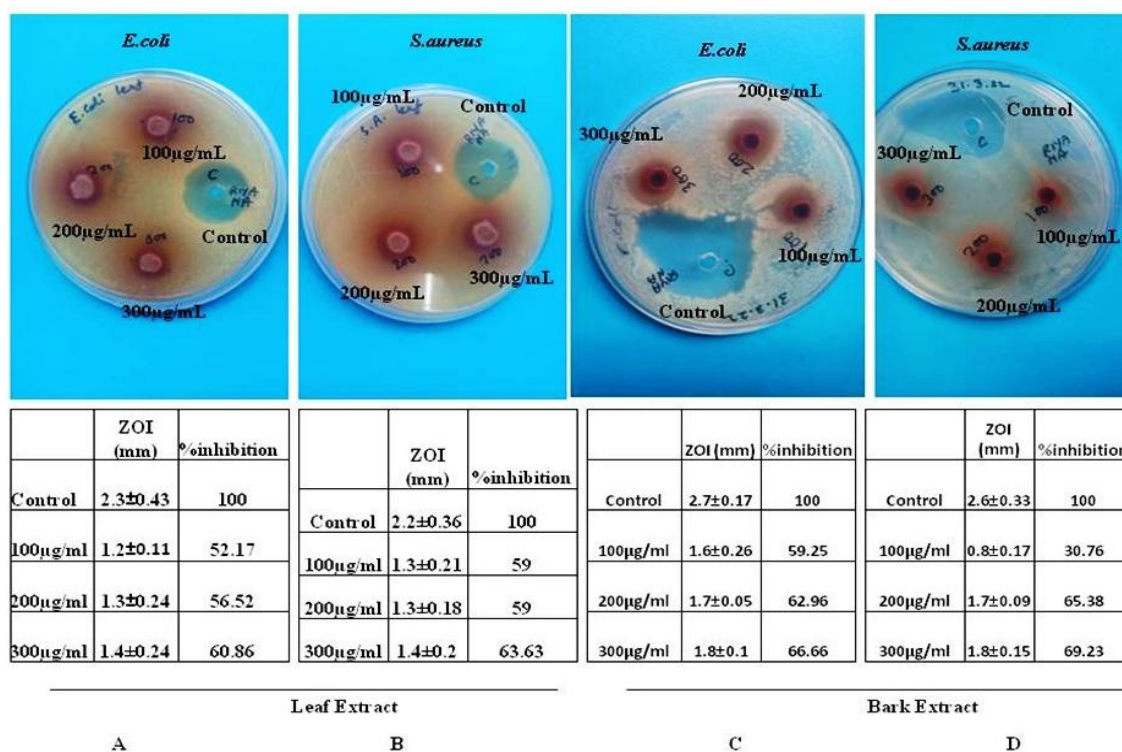


Figure 2 Antimicrobial activity of leaf & bark extracts of *K. linifolia*. Zone of inhibition (mm) produced by three different concentrations (100µg/mL, 200µg/mL & 300µg/mL) of leaf extract against *E.coli* (A) and *S.aureus* (B); Zone of inhibition (mm) produced by three different concentrations (100µg/mL, 200µg/mL & 300µg/mL) of bark extract against *E.coli* (C) and *S.aureus* (D). Ampicillin has been used as control (100µg/mL). All the experiments repeated thrice (n=3) and data shown are mean±SD.

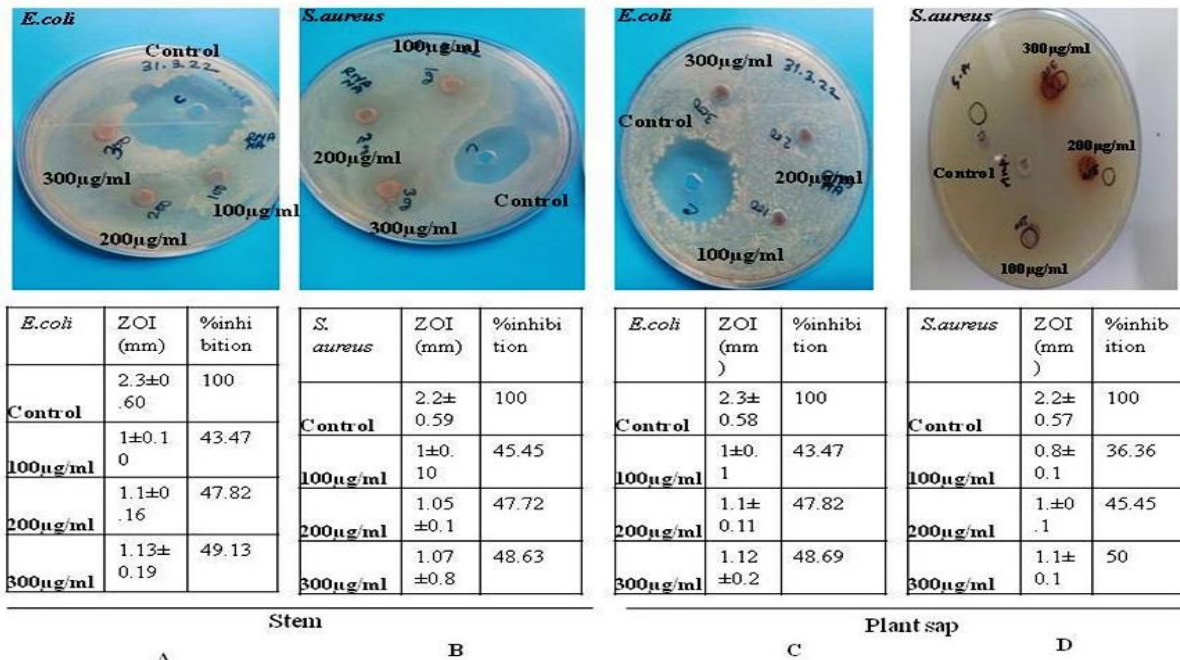


Figure 3 Antimicrobial activity of stem & plant sap extracts of *K. linifolia*. Zone of inhibition (mm) produced by three different concentrations (100µg/mL, 200µg/mL & 300µg/mL) of stem extract against *E. coli* (A) and *S. aureus* (B); Zone of inhibition (mm) produced by three different concentrations (100µg/mL, 200µg/mL & 300µg/mL) of plant sap extract against *E. coli* (C) and *S. aureus* (D). Ampicillin has been used as control (100µg/mL). All the experiments repeated thrice (n=3) and data shown are mean±SD.

Table 1 Minimum Inhibitory Concentrations of *K. linifolia* leaf and bark extract *S. aureus* and *E. coli*

Microorganism		Turbidity in broth (µg/ml)								
		3.9	7.8	15.6	31.2	62.5	125	250	500	1000
<i>E. coli</i>	Leaf Extract	+	+	+	+	+	+	+	-	-
	Bark Extract	+	+	+	+	+	+	-	-	-
<i>S. aureus</i>	Leaf Extract	+	+	+	+	+	+	+	+	-
	Bark Extract	+	+	+	+	+	+	-	-	-

S. aureus and gram-negative bacteria *E. coli*. Results presented in Figures 2 & 3 revealed the efficacy of leaf, bark, stem, and plant sap extracts. Among the tested various extracts, 300 µg/mL of both the leaf and bark extracts were shown to have significant antibacterial efficacy as both can kill more than 60% of both *S. aureus* and *E. coli*, compared with the ampicillin control (Figure 3). The stem and plant sap extracts failed to show considerable bactericidal properties ($\leq 50\%$; Figure 3). As the leaf and bark crude extracts were more potent than the stem and plant sap crude extracts, all the further experiments were performed using only the leaf and bark crude extracts.

3.2 Minimal inhibitory concentration of *K. linifolia* leaf and Bark extracts

The growth inhibitory potential of leaf and bark extracts of *K. linifolia* against both *S. aureus* & *E. coli* were determined through

MIC values (Table 1). To decide the MIC value, the concentrations of the leaf and bark extracts used were 3.9, 7.8, 15.6, 31.2, 62.5, 125, 250, 500 & 1000 µg/mL. Among these, the MIC for the leaf extract was 500µg/mL and 1000 µg/mL for *E. coli* and *S. aureus*, respectively. In the case of bark extract, the MIC value was recorded at 250µg/mL for *E. coli* and *S. aureus* (Table 1). The MIC values for leaf and bark extracts were $\leq 1000\mu\text{g/mL}$ & $\leq 500\mu\text{g/mL}$ for *E. coli* and *S. aureus*, respectively. These results show that bark crude extract has more potential to kill both the *E. coli* and *S. aureus* strains.

3.3 Quantitative phytochemical analysis of *Knema linifolia* aqueous extracts

The phytochemical studies of leaf and bark crude extracts of *K. linifolia* were carried out in this study to find out the presence of different phytocompounds, namely, tannins, terpenoids, saponins,

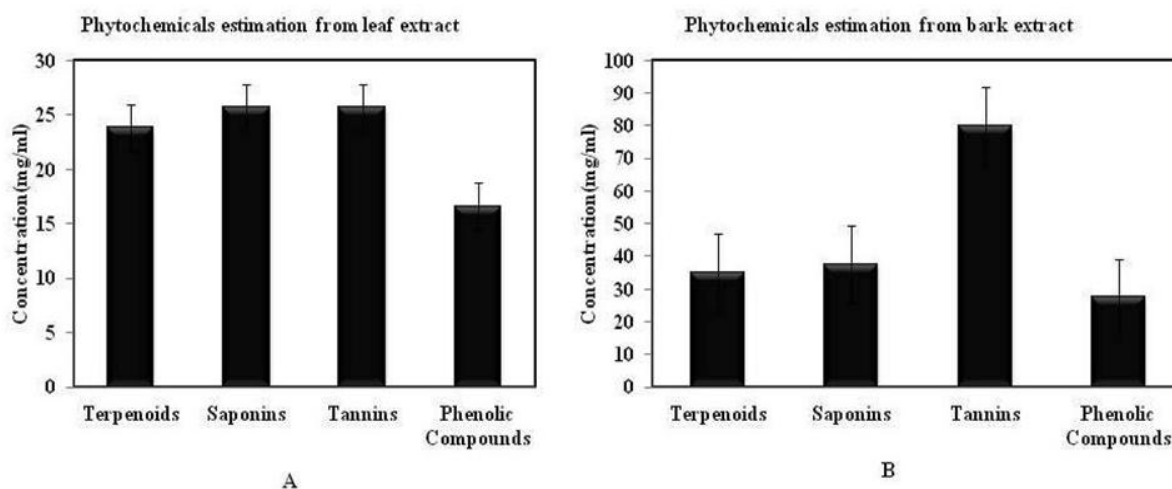


Figure 4 Quantitative estimation of phytochemicals from leaf and bark *K. linifolia* (A) Quantitative analysis of tannins, terpenoids, saponins & phenolic compounds in the leaf extract; (B) Quantitative analysis of tannins, terpenoids, saponins & phenolic compounds in the bark extract. All the experiments repeated thrice (n=3) and data shown are mean±SD.

Table 2 Qualitative analysis of phytochemical from bark and leaf extract of, sap and stem of *K. linifolia*

Components	Bark	Leaf
Flavonoids	-	+
Tannins	+++	+++
Saponins	++	++
Anthraquinones	-	-
Alkaloids	-	-
Anthocyanins	-	-
Terpenes/Terpenoids	-	++
Phenolic Compounds	+	+

flavonoids and phenolics by the standard techniques (Mujeeb et al. 2014). The presence of considerable terpenoids, tannins, phenolic compounds and saponins in the bark and leaf extracts of *K. linifolia* has been confirmed when compared against the respective standards (Figure 4; Table 2). No or negligible quantity of flavonoids was present in both the extracts (data not shown). The concentration of terpenoids, saponins, and phenolics was almost equivalent (23-38 µg/g) in leaf and bark extracts. But, the amount of tannin varies greatly in bark compared to the concentrations of other phytochemicals. The bark extract of *K. linifolia* contained more than 80µg/g of tannin (Figure 4).

4 Discussion

India is a country with great ethno-medicinal diversity. With the growing cost of medicines, reoccurrence of drug-resistant strains and side effects of medicine, it is important to discover alternate phytochemical sources that might be proven as a solution to combat this situation (Roy Chowdhury et al. 2022). *K. linifolia* is

a plant of high ethnomedicinal values among the local tribes of the eastern and northeastern parts of India (Supriya and Sreekanth 2021). However, lack of proper documentation leads to the confinement of this knowledge only to the local peoples, leading to less preservation and plantation of this plant and the probable extinction of this plant species shortly (Barstow and Timberlake 2018). In this research, we are trying to outline the antimicrobial potency of the aqueous extract of different parts (leaf, bark, stem, and plant sap) of *K. linifolia*. Also this study is, however, the first-ever documentation to quantify the phytochemicals present in the bark and leaf of *K. linifolia* to the best of our knowledge.

The taxonomical analysis was done through morphological characterization by the BSI office, Kolkata, based on the herbarium sheet, fruit and seed samples collected from Jaldapara National Park, Alipurduar district, west Bengal (Figure 1). This study is of notable significance as it showed that *K. linifolia* plant aqueous extract can kill gram-negative and gram-positive bacteria

(Figure 2, Table 1). The sequential antimicrobial study used aqueous leaf, bark, stem and plant sap extracts against *E. coli* and *S. aureus* strains. A cup plate assay with crude extracts from various plant organs showed that leaf and bark crude extracts are more potent in inhibiting the gram-negative and gram-positive strains. The inhibition percentages for leaf extracts are 60.86 and 63.63 against *E. coli* and *S. aureus*, respectively. Bark extract shows more potential by killing 66.66% of *E. coli* and 69.23% of *S. aureus* with the same concentration (300µg/mL) as leaf extract (Figure 2). This data has also been supported by the MIC values for the aqueous bark extract, i.e. 500µg/mL & 250µg/mL for *S. aureus* and *E. coli*, respectively (Table 1).

To find out the probable reason behind the antimicrobial properties of the leaf and bark crude extracts, the phytochemical analysis for certain natural compounds, such as tannins, terpenoids, saponins, flavonoids and phenolic compounds, were assessed against their respective standard compounds. Flavonoids were present in nominal quantity in leaf and bark (data not shown). Terpenoids, saponins and phenolic compounds are almost equivalent in leaf and bark extracts (ranging from 23µg/mL to 38µg/mL; Figure 4 and Table 2). In contrast, bark extract contains an elevated amount of tannins (80µg/mL), which could probably be the rationale for the high microbicidal potential of crude extract of *K. linifolia* bark against both the *E. coli* and *S. aureus* strains (Figure 4 & Table 2). The medicinal properties of tannins have been well documented in various literature (Chung et al. 1988; Kaczmarek 2020). The *K. linifolia* plant sap is also dark red or maroon coloured, resembling that of the blood, which might be due to the very high concentration of tannins present in the plant (Roy Chowdhury et al. 2022), as evident from Table 2.

Conclusion and Future Prospects

In conclusion, it can be summarized that the bark and leaf aqueous extracts of *K. linifolia* showed impressive antimicrobial potency against gram-negative and gram-positive bacteria, possibly due to the high concentration of tannins in the plant. Based on the data, it is evident that *K. linifolia* could be used as a potential alternative phytomedicinal source, but more studies need to be done in this aspect. Further, the antimicrobial, anti-fungal and anti-protozoan efficacy of different fractions of *K. linifolia* leaf and bark extract could be explored soon.

Acknowledgements

The authors want to acknowledge the support of the internal seed grant provided by Adamas University (No.-AU/R&D/SEED/28/03-2020-21). Also, the authors wish to thank Dr. Arijit Bhattacharya, Associate Professor, Department of Biological Sciences, Adamas University, for his valuable input to improve the manuscript further.

Conflict of interest

No conflict of interest has been declared by any of the authors.

References

- Alen, Y., Nakajima, S., Nitoda, T., Baba, N., Kanzaki, H., & Kawazu, K. (2000). Two antinematodal phenolics from *Knema hookeriana*, a Sumatran rainforest plant. *Zeitschrift fur Naturforschung. C, Journal of biosciences*, 55(3-4), 300–303. <https://doi.org/10.1515/znc-2000-3-426>
- Barstow, M., & Timberlake, J. (2018). *Pterocarpus angolensis*. *The IUCN Red List of Threatened*, 8235, 2018-1.
- Bhaumik, S. K., Singh, M. K., Karmakar, S., & De, T. (2009). UDP-Gal: N-acetylglucosamine beta 1-4 galactosyltransferase expressing live attenuated parasites as vaccine for visceral leishmaniasis. *Glycoconjugate journal*, 26(6), 663–673. <https://doi.org/10.1007/s10719-008-9212-y>
- Brantner, A., Pfeiffer, K.P., & Brantner, H. (1994). Applicability of diffusion methods required by the pharmacopoeias for testing antibacterial activity of natural compounds. *Pharmazie*, 49, 512–516.
- Chipinga, J. V., Kamanula, & J. F., Moyo, P.B.B. (2018). Efficacy of *Pterocarpus angolensis* crude extracts against *Candida krusei*, *Staphylococcus aureus*, *Streptococcus agalactiae* and *Escherichia coli*. *Malawi Medical Journal*, 30 (4), 219-224.
- Chung, K. T., Wong, T. Y., Wei, C. I., Huang, Y. W., & Lin, Y. (1998). Tannins and human health: a review. *Critical reviews in food science and nutrition*, 38(6), 421–464. <https://doi.org/10.1080/10408699891274273>
- Das, A., Raychaudhuri, U., & Chakraborty, R. (2012). Antimicrobial effect of edible plant extracts on the growth of some food borne bacteria including pathogens. *Nutrafoods*, 11, 99–104.
- Dhawan, B. N. (2012). Anti-Viral Activity of Indian Plants. *Proceedings of the National Academy of Sciences, India Section B*, 82(1), 209-224.
- Kaczmarek, B. (2020). Tannic Acid with Antiviral and Antibacterial Activity as A Promising Component of Biomaterials- A Minireview. *Materials (Basel)*, 13(14), 3224.
- Kamanula, J. F., Belmain, S. R., Hall, D. R., Farman, D. I., et al. (2017). Chemical variation and insecticidal activity of *Lippia javanica* (Burm. f.) Spreng essential oil against *Sitophilus zeamais* Motschulsky. *Industrial Crops and Products*, 110, 75–82.

- Malik, S.K., Ahmad, M., & Khan, F. (2017). Qualitative and quantitative estimation of terpenoid contents in some important plants of Punjab, Pakistan. *Pakistan Journal of Science*, 69(2), 150.
- Mandal, S., Patra, A., Samanta, A., Roy, S., Mandal, A., et al. (2013). Analysis of phytochemical profile of *Terminalia arjuna* bark extract with antioxidative and antimicrobial properties. *Asian Pacific journal of tropical biomedicine*, 3(12), 960–966. [https://doi.org/10.1016/S2221-1691\(13\)60186-0](https://doi.org/10.1016/S2221-1691(13)60186-0).
- Mujeeb, F., Bajpai, P., & Pathak, N. (2014). Phytochemical evaluation, antimicrobial activity, and determination of bioactive components from leaves of *Aegle marmelos*. *BioMed research international*, 2014, 497606. <https://doi.org/10.1155/2014/497606>
- Ndamba, J., Nyazema, N., Makaza, N., Anderson, C., & Kaondera, K. C. (1994). Traditional herbal remedies used for the treatment of urinary schistosomiasis in Zimbabwe. *Journal of ethnopharmacology*, 42(2), 125–132. [https://doi.org/10.1016/0378-8741\(94\)90106-6](https://doi.org/10.1016/0378-8741(94)90106-6)
- Paul Bhattacharya, S., Mitra, A., Bhattacharya, A., & Sen, A. (2020). Quorum quenching activity of pentacyclic triterpenoids leads to inhibition of biofilm formation by *Acinetobacter baumannii*. *Biofouling*, 36(8), 922–937. <https://doi.org/10.1080/08927014.2020.1831480>
- Roy Chowdhury, S., Haldar, S., Bhar, R., Das, S., Saha, A., Pal, K., Bandyopadhyay, S., & Paul, J. (2022). *Pterocarpus angolensis*: Botanical, Chemical and Pharmacological Review of an Endangered Medicinal Plant of India. *Journal of Experimental Biology and Agricultural Sciences*, 10(1), 150–156.
- Saising, J., Maneenoon, K., Sakulkeo, O., Limsuwan, S., Götz, F., & Voravuthikunchai, S. P. (2022). Ethnomedicinal Plants in Herbal Remedies Used for Treatment of Skin Diseases by Traditional Healers in Songkhla Province, Thailand. *Plants (Basel, Switzerland)*, 11(7), 880. <https://doi.org/10.3390/plants11070880>
- Salleh, W. M. N. H. W., & Ahmad, F. (2017). Phytochemistry and biological activities of the Genus *Knema* (Myristicaceae). *Pharmaceutical Sciences*, 24(4), 249–255.
- Sheeja, T. E., Anju, P. R., Shalini, R. S., Siju, S., Dhanya, K., & Krishnamoorthy, B. (2013). RAPD, SCAR and conserved 18S rDNA markers for a red-listed and endemic medicinal plant species, *Knema andamanica* (Myristicaceae). *Physiology and molecular biology of plants: an international journal of functional plant biology*, 19(2), 245–250. <https://doi.org/10.1007/s12298-013-0166-6>
- Steenkamp, V., Mathivha, E., Gouws, M. C., & van Rensburg, C. E. (2004). Studies on antibacterial, antioxidant and fibroblast growth stimulation of wound healing remedies from South Africa. *Journal of Ethnopharmacology*, 95(2-3), 353–357. <https://doi.org/10.1016/j.jep.2004.08.020>
- Supriya, R.H., & Sreekanth, G. B. (2021). Phytopharmacological review of *Knema attenuata* (Hook. F and Thoms) Warb. *International Journal of Current Pharmaceutical Research*, 13(3), 1–3.
- Wiar, C., Mogana, S., Khalifah, S., Mahan, M., Ismail, S., Buckle, M., Narayana, A. K., & Sulaiman, M. (2004). Antimicrobial screening of plants used for traditional medicine in the state of Perak, Peninsular Malaysia. *Fitoterapia*, 75(1), 68–73. <https://doi.org/10.1016/j.fitote.2003.07.013>
- Yang, Z., Li, L., Chen, C. H., Zhang, Y. Y., Yang, Y., Zhang, P., & Bao, G. H. (2022). Chemical composition and antibacterial activity of 12 medicinal plant ethyl acetate extracts using LC-MS feature-based molecular networking. *Phytochemical analysis: PCA*, 33(3), 473–489. <https://doi.org/10.1002/pca.3103>
- Zaika, L. L. (1988). Spices and herbs: their antimicrobial activity and its determination. *The Journal of Food Safety*, 9, 97–118.



Journal of Experimental Biology and Agricultural Sciences

<http://www.jebas.org>

ISSN No. 2320 – 8694

Molecular regulation of *Mycobacterium tuberculosis* Sigma factor H with Anti-sigma factor RshA under stress condition

Syantee Sen¹ , Swarnav Bhakta^{1,2} , Kuntal Pal^{1,3*} 

¹Department of Biotechnology, Adamas University, West Bengal, India

²Department of Developmental Biology, Agharkar Research Institute, Pune 411004, India

³Department of Bioscience, School of Bio Sciences and Technology, Vellore Institute of Technology, Tamil Nadu 632014, India

Received – October 31, 2023; Revision – December 31, 2023; Accepted – January 15, 2024

Available Online – March 15, 2024

DOI: [http://dx.doi.org/10.18006/2024.12\(1\).153.162](http://dx.doi.org/10.18006/2024.12(1).153.162)

KEYWORDS

Sigma Factor

SigH

Anti-sigma factor

RshA

Mycobacterium tuberculosis

Bacterial transcription

ABSTRACT

Mycobacterium tuberculosis is the causative agent of tuberculosis, the leading fatal infectious disease that claims millions of lives every year. *M. tuberculosis* regulates its stress condition response using its regulatory protein, Sigma Factor H, which binds with its cognate anti-sigma factor RshA in normal conditions, forming a complex inhibiting transcription. During oxidative stress, SigH is released from the complex and binds to RNA Polymerase (RNAP) to initiate transcription. Thus, it is important to understand the molecular conformational state of SigH in complex with different protein partners under different cellular or environmental contexts. This work intends to analyze the SigH-RshA complex, which revealed the variation in SigH shown during complex formation with RNAP and RshA, respectively. Previously, Hydrogen Deuterium Exchange-Mass Spectrometry (HDX-MS) analysis of SigH-RshA interaction provided a detailed insight into the critical residues participating in the interaction. The HDX-MS data were used to dock RshA on the open conformation of SigH from the SigH-RNAP complex structure (PDB: 5ZX2), and closed conformation was obtained from protein modelling. The docking revealed that closed conformation of SigH complexing with RshA in terms of HDX-MS data revealed a major structural shift in SigH while interacting with two different binding partners, RshA and RNAP, under variable environmental conditions. This structural shift of SigH with RshA and RNAP has significance in understanding the stress response of *M. tuberculosis*, and SigH could prove to be a potential drug target.

* Corresponding author

E-mail: Kuntal.pal@vit.ac.in (Kuntal Pal)

Peer review under responsibility of Journal of Experimental Biology and Agricultural Sciences.

Production and Hosting by Horizon Publisher India [HPI]
(<http://www.horizonpublisherindia.in/>).
All rights reserved.

All the articles published by [Journal of Experimental Biology and Agricultural Sciences](#) are licensed under a [Creative Commons Attribution-NonCommercial 4.0 International License](#) Based on a work at www.jebas.org.



1 Introduction

Mycobacterium tuberculosis is the causative agent of one of the most infectious diseases that has ever struck humans. This bacterium's ability to perceive its environment and adapt its physiology accordingly necessitates delicate gene expression regulation for survival in the varying immune signals by the host (Shi et al. 2003; Rohde et al. 2007). Gene expression in bacteria relies on transcription, whose initiation depends on multiple factors, including RNA Polymerase (RNAP), which comprises several subunits, including the sigma factor. Sigma factors, a separable class of RNAP, play a vital role in transcription initiation (Feklístov et al. 2014). They are responsible for linking to the core RNA Polymerase and guiding it through the steps leading to initiation (Manganelli et al. 1999). These include specific recognition of the promoter, separation of the DNA strand and synthesis of the initial nucleotides. This might result in the dissociation of the sigma factor from the RNAP (Borukhov and Nudler 2003).

Among two classes of σ^{70} and σ^{54} , the sigma 70 family includes several primary sigma factors with linked alternative sigma factors. Another group of a phylogenetically unrelated subfamily called the extracytoplasmic function factors, or ECF lies among the Sigma 70 families (Helmann 2002). SigH is one alternative sigma factor found in Mycobacterial species and regulates stress response conditions like heat and oxidative stresses (Raman et al. 2001). It has been demonstrated that SigH is necessary for the stress-induced expression of the genes for SigE and SigB, the two additional alternative sigma factors implicated in the *Mycobacterial* response to various stimuli (Manganelli et al. 2001). Thus, an upregulation in the transcription of auto-regulated (SigH-dependent) promoter causes an increase in SigH expression to adapt to oxidative or heat stress (Raman et al. 2001)

Despite the increased expression of SigH, its enzymatic activities are inhibited by a family of proteins known as the anti-sigma factors. These factors bind SigH and prevent its participation in the RNAP-mediated transcription process. Among these anti-sigma factors, RshA expression is controlled by a gene present in the SigH operon. RshA inhibits SigH-dependent transcription in *M. tuberculosis* (Raman et al. 2001; Song et al. 2003). The autoregulation of the SigH promoter controls RshA function at transcriptional, translational and post-translational levels. During post-translational modification, SigH interacts with its associated anti-sigma factor RshA (Newman et al. 2001; Li et al. 2003). RshA binds to SigH as a redox response signal, and upon oxidation of particular cysteine residues, a conformational change in the sigma factor leads to its release and allows binding with the RNA polymerase holoenzyme. This SigH-RshA complex gets disrupted under oxidizing conditions, allowing SigH to interact with RNAP, leading to transcription initiation. Until SigH rebinds with RshA, a

stable transcription of the SigH regulon is maintained (Song et al. 2003). This leads to the activation of the sigmulon (Kang 1999; Song et al. 2003). On reversal of favourable conditions, the reduction state is induced, during which the SigH binding capability of RshA is regained, and thus, expression is inhibited again (Jung et al. 2011).

There are 10 ECFs present in *M. tuberculosis*. Each member of the ECF sigma factors, along with RNAP, identifies and interacts with promoters and σ_4 and σ_2 recognizes the distinct sequence present at -35 and -10 elements, respectively (Campagne et al. 2014). Further, SigH binds to the RNAP- β subunit and creates a channel for the entry of template ssDNA, which binds to the active site of RNAP and initiates the transcription process. The channel exit is destined for the release of transcribed RNA but is blocked by the SigH-RNAP- β initiation complex. A conformation change in SigH dissociates the SigH-RNAP- β complex, opening the channel exit (Zhang et al. 2012; Dolatshahi et al. 2016; Li et al. 2019). Another transcription initiation complex, SigH-Rpo, represents a similar binding interface in SigH-RNAP binding. The active site cleft holds the DNA/RNA hybrid at a post-translational condition while the duplex DNA settles in the main channel (Campagne et al. 2014, 2015). Various interactions involved in the recognition and unwinding of the promoter by SigH-RNAP were also observed in SigH-RPo. A decrease in infectivity occurred in SigC and SigD's deletion, while SigE and SigH's deletion was responsible for virulence (Rodrigue et al. 2006; Sachdeva et al. 2010).

The inhibition of the Sigma factor by its associated anti-sigma factor depends on the reversible protein-protein interaction (ppi) (Duncan and Losick 1993; Hughes and Mathee 1998). In earlier biochemical studies, the purified SigH and RshA were shown to form a stable complex only in reducing conditions (Song et al. 2003; Jamithreddy et al. 2017). Although they interact in reducing conditions, their stability gets affected at temperatures higher than 50°C, leading to dissociation of complex and release of SigH. Thus, RshA acts as a heat sensor/ oxidative stress sensor to regulate the transcriptional role of SigH (Song et al. 2003).

The disc diffusion assays with diamide showed that mutated SigH is more sensitive than wild-type parental strain, indicating the importance of SigH in bacterial survivability (Fernandes et al. 1999). A wider zone of inhibition was observed in inducing the expression of RshA into the wild-type strain. This may be due to the inhibition of WT SigH for transcription activity in excess RshA (Raman et al. 2001). The sequence analysis of RshA shows that certain portions were conserved among *Mycobacterium sp.* Among these conserved regions, five cysteine residues were tested by swapping them with alanine to study the effect on inhibition of SigH. Three of them (Cys11, Cys41, Cys44) showed decreased effectivity, while two of them

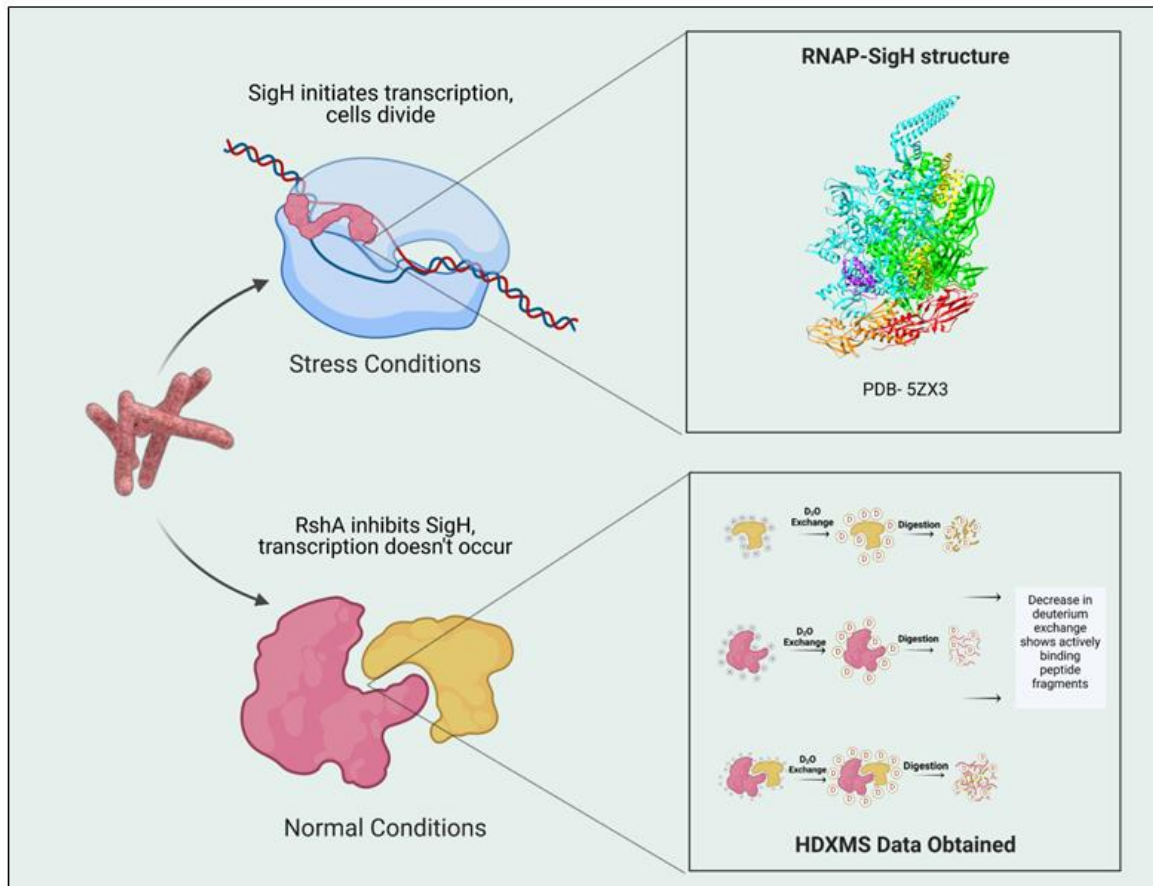


Figure 1 Schematic representation of *Mycobacterium tuberculosis* regulating transcription using Sigma Factor SigH. In stress conditions SigH binds to RNA Polymerase to initiate transcription. In normal conditions, Anti sigma factor RshA binds to SigH and inhibits transcription. The SigH-RshA interaction was analyzed by performing HDXMS (Image Created by Biorender).

(Cys61 & Cys62) showed no effect, which suggested the necessity of cysteine residues for the proper functioning of RshA in inhibiting SigH transcription (Paget et al. 2001).

A comparative study between the survival capacity of wild-type *M. tuberculosis* H37Rv, the SigH mutant strain RH349, and the SigH-complemented mutant strains RH377 and RH395 showed that the SigH mutant has more susceptibility to both diamide and plumbagin (Hassan and Fridovich 1979).

These studies showed the significance of the SigH-RshA complex in regulating the transcription process under both normal and stress conditions of *M. tuberculosis*. Without any molecular structure of this complex, a Hydrogen Deuterium Exchange Mass Spectrometry (HDX-MS) study was performed to identify the interface between SigH and RshA. In this study, we analyze the conformation of SigH while forming a complex with RshA compared to a SigH-RNAP complex. Here, we are using previously published HDX-MS data of interaction between SigH and RshA to predict an accurate model of interaction which will

decipher the conformation changes associated with SigH in different physiological conditions (Kumar et al. 2012).

2 Materials and Methods

2.1 Amino acid sequence retrieval

The National Centre for Biotechnological Information (NCBI) database was used for retrieval of amino acid sequences in FASTA format for both SigH and RshA proteins. After this, homology modelling was done, followed by further computational analysis.

2.2 Homology Modelling and Validation of 3D models

SWISS-MODEL and DISTILL 2.0 were used to carry out three-dimensional modelling of the protein sequences (Baú et al. 2006; Waterhouse et al. 2018). After creating the models, UCSF Chimera and PyMOL were used to visualize and analyze them (Pettersen et al. 2004). The predicted three-dimensional models were validated using the servers- PROCHECK v.3.5 and ProSA-web (Protein Structure Analysis) (Laskowski et al. 1993; Wiederstein and Sippl

Table 1 List of the values for the Most favoured region and disallowed regions as validated using PROCHECK for Models 1-6

Model	RM Plot	
	Most Favoured Region	Disallowed Region
1	82.6	0.6
2	93.4	0
3	91.1	0
4	75	4.2
5	87	1.3
6	79.6	1.9

1, 2 - Closed and Open conformation of SigH; 3,4 - Closed and Open conformation of RshA; 5,6 – Closed and Open conformation of docked SigH-RshA

2007). Ramachandran plot was also predicted using PROCHECK. Residues were present in disallowed regions, allowed regions, additional allowed regions and most favoured regions. The quality of the analytical structure of these 3-D models were determined by these values. Additional validation involved the calculation of the Z score of both models using ProSA-web. Protein position is determined by the Z score within experimental NMR and X-ray structure of equal residue length. The model's energy was also obtained from it (Sippl 1995).

2.3 Data from Previous HDX-MS of SigH and RshA

HDX-MS was used for free SigH, free RshA and the SigH-RshA complex. After comparison and analysis of all three, pepsin digest fragments between SigH and the SigH-RshA complex were identified in 32 regions and for RshA and the complex, 20 common fragments were identified. For SigH, 71% of the primary sequence was covered by the pepsin digest fragments, and in the case of RshA, 88% coverage was shown. Observations on carrying out Deuterium exchange for 10 minutes for all three were listed. Excluding two fragments, all showed a decrease in exchange after complex formation. Five of these regions (1-25, 58-69, 90-111, 115-132, 157-171) showed >1 decrease in

exchange (Table 2). In the case of RshA, compared to the SigH-RshA complex, only two overlapping sequences (34-49, 35-57) showed a decrease in exchange more than 1 (table 3). This decrease in exchange indicates the involvement of these regions in the RshA-SigH complex formation. Four of the fragments showed an increase in exchange, which could have been a result of a shifted domain due to the binding of RshA with SigH (Kumar et al. 2012).

2.4 Molecular docking analysis

Molecular docking analysis is a basic procedure for characterizing the interaction between two proteins and their binding affinity. The molecular docking for the predicted models of SigH and RshA was done using High Ambiguity Driven protein-protein DOCKing @BonvinLab (HADDOCK 2.4) web server (de Vries et al. 2010). Two input data were provided for the docking analysis: Molecule 1 was SigH, and Molecule 2 was RshA. The active residues were identified from the HDX-MS data of the previous studies as they are predicted to be directly involved in the complex formation. These residues were provided as input parameters. Once the molecular docking was successfully completed, the docked complex was visualized using PyMOL.

Table 2 Peptide fragments showing >1 decrease in Deuterium Exchange

No.	Pepsin digest fragment	Peptide, m/z, Charge state	SigH in complex with RshA	SigH
1	1-25	MADIDGVTGSAGLQPGPSEETDEEL (1259.56), +2	9.360.1	12.060.1
2	58-69	LQETMVKAYAGF (679.35), +2	6.560.1	7.760.4
3	90-111	YINSYRKKQRQPAEYPTEQITD (910.12), +3	7.860.3	10.060.0
4	115-132	ASNAEHSSTGLRSAEVEA (908.43), +2	5.460.1	7.360.0
5	157-171	YYADVEGFPYKEIAE (897.418), +2	8.260.2	9.460.1

Table 3 Peptide fragments showing >1 decrease in Deuterium Exchange

No.	Pepsin digest fragment	Peptide, m/z, Charge state	SigH in complex with RshA	RshA
1	34-49	LDGECTPETRELRH (656.664), +3	8.660.4	10.260.7
2	35-57	DGECTPETRELRHLEACPGL (881.084), +3	13.160.0	15.060.1

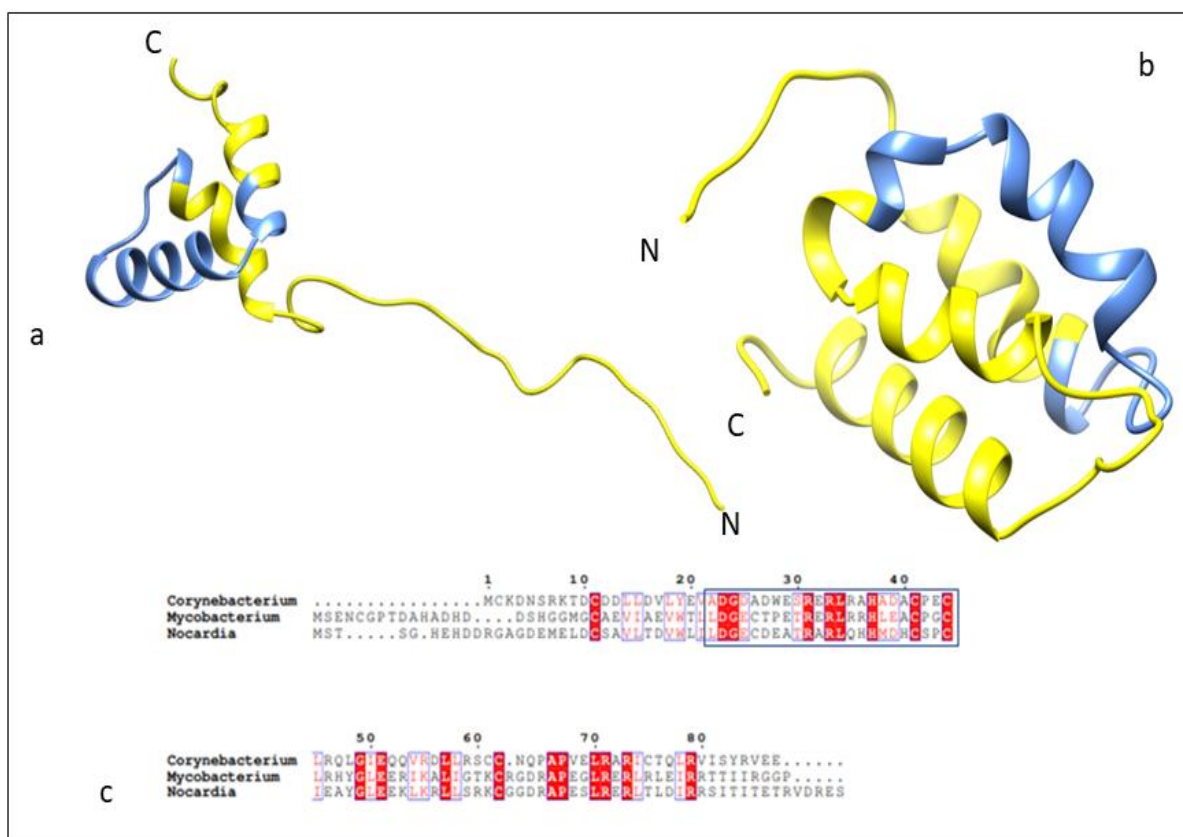


Figure 3 RshA a) The open conformation RshA model with a long loop at N-termini (Model 3) was predicted by using the server Distill 2.0, b) The closed conformation RshA model with a short helix at N-termini (Model 4) was predicted by using SWISS-MODEL, The protein is shown in yellow and blue indicates the regions showing decreased exchange level upon interaction with its cognate anti-sigma factor RshA. The actively binding sites are listed in Table 3, c) Multiple Sequence Alignment of RshA present across various pathogenic bacterial species shows that the actively binding regions (shown in the blue box) are conserved (shown in red) among them.

3.2 Molecular Docking of SigH-RshA

Previously, there was a known structure for SigH-RNAP where SigH encircles the β subunit of RNAP, and its complex unwinds the promoter and initiates transcription. There was still a lack of any known structure of SigH-RshA even though their residual details participating in interaction, complex formation and correspondence were proved through many experimental observations. Molecular docking of the designed protein models and their analysis provided both open and closed conformation models (Model 5 and 6) of the SigH-RshA interaction. Proper binding of the two proteins was not observed in the open conformation as it did not follow the experimental HDX-MS data, although the molecular docking of RshA with the closed conformation of SigH matched the stabilized regions represented by HDX-MS of SigH-RshA complex. So, the closed conformation model was chosen for further analysis. Even though the open conformation of SigH didn't comply with the HDX-MS data, it resembles its conformation in the SigH-RNAP complex ((PDB: 5ZX3). These also represent the structural flexibility of SigH in two different conditions.

3.3 Conformational variations in SigH at different environmental conditions of *Mycobacterium sp.*

Even though SigH has been known to keep an open conformation, as observed from the SigH-RNAP structure (PDB-5ZX3), the same conformation did not follow the HDX-MS data during protein-protein docking of SigH-RshA. Instead, a different closed conformation model of SigH seems to dock with RshA while following the experimental data (Table 2). On comparing the conformation of SigH from the SigH-RNAP crystal structure with the HDX-MS guided docked model of SigH-RshA, it was evident that SigH undergoes a major conformational shift while interacting with two different protein partners. The SigH chain has an open conformation not only when in complex with RNAP but also when it's free and a closed conformation following the interaction with RshA. This conformational change is also evident when the two complexes of SigH-RNAP and SigH-RshA are contrasted. This indicates the presence of certain specific regions, whose accessibility changes due to the conformational change and hence acts as a key to the specific interactions.

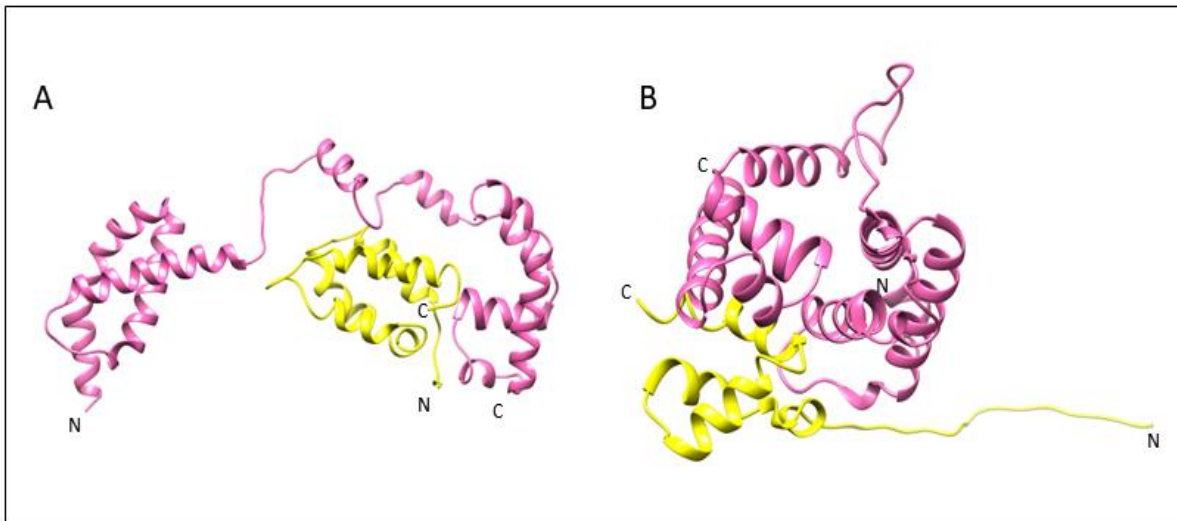


Figure 4 Docked models of SigH-RshA interaction, the models (Model 5 and 6) were prepared by molecular docking using the server PatchDock; SigH is shown in Pink and its partner RshA is shown in yellow; (A) the open conformation models, SigH in its open conformation was obtained from the SigH-RNAP structure (PDB-5ZX2); (B) The closed conformation model, the predicted 3D Model of SigH was used for this model

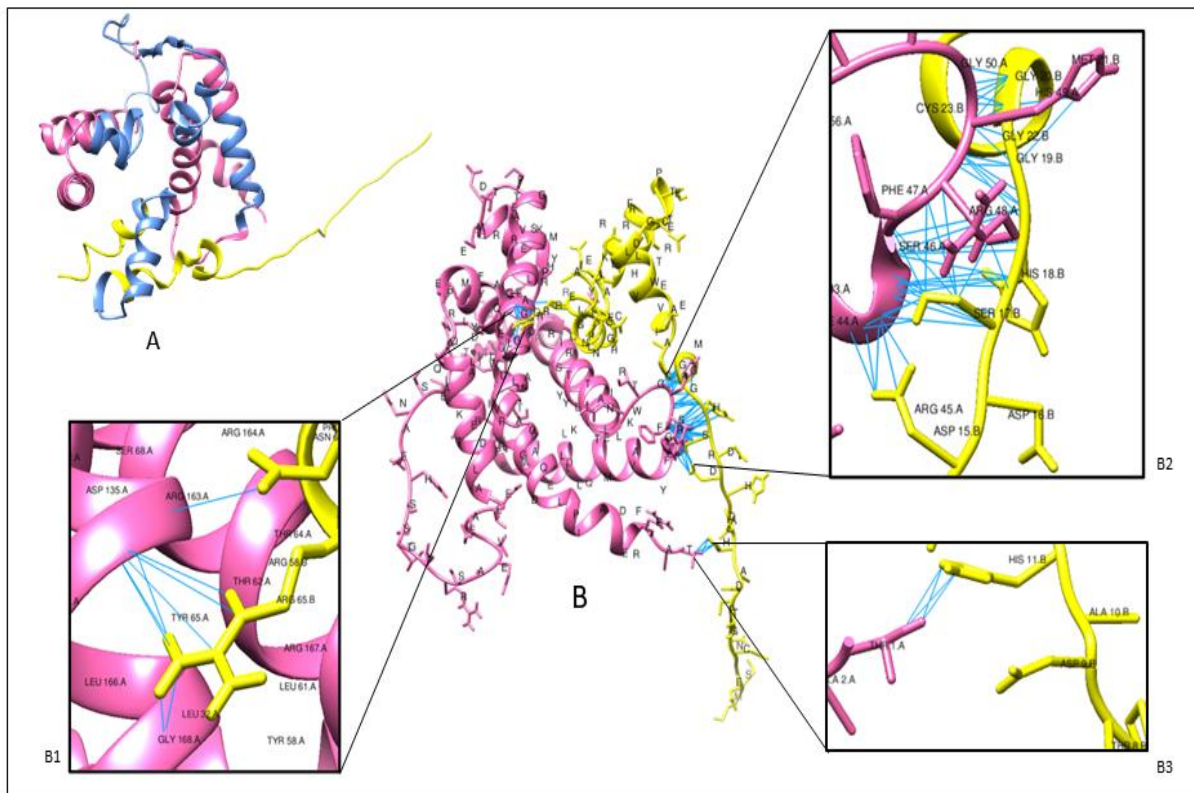


Figure 5 Model of Interaction A) A model for the interaction of SigH-RshA is proposed, which was prepared through docking, using PatchDock; SigH is shown in pink, RshA is shown in yellow and blue represents the regions showing decreased exchange upon interaction; B) The interactions between the two proteins are shown in light blue. These bonds were found to comply with the experimental data previously obtained through HDXMS. These actively binding residues did not resemble the ones involved in SigH-RNA Polymerase structure and hence showed a simultaneous change in accessibility with the conformational change. The binding residues are listed in Table 2 and 3.

3.4 Non-overlapping interacting residues

Previous findings showed that SigH interaction with the β subunit of RNAP unwinds the promoter and creates a channel for the passage of ssDNA, hence initiating transcription (PDB-5ZX2). Without any SigH-RshA structure, the proposed closed conformation model supported by HDX-MS experimental represents a different SigH conformation. The interacting residues were observed using PyMol and paralleled with the ones involved in SigH-RNAP interaction. The residues of SigH in the former case were not identical to the residues that are involved in SigH-RNAP complex formation. Hence, this distinct involvement shows the significance of these particular residues in the protein's specificity towards RshA. The conformational change that the protein goes through between the two complexes can be the reason for the accessibility of these particular residues, which have been observed to play a vital role in the SigH-RshA complex formation.

Conclusion

Mycobacterium tuberculosis, the causative agent of the infectious disease tuberculosis, survives in stress conditions due to the stress response mechanism regulated by the sigma factor SigH. SigH acts during both oxidative stress and heat shock. SigH, in turn, is regulated by RshA, its corresponding anti-sigma factor. In normal conditions of the host cell, SigH stays bound to RshA, which inhibits its transcription and, hence, advances the infection. However, when faced with stress conditions, RshA is released from the complex, and the free SigH binds with RNA polymerase and initiates transcription. SigH mainly interacts with the DNA-directed RNA polymerase subunit beta. The Arg-rich C terminal of the SigH protein interacts with the phosphate backbone and, along with RNAP, unwinds the DNA promoter.

The predicted docked models of SigH-RshA were in both open and closed conformation, but the closed model matched the previously obtained HDXMS experimental data. So, the closed conformation model was chosen for further analysis. It has been observed that there is a major conformational change of SigH when compared between its complexes with RNAP and RshA. SigH shows an open conformation with RNAP and a closed one with RshA. This conformational change was analyzed. It was noted that the C-terminal and N-terminal regions of SigH interact with RNAP β -subunit. However, none of the residues overlapped with the regions that actively interact with RshA. Free SigH, also in an open conformation, shows the significance of the distinct residues involved in the protein-protein interaction. The conformational change leads to the varying accessibility of certain residues, which are vital for the interaction.

Hence, these conformational changes in SigH and the difference in its model of interaction with two different regulatory proteins raise

the question of whether SigH can be a potential target for a drug against tuberculosis. To establish SigH as a molecular drug target, an experimental structure of its complex with RshA is necessary, which might be more important to understand the conformation accurately.

Acknowledgement

We would like to thank all the open-access free software and web servers used in this study.

Conflict of Interest

The authors declare that there is no conflict of interest

Financial Discloser

Nil

References

- Baú, D., Martin, A. J., Mooney, C., Vullo, A., Walsh, I., & Pollastri, G. (2006). Distill: A suite of web servers for the prediction of one-, two- and three-dimensional structural features of proteins. *BMC Bioinformatics*, 7(1), 402. <https://doi.org/10.1186/1471-2105-7-402>
- Borukhov, S., & Nudler, E. (2003). RNA polymerase holoenzyme: Structure, function and biological implications. *Current Opinion in Microbiology*, 6(2), 93–100. [https://doi.org/10.1016/S1369-5274\(03\)00036-5](https://doi.org/10.1016/S1369-5274(03)00036-5)
- Campagne, S., Allain, F. H.-T., & Vorholt, J. A. (2015). Extra Cytoplasmic Function sigma factors, recent structural insights into promoter recognition and regulation. *Current Opinion in Structural Biology*, 30, 71–78. <https://doi.org/10.1016/j.sbi.2015.01.006>
- Campagne, S., Marsh, M. E., Capitani, G., Vorholt, J. A., & Allain, F. H.-T. (2014). Structural basis for -10 promoter element melting by environmentally induced sigma factors. *Nature Structural & Molecular Biology*, 21(3), 269–276. <https://doi.org/10.1038/nsmb.2777>
- de Vries, S. J., van Dijk, M., & Bonvin, A. M. J. J. (2010). The HADDOCK web server for data-driven biomolecular docking. *Nature Protocols*, 5(5), 883–897. <https://doi.org/10.1038/nprot.2010.32>
- Dolatshahi, S., Fonseca, L. L., & Voit, E. O. (2016). New insights into the complex regulation of the glycolytic pathway in *Lactococcus lactis*. I. Construction and diagnosis of a comprehensive dynamic model. *Molecular BioSystems*, 12(1), 23–36. <https://doi.org/10.1039/C5MB00331H>
- Duncan, L., & Losick, R. (1993). SpoIIAB is an anti-sigma factor that binds to and inhibits transcription by regulatory protein sigma

- F from *Bacillus subtilis*. *Proceedings of the National Academy of Sciences of the United States of America*, 90(6), 2325–2329. <https://doi.org/10.1073/pnas.90.6.2325>
- Feklistov, A., Sharon, B. D., Darst, S. A., & Gross, C. A. (2014). Bacterial Sigma Factors: A Historical, Structural, and Genomic Perspective. *Annual Review of Microbiology*, 68(1), 357–376. <https://doi.org/10.1146/annurev-micro-092412-155737>
- Fernandes, N. D., Wu, Q. L., Kong, D., Puyang, X., Garg, S., & Husson, R. N. (1999). A mycobacterial extracytoplasmic sigma factor involved in survival following heat shock and oxidative stress. *Journal of bacteriology*, 181(14), 4266–4274. <https://doi.org/10.1128/JB.181.14.4266-4274.1999>
- Hassan, H. M., & Fridovich, I. (1979). Intracellular production of superoxide radical and of hydrogen peroxide by redox active compounds. *Archives of Biochemistry and Biophysics*, 196(2), 385–395. [https://doi.org/10.1016/0003-9861\(79\)90289-3](https://doi.org/10.1016/0003-9861(79)90289-3)
- Helmans J. D. (2002). The extracytoplasmic function (ECF) sigma factors. *Advances in microbial physiology*, 46, 47–110. [https://doi.org/10.1016/s0065-2911\(02\)46002-x](https://doi.org/10.1016/s0065-2911(02)46002-x)
- Hughes, K. T., & Mathee, K. (1998). The Anti-Sigma Factors. *Annual Review of Microbiology*, 52(1), 231–286. <https://doi.org/10.1146/annurev.micro.52.1.231>
- Jamithreddy, A. K., Samajdar, R. N., Gopal, B., & Bhattacharyya, A. J. (2017). Determination of Redox Sensitivity in Structurally Similar Biological Redox Sensors. *The Journal of Physical Chemistry B*, 121(29), 7005–7015. <https://doi.org/10.1021/acs.jpcc.7b02081>
- Jung, Y.G., Cho, Y.B., Kim, M.S., Yoo, J.S., Hong, S.H., & Roe, J.H. (2011). Determinants of redox sensitivity in RsrA, a zinc-containing anti-sigma factor for regulating thiol oxidative stress response. *Nucleic Acids Research*, 39(17), 7586–7597. <https://doi.org/10.1093/nar/gkr477>
- Kang, J.G. (1999). RsrA, an anti-sigma factor regulated by redox change. *The EMBO Journal*, 18(15), 4292–4298. <https://doi.org/10.1093/emboj/18.15.4292>
- Kumar, S., Badireddy, S., Pal, K., Sharma, S., Arora, C., Garg, S. K., Alam, M. S., Agrawal, P., Anand, G. S., & Swaminathan, K. (2012). Interaction of *Mycobacterium tuberculosis* RshA and SigH Is Mediated by Salt Bridges. *PLoS ONE*, 7(8), e43676. <https://doi.org/10.1371/journal.pone.0043676>
- Laskowski, R. A., MacArthur, M. W., Moss, D. S., & Thornton, J. M. (1993). PROCHECK: A program to check the stereochemical quality of protein structures. *Journal of Applied Crystallography*, 26(2), 283–291. <https://doi.org/10.1107/S0021889892009944>
- Li, L., Fang, C., Zhuang, N., Wang, T., & Zhang, Y. (2019). Structural basis for transcription initiation by bacterial ECF σ factors. *Nature Communications*, 10(1), 1153. <https://doi.org/10.1038/s41467-019-09096-y>
- Li, W., Bottrill, A. R., Bibb, M. J., Buttner, M. J., Paget, M. S. B., & Kleanthous, C. (2003). The Role of Zinc in the Disulphide Stress-regulated Anti-sigma Factor RsrA from *Streptomyces coelicolor*. *Journal of Molecular Biology*, 333(2), 461–472. <https://doi.org/10.1016/j.jmb.2003.08.038>
- Manganelli, R., Dubnau, E., Tyagi, S., Kramer, F. R., & Smith, I. (1999). Differential expression of 10 sigma factor genes in *Mycobacterium tuberculosis*. *Molecular Microbiology*, 31(2), 715–724. <https://doi.org/10.1046/j.1365-2958.1999.01212.x>
- Manganelli, R., Voskuil, M. I., Schoolnik, G. K., & Smith, I. (2001). The *Mycobacterium tuberculosis* ECF sigma factor σ_E : Role in global gene expression and survival in macrophages: sigE mutant of *M. tuberculosis*. *Molecular Microbiology*, 41(2), 423–437. <https://doi.org/10.1046/j.1365-2958.2001.02525.x>
- Morris, A. L., MacArthur, M. W., Hutchinson, E. G., & Thornton, J. M. (1992). Stereochemical quality of protein structure coordinates. *Proteins: Structure, Function, and Genetics*, 12(4), 345–364. <https://doi.org/10.1002/prot.340120407>
- Newman, J. D., Anthony, J. R., & Donohue, T. J. (2001). The importance of zinc-binding to the function of *Rhodobacter sphaeroides* ChrR as an anti-sigma factor. *Journal of Molecular Biology*, 313(3), 485–499. <https://doi.org/10.1006/jmbi.2001.5069>
- Paget, M. S. B., Bae, J.B., Hahn, M.Y., Li, W., Kleanthous, C., Roe, J.H., & Buttner, M. J. (2001). Mutational analysis of RsrA, a zinc-binding anti-sigma factor with a thiol-disulphide redox switch: Mutational analysis of RsrA. *Molecular Microbiology*, 39(4), 1036–1047. <https://doi.org/10.1046/j.1365-2958.2001.02298.x>
- Pettersen, E. F., Goddard, T. D., Huang, C. C., Couch, G. S., Greenblatt, D. M., Meng, E. C., & Ferrin, T. E. (2004). UCSF Chimera?A visualization system for exploratory research and analysis. *Journal of Computational Chemistry*, 25(13), 1605–1612. <https://doi.org/10.1002/jcc.20084>
- Raman, S., Song, T., Puyang, X., Bardarov, S., Jacobs, W. R., & Husson, R. N. (2001). The Alternative Sigma Factor SigH Regulates Major Components of Oxidative and Heat Stress Responses in *Mycobacterium tuberculosis*. *Journal of Bacteriology*, 183(20), 6119–6125. <https://doi.org/10.1128/JB.183.20.6119-6125.2001>
- Rodrigue, S., Provvedi, R., Jacques, P.É., Gaudreau, L., & Manganelli, R. (2006). The σ factors of *Mycobacterium tuberculosis*. *FEMS Microbiology Reviews*, 30(6), 926–941. <https://doi.org/10.1111/j.1574-6976.2006.00040.x>

- Rohde, K., Yates, R. M., Purdy, G. E., & Russell, D. G. (2007). *Mycobacterium tuberculosis* and the environment within the phagosome. *Immunological Reviews*, 219(1), 37–54. <https://doi.org/10.1111/j.1600-065X.2007.00547.x>
- Sachdeva, P., Misra, R., Tyagi, A. K., & Singh, Y. (2010). The sigma factors of *Mycobacterium tuberculosis*: Regulation of the regulators: The σ -factors of *M. tuberculosis*. *FEBS Journal*, 277(3), 605–626. <https://doi.org/10.1111/j.1742-4658.2009.07479.x>
- Saha, R. P., Bahadur, R. P., Pal, A., Mandal, S., & Chakrabarti, P. (2006). ProFace: A server for the analysis of the physicochemical features of protein-protein interfaces. *BMC Structural Biology*, 6(1), 11. <https://doi.org/10.1186/1472-6807-6-11>
- Shi, L., Jung, Y.J., Tyagi, S., Gennaro, M. L., & North, R. J. (2003). Expression of Th1-mediated immunity in mouse lungs induces a *Mycobacterium tuberculosis* transcription pattern characteristic of nonreplicating persistence. *Proceedings of the National Academy of Sciences*, 100(1), 241–246. <https://doi.org/10.1073/pnas.0136863100>
- Sippl, M. J. (1995). Knowledge-based potentials for proteins. *Current Opinion in Structural Biology*, 5(2), 229–235. [https://doi.org/10.1016/0959-440X\(95\)80081-6](https://doi.org/10.1016/0959-440X(95)80081-6)
- Song, T., Dove, S. L., Lee, K. H., & Husson, R. N. (2003). RshA, an anti-sigma factor that regulates the activity of the mycobacterial stress response sigma factor SigH. *Molecular Microbiology*, 50(3), 949–959. <https://doi.org/10.1046/j.1365-2958.2003.03739.x>
- Waterhouse, A., Bertoni, M., Bienert, S., Studer, G., Tauriello, G., et al. (2018). SWISS-MODEL: Homology modelling of protein structures and complexes. *Nucleic Acids Research*, 46(W1), W296–W303. <https://doi.org/10.1093/nar/gky427>
- Wiederstein, M., & Sippl, M. J. (2007). ProSA-web: Interactive web service for the recognition of errors in three-dimensional structures of proteins. *Nucleic Acids Research*, 35, W407–W410. <https://doi.org/10.1093/nar/gkm290>
- Xue, L. C., Rodrigues, J. P., Kastiris, P. L., Bonvin, A. M., & Vangone, A. (2016). PRODIGY: A web server for predicting the binding affinity of protein-protein complexes. *Bioinformatics*, btw514. <https://doi.org/10.1093/bioinformatics/btw514>
- Zhang, Y., Feng, Y., Chatterjee, S., Tuske, S., Ho, M. X., Arnold, E., & Ebright, R. H. (2012). Structural Basis of Transcription Initiation. *Science*, 338(6110), 1076–1080. <https://doi.org/10.1126/science.1227786>